

Electronic Thesis and Dissertation Repository

6-14-2016 12:00 AM

Cycloaddition Reactions of (Di)tetrelenes

Nada Yahya Tashkandi
The University of Western Ontario

Supervisor
Prof. Kim. M. Baines
The University of Western Ontario

Graduate Program in Chemistry
A thesis submitted in partial fulfillment of the requirements for the degree in Doctor of
Philosophy
© Nada Yahya Tashkandi 2016

Follow this and additional works at: <https://ir.lib.uwo.ca/etd>

 Part of the [Life Sciences Commons](#)

Recommended Citation

Tashkandi, Nada Yahya, "Cycloaddition Reactions of (Di)tetrelenes" (2016). *Electronic Thesis and Dissertation Repository*. 3818.
<https://ir.lib.uwo.ca/etd/3818>

This Dissertation/Thesis is brought to you for free and open access by Scholarship@Western. It has been accepted for inclusion in Electronic Thesis and Dissertation Repository by an authorized administrator of Scholarship@Western. For more information, please contact wlsadmin@uwo.ca.

Abstract

This thesis examines a variety of cycloaddition reactions of multiply-bonded heavy analogues of carbon. With the aid of a mechanistic probe, *trans*-(2-phenylcyclopropyl)acetylene and *trans,trans*-2-methoxy-1-methyl-3-phenylcyclopropyl)ethyne, the mechanism of the addition of alkynes to a germene and a digermene was examined. In both cases, the addition does not involve the intermediacy of a vinyl radical or cation.

The addition of a variety of nitro compounds to tetramesityldisilene and tetramesityldigermene was examined. The facile formation of the novel 1,3,2,4,5-dioxazadisil- and digermolidine ring systems, respectively, was observed. In general, 1,3,2,4,5-dioxazadisilolidines and -digermolidines isomerize under thermal conditions to the 1,4,2,3,5-dioxazadisilolidines and -digermolidines ring system. The 1,3,2,4,5-dioxazadisilolidine and digermolidine systems were found also to undergo ring opening to the isomeric oximes. The addition of nitro compounds to ditetrelenes is a general reaction; the variability of products obtained from the reaction can be understood based on the nature of the substituents on the nitrogen in the nitro compound. For most part, the chemistry of ditetrelenes and the Si and Ge(100)- 2×1 surfaces were quite comparable although the apparent relative stabilities of the adducts varied.

The addition of sulfonyl chloride compounds to tetramesityldisilene (or tetramesityldigermene) lead to the facile formation of a 1,2 addition product, a β -disilyl (or digermyl) halosulfinate. The formation of the sulfinate compounds revealed an interesting, 2-electron reduction of the sulfur centre using a ditetrelene. The addition

reactions of sulfonyl compounds with ditetrelenes illustrates the potential of ditetrelenes to serve as effective reducing agents which react rapidly, at room temperature and under mild conditions.

The addition of isocyanide to tetramesityldisilene differs greatly from the addition of isocyanide to tetramesityldigermene. A C-N bond activation product was obtained from the addition of benzyl isocyanide to tetramesityldigermene. In the presence of the bulkier 2,6-dimethylphenyl- or *t*-butyl isocyanide, the conversion of the digermene to the cyclotrigermane is accelerated. While one equivalent of 2,6-dimethylphenyl- or *t*-butyl isocyanide add to tetramesityldisilene forming [2+1] cycloaddition products, the addition of two equivalent of *t*-butyl isocyanide yields a novel double enamine cycloadduct. The reaction was examined computationally to provide an understanding on the reaction pathway and the intermediates involved.

Keywords: Cycloaddition, Ditetrelene, Alkyne addition, Germene, Digermene, Digermene, Disilene, Mechanism, Sulfonyls, Isocyanides, Nitro compounds

Co-Authorship Statement

A version of Chapter 2 has been published as a full paper authored by Nada Y. Tashkandi, Laura C. Pavelka, Margaret A. Hanson and Kim M. Baines. I am the primary author and conducted all synthetic experiments under the supervision of Dr. Laura C. Pavelka and Prof. Kim M. Baines; Margaret A. Hanson performed the calculations of the energies of the compounds. The written work was a collaborative effort between Prof. Kim M. Baines and myself.

A version of Chapter 3 has been published as a communication authored by Nada Y. Tashkandi, Laura C. Pavelka, Christine A. Caputo, Paul D. Boyle, Philip P. Power and Kim M. Baines. I am the primary author and conducted all experimental work under the supervision of Dr. Laura C. Pavelka and Prof. Kim M. Baines. Digermyne (compound **1.3**) was provided by Christine A. Caputo and Philip P. Power (University of California at Davis). The X-ray structure determination was performed by Dr. Paul Boyle. The written work was a collaborative effort between Prof. Kim M. Baines and myself.

A version of Chapter 4 has been published as a communication authored by Nada Y. Tashkandi, Frederick Parsons, Jiacheng Guo and Kim M. Baines. I am the primary author and conducted most of the experimental work under supervision of Prof. Kim M. Baines. Frederick Parsons conducted some preliminary experiments. The X-ray structure determination and the calculations of the energies of the compounds was performed by Jiacheng Guo. The written work was a collaborative effort between Prof. Kim M. Baines and myself.

For Chapter 5, Jiacheng Guo and Jeremy L. Bourque performed the X- ray structure determination experiments.

For Chapter 6, the computational work and the X- ray structure determination experiments were performed by Jeremy L. Bourque.

For Chapter 7, the addition of bulky isocyanides to tetramesityldigermene was performed by Emily E. Cook, while the X- ray structure determination was performed by Jeremy L. Bourque. Prof. Kim M. Baines and Jeremy L. Bourque performed the computational work of Chapter 7.

Acknowledgements

First, I must thank my supervisor, Kim Baines, for allowing me to continue my studies with her in graduate school. I appreciate all of the time, dedication, and patience. It has been pleasure to work for her. I couldn't have done this work without her guidance. I also thank my Baines group lab mates, especially Bahar. They have made time spent in the lab enjoyable and I am thankful for the many friendships I have gained during my time here.

I would also like to extend my gratitude to all of the faculty and staff in the department for providing me with such an incredible university education. I would especially like to thank Mat Willans, Doug Hairsine and Paul Boyle for their assistance with NMR spectroscopy, mass spectrometry and X-ray diffraction, respectively.

I need to thank my family, my parents and siblings, my biggest support and love of my life my husband, and my children, for encouraging me to achieve my goals and for believing in me to cross the world and come here to make my dream come true.

Table of Contents

	Page
Certificate of Examination	ii
Abstract and Keywords.....	iii
Co-Authorship.....	v
Acknowledgements.....	vi
Table of Contents.....	viii
List of Tables	xiii
List of Figures.....	xiv
List of Abbreviations	xvi
Cast of Characters.....	xix
 Chapter 1: The Chemistry of Unsaturated Heavy Analogues of Carbon	
1.1 General Introduction	1
1.2 Structure and Bonding of Tetrelenes	2
1.3 Structure and Bonding of Ditetrelenes.....	3
1.4 Structure and Bonding of Ditetrelynes	5
1.5 Reactivity of (Di)tetrelenes and Ditetrelynes	7
1.6 Mechanistic Alkyne Probe.....	8

1.7	Disilenes and Digermenes as Models of the Silicon and Germanium(100)- 2×1 Surfaces.....	11
1.8	Nature of Si and Ge(100)- 2×1 Surfaces.....	11
1.9	Preparation of (Di)tetrelenes and Ditetrelynes	17
1.10	References.....	18

Chapter 2: The Addition of Terminal Alkynes to Dimesitylfluorenylidene-germane

2.1	Introduction.....	25
2.2	Results.....	28
2.2.1	Addition of Terminal Alkynes to Dimesitylfluorenylidene-germane	28
2.2.2	Addition of Alkyne Probe to Dimesitylfluorenylidene-germane	32
2.2.3	Addition of Ethoxyacetylene to Dimesitylfluorenylidene-germane	32
2.3	Discussion.....	36
2.4	Conclusions.....	43
2.5	Experimental.....	43
2.6	References.....	53

Chapter 3: Addition of Alkynes to Digermynes: Experimental Insight into the Reaction Pathway

3.1	Introduction.....	56
3.2	Results.....	60
3.3	Discussion.....	61

3.4	Conclusions.....	65
3.5	Experimental.....	66
3.6	References.....	69

Chapter 4: Addition of Nitromethane to a Disilene and a Digermene: Comparison to Surface Reactivity and the Facile Formation of 1,3,2-dioxazolidines

4.1	Introduction.....	73
4.2	Results.....	75
4.2.1	Addition of Nitromethane to Tetramesityldisilene.....	75
4.2.3	Addition of Nitromethane to Tetramesityldigermene.....	77
4.3	Discussion.....	79
4.4	Conclusions.....	84
4.5	Experimental.....	84
4.6	References.....	90

Chapter 5: The Addition of Nitro Compounds to Tetramesityldisilene and Tetramesityldigermene: Substituent Effects and Comparison to Surface Reactivity

5.1	Introduction.....	94
5.2	Results.....	97
5.2.1	Addition of Nitro Compounds to Disilene 1.4	97
5.2.2	Addition of Nitro Compounds to Digermene 1.2	102
5.3	Discussion.....	108

5.4	Conclusion	119
5.5	Experimental	120
5.5	References	131

Chapter 6: Reactivity of Sulfonyl-Containing Compounds with Ditetrelenes

6.1	Introduction	136
6.2	Results	137
6.3	Discussion	145
6.4	Summary and Conclusions	154
6.5	Experimental	154
6.6	References	163

Chapter 7: The Reactivity of Ditetrelenes Toward Isocyanides

7.1	Introduction	168
7.2	Results	171
7.2.1	Addition of Isocyanides to Digermene 1.2	171
7.2.1.1	Addition of a Small Isocyanide to Digermene 1.2	172
7.2.1.2	Addition of Bulky Isocyanides to Digermene 1.2	174
7.2.2	Addition of Isocyanides to Disilene 1.4	181
7.2.2.1	Addition of <i>t</i> -Butyl Isocyanides to Disilene 1.4	181

7.2.2.2	Addition of 2,6-dimethylphenyl Isocyanides to Disilene 1.4	184
7.3	Discussion	176
7.3.1	The Addition of Isocyanides to Digermene 1.2	176
7.3.2	Addition of Isocyanides to Disilene 1.4	186
7.4	Conclusions.....	193
7.5	Experimental	194
7.6	References.....	202
 Chapter 8: Summary and Future work		
8.1	Summary and Conclusions	207
8.2	Future Directions	212
8.3	References.....	213
 Appendix 1: Illustrative Example of NMR Spectra for Characterization of New Compounds		
		215
 Appendix 2: Copyrighted Material and Permissions		
		221
 Curriculum Vitae		
		225

List of Tables

	Page
Table 2.1	Crystallographic data for compounds 2.9a and 2.9b53
Table 3.1	Crystallographic data for compound 3.5c68
Table 4.1	Crystallographic data for compounds 4.4 and 4.789
Table 5.1	Crystallographic data for compounds 5.5a , 5.7b , 5.7c , 5.9c and 5.13130
Table 6.1	Crystallographic data for compounds 6.2 , 6.3 , 6.4 , 6.6 and 6.7163
Table 7.1	Summary of the reactivity of disilenes toward isocyanides.189
Table 7.2	Crystallographic data for compounds 7.8 , 7.19 and 7.21202

List of Figures

	Page
Figure 2.1 Displacement ellipsoid plot of 2.9a	31
Figure 2.2 Displacement ellipsoid plot of 2.9b	31
Figure 2.3 HOMO and LUMO of (A) butadiene, (B) 1-germabutadiene, (C) phenylacetylene, and (D) ethoxyacetylene.	41
Figure 3.1 Displacement ellipsoid plot of 3.5c	61
Figure 4.1 Displacement ellipsoid plot of 4.4	76
Figure 4.2 Displacement ellipsoid plot of 4.7	79
Figure 5.1 Displacement ellipsoid plot of 5.5a	99
Figure 5.2 Displacement ellipsoid plot of 5.7b	101
Figure 5.3 Displacement ellipsoid plot of 5.9c	104
Figure 5.4 Displacement ellipsoid plot of 5.13	106
Figure 5.5 Displacement ellipsoid plot of 5.7c	110
Figure 6.1 Displacement ellipsoid plot of 6.2	139
Figure 6.2 Displacement ellipsoid plot of 6.3	139
Figure 6.3 Displacement ellipsoid plot of 6.4	140
Figure 6.4 Displacement ellipsoid plot of 6.6	142

Figure 6.5	Displacement ellipsoid plot of 6.7	143
Figure 7.1	Displacement ellipsoid plot of 7.8	173
Figure 7.2	Effect of adding 2,6-dimethylphenyl isocyanide on the conversion of 1.2 to 7.9	175
Figure 7.3	Displacement ellipsoid plot of 7.19	183
Figure 7.4	Displacement ellipsoid plot of 7.21	185

List of Abbreviations

Å = Angstrom

Ad = admantyl

br = broad

Bu = butyl

calcd = calculated

d = doublet (NMR)

DCM = dichloromethane

DFT = density functional theory

Dipp = 2,6-diisopropylphenyl

DMB = 2,3-dimethylbutadiene

EI = electron impact

ESI = electrospray ionization

Et = ethyl

FT = fourier transform

gCOSY = gradient correlation spectroscopy

gHMBC = gradient heteronuclear multiple bond correlation

gHMQC = gradient heteronuclear multiple quantum coherence

gHSQC = gradient homonuclear spin quantum coherence

HOMO = highest occupied molecular orbital

hr = hour

Hz = hertz

i-Pr = isopropyl

IR = infrared

J = coupling constant

LUMO = lowest unoccupied molecular orbital

m = multiplet (NMR); medium (IR)

m-cpba = *meta*-chloroperbenzoic acid

Me = methyl

Mes = mesityl = 2,4,6-trimethylphenyl

MHz = megahertz

MO = molecular orbital

MS = mass spectrometry

m/z = mass-to-charge units

Ph = phenyl

ppm = parts per million

RT = room temperature

s = singlet (NMR); strong (IR)

STM = Scanning tunneling microscopy

t = triplet

t-Bu = *tertiary* butyl

Tip = triisopropylphenyl

THF = tetrahydrofuran

TMS = trimethylsilyl

w = weak

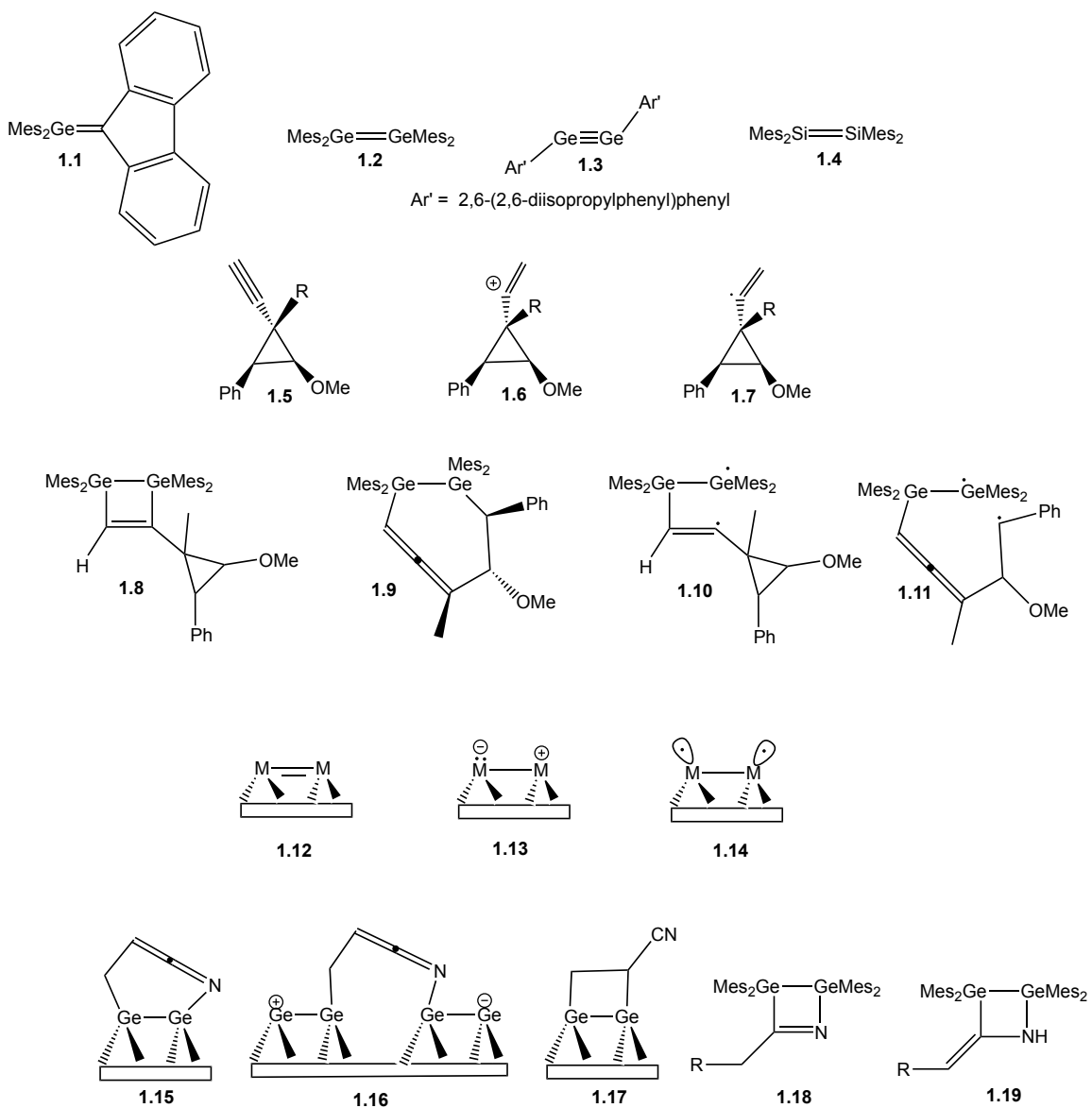
XPS = X-ray Photoelectron spectroscopy

Xyl = 2,6-dimethylphenyl

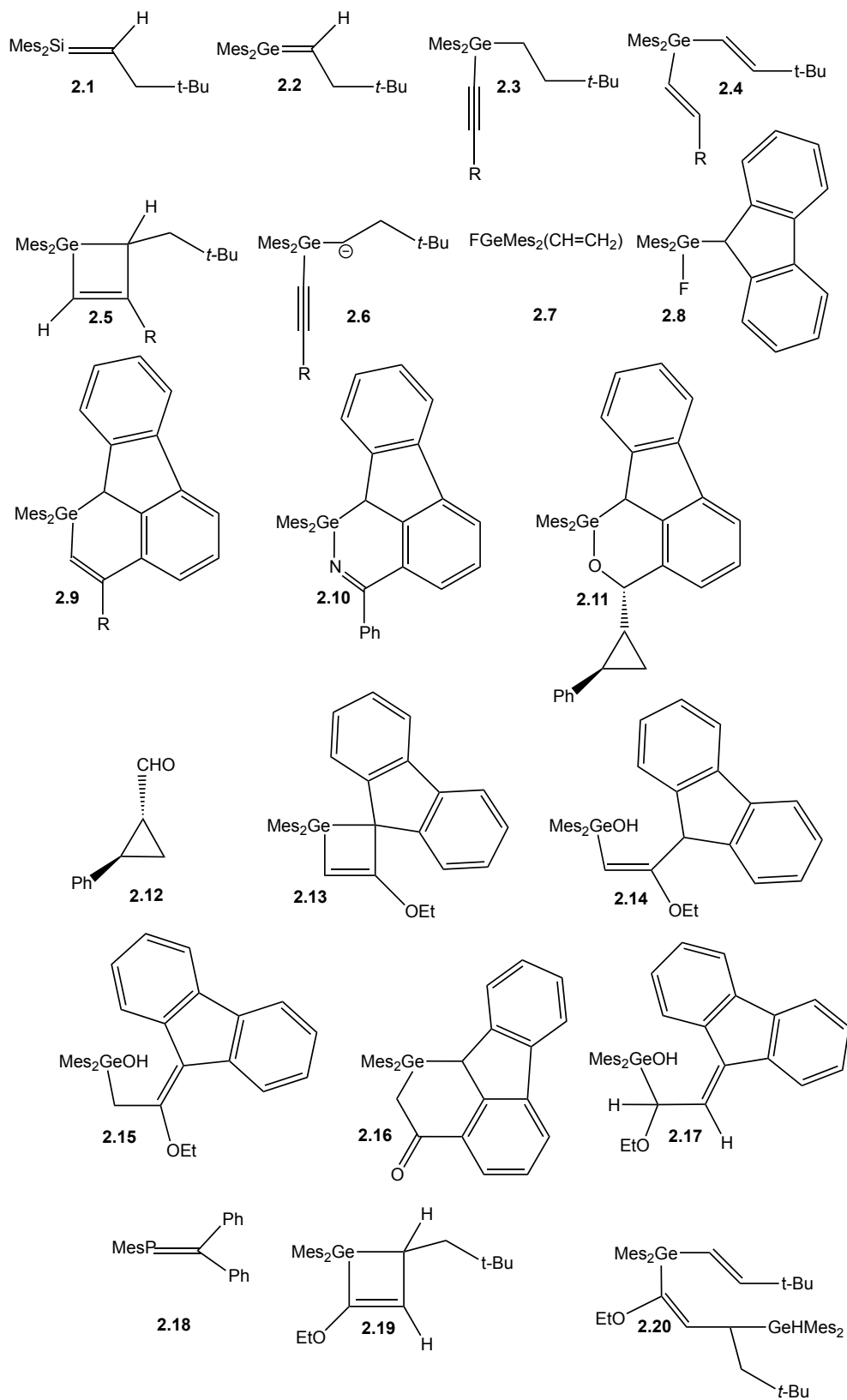
δ = chemical shift

Cast of Characters

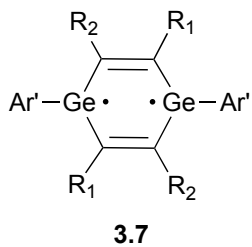
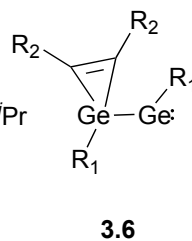
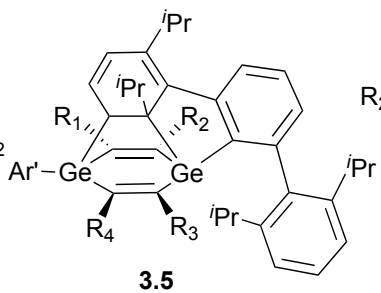
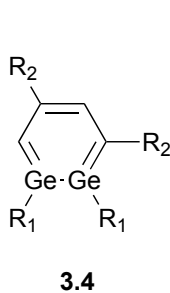
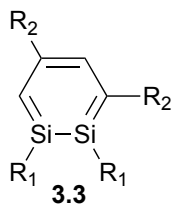
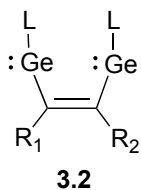
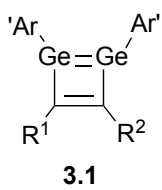
Chapter 1



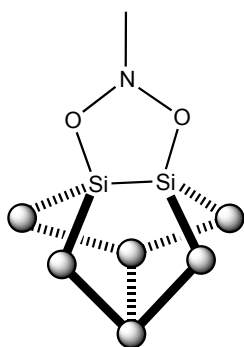
Chapter 2



Chapter 3

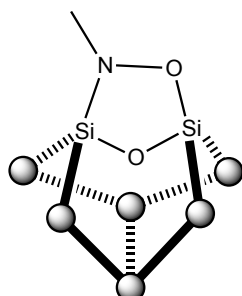


Chapter 4

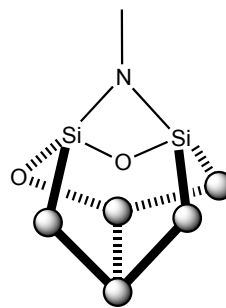


4.1

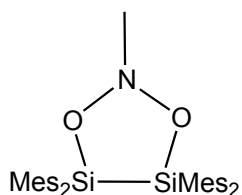
● = Si



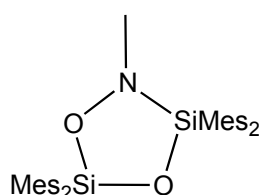
4.2



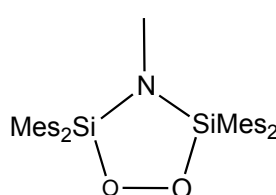
4.3



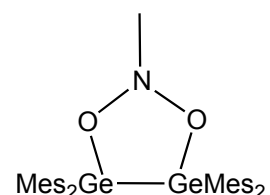
4.4



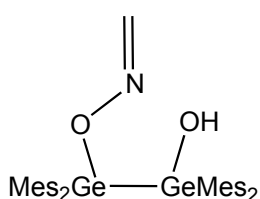
4.5



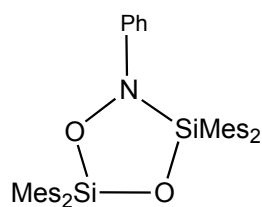
4.6



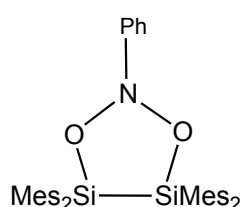
4.7



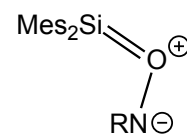
4.8



4.9

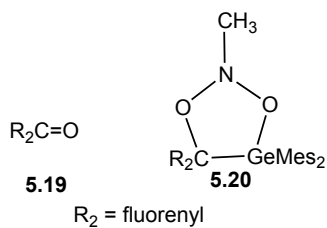
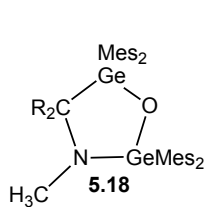
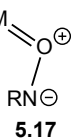
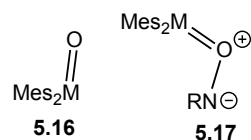
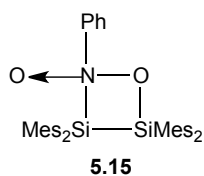
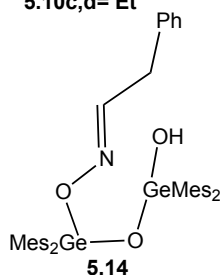
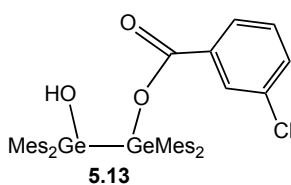
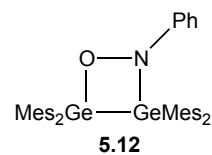
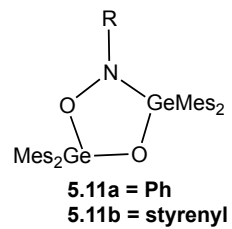
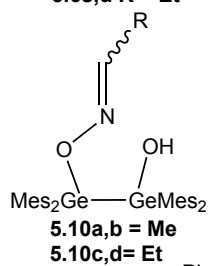
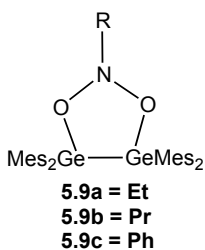
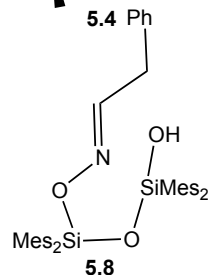
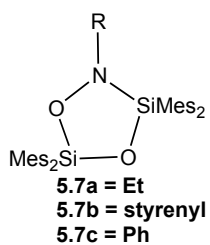
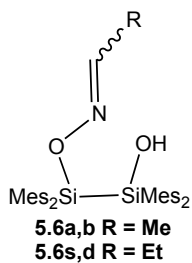
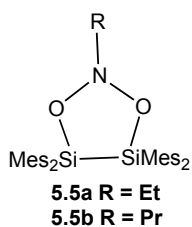
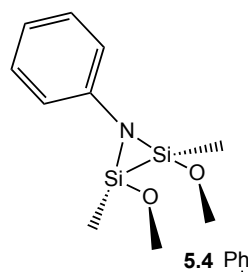
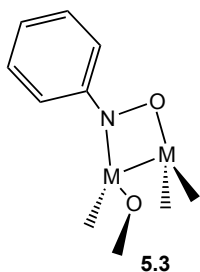
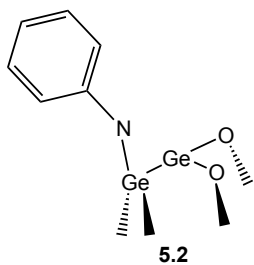
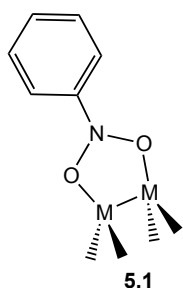


4.10

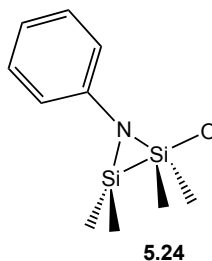
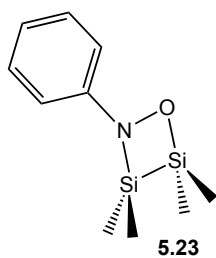
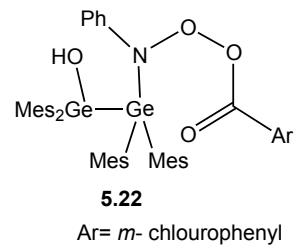
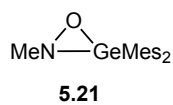
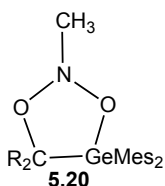


4.11

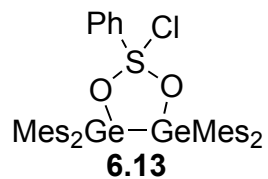
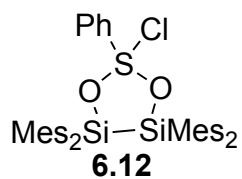
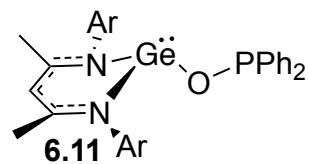
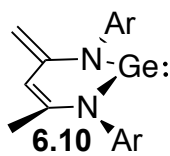
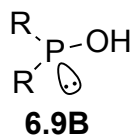
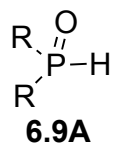
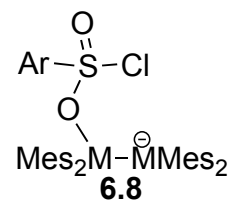
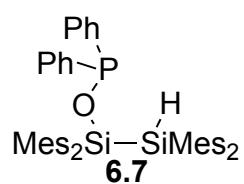
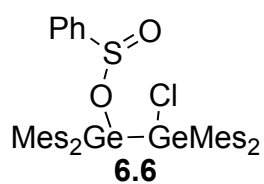
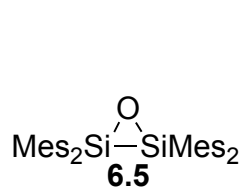
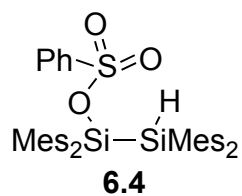
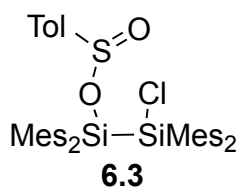
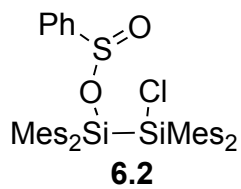
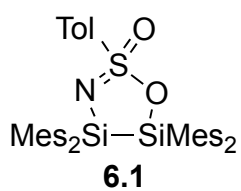
Chapter 5



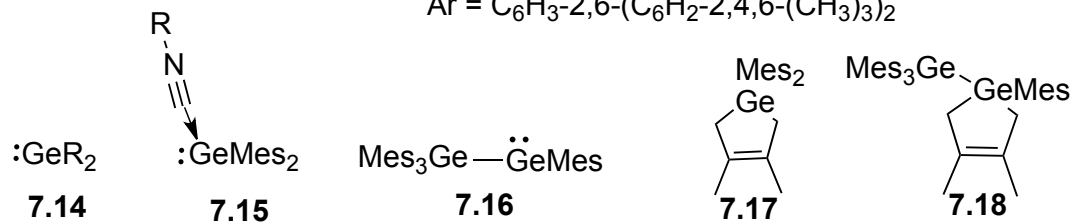
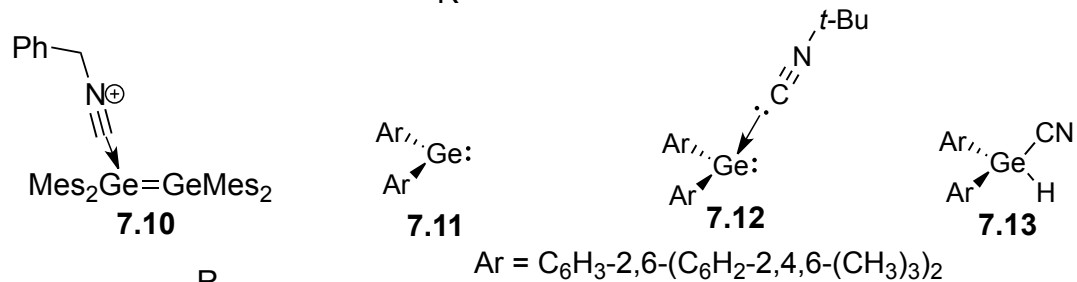
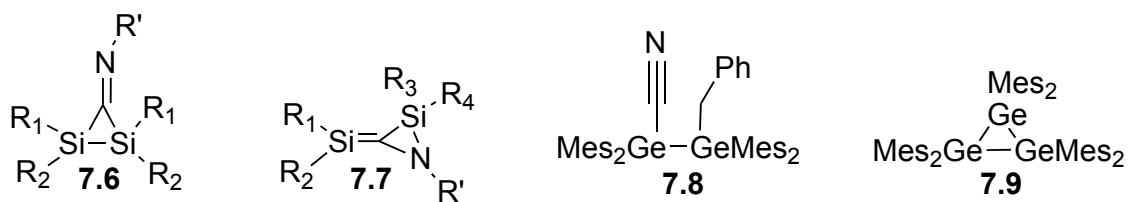
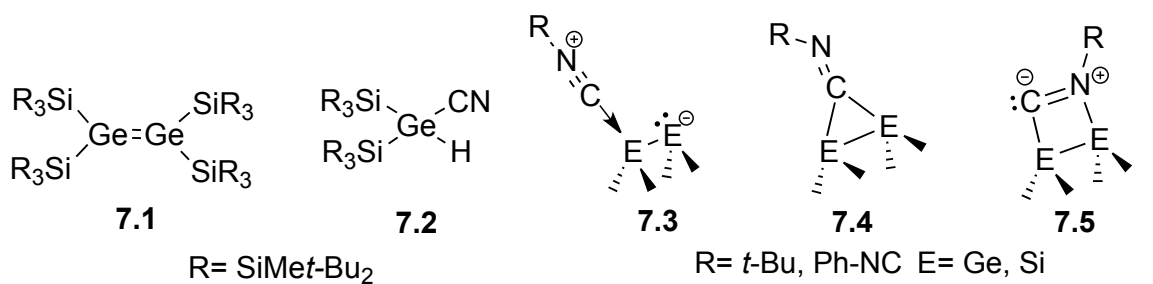
R₂ = fluorenyl



Chapter 6

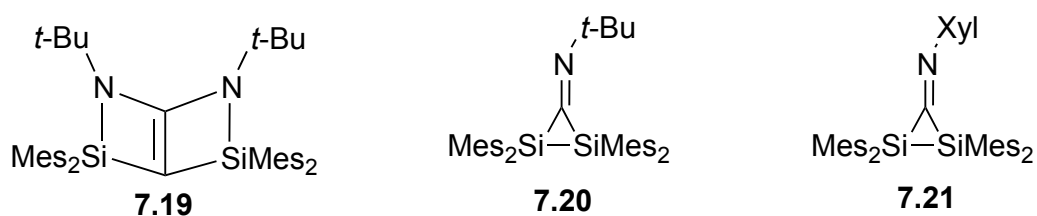


Chapter 7



R' = 2,6-dimethylphenyl, t -Bu

R = Mes, SiMe t -Bu $_2$



Chapter 1

The Chemistry of Unsaturated Heavy Analogues of Carbon

1.1 General Introduction

The field of low valent main group chemistry has experienced a renaissance over the last five years, taking advantage of the unique properties and high reactivities of this class of compounds. It has been recognized that low valent main group compounds have similar reactivity to transition metals.¹ Like transition metals, many heavier carbon analogues are able to activate small molecules such as H₂, CO₂, CO and NH₃ under ambient temperature² and have been used as catalysts or as reagents to effect organic transformations under mild conditions.^{3,2d}

(Di)tetrelenes (referring to the heavy Group 14 derivatives: tetrelenes (R₂M=CR₂) and ditetrelenes (R₂M=MR₂) M = Si, Ge, Sn, Pb) are a fundamental class of molecules. The spectroscopic and structural characterization of these unsaturated species and computational studies of their electronic structure has greatly influenced our understanding of structure, bonding and reactivity. In comparison to alkenes, ditetrelenes are more reactive, which should enable new modes of reactivity as well as introduce functionality and new synthetic routes not available using other organometallic species. Doubly-bonded compounds of the heavy main group elements have proven to be powerful building blocks in organometallic/inorganic synthesis just as alkenes have proven to be in organic synthesis.⁴ Moreover, (di)tetrelenes have been utilized as monomers in the development of novel organometallic polymers⁵ and also have been used as models to study the reactivity of their surfaces analogues.⁶

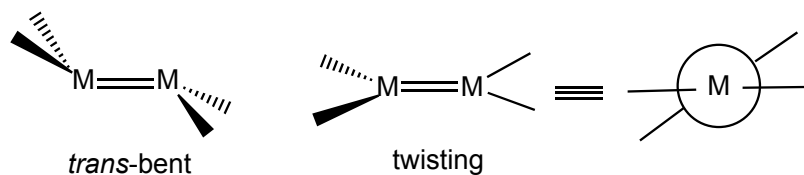
The focus of this thesis will be on the chemistry of multiply-bonded derivatives of the heavier Group 14 elements, specifically the germanium derivatives, namely: germenes, digermenes and digermynes. In addition, in some cases, the comparative reactivity of disilenes will be examined. As prototypical examples, the chemistry of the following compounds will be studied: $\text{Mes}_2\text{Ge}=\text{CR}_2$ (where CR_2 =fluorenylidene) **1.1**, $\text{Mes}_2\text{Ge}=\text{GeMes}_2$, (where Mes = 2,4,6- $\text{Me}_3\text{C}_6\text{H}_2$) **1.2**, $\text{Ar}'\text{GeGeAr}'$ (where Ar' =2,6-(2,6-diisopropylphenyl)phenyl) **1.3**, and $\text{Mes}_2\text{Si}=\text{SiMes}_2$ **1.4**. Given the central role of these compounds to this thesis, the structure and bonding of these unsaturated molecules will be reviewed here.

1.2 Structure and Bonding of Tetrelenes

The first isolable tetrelene was $(\text{Mes}_3\text{Si})_2\text{Si}=\text{C}(1\text{-Ad})(\text{OSiMe}_3)$, which was synthesized by Brook in 1981 and utilized bulky substituents to kinetically stabilize the compound from dimerization.⁷ The geometry about the double bond in both germenes and silenes is planar similar to their lighter congeners, the alkenes. The π bond in silenes ($\text{Si}=\text{C}$) and germenes ($\text{Ge}=\text{C}$) is a traditional π bond; albeit, it is weaker than the π bond of alkenes. As a result, tetrelenes are far more reactive than alkenes.⁸ In contrast to alkenes, the double bonds of silenes and germenes are polarized due to the electronegativity difference between carbon ($\chi= 2.5$) and silicon ($\chi= 1.8$) or germanium ($\chi= 1.9$). The polarized $\text{M}=\text{C}$ bond in a silene or germene leads to the regioselective addition of polar reagents: electronegative elements prefer to add to the electropositive atom (silicon or germanium).

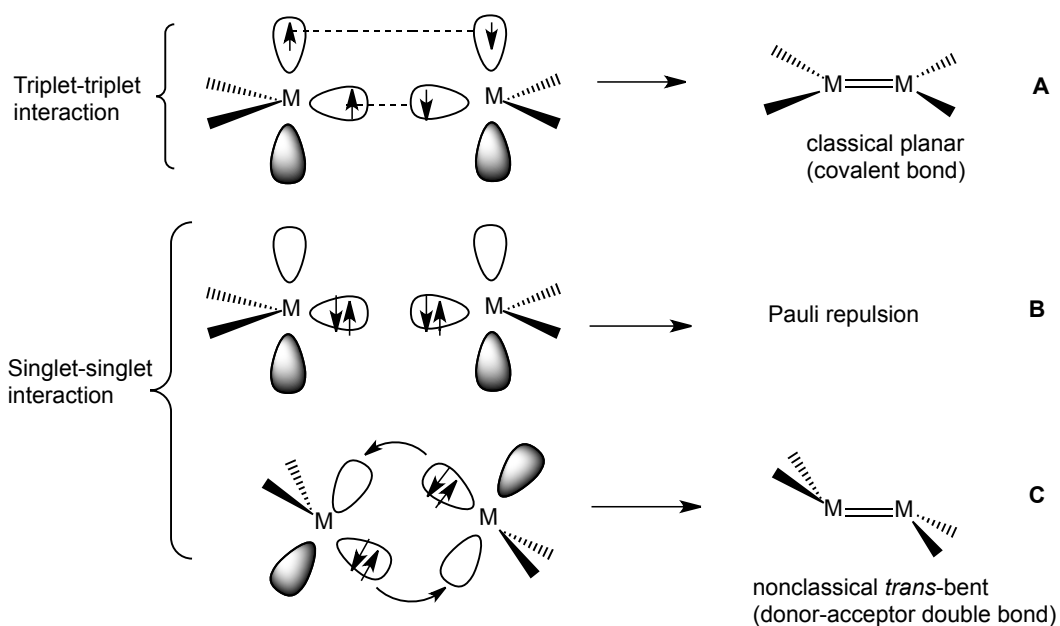
1.3 Structure and Bonding of Ditetrelenes

In contrast to tetrelenes which are typically planar, ditetrelenes have a *trans*-bent geometry at the silicon or germanium centre and exhibit twisting about the M=M bond (Scheme 1.1).



Scheme 1.1

The bonding in ditetrelenes can be understood as the interaction of two monomeric divalent species. For alkenes, the interaction of two monomeric carbenes, which typically are ground state triplets, results in two covalent interactions between singly occupied MOs forming the classic planar C=C double bond (Scheme 1.2, A). In contrast to carbenes, the heavier analogues (silylenes and germylenes) are ground state singlets, and therefore, the classic planar interaction (model A) of singlet silylenes or germylenes gives rise to a significant Pauli repulsion between the doubly-occupied n-orbitals (Scheme 1.2, B). As consequence, the two heavy analogues (silylenes and germylenes) interact in a donor-acceptor manner which results in the formation of a non-classical M=M bond with *trans*-bent geometry (Scheme 1.2, C).^{8a,9}



Scheme 1.2

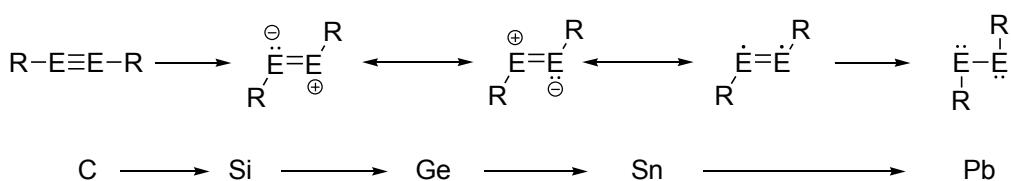
The π bond in ditionenes is inherently weak and many computational studies have focused on understanding the weakness of the π bond.⁹ The bonding in H_2 arises nearly exclusively from orbital interactions, and thus, covalent interactions in nonpolar bonds are often described only in terms of molecular orbitals. However, Frenking and co-workers have extensively investigated the nature of non-polar chemical bonds using energy-partitioning analysis and have found that the bonding interactions in a covalent bond are more readily understood in terms of three major components, that is, the repulsive Pauli term, quasiclassical electrostatic interactions (E_{elstat}), and orbital interactions.¹⁰ The interaction energy in H_3E-EH_3 ($E = C$ to Pb) decreases monotonically as the element E becomes heavier. The electrostatic character of the $E-E$ bond increases from $E=C$ (41.4%) to $E=Sn$ (55.1%). Doubly-bonded species ($HB=BH$, $H_2C=CH_2$, and *trans*- $HN=NH$), on the other hand, have a higher degree of orbital interactions compared to the analogous single bonds in H_nE-EH_n . The relative contribution of the ΔE_{elstat} term

increases whilst that of the π -bonding decreases as E becomes more electronegative. Meanwhile, the Pauli repulsion term increases significantly from HB=BH (116.3 kcal/mol), to H₂C=CH₂ (281.9 kcal/mol), to HN=NH (599.4 kcal/mol). The absolute values of the energy components of HN=NH are significantly higher than those of ethylene, but the very strong Pauli repulsion in diazene leads to a weaker net attraction.¹⁰ Similar to diazene, (di)tetrelenes have a strong Pauli repulsion causing them to have weak π -bond.

1.4 Structure and Bonding of Ditetrelynes

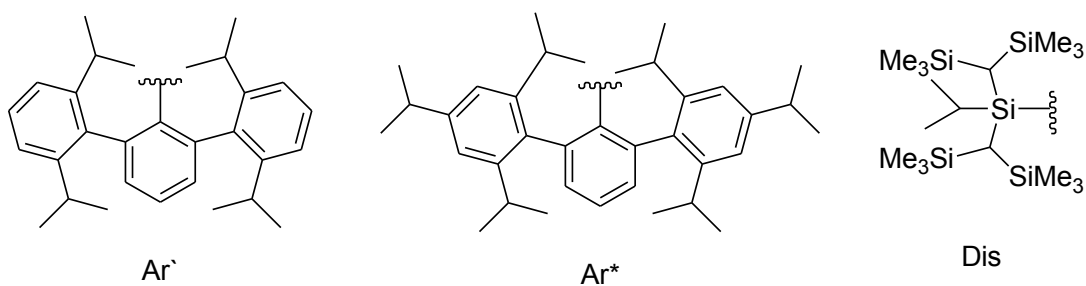
The synthesis and chemistry of the heavier Group 14 congeners of alkynes is of fundamental interest to main group chemists. The bonding in these species has received much theoretical consideration. One of the major findings is that the familiar linear geometry of acetylene is energetically unfavorable for all heavier group 14 elements.^{9a,11} The hydrogen-bridged structure of Si₂H₂ is favoured over a linear disilyne; however, a *trans*-bent structure, featuring a Si-Si triple bond, is also a local minimum. When the hydrogens are replaced with methyl groups, the *trans*-bent structure becomes more favorable than the bridged structure.¹² This provided reassurance that, with the right substituents, the synthesis of a ditetrelene may be possible. Although the existing ditetrelenes feature the defining REER formula of the heavier congeners of alkynes, there is still controversy as to whether such species can truly be said to contain a triple bond. The calculated bond order decreases down the group, which is believed to be due to the intermixing of the σ^* orbital with the π bonding orbitals due to a second order Jahn-Teller distortion. As a result, an increasingly *trans*-bent geometry is observed as one descends the group. In diplumbynes, the C-Pb-Pb angle is closer to 90° than 180°. There

is general agreement that these are not *classical* triple bonds, having some degree of either lone pair or diradical character. With lead, the bonding is thought to be best described as a single bond with a lone pair on each atom, but the bonding in the intermediate group 14 elements is much less clearly defined (Scheme 1.3). All the depictions of the bonding lead to even higher expected reactivity than the already reactive classical triple bond.¹³



Scheme 1.3

Ditetrelynes are highly reactive and require kinetic stabilization to enable isolation. Nonetheless, the full series of heavy group 14 ditetrelynes have been synthesized. Since steric protection of the reactive triple bond of the disilynes and digermynes must be achieved using only a single ligand, the synthesis of stable derivatives has proven to be very challenging. Very bulky ligands are required. Power has effectively utilized the terphenyl ligands for example, 2,6-(2,6-diisopropylphenyl)phenyl (Ar¹) and 2,6-(2,4,6-triisopropylphenyl)phenyl (Ar^{*}) for the synthesis of stable digermynes.¹⁴ Sekiguchi, on the other hand, has used bulky silyl substituents, such as 1,1,4,4-tetrakis[bis(trimethylsilyl)methyl]1,4-triisopropylsilyl (Dis), for the synthesis of stable disilynes (Scheme 1.4).¹⁵



Scheme 1.4

1.5 Reactivity of (Di)tetrelenes and Ditetrelynes

(Di)tetrelenes and ditetrelynes have a much higher reactivity in contrast to their lighter congeners, alkenes; they react almost instantly with many reagents at room temperature without the use of a catalyst, heat, or pressure.^{8,16,17,18,19} One of the most common classes of reactions, which has been studied in detail and still receives much attention, is cycloaddition reactions. Cycloaddition reactions have fascinated the chemical community for generations because a great variety of ring systems can be constructed directly from simple building blocks. Not surprisingly then, cycloadditions of the ditetrelenes and ditetrelynes were among the first reactions investigated upon the discovery of a new species of this class. Many modes of cycloaddition have been reported with many different unsaturated compounds leading to many exciting developments in the area of unsaturated Group14 analogues. For example, an organosilicon hybrid polymer was obtained via the regiospecific [2+2] cycloaddition of alkynes to the Si=Si double bonds of a tetradisilene, providing a catalyst-free and by-product free protocol for the synthesis of conjugated organosilicon polymers.^{5b} The cycloaddition reactions of low valent main group species has provided some exciting new modes of reactivity that inspired us to further pursue these reactions. The exploration and understanding of the cycloaddition reactions of (di)tetrelenes and ditetrelynes is the

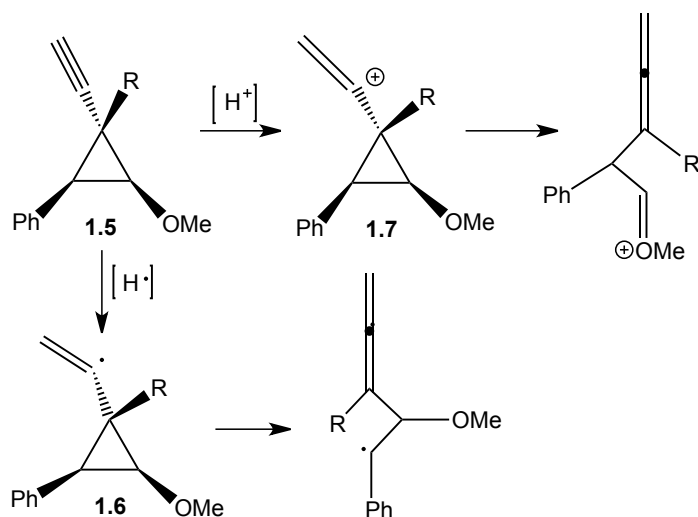
overarching theme in this thesis.

1.6 Mechanistic Alkyne Probe

A clear understanding of the mechanisms of the reactions of (di)tetrelenes and ditetrelynes is essential for the development of applications of this chemistry. However, mechanistic studies on (di)tetrelenes/ditetrelynes are challenging. (Di)tetrelenes and ditetrelynes readily react with oxygen and water often giving by-products complicating the mechanistic studies. Furthermore, (di)tetrelenes and ditetrelynes react with many common functional groups limiting the solvents that can be utilized. Few *E/Z* isomers of (di)tetrelenes are known and have only become readily available recently,¹⁷ and thus, examination of the stereo- and regiochemistry of the addition reactions of these species is limited. Finally, the rates of many reactions are quite fast requiring specialty equipment to monitor them. As a result, detailed mechanistic studies of these classes of compounds are still relatively rare. One of the few reactions of (di)tetrelenes that has been studied in detail mechanistically is the addition of alcohols or water to (di)silenes.²⁰

Mechanistic probes have been utilized as a means to understand the reactivity of (di)tetrelenes.²¹ Newcomb developed hypersensitive phenylcyclopropylcarbinyll mechanistic probes.²² The term “hypersensitive” means that these probes can reveal transformations that occur on the nano- to picosecond time scale.²² Mechanistic probes operate on the following basis: depending on the nature of the intermediate located adjacent to the cyclopropyl ring, structurally different products are formed and the presence of a given type of reaction intermediate can be concluded by recognizing the regiochemically different rearrangements of the products (Scheme 1.5). For example, α -

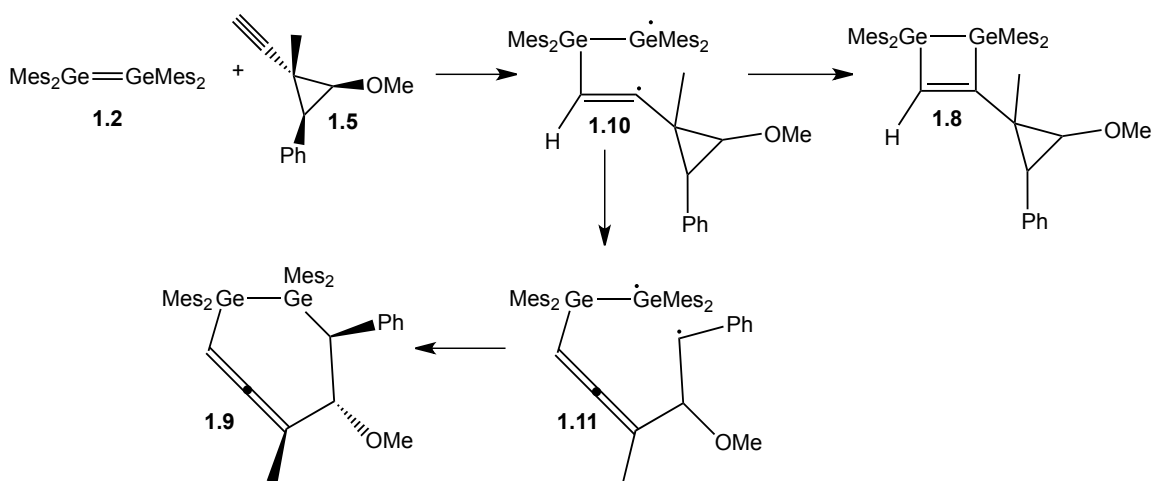
cyclopropylvinyl radical **1.6** opens rapidly and regioselectively towards the phenyl substituent yielding a benzyl radical. In contrast, the α -cyclopropylvinyl cation **1.7** rearranges selectively towards the methoxy substituent. Therefore, the cyclopropyl alkyne probe **1.5** can be used to discriminate between the formation of vinyl-substituted cyclopropylcarbinyl radicals and cations.



Scheme 1.5

To be an effective probe, the rate constant for the rearrangement reaction must be large enough such that the rearrangement effectively competes with other processes that may occur during the reaction, such as ring closure; probe **1.5** was shown to have an appropriate magnitude for the rate constants of the rearrangements. The following example is an illustration of the application of the alkynyl mechanistic probe in the study of the addition of alkynes to a Group 14 ditetrelene. The addition of alkyne mechanistic probe **1.5** to tetramesityldigermene **1.2** resulted in the formation of two isomeric digermacyclobutenes **1.8** and digermacyclohepta-1,2-diene **1.9**, in addition to other by-products (Scheme 1.6). The key piece of evidence is the location of the phenyl group: on

the carbon adjacent to the germanium atom in the 7-membered ring of **1.9**. As a consequence, the mechanism of the addition reaction was postulated to proceed via a *biradical* intermediate since the cyclopropyl ring rearranged exclusively toward the phenyl. The initially formed 1,4-biradical intermediate, **1.10**, also appears to cyclize at a comparable rate to give digermacyclobutene **1.8**.



Scheme 1.6

Using the same approach, the mechanism of the addition of alkynes to disilenes was determined to proceed via a biradical intermediate.²³ Similarly, the addition of the cyclopropyl alkyne probe to Brook silenes, which are silenes with the general structure $(\text{Mes}_3\text{Si})_2\text{Si}=\text{C}(\text{R})(\text{OSiMe}_3)$, was also determined to proceed via a biradical intermediate.²⁴ In contrast to Brook silenes, the naturally polarized silene $\text{Mes}_2\text{Si}=\text{CHCH}_2t\text{-Bu}$ reacted with the alkyne mechanistic probe exclusively through insertion of the acetylenic C-H across the Si=C bond to form silylacetylenes, and therefore, no information on the cycloaddition reaction could be inferred.²⁵ The addition of alkynes to disilynes^{26,27} and digermynes^{13,28,29,30,31} was one of the first reactions explored to test the reactivity of this fundamental class of molecules. The mechanism of

the addition reaction has received a great deal of interest; however, it has only been explored computationally. The mechanism of the addition of alkynes to a germene or a ditetrelyne has not been explored experimentally, and thus, the mechanism of the addition of alkynes to germene **1.1** and digermene **1.3** will be examined in this thesis using the mechanistic probe approach (Chapters 2 and 3, respectively).

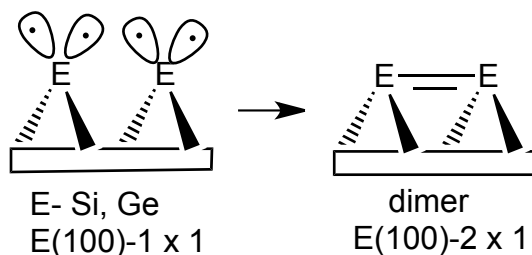
1.7 Disilenes and Digermenes as Models of the Silicon and Germanium(100)- 2×1 Surfaces

The attachment of organic compounds to silicon surfaces has gained significant interest over the years.³² Understanding the functionalization of semiconductor surfaces by the direct attachment of organic molecules is critical to achieving molecular level control of organic-inorganic interfaces.³³ Microelectronics, catalysis and sensors are among the fields where this research might be relevant.³⁴ Especially of interest are those compounds that can alter the electronic properties of the substrate surface. Ditetrelenes (digermene **1.2** and disilene **1.4**) have been successfully used as models for the reactivity of the Si and Ge(100)- 2×1 reconstructed surfaces, and therefore, the nature, bonding and reactivity of these surfaces will be briefly discussed.

1.8 Nature of Si and Ge(100)- 2×1 Surfaces

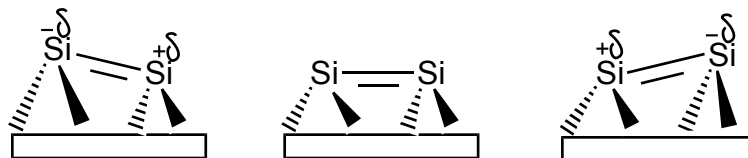
The surfaces of silicon or germanium are usually prepared by bombardment of the oxidized layer with argon ions (Ar^+) or by heating to 900 °C under ultrahigh vacuum atmosphere.^{33a} The removal of the oxide layer on the surface results in the interfacial atoms being connected only to two atoms rather than the preferred four. Two unpaired electrons are obtained on each surface atom and are referred to as dangling bonds. This

type of surface is referred to as the Si (or Ge)(100)- 1×1 surface.^{32g} The numbers in parentheses are the Miller indices, a notation referring to the orientation at which the bulk surface is terminated. The notation following the hyphen indicates the periodicity of the surface atoms.^{32g} The number of dangling bonds is reduced, as they recombine to form dimers to reduce the total free energy of the system (Scheme 1.7). The surface is now indicated as the Si or Ge(100)- 2×1 reconstructed surface. This surface is made up of silicon or germanium atoms in a 2×1 dimer arrangement with a trench between the dimer rows.^{32a}



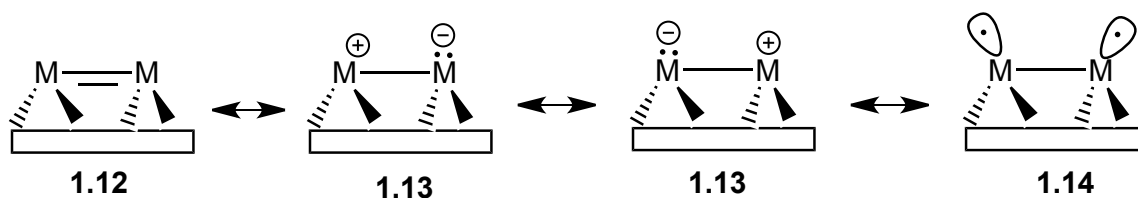
Scheme 1.7

The dimers then tilt to further reduce the energy of the system.^{32d} At room temperature, the silicon dimers appear symmetric due to the thermal energy of the system causing the dimers to rapidly oscillate. Meanwhile, for germanium, the tilting is apparent even at room temperature. The reactivity is greatly affected by this tilting since the electronic properties of the dimer are altered by the tilting.^{32a} The “up” atom exhibits a nucleophilic character since it possesses most of the electron density. Consequently, the “down” atom is expected to exhibit significant electrophilic character since it possesses the least electron density (Scheme 1.8). This leads to Lewis acid donor/acceptor type behavior of the dimer species.^{32a}



Scheme 1.8

Both molecular (di)tetrelenes and the surface dimers can be represented by four resonance structures: as a full double bond **1.12**, a set of zwitterions **1.13**, or a biradical species **1.14** (Scheme 1.9). The exact structure of the surface is still debateable.^{32d,h,i}



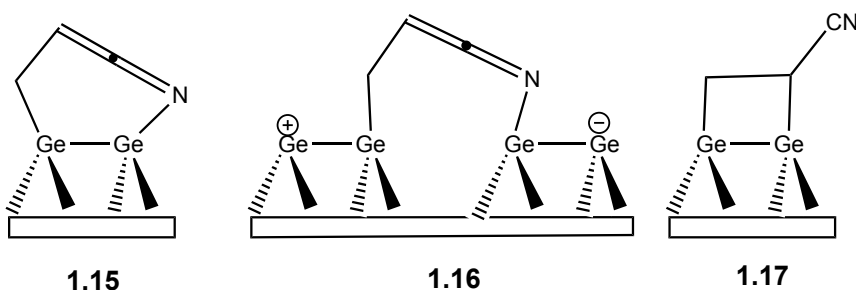
Scheme 1.9

Extensive experimental and computational studies of the functionalization of the Si/Ge(100)- 2×1 surfaces have been carried out. In general, an excess amount of reagent is added to the surface forming surface adducts. However, characterization of those adducts on the surface is challenging. X-ray photoelectron spectroscopy (XPS) is used to identify which elements are present and their oxidation state, Fourier transform infrared spectroscopy (FTIR) can provide information on the types of functional groups present in the surface adducts. Scanning tunneling microscopy (STM) can provide insight into the electronic structure of the surface atoms. Although these techniques provide valuable information on the reaction products, the structure of the surface adducts often remains ambiguous.

In contrast to surface adducts, the structures of molecular compounds can be identified unequivocally using various techniques which are not available to surface scientists, such as NMR spectroscopy, mass spectrometry and X-ray crystallography. Additionally, molecular compounds and surface adducts can be characterized by FTIR spectroscopy which allows for a comparison between the data sets. Furthermore, the reactivity of molecular compounds can be examined more easily than the reactivity of surface adducts, especially when the surface layer contains several reactive functionalities.

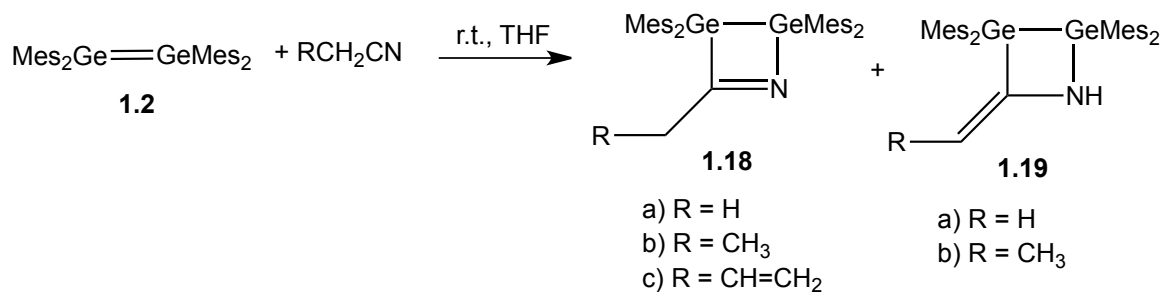
Our group has demonstrated that tetramesityldisilene (**1.4**) and tetramesityldigermene (**1.2**) are reasonable models for the Si and Ge(100)- 2×1 surface, respectively. Ditetrelenes (disilene **1.4** and digermene **1.2**) are similar in structure to the Si and Ge(100)- 2×1 surfaces dimers. The main differences between the molecular and surface species are the geometry about the double bond (planar in the case of the disilene³⁵ and *trans*-bent in the case of the digermene^{6c} versus *cis* bent on the surface) and the nature of the substituents (aryl versus silyl/germyl). We believe that tetramesityldigermene (**1.2**) and tetramesityldisilene (**1.4**) can serve as appropriate molecular models for the corresponding Si and Ge(100)- 2×1 surfaces⁶ and we have shown that the reactivity of silicon and germanium surfaces are comparable to their molecular counterparts. As an example, the addition of nitriles to digermenes and the Ge(100)- 2×1 will be discussed. The addition of acetonitrile to the germanium surface Ge(100)- 2×1 was examined and showed no evidence for a stable adduct on the germanium surface.³⁶ DFT calculations showed that acetonitrile forms a very weak dative bond to the surface before rearranging to either a cycloadduct (by addition through the

CN triple bond) or a ketenimine.³⁶ Acrylonitrile, on the other hand, reacts with the Ge(100)-2 × 1 surface to give two types of stable products. The structures of the cycloadducts on the surface were proposed on the basis of IR data and DFT calculations: ketenimines (cyclic single-dimer adducts **1.15** and/or interdimer adducts **1.16**) and a cycloadduct between the surface dimer and the C=C bond of acrylonitrile **1.17** (Scheme 1.10).^{36,37}



Scheme 1.10

In comparison, addition of acetonitrile, propionitrile and acrylonitrile to the molecular analogue, tetramesityldigermene (**1.2**), yielded the 4-membered ring 1,2,3-azadigermetines **1.18a-c** as the major products accompanied by a trace of the enamine isomer **1.19a-b** (Scheme 1.11).^{6a}



Scheme 1.11

The addition of nitriles to molecular digermenes was found to be reversible as was evident from trapping reactions using dimethylbutadiene (DMB).^{6a}

The addition of acrylonitrile to the Ge(100)- 2×1 surface at room temperature results in the formation of cyclic ketenimines (**1.15** and **1.16**) and a cyano-substituted digermetane (**1.17**), whereas in the molecular system, the formation of only an azadigermetine was observed (**1.18c**); no evidence for ketenimine formation or cycloaddition through the C=C bond of acrylonitrile was obtained. The lack of formation of a six-membered cyclic ketenimine in the molecular system suggests that the surface ketenimine formed upon the addition of acrylonitrile is likely **1.16** and not **1.15**. Furthermore, no [2+2] cycloadduct between the C=C of acrylonitrile and digermene **1.2** was observed, calling into question the assignment of the structure of **1.17**. This example demonstrates that reactivity studies of tetramesityldigermene (**1.2**) can provide useful insights into the reactivity of the surfaces.

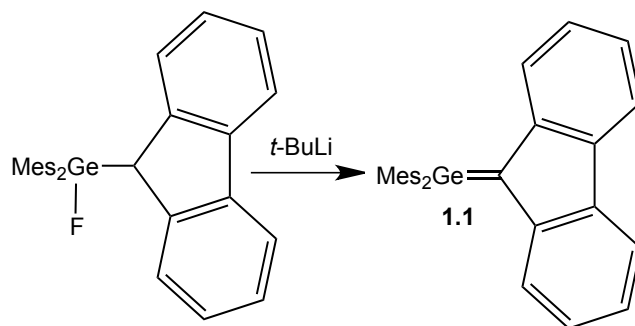
In this thesis, the addition of nitromethane to ditetrelenes will be examined and the chemistry of the disilene will be compared to the analogous Si(100)- 2×1 surface chemistry (Chapter 4). For a broader understanding of the reactivity, the addition of a series of nitro compounds to ditetrelenes will be examined and, again, the chemistry will be compared to the chemistry of the Si(100) and Ge(100)- 2×1 reconstructed surfaces, where appropriate (Chapter 5). The addition of the nitro compounds to ditetrelenes revealed the ability of ditetrelenes to act as reducing agents and this concept is further explored through examination of the addition of sulfonyl compounds and related derivatives to ditetrelenes (Chapter 6). Along the same lines, the addition of a range of isocyanides to ditetrelenes is examined and compared to the analogous chemistry on the

Si(100) and the Ge(100)- 2×1 reconstructed surface (Chapter 7).

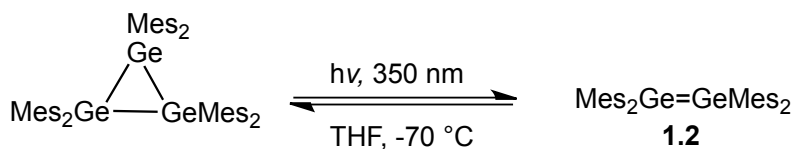
1.9 Preparation of (Di)tetrelenes and Ditetrelyne

This thesis focuses on the reactivity of a variety of multiply-bonded Group 14 compounds: $\text{Mes}_2\text{Ge}=\text{CR}_2$ (where CR_2 =fluorenylidene) (**1.1**), $\text{Mes}_2\text{Ge}=\text{GeMes}_2$ (**1.2**), $\text{Ar}'\text{GeGeAr}'$ (where $\text{Ar}'=2,6$ -(2,6 diisopropylphenyl)phenyl) (**1.3**), and $\text{Mes}_2\text{Si}=\text{SiMes}_2$ (**1.4**). The syntheses of these compounds is described briefly.

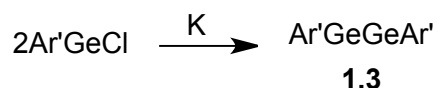
Germene **1.1** was the first isolable, stable germene to be synthesized.³⁸ It is synthesized by the dehydrohalogenation of fluorofluorenyldimesitylgermane using *t*-butyllithium in diethyl ether solution at -78°C (Scheme 1.12).³⁸ To avoid the formation of reduction products, less than one equivalent of *t*-BuLi is utilized.



Tetramesityldigermene **1.2** is formed by irradiation of a THF solution of hexamesitylcyclotrigermene (Scheme 1.13). Digermene **1.2** is not stable in solution for extended periods of time and slowly reverts back to cyclotrigermene.^{6c}

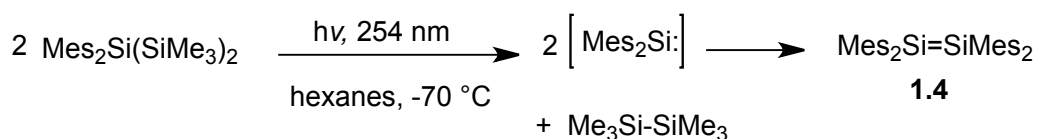


For the studies reported in this thesis, digermyne **1.3** was generously provided by the Power research group (University of California at Davis). It is synthesized by the reduction of Ar'GeCl (Ar'=2,6-(2,6 diisopropylphenyl)phenyl) with potassium in THF (Scheme 1.14).³⁹



Scheme 1.14

Tetramesityldisilene **1.4** is synthesized by the photolysis of 2,2-dimesitylhexamethyltrisilane in hexanes (Scheme 1.15). Dimesitylsilylene is the primary photoproduct of the reaction which, in absence of trapping agent, dimerizes to give the bright yellow disilene **1.4**.⁴⁰



Scheme 1.15

1.10 References

- (a) Power, P.P. *Nature* **2010**, *463*, 171; (b) Melaimi, M.; Soleilhavoup, M.; Bertrand, G. *Angew. Chem. Int. Ed.* **2010**, *49*, 8810; (c) Martin, D.; Soleilhavoup, M.; Bertrand, G.; *Chem. Sci.* **2011**, *2*, 389; (d) Power, P.P. *Acc. Chem. Res.* **2011**, *44*, 627; (e) Yao, S.; Xiong, Y.; Driess, M. *Organometallics* **2011**, *30*, 1748; (f) Power, P.P. *Chem. Rec.* **2012**,

12, 238; (g) Mandal, S. K.; Roesky, H. W. *Acc. Chem. Res.* **2012**, *45*, 298; (h) Yadav, S.; Saha, S.; Sen, S. S. *Chem. Cat. Chem.* **2016**, *8*, 486.

2. Selected examples: (a) Spikes, G. H.; Fettinger, J. C.; Power, P. P. *J. Am. Chem. Soc.* **2005**, *127*, 12232; (b) Li, J.; Schenk, C.; Goedecke, C.; Frenking, G.; Jones, C. *J. Am. Chem. Soc.* **2011**, *133*, 18622; (c) Peng, Y.; Guo, J. D.; Ellis, B. D.; Zhu, Z.; Fettinger, J. C.; Nagase, S.; Power, P. P. *J. Am. Chem. Soc.* **2009**, *131*, 16272; (d) Li, J.; Hermann, M.; Frenking, G.; Jones, C. *Angew. Chem. Int. Ed.* **2012**, *51*, 8611.

3. For example: (a) Hadlington, T. J.; Hermann, M.; Frenking, G.; Jones, C. *J. Am. Chem. Soc.* **2014**, *136*, 3028; (b) Jana, A.; Tavcar, G.; Roesky, H. W.; John, M. *Dalton Trans.* **2010**, *39*, 9487.

4. Ottosson, H.; Steel, P. G. *Chem. Eur. J.* **2006**, *12*, 1576.

5. For example: (a) Pavelka, L. C.; Milnes, K. K.; Baines, K. M. *Chem. Mater.* **2008**, *20*, 5948; (b) Majumdar, M.; Bejan, L.; Huch, V.; White, A. J. P.; Whittell, G. R.; Schäfer, A.; Manners, I.; Scheschkewitz, D. *Chem. Eur. J.* **2014**, *20*, 9225; (c) Bravo-Zhivotovskii, D.; Melamed, S.; Molev, V.; Sigal, N.; Tumanskii, B.; Botoshansky, M.; Molev, G.; Apeloig, Y. *Angew. Chem. Int. Ed.* **2009**, *48*, 1834; (d) Pavelka, L. C.; Holder, S. J.; Baines, K. M. *Chem. Commun.* **2008**, 2346.

6. (a) Hardwick, J. A.; Baines, K. M. *Angew. Chem. Int. Ed.* **2015**, *54*, 6600; (b) Hardwick, J. A.; Pavelka, L. C.; Baines, K. M. *Dalton Trans.* **2012**, *41*, 609; (c) Hurni, K. L.; Baines, K. M. *Chem. Comm.* **2011**, *47*, 8382; (d) Hurni, K. L.; Rupar, P. A.; Payne, N. C.; Baines, K. M. *Organometallics* **2007**, *26*, 5569; (e) Gottschling, S. E.; Milnes, K. K.; Jennings, M. C.; Baines, K. M. *Organometallics* **2005**, *24*, 3811; (f) Gottschling, S. E.;

- Jennings, M. C.; Baines, K. M. *Can. J. Chem.* **2005**, *83*, 1568; (f) Samuel, M. S.; Baines, K. M. *J. Am Chem. Soc.* **2003**, *125*, 12702; (g) Samuel, M. S.; Jenkins, H. A.; Hughes, D.W.; Baines, K. M. *Organometallics* **2003**, *22*, 1603.
7. Brook, A. G.; Abdesaken, F.; Gutekunst, B.; Gutekunst, G.; Kallury, R. K. *J. Chem. Soc. Chem. Commun.* **1981**, 191.
8. General reviews: (a) Lee, V. Y.; Sekiguchi, A. *Organometallic Compounds of Low-Coordinate Si, Ge, S, and Pb, From Phantom Species to Stable Compounds*; John Wiley & Sons, Ltd, Chichester, 2010; Chapter 5; (b) Lee V. Y.; Sekiguchi, A. *Organometallics* **2004**, *23*, 2822.
9. (a) Power, P.P. *Chem. Rev.* **1999**, *99*, 3463; (b) Karni, M.; Apeloig, Y.; Kapp, J. Schleyer, P. *The Chemistry of Organic Silicon Compounds*; Rappoport, Z.; Apeloig, Y., Eds.; John Wiley & Sons: New York, 2001; Chichester, Vol. 3 Chapter 1; (c) Klinkammer, K. W. *The Chemistry of Organic Germanium, Tin and Lead Compounds*; Rappoport, Z., Eds.; John Wiley & Sons, Ltd, 2002; Chichester, Vol. 2, Part 1, Chapter 4.
10. Kovács A.; Esterhuysen, C.; Frenking, G. *Chem. Eur. J.* **2005**, *11*, 1813.
11. For reviews on triple bond chemistry of heavier group 14 elements: (a) Robinson, G. H. *Acc. Chem. Res.* **1999**, *32*, 773; (b) Jutzi, P. *Angew. Chem. Int. Ed.* **2000**, *39*, 3797; (d) Weidenbruch, M. *J. Organomet. Chem.* **2002**, *39*, 646; (c) Power, P. P. *Chem. Commun.* **2003**, 2091; (d) Weidenbruch, M. *Angew. Chem. Int. Ed.* **2004**, *43*, 2; (g) Power, P. P. *Appl. Organomet. Chem.* **2005**, *19*, 488; (e) Rivard, E.; Power, P. *Inorg. Chem.* **2007**, *46*, 10047.
12. Kobayashi, K.; Nagase, S. *Organometallics* **1997**, *16*, 2489.

13. Cui, C.; Olmstead, M. M.; Fettinger, J. C.; Spikes, G. H.; Power, P. P. *J. Am. Chem. Soc.* **2005**, *127*, 17530.
14. Stender, M.; Phillips, A. D.; Wright, R. J.; Power, P. P. *Angew. Chem. Int. Ed.* **2002**, *41*, 1785.
15. Sekiguchi, A.; Kinjo, R.; Ichinohe, M. *Science* **2004**, *305*, 1755.
16. For recent accounts on various aspects of silene chemistry: (a) Ottosson H.; Rouf, A. M. *Science of Synthesis: Knowledge Updates*; 2011/3, Oestreich, M., Eds.; Thieme, Stuttgart, 2011; Chapters 4.4.25; (b) Baines, K. M. *Chem. Comm.* **2013**, *49*, 6366; (c) Ottosson H.; Eklof, A. M. *Coord. Chem. Rev.* **2008**, *252*, 1287; (d) Ottosson H.; Steel, P. G. *Chem. Eur. J.* **2006**, *12*, 1576; (e) Gusel'nikov, L. E. *Coord. Chem. Rev.* **2003**, *244*, 149; (f) Escudié, J.; Couret C.; Ranaivonjatovo, H. *Coord. Chem. Rev.* **1998**, *565*, 178.
17. For recent accounts on various aspects of disilene chemistry: (a) Iwamoto, T.; Ishida, S. *Struct. Bonding* **2014**, *156*, 125; (b) Sasamori, T.; Tokitoh, N. *Bull. Chem. Soc. Jpn.* **2013**, *86*, 1005; (c) Kira, M. *Proc. Jpn. Acad., Ser. B* **2012**, *88*, 167; (d) Matsuo, T. Kobayashi M.; Tamao, K. *Dalton Trans.* **2010**, *39*, 9203; (e) Abersfelder, K.; Scheschkewitz, D. *Pure Appl. Chem.* **2010**, *82*, 595; (f) Scheschkewitz, D. *Chem. Eur. J.* **2009**, *15*, 2476; (g) Kira, M. *J. Organomet. Chem.* **2004**, *689*, 4475; (h) Weidenbruch, M. *Organometallics* **2003**, *22*, 4348.
18. For recent accounts of the chemistry of germenenes and digermenenes see: (a) Plyusnin, V. F.; Kaletina M. V.; Leshina, T. V. *Russ. Chem. Rev.* **2007**, *76*, 931; (b) Takeda, N.; Tokitoh N.; Okazaki, R. *Science of Synthesis*; Moloney, M. G., Eds.; Thieme, Stuttgart, 2003; Chapters 5.1.2.
19. Power, P.P. *Organometallics* **2007**, *26*, 4362.

20. (a) Morkin T. L.; Leigh, W. J. *Acc. Chem. Res.* **2001**, *34*, 129; (b) Morkin, T. L.; Owens, T. R.; Leigh, W. J. *The Chemistry of Organic Silicon Compounds*; Rappoport, Z.; Apeloig, Y., Eds.; Wiley and Sons: New York, 2001; Vol. 3, Chapter 17; (c) Leigh, W. J. *Pure Appl. Chem.* **1999**, *71*, 453; (d) Sakurai, H. *The Chemistry of Organic Silicon Compounds*; Rappoport Z.; Apeloig, Y., Eds.; Wiley and Sons Ltd, New York, 1998; Chapter 15.
21. Milnes, K. K.; Pavelka, L. C.; Baines, K. M. *Chem. Soc. Rev.* **2015**, *45*, 1019.
22. (a) Newcomb, M.; Toy, P. H. *Acc. Chem. Res.* **2000**, *33*, 449; (b) Le Tadic-Biadatti, M. H.; Newcomb, M. *J. Chem. Soc., Perkin Trans.2* **1996**, 1467; (c) Newcomb, M.; Chestney, D. L. *J. Am. Chem. Soc.* **1994**, *116*, 9753; (d) Newcomb, M.; Johnson, C. C.; Manek, M. B.; Varick, T. R. *J. Am. Chem. Soc.* **1992**, *114*, 10915; (e) Newcomb, M.; Manek, M. B. *J. Am. Chem. Soc.* **1990**, *112*, 9662.
23. Gottschling, S. E.; Jennings, M. C.; Baines, K. M. *Can. J. Chem.* **2005**, *83*, 1568.
24. (a) Milnes, K. K.; Gottschling, S. E.; Baines, K. M. *Org. Biomol. Chem.* **2004**, *2*, 3530; (b) Milnes, K. K.; Baines, K. M. *Can. J. Chem.* **2009**, *87*, 307.
25. Milnes, K. K.; Pavelka L. C.; Baines, K. M. *Organometallics* **2010**, *29*, 5972.
26. Kinjo, R.; Ichinohe, M.; Sekiguchi, A.; Takagi, N.; Sumimoto, M.; Nagase, S. *J. Am. Chem. Soc.* **2007**, *129*, 7766.
27. Han, J. S.; Sasamori, T.; Mizuhata Y.; Tokitoh, N. *Dalton Trans.* **2010**, *39*, 9238.
28. Cui, C.; Olmstead M. M.; Power, P. P. *J. Am. Chem. Soc.* **2004**, *126*, 5062.
29. Hadlington, T. J.; Li, J.; Hermann, M.; Davey, A.; Frenking G.; Jones, C. *Organometallics* **2015**, *34*, 3175.
30. Zhao, L.; Jones C.; Frenking, G. *Chem. Eur. J.* **2015**, *21*, 12405.

31. Sasamori, T.; Sugahara, T.; Agou, T.; Guo, J. D.; Nagase, S.; Streubel R.; Tokitoh, N. *Organometallics* **2015**, *34*, 2106.
32. For recent reviews, see: (a) Kachian, J. S.; Wong, K. T.; Bent, S. F. *Acc. Chem. Res.* **2010**, *43*, 346; (b) Hamers, R. J. *Annu. Rev. Anal. Chem.* **2008**, *1*, 707; (c) Loscutoff, P. W.; Bent, S. F. *Annu. Rev. Phys. Chem.* **2006**, *57*, 467; (d) Lu, X.; Lin, M. C. *Int. Rev. Phys. Chem.* **2002**, *21*, 137; (e) Bent, S. F. *J. Phys. Chem. B* **2002**, *106*, 2830; (f) Bent, S. F. *Surf. Sci.* **2002**, *500*, 879; (g) Buriak, J. M. *Chem. Rev.* **2002**, *102*, 1271; (h) Hamers, R. J.; Coulter, S. K.; Ellison, M. D.; Hovis, J. S.; Padowitz, D. F.; Schwartz, M. P.; Greenlief, C. M.; Russell, J. N., Jr. *Acc. Chem. Res.* **2000**, *33*, 617; (j) Wolkow, R. A. *Annu. Rev. Phys. Chem.* **1999**, *50*, 413; (h) Hamers, R. J.; Wang, Y. *Chem. Rev.* **1996**, *96*, 1261; (i) Duke, C. B. *Chem. Rev.* **1996**, *96*, 1237.
33. Tao, F.; Bernasek, S. *Functionalization of Semiconductor Surfaces*; Wiley: Hoboken, N. J., Eds.; 2012.
34. Bent, S. F. *Surface Science* **2002**, *500*, 879.
35. Fink, M. J.; Michalczyk, M. J.; Haller, K. J.; West, R. Michl, J. *J. Chem. Soc., Chem. Commun.* **1983**, 1010.
36. Mui, C.; Filler, M. A.; Bent, S. F.; Musgrave, C. B. *J. Phys. Chem. B* **2003**, *107*, 12256.
37. Filler, M. A.; Mui, C.; Musgrave, C. B.; Bent, S. F. *J. Am. Chem. Soc.* **2003**, *125*, 4928.
38. Couret, C.; Stage, J.; Escudié, J.; Lazraq, M. *J. Am. Chem. Soc.* **1987**, *27*, 828.

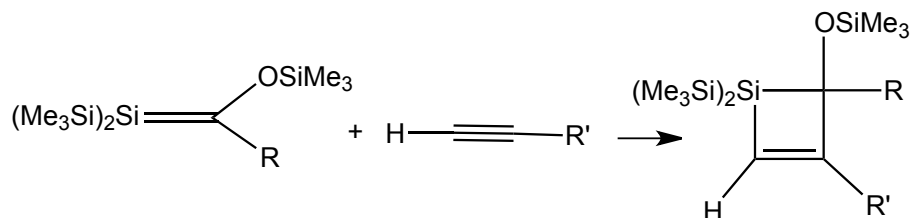
39. Pu, L. H.; Philips, A. D.; Richards, A. F.; Stender, M.; Simon, R. S.; Olmstead, M., M.; Power, P.P. *J. Am. Chem. Soc.* **2003**, *125*, 11626.
40. Fink, M. J.; Michalczyk, M. J.; Haller, K. J.; Michl, J.; West, R. *Organometallics* **1984**, *3*, 793.

Chapter 2

The Addition of Terminal Alkynes to Dimesitylfluorenylidengermane*

2.1 Introduction

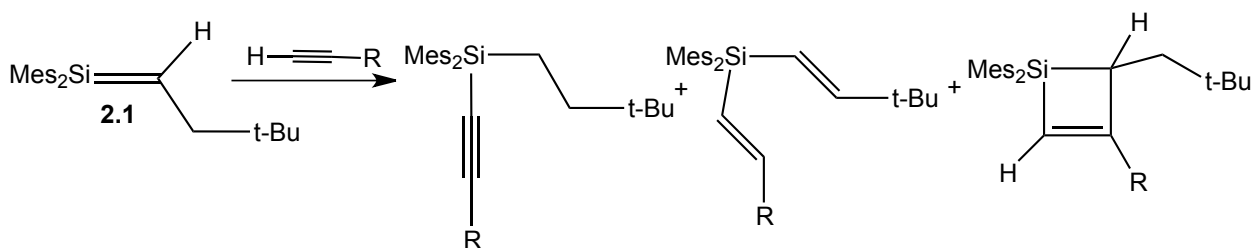
Cycloaddition reactions of Group 14 tetrelenes have been attracting the interest of chemists for more than 35 years due to the high levels of regio- and stereospecificity.¹ The addition of alkynes to Brook silenes $(\text{Me}_3\text{Si})_2\text{Si}=\text{C}(\text{R})(\text{OSiMe}_3)$ is a classic example; the reaction produces silacyclobutenes rapidly and quantitatively (Scheme 2.1).² Through the use of a phenyl cyclopropyl-substituted alkyne mechanistic probe,³ the cycloaddition of alkynes to Brook silenes was determined to proceed via a biradical intermediate.⁴



Scheme 2.1

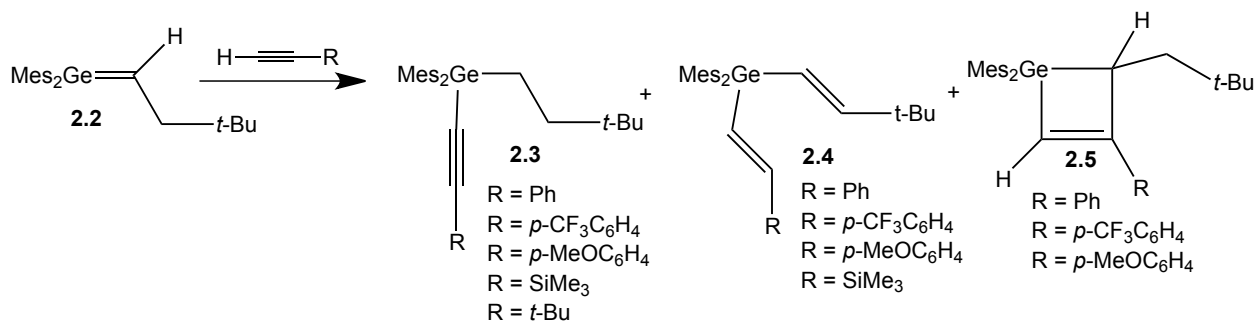
In contrast, when a variety of terminal alkynes were added to the neopentylsilene **2.1**, a preference for the formation of a C-H insertion product over the formation of formal ene- and/ or [2+2] cycloadduct(s) was observed (Scheme 2.2).⁵

*A version of sections 2.2 and 2.3 of this chapter have been published. Nada Y. Tashkandi, Laura C. Pavelka, Margaret A. Hanson, Kim M. Baines. The Addition of Terminal Alkynes to Dimesitylfluorenylidengermane. *Can. J. Chem.* **2014**, 92, 462.



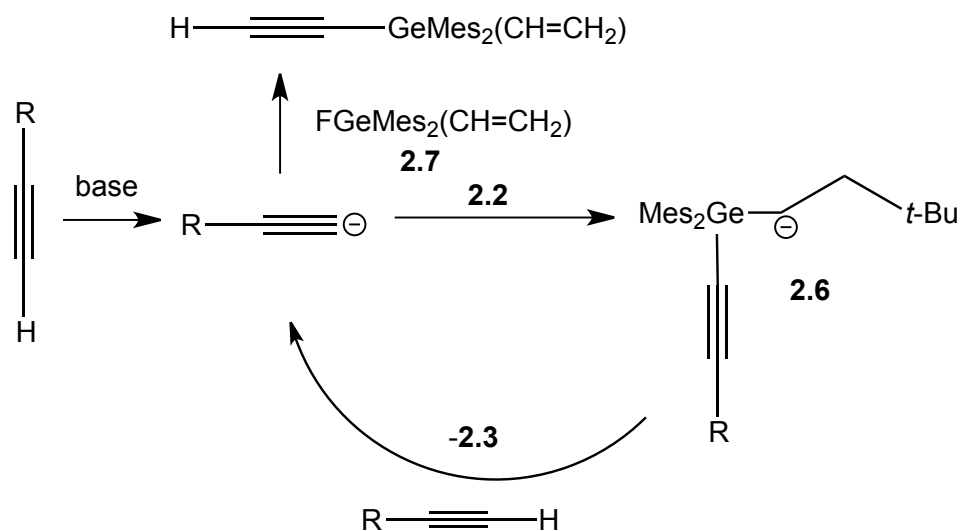
Scheme 2.2

A comparison between the reactivity of neopentylsilene **2.1** with that of neopentylgermene **2.2** towards alkynes revealed similar activity. Like silenes, three different modes of reactivity were observed for germenes: insertion of the acetylenic C-H bond to give germylacetylenes **2.3**, ene-addition to give vinylgermanes **2.4**, and cycloaddition to give germacyclobutenes **2.5** (Scheme 2.3).⁶



Scheme 2.3

A biradical pathway was proposed to account for the formation of the cycloadducts with aromatic alkynes based on the effect of the substituents on the rate of the reaction.⁶ A chain reaction mechanism was proposed to explain the rapid formation of germylacetylenes **2.3**. The initiator of the reaction is believed to be a trace amount of a strong base such as fluoride or the anion, Mes₂Ge(F)CHCH₂*t*-Bu, creating the acetylide anion which then adds to germene **2.2** producing an α -germyl carbanion **2.6**. The carbanion can deprotonate another equivalent of alkyne, reforming an acetylide anion, and the cycle can continue until it is quenched, presumably by residual Mes₂GeF(CH=CH₂) (**2.7**) (Scheme 2.4).⁶



Scheme 2.4

The presence of the α -hydrogen in germyne **2.2** facilitates the formation of the ene-adduct **2.4**, while the basicity of the anion generated from **2.2** (**2.6**) leads to the CH-insertion product, **2.3**. In contrast dimesitylfluorenylidengermyne, **1.1**, lacks an α -hydrogen, which should eliminate the formation of ene-type adducts. Moreover, the amount of C-H insertion product may be reduced since the corresponding anion is less basic than anion **2.6**. Thus, we examined the addition of terminal alkynes to dimesitylfluorenylidengermyne, **1.1**, with the expectation that the reaction will not be as complex as those of germyne **2.2**.

Mechanistic studies of tetrelenes are challenging: the reactivity of tetrelenes towards air and moisture as well as many common functional groups limits the variability of substituents and solvents that can be utilized. Our group has employed cyclopropyl-based hypersensitive mechanistic probes as a means to understand the reactivity of tetrelenes and their reaction pathways. *Trans*-(2-phenylcyclopropyl)acetylene³ can be used as a probe to detect the formation of a reactive vinylic intermediate. During the cycloaddition of the alkyne moiety, rapid and regioselective cyclopropyl ring opening can occur upon the formation of a vinylic biradical or

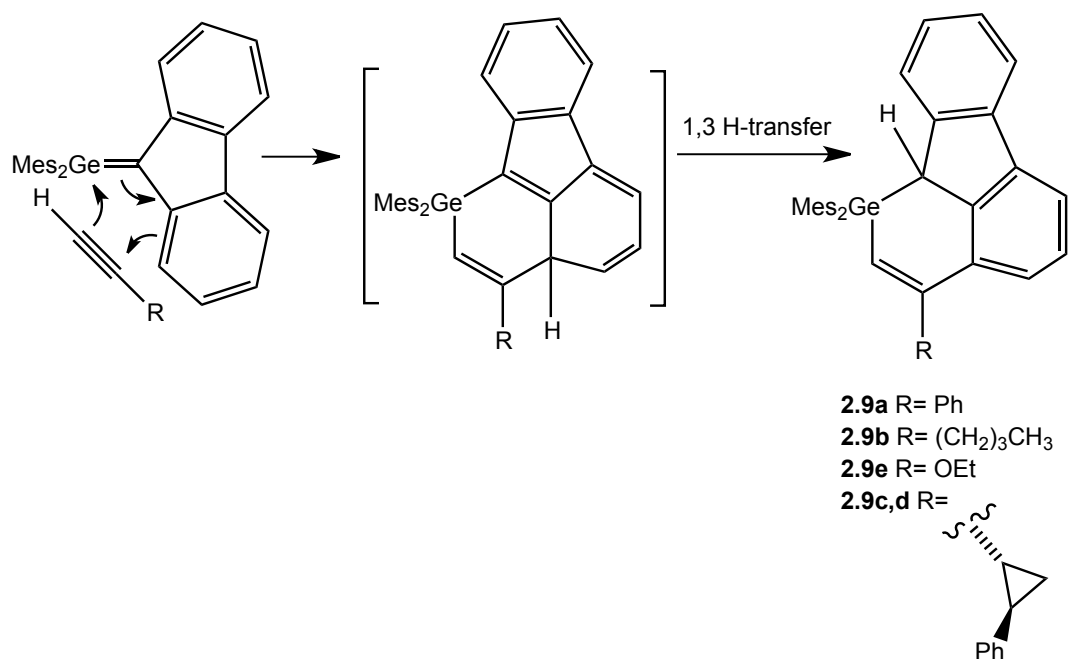
cationic intermediate. In contrast, no rearrangement of the probe will occur during a concerted addition. Thus, the isolation of ring-opened adducts of alkyne probe provides strong evidence for the formation of an intermediate. In an attempt to elucidate the mechanism of the addition of alkynes to germenes, we have also examined the addition of *trans*-(2-phenylcyclopropyl)acetylene to germene **1.1**.

2.2 Results

2.2.1 Addition of Terminal Alkynes to Dimesitylfluorenylidengermane

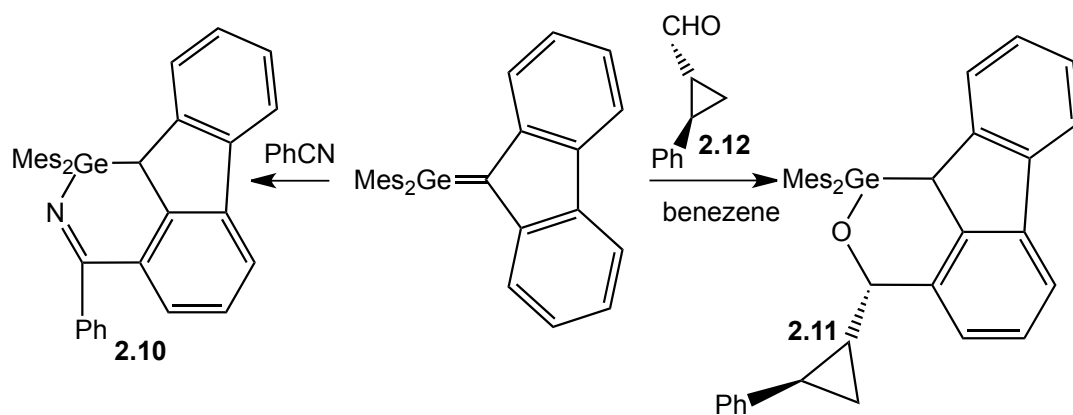
Germene **1.1** was synthesized prior to each reaction and used *in situ* without purification. A pale yellow ethereal solution of fluorenylfluorodimesitylgermane **2.8** was cooled in a Dry Ice/acetone bath and then treated with *t*-BuLi. To avoid the formation of reduction products, less than one equivalent of *t*-BuLi was utilized, and thus, germene **1.1** was always contaminated with residual fluorogermane **2.8**. After warming the solution to room temperature, the colour of the solution changed from pale yellow to bright orange.⁷ The orange solution of germene **1.1** is extremely air- and moisture-sensitive; the colour of the solution changes dramatically from bright orange to olive-green upon exposure to traces of moisture or oxygen. The presence of germene **1.1** was confirmed by ¹H NMR spectroscopy before subsequent reactions. The germene was then dissolved in C₆D₆, diethyl ether or THF, and excess alkyne was added. The reaction was kept at room temperature and monitored by ¹H NMR spectroscopy for up to 3 days. Germacyclohexene **2.9** was the only product formed from the reaction of germene **1.1** with phenylacetylene, 1-hexyne or *trans*-(2-phenylcyclopropyl)acetylene (Scheme 2.5). The reactions of germene **1.1** with phenylacetylene or *trans*-(2-phenylcyclopropyl)acetylene were faster than that with 1-hexyne; the addition of phenylacetylene or *trans*-(2-phenylcyclopropyl)acetylene to **1.1** was complete within

minutes, whereas the addition of 1-hexyne required approximately 24-72 hours to go to completion. The products were isolated by preparative silica gel chromatography to give a yellow oil in each case and were identified by ^1H , ^{13}C , ^1H - ^1H COSY, ^{13}C - ^1H gHSQC and ^{13}C - ^1H gHMBC NMR and FTIR spectroscopy, EI-mass spectrometry and, in some cases, X-ray crystallography. Due to similarities between the spectroscopic data of **2.9a**, **2.9b** and **2.9c,d**, only the data of **2.9a** will be discussed.



Scheme 2.5

The high resolution mass spectral data of **2.9a** and the isotopic pattern of the signal assigned to the molecular ion were consistent with the molecular formula, $\text{GeC}_{39}\text{H}_{36}$. The ^1H NMR spectral data of germacyclohexene **2.9a** were similar to those reported for the germaisoquinoline **2.10** formed upon the addition of benzonitrile to germene **1.1**⁸ and oxagermin **2.11** produced in the addition of aldehyde **2.12** to germene **1.1** (Scheme 2.6).⁹



Scheme 2.6

Broad singlets were observed at 1.64 and 2.32 ppm in the ^1H NMR spectrum of **2.9a** and were assigned to two *ortho*-methyl groups of non-equivalent mesityl substituents. A singlet at 4.65 ppm was observed and assigned to the Ge-C_(saturated)H in the germacyclohexene ring. The chemical shift of this signal was in reasonable agreement with the chemical shifts of the analogous signals assigned to the Ge-CH in germaisoquinoline **2.10** (4.55 ppm)⁸ and oxagermin **2.11** (4.62 ppm).⁹ Integration of the signals assigned to the fluorenyl moiety did not correspond to the eight hydrogens present in the starting material; there was one hydrogen less than expected. The signal at 7.03 ppm in the ^1H NMR spectrum of **2.9a** was assigned to the vinylic hydrogen of the germacyclohexene ring. This signal correlated to the signal assigned to the *ipso*-carbon of the phenyl substituent in the ^{13}C - ^1H gHMBC spectrum of **2.9a**. All data are in agreement with the proposed structure of germacyclohexene **2.9a**.

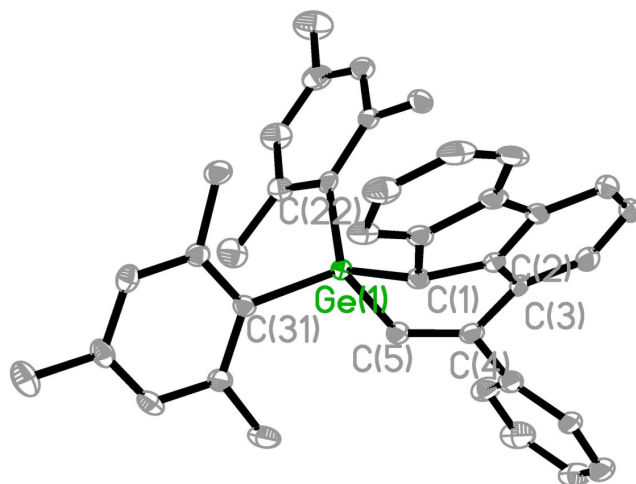


Figure 2.1 Thermal ellipsoid plot of **2.9a** (30% probability surface). Selected bond lengths (Å) and angles (deg): Ge1-C1 = 1.994(3); Ge1-C5 = 1.963(3); Ge1-C31 = 1.971(3); Ge1-C22 = 1.984(3); C1-C2 = 1.490(5); C2-C3 = 1.380(5); C3-C4 = 1.499(5); C4-C5 = 1.336(5). C5-Ge1-C1 = 92.85(15); C2-C1-Ge1 = 107.5(2), C3-C2-C1 = 127.2(3); C2-C3-C4 = 120.5(3); C5-C4-C3 = 122.2(3); C4-C5-Ge1 = 122.0(3).

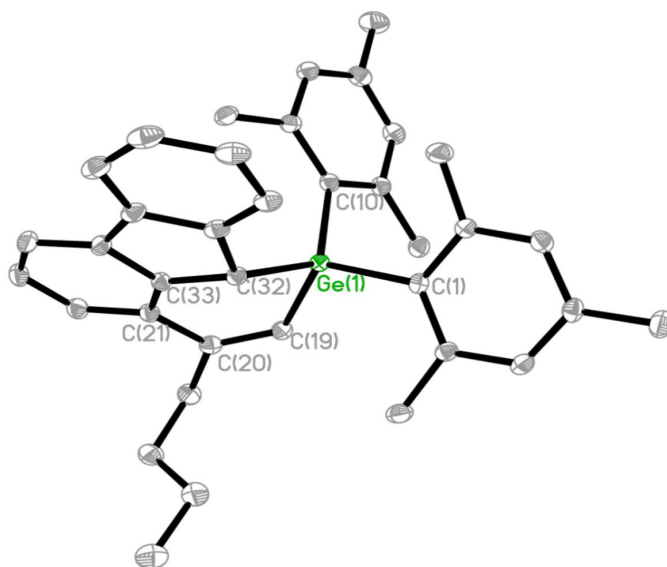


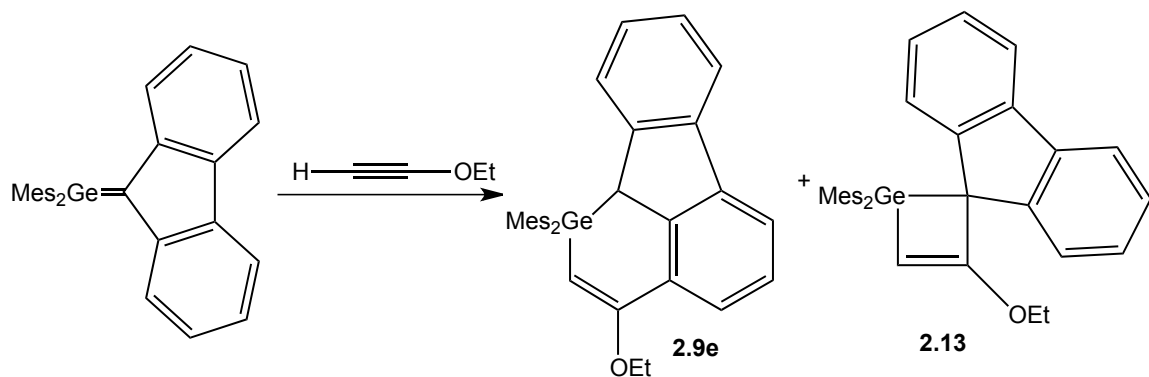
Figure 2.2 Thermal ellipsoid plot of **2.9b** (30% probability surface). Selected bond lengths (Å) and angles (deg): Ge1-C19 = 1.924(2); Ge1-C32 = 1.961(2); Ge1-C1 = 1.961(2); Ge1-C10 = 1.964(2); C32-C33 = 1.490(3); C33-C21 = 1.378(3); C20-C21 = 1.467(3); C19-C20 = 1.334(3). C20-C19-Ge1 = 123.75(18); C19-C20-C21 = 122.8(2); C33-C21-C20 = 121.3(2); C19-Ge1-C32 = 94.40(10); C33-C32-Ge1 = 109.67(15); C21-C33-C32 = 127.6(2).

2.2.2 Addition of Alkyne Probe to Dimesitylfluorenylidengermane

Addition of *trans*-(2-phenylcyclopropyl)acetylene to germene **1.1** yielded two diastereomers **2.9c,d** in a ratio of 1:1, the coupling constants extracted from the multiplets of the two cyclopropyl spin systems showed maintenance of the original *trans* relationship between the cyclopropyl substituents (Scheme 2.5). The regiochemistry of compounds **2.9a,b** was confirmed by the X-ray diffraction (Figures 2.1 and 2.2, respectively), whereas the regiochemistry of **2.9c,d** was assigned based on the known regiochemistry of **2.9a,b**. The germacyclohexene ring is puckered in a half chair conformation (Figures 2.1 and 2.2). All bond lengths and angles are within normal ranges. In contrast, no reaction was observed upon the addition of *t*-butylacetylene and trimethylsilylacetylene to germene **1.1**, even with gentle heating for two days.

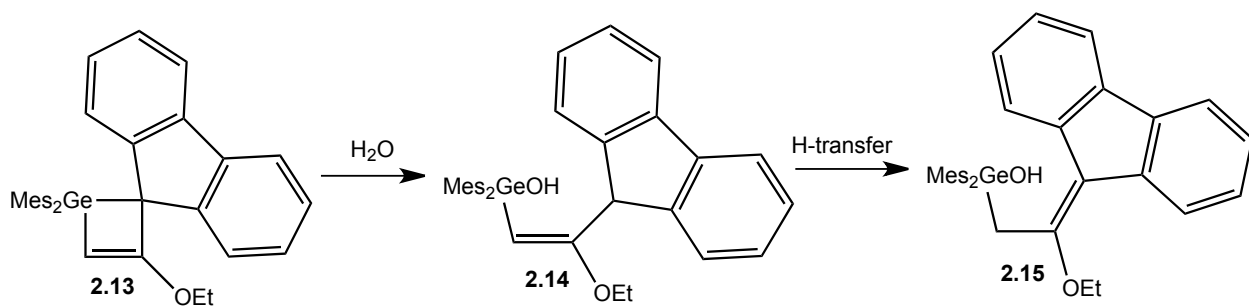
2.2.3 Addition of Ethoxyacetylene to Dimesitylfluorenylidengermane

The addition of ethoxyacetylene to germene **1.1** showed different reactivity. In this case, both the six-membered ring germacyclohexene **2.9e**, and the four-membered ring, germacyclobutene **2.13**, are formed in the reaction (Scheme 2.7). The ratio of **2.9e** to **2.13** was 1:1 when the reaction was performed in Et₂O. This ratio changed to 1:3, when THF was employed as the solvent of the reaction. Germacyclohexene **2.9e** and germacyclobutene **2.13** were the only products of the reaction and they were identified as part of the crude product mixture by ¹H NMR spectroscopy due to their sensitivity to moisture.



Scheme 2.7

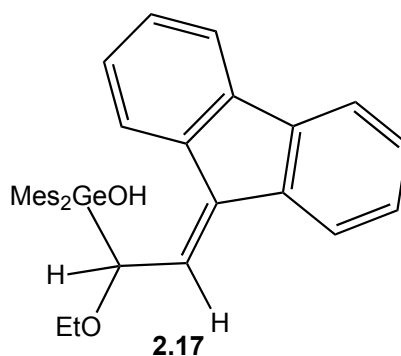
Germacyclobutene **2.13** hydrolyzed rapidly upon exposure to air, yielding germanol **2.14**, which then isomerizes to **2.15** upon adsorption to silica (Scheme 2.8). Germacyclohexene **2.9e** also hydrolyzed, presumably through the hemiacetal, to yield germacyclohexanone **2.16** at slower rate (Scheme 2.10). The regiochemistry of the addition of ethoxyacetylene to germene **1.1** was inferred from the structures elucidated for **2.15** and **2.16**.



Scheme 2.8

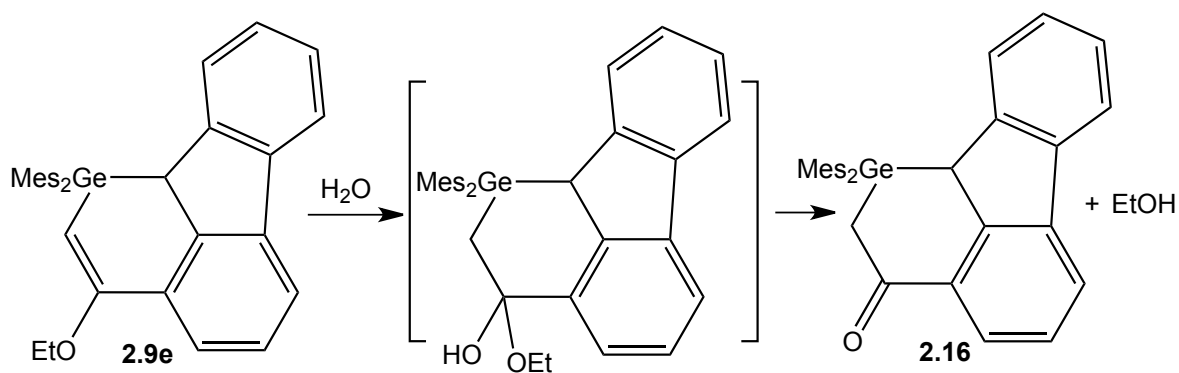
The highest mass signal in the mass spectra of **2.14** and **2.15** was observed at m/z 564.2078 and 564.2106, respectively, corresponding to a 1:1 adduct between ethoxyacetylene and germene **1.1** and one molecule of H_2O for each isomer. The 1H NMR spectrum of **2.14** revealed a singlet at 4.54 ppm which was assigned to the sp^3 C-H in the fluorenyl moiety; the absence of coupling is consistent with the regiochemistry assigned. A strong absorption at 3444 cm^{-1} in the

IR spectrum of **2.15** was assigned to the hydroxyl group. The key to assigning the regiochemistry in **2.15** lies in the identification of the linker between the Mes₂GeOH- and the fluorenyl moiety. Two signals were observed in the ¹³C NMR spectrum of **2.15** at 159.30 and 119.73 ppm, characteristic of a vinyl ether moiety. Neither of these signals correlated to a signal in the ¹H NMR spectrum of **2.15** as was evident in the ¹³C-¹H gHSQC spectrum of **2.15**. Furthermore, there were no signals in the ¹H NMR spectrum of **2.15** between 4 and 6 ppm indicating the absence of a vinylic-type hydrogen. A correlation was observed in the ¹H-¹³C gHMBC spectrum of **2.15** between the signals at 159.30 and 119.73 ppm in the ¹³C NMR spectrum and the signal at 3.32 ppm in the ¹H NMR spectrum of **2.15** which was assigned to the CH₂Ge moiety. Moreover, the signal at 3.32 ppm is a singlet and integrates for two hydrogens. If ethoxyacetylene had added to germene **1.1** with the opposite regiochemistry followed by hydrolysis (that is, to produce **2.17**, see Scheme 2.9), the corresponding signal would integrate for a single hydrogen and exhibit coupling to the vinylic hydrogen. Furthermore, if **2.17** were indeed the structure, the characteristic signals for the vinyl ether moiety would be absent. All data observed are completely consistent with the regiochemistry elucidated for **2.15**.



Scheme 2.9

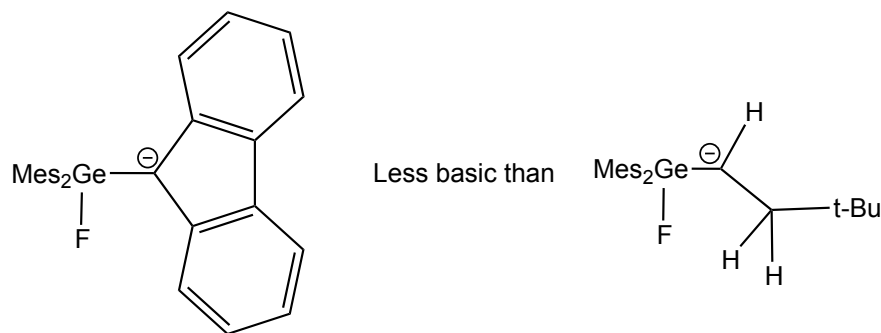
The highest mass signal in the mass spectrum of **2.16** was observed at m/z 518.1668, which is consistent with the mass of a 1:1 adduct between ethoxyacetylene and germene **1.1**, with the addition of H₂O and the loss of an ethoxy group (Scheme 2.10). The presence of a carbonyl group was evident from the signal at 196.30 ppm in the ¹³C NMR spectrum of **2.16**. The chemical shift of this signal is consistent with that reported for a typical β-germyl ketone (194.2 ppm).¹⁰ The IR spectrum of **2.16** exhibits a strong absorption at 1664 cm⁻¹. The C=O moieties of related β-keto germanes absorb at approximately 1660 cm⁻¹ (for example, Ph₃GeCH₂COPh at 1661 cm⁻¹) whereas the corresponding carbonyl moiety in α-keto germanes absorb at lower wavenumbers (for example, 1629 cm⁻¹ for Ph₃GeCOPh).¹¹ The position of the IR absorption of **2.16** supports the carbonyl group being in the β-position to Ge. The signal(s) assigned to the inequivalent CH₂ hydrogens, at 3.11 and 3.39 ppm, correlate to the signal at 196.30 ppm in the ¹³C NMR spectrum of **2.16** assigned to the carbonyl group, to the signal assigned to one of the *ipso*-mesityl carbons, to the signal assigned to the GeCH at 45.43 ppm, and to the unsaturated carbon on the opposite side of the carbonyl at 133.07 ppm. Given that the ¹³C-¹H gHMBC spectroscopy experiment is optimized for 3-bond correlations (8 Hz), the regiochemistry assigned is most consistent with the observed correlations. All these data unambiguously confirm the regiochemistry of germacyclohexanone **2.16**. Germacyclohexanone **2.16** was also synthesized by deliberate treatment of the product mixture containing **2.9e** with aqueous NH₄Cl in THF. Germacyclohexanone **2.16** is unstable and decomposes to unidentified products upon prolonged exposure to the ambient atmosphere.



Scheme 2.10

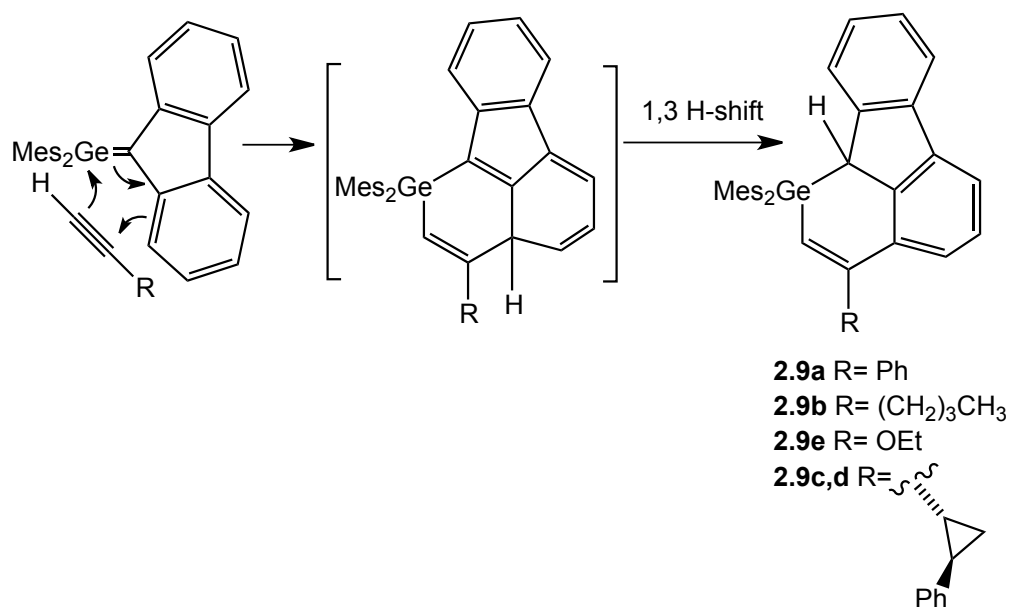
2.3 Discussion

The addition of alkyl and aromatic terminal alkynes to germene **1.1** is clean and quantitative and produces germacyclohexenes **2.9a-d**. As anticipated, there was no evidence for the formation of an ene adduct which was attributed to the lack of an α -hydrogen in germene **1.1**. A product derived from insertion of the C-H of the terminal alkyne across the Ge=C of **1.1** was also not observed in any of the reactions. The absence of a C-H insertion product is attributed to the low basicity of the α -germyl anion derived from germene **1.1** (Scheme 2.11). The lack of a C-H insertion product supports the proposed chain mechanism for the formation of the C-H insertion adduct in the addition of terminal alkynes to germene **2.2**.⁵



Scheme 2.11

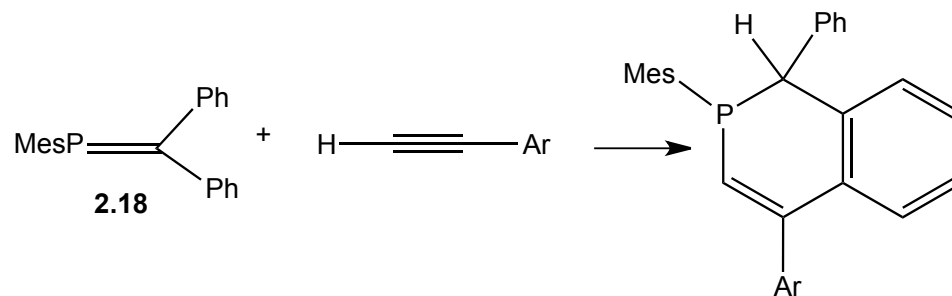
The addition of *trans*-(2-phenylcyclopropyl)acetylene to germene **1.1** resulted in the formation of germacyclohexenes **2.9c,d** with the cyclopropyl ring still intact, which rules out the presence of a cyclopropyl vinyl radical or cationic intermediate along the reaction pathway. Thus, the mechanism of the addition of alkynes to germene **1.1** is proposed to proceed via a concerted [2+4] cycloaddition where germene **1.1** acts as the diene (4π component) and the alkyne acts as the dienophile (2π component), followed by hydrogen transfer to give the corresponding germacyclohexene (Scheme 2.12). The stereochemistry of the cyclopropyl ring in **2.9c,d** remains *trans*; it does not scramble which rules out the cyclopropyl ring opening and closing during the reaction. Analogous products were also observed in the addition of cyclopropylaldehyde **2.12** to germene **1.1**, to yield oxagermin **2.11** with the cyclopropyl ring still intact.⁹



Scheme 2.12

For a [2+4] cycloaddition reaction to take place, the diene must be in a cisoid conformation; the fluorenylidene substituent forces the coplanar cisoid conformation needed for the cycloaddition. A similar cycloaddition was observed in the addition of alkynes to P-

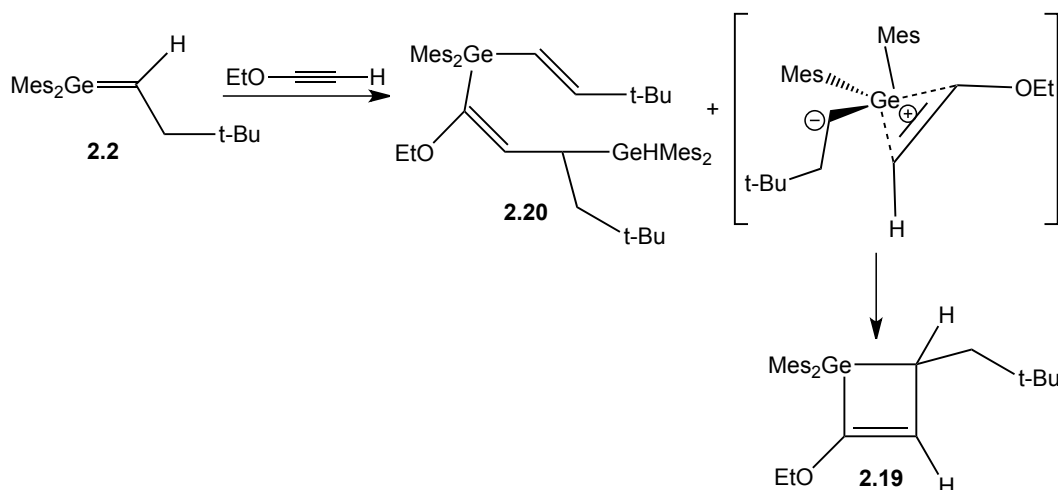
mesityldiphenylmethylenephosphine **2.18** (Scheme 2.13) even with the phenyl group not being held in a planar conformation.¹²



Scheme 2.13

t-Butylacetylene and trimethylsilylacetylene did not react with germene **1.1**, even after gentle heating for two days. Similarly, no cycloadduct was reported upon the addition of those alkynes to neopentylsilene **2.1**⁵ or neopentylgermene **2.2**.⁶ The lack of reaction was attributed to the steric bulk of the substituents.

Previous work in our group showed that the addition of ethoxyacetylene to germene **2.2** resulted in the formation of germacyclobutene **2.19** and vinylgermane **2.20**, which have the opposite regiochemistry compared to germacyclohexene **2.9a-e**. Complexation between the alkyne and germene **2.2** was suggested to account for the unusual regiochemistry (Scheme 2.14).⁶



Scheme 2.14

The regiochemistry observed in the addition of ethoxyacetylene to germene **1.1** is consistent with regiochemistry observed in the addition of phenylacetylene, 1-hexyne and *trans*-(2-phenylcyclopropyl)acetylene forming **2.9a-d**. The regiochemistry in **2.9a-e** and **2.14** is also consistent with the regiochemistry observed in the addition of alkynes to Brook silenes (Scheme **2.1**)² and the addition of aromatic alkynes to germene **2.2** (Scheme 2.2).⁶

To gain more insight into the addition of alkynes to germenes, DFT calculations were performed at the TPSS/6-31G(d) level of theory. Dimethylfluorenylidengermane **1.1** was modeled by (1,1-dimethyl)germabutadiene or 1,1-dimethylgermastylene; acetylene was used to model 1-hexyne. All geometries were optimized at the same level. As was observed for (adamantyl)C=Ge(SiMe₃)(SiMe₂tBu),¹³ the HOMO-LUMO energy gap of 1-germabutadiene (257 kJ/mol) was much less than in butadiene (399 kJ/mol).

The largest orbital coefficient in the LUMO of 1,1-dimethylgermabutadiene is located on the germanium atom (0.7633) and contributes 58% to the molecular orbital. In ethoxyacetylene, the largest orbital coefficient in the HOMO is located on the carbon bearing the hydrogen

(0.7206, 52%) rather than the carbon bearing the ethoxy group (0.6933, 48%), which is consistent with the observed regiochemistry. In acetylene and phenylacetylene, the orbital coefficient on each carbon is equal. Since no difference in the frontier molecular orbital coefficients was observed in these cases, the observed regiochemistry is likely governed by minimization of steric interactions.

Two possibilities for the reaction pathway were considered: the HOMO of the conjugated germene interacting with the LUMO of the alkyne, known as a normal demand Diels-Alder reaction, or the LUMO of the conjugated germene interacting with the HOMO of the alkyne, known as an inverse demand Diels Alder reaction. Our DFT calculations suggests that in the case of phenylacetylene, the difference between the energy levels is the same. However, when ethoxyacetylene or acetylene was employed, the LUMO of the germene and the HOMO of the alkyne are closer in energy than the reverse. Thus, we believe these reactions are best classified as inverse demand Diels Alder reactions. In general, inverse demand Diels-Alder reactions are favoured when a dienophile with electron-donating substituents reacts with a diene. The electron-donating groups on the dienophile raise the energy of the HOMO, and thus, contribute towards a decrease in the HOMO-LUMO gap between the diene and dienophile, and thus, accelerate the rate of the reaction. Phenylacetylene, *trans*-(2-phenylcyclopropyl)acetylene and ethoxyacetylene are conjugated alkynes with electron-donating groups. Accordingly, the addition of all of these alkynes to germene **1.1** took only few minutes to go to completion, whereas the addition of 1-hexyne to germene **1.1** took several days. Correspondingly, the HOMO-LUMO gap between 1,1-dimethylgermastyrene and acetylene (440 kJ/mol) decreases significantly to 303 kJ/mole when the alkyne is changed to ethoxyacetylene and to 328 kJ/mol when it is changed to phenylacetylene (Figure 2.3) in agreement with the qualitative experimental observations. Thus,

the formation of germacyclohexenes **2.9a-d** follows the trends established for carbon chemistry. Even though the reaction of 1-hexyne with germene **1.1** took longer to go to completion compared to the conjugated alkynes, the reaction proceeds much faster than the analogous all-carbon systems. In comparison, the addition of non-activated alkynes to dienes requires high temperature and/or the presence of a catalyst to proceed at a reasonable rate.¹⁴

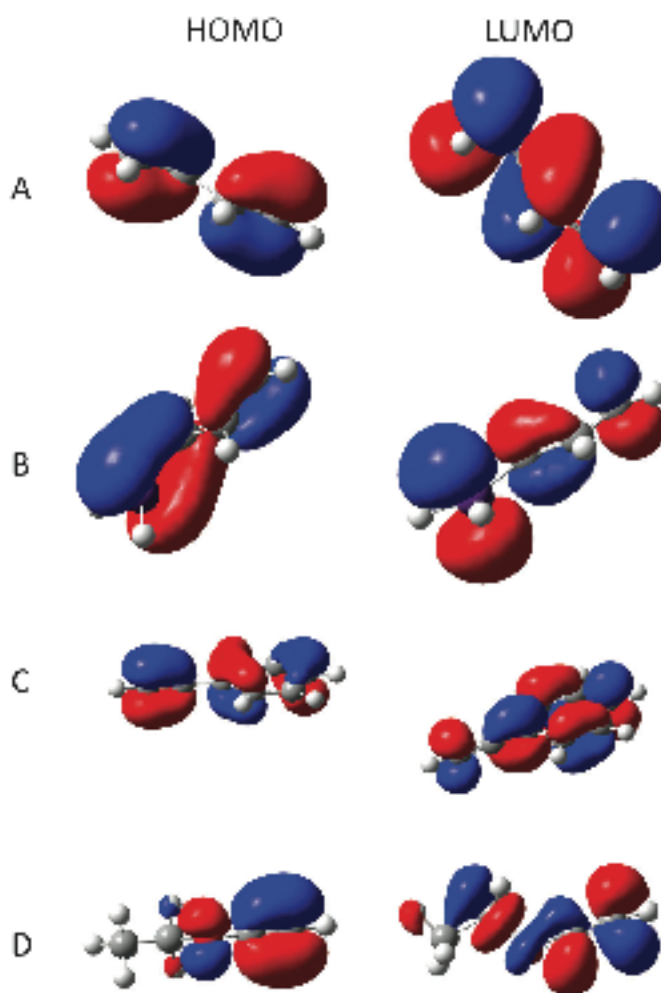
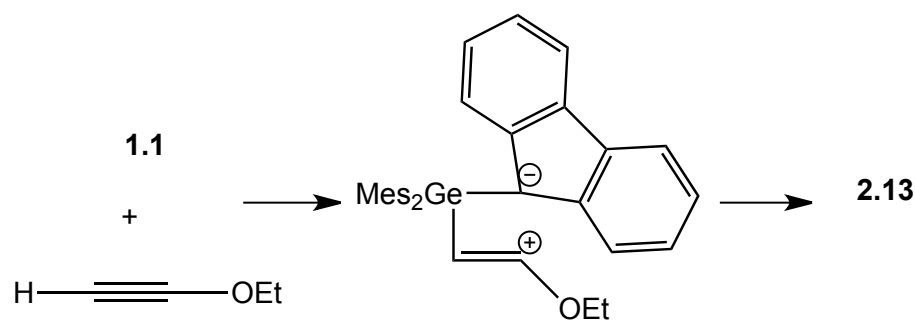


Figure 2.3 Highest occupied and lowest unoccupied molecular orbitals of (A) butadiene, (B) 1-germabutadiene, (C) phenylacetylene, and (D) ethoxyacetylene. All molecular orbitals were calculated at the TPSSTPSS/6-31G(d) level.

The ethoxy substituent in ethoxyacetylene is strongly electron donating. In this case, both the dienophile (ethoxyacetylene) and the diene (germene **1.1**) are electron rich species. The mismatch in electron-demand presumably slows the rate of Diels-Alder reaction and opens up a new cycloaddition pathway. The mechanism for the formation of germacyclobutene **2.13** is likely stepwise, where the nucleophile (ethoxyacetylene) attacks germene **1.1** to give a zwitterionic intermediate, followed by cyclization (Scheme 2.15). This is in contrast to the formation of germacyclobutene **2.19**, from the addition of ethoxyacetylene to germene **2.2**, which had opposite regiochemistry of alkyne addition and was proposed to proceed via complexation (Scheme 2.14). The regiochemistry observed in **2.13** was found to follow that for the formation of **2.9a-d**. Furthermore, the zwitterionic intermediate proposed from the nucleophilic addition of ethoxyacetylene to germene **1.1** (Scheme 2.15) would be stabilized due to the delocalization of the negative charge over the fluorenyl group¹⁵ and the positive charge can be stabilized by the ethoxy group. The observed increase in the ratio of the germacyclobutene **2.13** over germacyclohexene **2.9e** when the reaction is carried out in THF rather than in diethyl ether also supports our proposed stepwise, zwitterionic cycloaddition mechanism, as the solvent (THF) with the greater dielectric constant can stabilize the zwitterionic intermediate and lead to an increase in the rate of germacyclobutene **2.13** formation.



Scheme 2.15

2.4 Conclusions

In summary, the addition of terminal alkynes to germene **1.1** yielded germacyclohexenes **2.9a-e**, quantitatively. Rearrangement of the cyclopropyl ring did not occur in the formation of **2.9c,d** which rules out the presence of a radical or cationic intermediate along the reaction pathway. Thus, the formation of germacyclohexenes **2.9a-e** are proposed to occur via a concerted [2+4] cycloaddition followed by hydrogen transfer. The addition of ethoxyacetylene to germene **1.1** produced germacyclobutene **2.13** and germacyclohexene **2.9e**, where **2.13** is likely formed via a stepwise [2+2] cycloaddition through a zwitterionic intermediate. The difference in reaction rate between aromatic and aliphatic alkynes toward germene **1.1** reveals that conjugated germenes mimic carbon-based dienes in terms of their cycloaddition chemistry. Indeed, our hypothesis that the reaction of germene **1.1** would indeed be simpler than the reactions of germene **2.2** because of the lack of an α -hydrogen and the reduced basicity of the conjugate base of **1.1** proved to be correct. The addition reactions of alkynes to germene **1.1** are cleaner; they undergo cycloaddition exclusively. As in carbon chemistry, a [4+2] cycloaddition pathway is favoured over a [2+2] cycloaddition pathway unless an extremely electron-rich alkyne is utilized. We continue to investigate the cycloaddition reactions of germenes with the goal of understanding their reactivity more completely.

2.5 Experimental

General Experimental Details

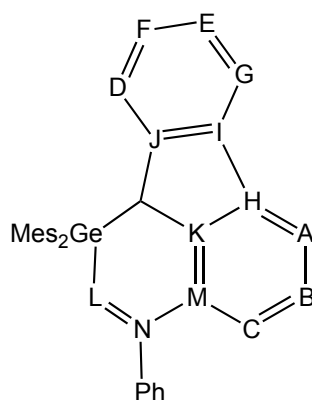
All manipulations were performed in flame-dried Schlenk tubes, or NMR tubes sealed with a septum, under an inert atmosphere of argon. Benzene- d_6 was distilled from LiAlH_4 , stored over 4 Å molecular sieves, and degassed prior to use. *t*-BuLi was purchased from the Aldrich

Chemical Co. The NMR standards used were: residual C₆D₅H (7.15 ppm) for ¹H NMR spectra, C₆D₆ central transition (128.00 ppm) for ¹³C NMR spectra, residual CHCl₃ (7.26 ppm) for ¹H NMR spectra, CDCl₃ central transition (77.00 ppm) for ¹³C NMR spectra. IR spectra were recorded (cm⁻¹) from thin films on a Bruker Tensor 27 FT-IR spectrometer. Electron impact mass spectra were obtained using MAT model 8400 mass spectrometer using an ionizing voltage of 70 eV. Mass spectral data are reported in mass-to-charge units, *m/z*. *Trans*-(2-phenylcyclopropyl)acetylene was synthesized as follows: reduction of *trans*-2 phenylcyclopropylcarboxylic acid using excess LiAlH₄ produced the corresponding alcohol, which was oxidized under Swern conditions. The resulting aldehyde was converted to the dibromoolefin and then to *trans*-(2-phenylcyclopropyl)acetylene using Corey-Fuchs conditions. The product was identified by comparison of the ¹H NMR data to those in the literature.⁶ A modified route to synthesize fluorenylfluorodimesitylgermane **2.8** was developed due to the complexity of the purification step in the reported procedure.⁹ Hydrolysis using NaOH solution of chlorofluorenyldimesitylgermane to give the hydroxy analog followed by fluorination using HF gave **2.8**. The overall yield (40%) is comparable to the yield from the original route (41%).⁹

General Procedure for the Reaction of Alkynes with Germene 1.1

A solution of fluorenylfluorodimesitylgermane (50 mg, 0.1 mmol) dissolved in diethyl ether (3 mL), was cooled to -78 °C. *t*-BuLi (0.06 mL, 1.7 M in pentane, 0.1 mmol) was added slowly. The colour of the solution changed from pale yellow to bright orange. The reaction mixture was allowed to stir at room temperature for 2 h. An aliquot was analyzed by ¹H NMR spectroscopy (C₆D₆) and was found to contain germene **1.1** (~88%). The ether was removed in *vacuo* (if required), yielding a bright orange residue and the residue was dissolved in C₆D₆ (1.1 mL). Alkyne (1.2 equiv) was added directly to the germene solution. The progress of the reaction

was monitored by ^1H NMR spectroscopy for up to 3 days. The solvent was removed by rotary evaporation yielding a yellow residue. The ratio of products in the crude reaction mixture was determined by ^1H NMR spectroscopy. The product mixture was contaminated with residual alkyne and unreacted fluorogermane **2.8**. The products were separated from fluorogermane **2.8** and residual alkyne by preparative thin layer chromatography on silica gel (hexanes and dichloromethane, 50:50) followed by second preparative thin layer chromatography on silica gel (hexanes) yielding yellow oil (mixed with a colourless solid in the case of **2.9a** and **b**), **2.9a-d** (43-45%).

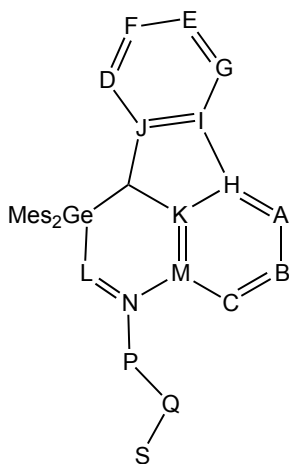


2.9a

2.9a IR (thin film, cm^{-1}) 2922 (s), 2851 (s), 1731 (m), 1603 (m), 1449 (s), 1377 (m), 1264 (m), 1028 (m), 847 (m), 810 (m), 740 (m); ^1H NMR (CDCl_3 , 600 MHz) δ 7.89 (d, 1H, G, $J = 7.8$ Hz), 7.76 (d, 1H, A, $J = 7.8$ Hz), 7.44-7.32 (m, 6H, Ph-H and F), 7.32- 7.28 (m, 1H, D), 7.27-7.22 (m, 2H, B and E), 7.03 (s, 1H, L), 6.93 (d, 1H, C, $J = 7.2$ Hz), 6.91 (s, 2H, *m*-Mes H), 6.55 (s, 2H, *m*-Mes-H), 4.65 (s, 1H, Q), 2.32 (br s, 9H, *o,p*-Mes), 2.11 (s, 3H, *p*-Mes), 1.64 (br s, 6H, *o*-Mes); ^{13}C NMR (CDCl_3 , 100 Hz) δ 150.92 (N), 145.80 (J), 143.81 (*i*-Ph), 143.24 (*o*-Mes), 142.98 (K), 141.56 (I), 141.53 (*o*-Mes), 140.37 (H), 138.51 (*p*-Mes), 138.07 (*p*-Mes), 137.71 (*i*-Mes), 134.81 (*i*-Mes), 134.06 (M), 132.91(L), 129.40 (*m*-Mes), 128.67 (*o*-Ph), 128.26 (*m*-Mes), 128.10 (*m*-Ph), 127.33 (*p*-Ph), 126.60 (C), 126.37 (E), 126.12 (B), 125.76 (F), 124.35 (D), 120.16 (G),

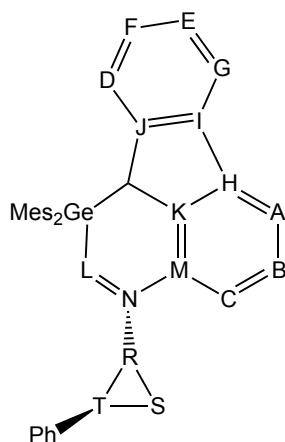
119.27 (A), 41.88 (GeCH), 25.56 (br s, *o*-Mes), 22.71 (*o*-Mes), 21.03 (*p*-Mes), 20.80 (*p*-Mes);

High-resolution MS (EI) for C₃₉H₃₆⁷⁰Ge (*m/z*), calc 574.206 found 574.204.



2.9b

2.9b ¹H NMR (CDCl₃, 600 MHz) δ 7.86 (d, 1H, D, J = 7.8 Hz), 7.74 (d, 1H, A, J = 7.8 Hz), 7.37-7.31 (m, 4H, B and G and C), 7.23-7.19 (m, 2H, F and E), 6.91 (s, 2H, *m*-Mes-H), 6.79 (s, 1H, L), 6.51 (s, 1H, *m*-Mes-H), 4.45 (s, 1H, L), 2.87 (dt, 1H, P, J = 7.8, 14.4 Hz), 2.53 (dt, 1H, P, J = 7.8, 14.9 Hz), 2.32 (s, 9H, *o,p*-Mes), 2.08 (s, 3H, *p*-Mes), 1.63-1.57 (m, 8H, *o*-Mes and Q), 1.4 (m, 2H, R), 0.93 (t, 3H, S, J = 7.2 Hz); ¹³C NMR (CDCl₃, 150 Hz) δ 149.07 (N), 145.96 (K), 143.22 (bs, *o*-Mes), 142.73 (I), 141.57 (J), 141.38 (*o*-Mes), 140.36 (H), 138.38 (*p*-Mes), 138.21 (*i*-Mes), 137.96 (*p*-Mes), 135.27 (*i*-Mes), 133.80 (M), 129.34 (*m*-Mes), 129.00 (L), 128.17 (*m*-Mes), 126.25 (B), 126.23 (F), 125.61 (E), 124.23 (D), 123.30 (C), 120.04 (G), 118.87 (A), 42.00 (Ge-CH), 37.21 (P), 30.48 (Q), 25.5 (br s, *o*-Mes), 22.60 (*o*-Mes), 22.50 (R), 21.05 (*p*-Mes), 20.78 (*p*-Mes), 14.02(S); High-resolution EI-MS for C₃₇H₄₀⁷⁰Ge (*m/z*), calc 554.2373 found 554.2369. Anal. Calc. for C₃₇H₄₀⁷⁰Ge: C, 79.73; H, 7.23 found C, 75.36; H, 7.13.



2.9c,d

2.9c,d: Mixture of diastereomers, colourless solid contaminated with $[\text{Mes}_2\text{Ge}(\text{fluorenyl})]_2\text{O}^7$ (1:1:0.13) and other minor impurities: ^1H NMR (C_6D_6 , 600 MHz) δ 7.79 (d, 1H, G, $J = 7.8$ Hz), 7.78 (d, 1H, G, $J = 7.8$ Hz), 7.67 (d, 1H, A, $J = 7.8$ Hz), 7.62 (d, 1H, A, $J = 7.8$ Hz), 7.57 (d, 1H, C, $J = 7.8$ Hz), 7.52 (d, 1H, C, $J = 7.2$ Hz), 7.50 (d, 2H, 2D, $J = 7.2$ Hz), 7.25 (m (2x td), 2H, 2E), 7.21 (t, 1H, B, $J = 7.2$ Hz), 7.16- 7.14 (m, B+ F+ Ph), 7.12 (t, F, $J = 7.8$ Hz), 7.07-7.02 (m, 5H, Ph), 6.99 (d, 1H, L, $J = 1\text{Hz}$), 6.92 (s, 1H, L), 6.86 (m, 1H, Ph), 6.85 (s, 4H, *m*-Mes2), 6.41 (s, 2H, *m*-Mes1), 6.39 (s, 2H, *m*-Mes1), 4.64 (s, 1H, Q), 4.54 (s, 1H, Q), 2.46 (s, 6H, *o*-Mes2), 2.43 (s, 6H, *o*- Mes2), 2.24- 2.20 (m, T'), 2.18, 2.17 (s each, 6H total, *p*-Mes2), 2.15- 2.10 (m, T), 2.08- 2.02 (m, R'), 1.87 (s, 3H, *p*-Mes1), 1.85 (s, 3H, *p*-Mes1), 1.80 (br s, 12H, *o*-Mes1), 1.80- 1.77 (m, R), 1.49 (ddd, 1H, S1, $J = 5.4, 6.3, 9.6$ Hz), 1.26 (ddd, 1H, S', $J = 4.8, 6.3, 9.0$ Hz), 1.18 (ddd, 1H, S', $J = 4.8, 6.6, 9.0$ Hz), 1.07 (ddd, 1H, S1, $J = 4.8, 5.4, 8.4$ Hz); ^{13}C NMR (C_6D_6 , 150 Hz) δ 149.43 (N), 149.34 (N), 146.42 (J), 146.56 (J), 143.62 (*o*-Mes2), 143.53 (*o*-Mes2), 143.20 (Ph), 143.16 (K), 143.07 (Ph), 142.94 (K), 142.35 (I), 142.31 (I), 141.61 (*o*-Mes1), 141.58 (*o*-Mes1), 140.93 (2H), 138.88 (*p*-Mes2), 138.35 (*p*-Mes1), 138.29 (*i*-Mes1), 138.09 (*i*-Mes1), 135.76 (*i*-Mes2), 135.66 (*i*-Mes2), 135.12 (M), 135.05 (M), 130.11 (*m*-Mes2), 129.09 (*m*-Mes1), 129.05 (*m*-Mes1), 128.89 (L), 127.15 (B), 127.05 (B), 126.94 (F), 126.92 (F), 126.50 (2E), 126.37 (Ph),

126.35 (Ph), 126.31 (L), 126.30 (Ph), 126.17 (Ph), 126.14 (Ph), 126.04 (Ph), 124.75 (D), 124.71 (D), 124.65 (C), 124.63 (C), 120.79 (G), 119.90 (A and G), 119.76 (A), 42.58 (Q), 42.52 (Q), 30.41 (T), 29.79 (T'), 28.19 (R'), 25.93 (*o*-Mes2), 25.85 (*o*-Mes2), 24.53 (R), 23.21 (*o*-Mes1), 21.23 (*p*-Mes2), 20.89 (*p*-Mes1), 20.71 (*p*-Mes1), 17.96 (S'), 14.64 (S); High-resolution EI-MS for C₄₂H₄₀⁷⁰Ge *m/z*, calc 614.2372 found 614.2373 (primes or numbers indicate the signals belong to the same diastereomer).

Addition of Ethoxyacetylene to Germene 1.1

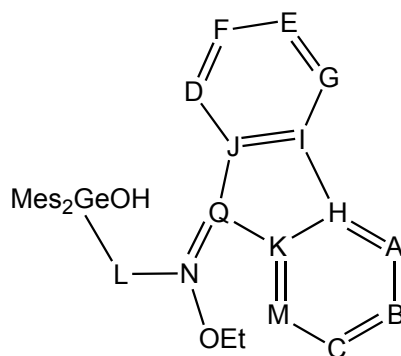
A solution of fluorogermene **2.8** (50 mg, 0.1 mmol) dissolved in diethyl ether (3 mL), was cooled to -78 °C. *t*-BuLi (0.06 mL, 1.7 M in pentane, 0.1 mmol) was added slowly. The colour of the solution changed from pale yellow to bright orange. The reaction mixture was allowed to stir at room temperature for 2 h. An aliquot was analyzed by ¹H NMR spectroscopy (C₆D₆) and was found to contain germene **1.1** (~88%). The ether was removed in *vacuo* (if required), yielding a bright orange residue. The residue was dissolved in one of three solvents: C₆D₆, diethyl ether or THF (1.1 mL). Ethoxyacetylene (1.2 equiv) was added directly to the germene solution. The solvent was removed by rotary evaporation yielding a yellow residue. The ratio of products (**2.9e**:**2.13**) in the crude reaction mixture was determined by ¹H NMR spectroscopy. The product mixture was contaminated with residual alkyne and unreacted fluorogermene **2.8**. The mixture was separated by preparative thin layer chromatography on silica gel (hexanes and dichloromethane, 50:50) to give contaminated samples of **2.9e** and **2.13**. Further attempts at purification by chromatography resulted in the hydrolysis of **2.9e** and **2.13**; compounds **2.14**, **2.15** and **2.16** were isolated from the plate. Compound **2.14** underwent isomerization to **2.15** in solution. A third attempt to purify compounds **2.15** and **2.16** by preparative thin layer

chromatography on silica gel (hexanes) gave **2.15** in acceptable purity, however, **2.16** was contaminated with $\text{Mes}_2\text{GeOHCHR}_2$.⁷

2.9e yellow oil contaminated with fluorene and other impurities (1: 0.8): $^1\text{H NMR}$ (C_6D_6 , 600 MHz) δ 7.96 (d, 1H, $J = 7.2$ Hz), 7.78 (d, 1H, $J = 7.8$ Hz), 7.71 (d, 1H, $J = 7.8$ Hz), 7.51 (d, 1H, $J = 7.2$ Hz), 7.35 (t, 1H, $J = 7.2$ Hz), ~ 7.23 (m) (all for fluorenyl-H), 6.85 (s, 2H, *m*-Mes), 6.44 (s, 2H, *m*-Mes), 5.58 (s, 1H, vinyl H), 4.58 (s, 1H, Ge-CH), 3.70 (dq, 1H, OCH $J = 16.8, 6$ Hz), 3.52 (dq, 1H, OCH, $J = 16.2, 6.6$ Hz), 2.47 (br s, 6H, *o*-Mes), 2.18 (s, 3H, *p*-Mes), 1.90 (s, 3H, *p*-Mes), 1.80 (br s, 6H, *o*-Mes), 1.15 (t, 3H, CH_3 , $J = 6.6$ Hz).

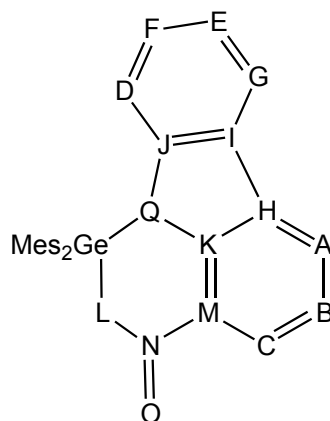
2.13 yellow oil: $^1\text{H NMR}$ (C_6D_6 , 600 MHz) δ 7.68 (d, 2H, $J = 7.2$ Hz), 7.29 (d, 2H, $J = 7.8$ Hz), 7.16 (t, 2H, $J = 7.8$ Hz), 7.00 (t, 2H, $J = 7.2$ Hz) (all for fluorenyl-H), 6.66 (s, 4H, *m*-Mes), 5.48 (s, 1H, vinyl H), 3.56 (q, 2H, OCH_2 $J = 7.2$ Hz), 2.12 (br s, 12H, *o*-Mes), 2.06 (s, 6H, *p* Mes), 0.74 (t, 3H, CH_3 , $J = 6.6$ Hz).

2.14 yellow oil: $^1\text{H NMR}$ (C_6D_6 , 400 MHz) δ 7.58- 7.54 (m, 2H), 7.2 (m, 6H) (all fluorenyl-H), 6.72 (s, 4H, *m*-Mes), 5.25 (s, 1H, vinyl), 4.54 (s, 1H, CHR_2), 3.09 (q, 2H, $J = 7.2$, OCH_2), 2.56 (s, 12H, *o*-Mes), 2.08 (s, 6H, *p*-Mes), 0.49 (t, 3H, $J = 7.2$ Hz, OCH_2CH_3); High-resolution MS (EI) for $\text{C}_{35}\text{H}_{38}\text{O}_2$ ⁷⁴Ge (m/z), calc 564.2088 found 564.2078.



2.15

2.15 yellow oil: IR (thin film, cm^{-1}) 3444 (br,s), 2923(m), 1612(w), 1734 (w), 1602 (w), 1303 (s), 1025 (w), 758 (s); ^1H NMR (C_6D_6 , 400 MHz) δ 8.54 (dt, 1H, M, $J = 7.8, 0.8$ Hz), 7.86 (d, 1H, G, $J = 7.6$ Hz), 7.72 (dt, 1H, A, $J = 7.8, 0.8$ Hz), 7.68 (ddd, 1H, D, $J = 6.8, 1.2, 0.8$ Hz), 7.39 (td, 1H, C, $J = 7.8, 1.2$ Hz), 7.27 (td, 1H, B, $J = 7.6, 1.2$ Hz), 7.12 (td, 1H, F, $J = 7.6, 1.2$ Hz), 7.07 (td, 1H, E, $J = 7.2, 1.6$ Hz), 6.60 (s, 4H, *m*-Mes), 3.50 (q, 2H, O-CH₂, $J = 6.8$ Hz), 3.32 (s, 2H, L), 2.37 (s, 12H, *o*-Mes), 2.03 (s, 6H, *p*-Mes), 0.92 (t, 3H, CH₃, $J = 7.2$ Hz); ^{13}C NMR (C_6D_6 , 100 Hz) δ 159.30 (N), 143.01 (*o*-Mes), 139.97 (J), 139.38 (*p*-Mes), 139.01 (K), 138.22 (H), 138.11 (I), 136.09 (*i*-Mes), 129.83 (*m*-Mes), 127.50 (C), 126.67 (E), 126.40 (B), 126.21 (M), 125.89 (F), 123.30 (G), 120.27 (D), 119.73 (Q), 119.65 (A), 64.63 (OCH₂), 27.83 (L), 23.85 (*o*- Mes), 21.16 (*p*-Mes), 15.02 (CH₃); High-resolution MS (EI) for $\text{C}_{35}\text{H}_{38}\text{O}_2^{74}\text{Ge}$ (m/z), calc 564.2088 found 564.2106.



2.16

2.16 yellow oil contaminated with $\text{Mes}_2\text{GeOHCHR}_2^7$ in (1:0.5) ratio: IR (thin film, cm^{-1}) 2919 (m), 2849 (m), 1665 (s), 1601 (m), 1448 (s), 1415(m), 1414 (m), 1276 (m), 1261 (m), 1025 (s), 849 (m), 795 (s), 765 (m), 737 (s); ^1H NMR (C_6D_6 , 600 MHz) δ 8.2 (d, 1H, C, $J = 7.8$ Hz), 7.71 (d, 1H, G, $J = 7.2$ Hz), 7.70 (d, 1H, A, $J = 6.6$ Hz), 7.34 (d, 1H, D, $J = 7.8$ Hz), 7.18 (t, 1H, B, $J = 7.2$ Hz), ~ 7.22 (E, overlap with signal from the germol), 7.11 (t, 1H, F, $J = 7.8$ Hz), 6.74 (s, 2H, *m*-Mes2), 6.35 (s, 2H, *m*-Mes2), 4.23 (s, 1H, Q), 3.39 (d, 1H, L, $J = 12$ Hz), 3.11 (d, 1H, L, $J = 12$ Hz), 2.20 (s, 6H, *o*-Mes2), 2.10 (s, 3H, *p*-Mes2), 1.82 (s, 3H, *p*-Mes1), 1.60 (s, 6H, *o*-Mes1); ^{13}C NMR (C_6D_6 , 100 Hz) δ 196.30 (N), 147.98 (K), 145.59 (J), 143.04 (*o*-Mes1), 142.05 (*o*-Mes2), 141.81 (H), 141.37 (I), 139.47 (*p*-Mes2), 138.78 (*p*-Mes1), 134.99 (*i*-Mes2), 133.48 (*i*-Mes1), 133.07 (M), 130.03 (*m*-Mes2), 129.27 (*m*-Mes1), 127.34 (F), 127.04 (B), 126.55 (E), 126.38 (C), 124.55 (D), 124.18 (A), 120.61 (G), 45.43 (Q), 42.74 (L), 24.70 (*o*-Mes2), 22.43 (*o*-Mes1), 20.98 (*p*-Mes2), 20.70 (*p*-Mes1)); High-resolution MS (EI) for $\text{C}_{33}\text{H}_{32}\text{O}^{74}\text{Ge}$ (m/z), calc 518.1642 found 518.1668.

DFT Calculations

First principles calculations were performed using Gaussian 09¹⁶ on the Shared Hierarchical Academic Research Computing Network (SHARCNET, www.sharcnet.ca). Calculations were performed on an 8 core Xeon 2.83 GHz CPU with 16 GB memory. All calculations were performed at the TPSSSTPSS¹⁷/6-31G(d) level of theory. Molecular orbitals were calculated using NBO version 3. Cube files were generated using the cubegen utility and visualized in Gaussview 3.09.

Single Crystal X-ray Diffraction Experimental Details

The crystal, **2.9a** or **2.9b**, was covered in Nujol and placed rapidly into the cold N₂ stream of a Kryo-Flex low temperature device. The data were collected either by employing the SMART software on a Bruker APEX CCD diffractometer or by using the COLLECT¹⁸ software on a Nonius KAPPA CCD diffractometer, each being equipped with a graphite monochromator with Mo K α radiation ($\lambda = 0.71073 \text{ \AA}$). For each sample, a hemisphere of data was collected using counting times of 10-30 seconds per frame. The data were collected at -123 °C. Data reductions were performed using the SAINT¹⁹ software and the data were corrected for absorption using SADABS²⁰ or using the DENZO-Scalepack application.²¹ The structures were solved by direct methods using the SHELX²² suite of programs and refined by full-matrix least-squares on F^2 with anisotropic displacement parameters for the non-H atoms using SHELXL-97 and the WinGX²³ software package. Details of the final structure solutions were evaluated using PLATON²⁴ and thermal ellipsoid plots were produced using SHELXTL.

Table 2.1: Crystallographic data of compounds **2.9a** and **2.9b**

Data	10a	10b
empirical formula	C ₃₉ H ₃₆ Ge	C ₃₇ H ₄₀ Ge
formula wt	577.27	557.28
cryst syst	triclinic	triclinic
space group	P-1	P-1
a (Å)	11.9691(5)	10.865(2)
b (Å)	12.1777(5)	11.650(2)
c (Å)	21.5063(10)	12.680(3)
α (deg)	85.934(2)	95.79(3)
β (deg)	84.697(2)	102.75(3)
γ (deg)	76.614(2)	114.48(3)
V (Å ³)	3032.5(2)	1390.9(5)
Z	4	2
no. of data/ restraints/ params	1447/ 0/ 733	6604/ 0/ 348
goodness of fit	1.000	1.043
R (I > 2σ (I))	0.1316	0.0540
wR2 (all data)	0.1198	0.1033
Largest diff peak, hole (e Å ⁻³)	0.402, -0.573	0.438, -0.585
CCDC reference #	960004	960005

2.6 References:

1. Ottosson, H.; Steel, P. G. *Chem. Eur. J.* **2006**, *12*, 1576.
2. (a) Brook, A. G.; Harris, J. W.; Lennon, J.; El Sheikh, M. *J. Am. Chem. Soc.* **1979**, *101*, 83; (b) Brook, A. G.; Baumegger, A.; Lough, A. I. *Organometallics* **1992**, *11*, 3088.
3. Gottschling, S. E.; Grant, T. N.; Milnes, K. K.; Jennings, M. C.; Baines, K. M. *J. Org. Chem.* **2005**, *70*, 2686.
4. Milnes, K. K.; Jennings, M. C.; Baines, K. M. *J. Am. Chem. Soc.* **2006**, *128*, 2491.
5. Milnes, K. K.; Pavelka, L. C.; Baines, K. M. *Organometallics* **2010**, *29*, 5972.
6. Pavelka, L. C.; Baines, K. M. *Organometallics* **2011**, *30*, 2261.
7. Couret, C.; Stage, J.; Escudie, J.; Lazraq, M. *J. Am. Chem. Soc.* **1987**, *27*, 828.

8. El Kettani, S. A.; Lazraq, M.; Ranaivonjatovo, H.; Escudié, J.; Couret, C.; Gornitzka, H.; Merceron, N. *Organometallics* **2004**, *23*, 5062.
9. Allan, C. J.; Reinhold, C.; Pavelka, L. C.; Baines, K. M. *Organometallics* **2011**, *30*, 3010.
10. Liang, Y.; Pitteloud, J.-P.; Wnuk, S. F. *J. Org. Chem.* **2013**, *78*, 5761.
11. Brook, A. G. *Adv. Organomet. Chem.* **1968**, *7*, 155.
12. Pavelka, L.C.; Baines, K. M. *Dalton Trans.* **2012**, *41*, 3294.
13. Ying, B.; Su, M. *Organometallics* **2011**, *41*, 3294.
14. Tonogaki, K.; Mori, M. *Tetrahedron Lett.* **2002**, *43*, 2235.
15. Lazraq, M.; Escudié, J.; Couret, C.; Stagé, J.; Dräger, M.; Dammel, R. *Angew. Chem. Int. Ed.* **1988**, *27*, 828.
16. Frisch, M. J.; Trucks, G. W.; Schlegel, H. B.; Scuseria, G. E.; Robb, M. A.; Cheeseman, J. R.; Scalmani, G.; Barone, V.; Mennucci, B.; Petersson, G. A.; Nakatsuji, H.; Caricato, M.; Li, X.; Hratchian, H. P.; Izmaylov, A. F.; Bloino, J.; Zheng, G.; Sonnenberg, J. L.; Hada, M.; Ehara, M.; Toyota, K.; Fukuda, R.; Hasegawa, J.; Ishida, M.; Nakajima, T.; Honda, Y.; Kitao, O.; Nakai, H.; Vreven, T.; Montgomery, J. A., Jr.; Peralta, J. E.; Ogliaro, F.; Bearpark, M.; Heyd, J. J.; Brothers, E.; Kudin, K. N.; Staroverov, V. N.; Kobayashi, R.; Normand, J.; Raghavachari, K.; Rendell, A.; Burant, J. C.; Iyengar, S. S.; Tomasi, J.; Cossi, M.; Rega, N.; Millam, N. J.; Klene, M.; Knox, J. E.; Cross, J. B.; Bakken, V.; Adamo, C.; Jaramillo, J.; Gomperts, R.; Stratmann, R. E.; Yazyev, O.; Austin, A. J.; Cammi, R.; Pomelli, C.; Ochterski, J. W.; Martin, R. L.; Morokuma, K.; Zakrzewski, V. G.; Voth, G. A.; Salvador, P.; Dannenberg, J. J.; Dapprich, S.; Daniels, A. D.; Farkas, Ö.; Foresman, J. B.; Ortiz, J. V.; Cioslowski, J.; Fox, D. J.; Revision A1 ed.; Gaussian Inc.: Wallingford, CT, **2009**.
17. Tao, J.; Perdew, J. P.; Staroverov, V. N.; Scuseria, G. E. *Phys. Rev. Lett.* **2003**, *91*, 146401.

18. COLLECT; Nonius BV: Delft, The Netherlands, **2001**.
19. SAINTPLUS; Bruker AXS Inc.: Madison, WI, **2001**.
20. SADABS; Bruker AXS Inc.: Madison, WI, **2001**.
21. Otwinowski, Z.; Minor, W. In *Macromolecular Crystallography*; Carter, C. W. J.; Sweet, R. M., Eds.; Academic Press: New York, 1997; Vol. Part A, p 307.
22. Sheldrick, G. M. *Acta Crystallogr. Sect. A: Found Crystallogr.* **2008**, *112*, 64.
23. Farrugia, L. J. *J. Appl. Crystallogr.* **1999**, *32*, 837.
24. Spek, A. L. *J. Appl. Crystallogr.* **2003**, *36*, 7.

Chapter 3

Addition of Alkynes to Digermynes: Experimental Insight into the Reaction

Pathway*

3.1 Introduction

With the landmark syntheses of several stable derivatives of disilynes¹ and digermynes,² attention has been focussed in recent years on the reactivity of these novel species.³ Of particular interest is the reactivity of the heavier ditetrelynes towards chemical feedstocks and their derivatives, in an effort to understand the ability of these unsaturated main group molecules to mimic the reactivity of transition metals in the activation of small molecules and in catalysis.⁴ Pertinent to this endeavour is the study of the reactivity of disilynes^{5,6} and digermynes^{7,8,9,10,11} towards alkynes. Several different modes of reaction have been observed: one equivalent of alkyne adds to a digermine to give a 1,2-digermete or a bis(germylidenyl)-substituted alkene (**3.1** or **3.2**, respectively, Chart 3.1) or two equivalents of alkyne add to a ditetrelyne to give a 1,2-ditetrelabenzene or a 1,4-dihydro-1,4-digermine (i.e. **3.3/3.4** or **3.5**, respectively, Chart 3.1).

* A version of sections 3.1, 3.2 and 3.3 of this chapter have been published. Nada Y. Tashkandi, Laura C. Pavelka, Christine A. Caputo, Paul D. Boyle, Philip P. Power, Kim M. Baines. Addition of Alkynes to Digermynes: Experimental Insight into the Reaction Pathway. *Dalton Trans.* **2016**, 45, 7226.

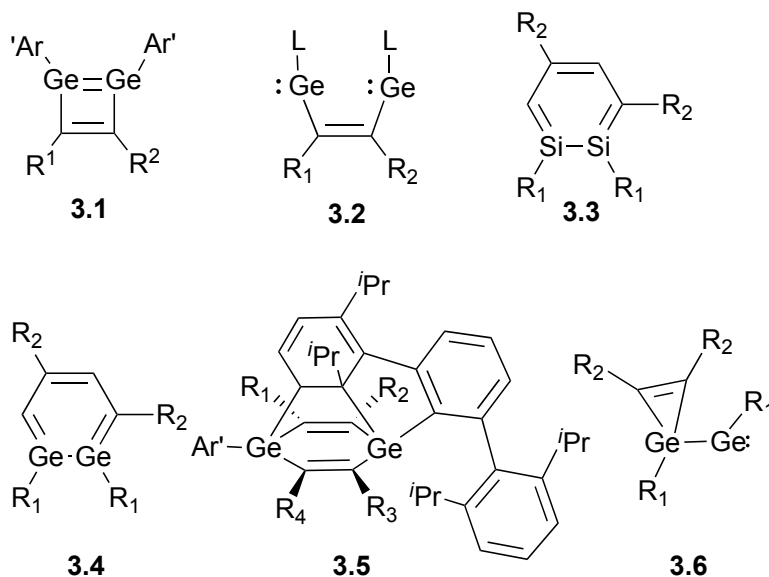
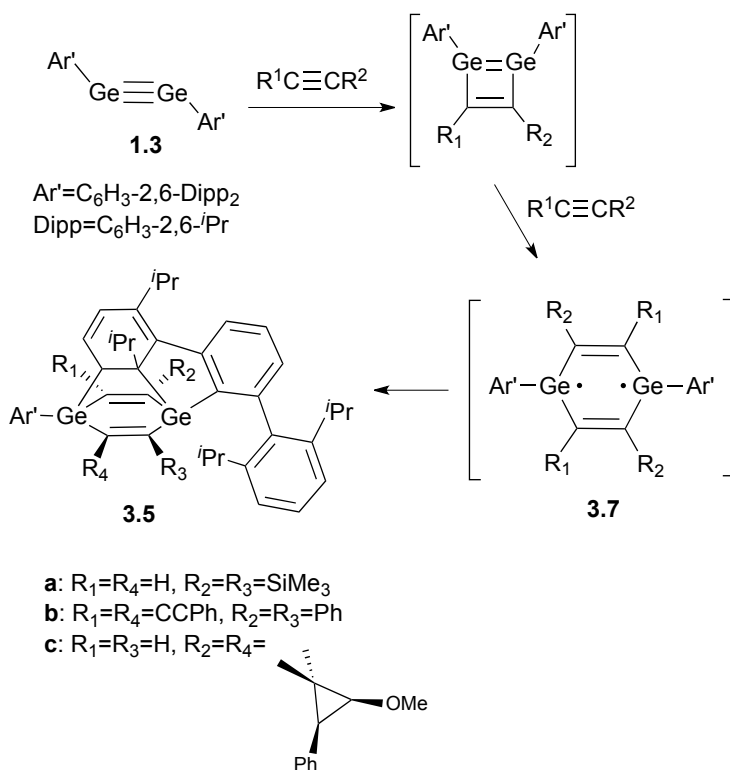


Chart 3.1 Products derived from the reaction of disilynes or digermynes with alkynes. **3.1**: Ar' = C₆H₃-2,6-Dipp₂, Dipp = C₆H₃-2,6-ⁱPr₂; R₁=R₂=Ph.⁷ **3.2a**: L=N(Ar)(SiⁱPr₃); Ar=C₆H₂-2,6-[CHPh₂]₂-4-ⁱPr, R₁=H, R₂=Me or **3.2b**: L=N(Ar)(SiMe₃); Ar=C₆H₂-2,6-[CHPh₂]₂-4-Me, R₁=CCSiMe₃, R₂=SiMe₃.⁹ **3.3a**: R₁=SiⁱPr[CH(SiMe₃)₂]₂; R₂=Ph (4,5-diPh isomer also formed).⁵ **3.3b**: R₁=C₆H₂-2,6-[CH(SiMe₃)₂]₂-4-[C(SiMe₃)₃]; R₂=H, Ph, or SiMe₃.⁶ **3.4**: R₁=C₆H₂-2,6-[CH(SiMe₃)₂]₂-4-[CMe₃], R₂=H.¹¹ **3.5a**: Ar' = C₆H₃-2,6-Dipp₂, Dipp = C₆H₃-2,6-ⁱPr₂, R₁=R₄=H, R₂=R₃=SiMe₃,⁷ **3.5b**: Ar' = C₆H₃-2,6-Dipp₂, Dipp = C₆H₃-2,6-ⁱPr₂, R₁=R₄=CCPh, R₂=R₃=Ph.⁸ **3.6**: R₁=NPh₂, R₂=H.

The reaction pathways have been considered. Compounds **3.2-3.5** have been proposed to form through a common intermediate, a ditetrelete.^{5,7-11} The possibility of a [2+2] cycloaddition between the digermene and the alkyne to give **3.1** was suggested in an early study.⁷ Subsequent calculations on the addition of alkynes to amido-substituted digermynes have shown that the alkyne initially adds to the digermene in a [2+1] fashion to give a germylidenyl-substituted germirene (**3.6** in Chart 3.1) which rearranges in a second step to give a digermene-like intermediate with a long Ge=Ge bond. The weak Ge=Ge bond of the germene dissociates to give the bis(germylidenyl)-substituted alkene derivatives, **3.2**.¹⁰ Similarly, a 1,2-disilete-type species was proposed as an intermediate in a computational study of the formation of **3.3**. However, in this case, subsequent [2+4]

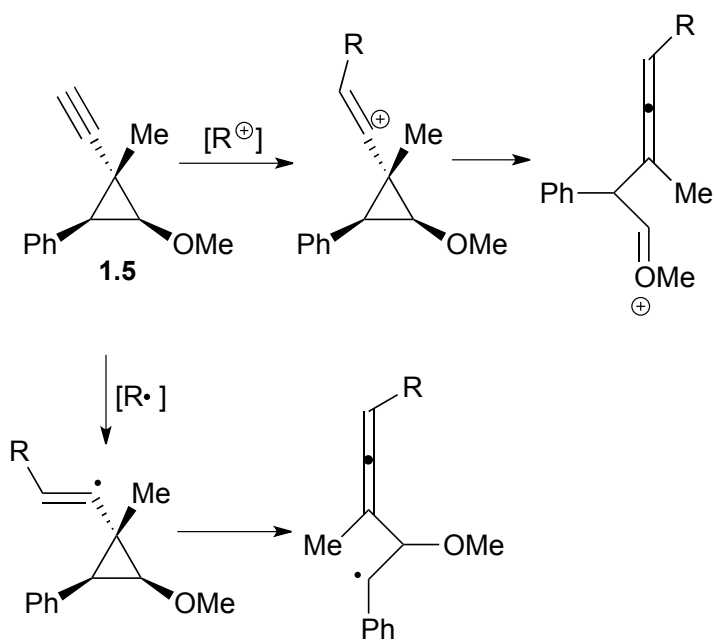
cycloaddition of another equivalent of alkyne to the 1,2-disilene followed by rearrangement leads to the disilabenzene **3.3**.⁵ The formation of the 1,4-dihydro-1,4-digermines **3.5a,b** (Chart 3.1) was speculated to take place via the addition of a second equivalent of alkyne to the Ge-Ge double bond of an initially formed digermene followed by (or concerted with) dissociation of the central Ge-Ge bond to give a diradical intermediate, **3.7**, which inserts into one of the flanking terphenyl groups to give **3.5a,b** (Scheme 3.1).⁷



Scheme 3.1

We have long been interested in the mechanism of cycloaddition reactions of (di)tetrelenes,¹² particularly those of alkynes, and have developed the mechanistic probe, **1.5**, which enables us to distinguish between the formation of an α -cyclopropyl vinyl

radical and cation during the course of a reaction by the formation of regioisomeric adducts. If a radical intermediate is formed adjacent to the cyclopropyl ring along the reaction pathway, the cyclopropyl ring will open preferentially toward the phenyl group; however, if the intermediate is cationic in nature, ring opening towards the methoxy group is favoured (Scheme 3.2).¹³ Thus, the different rearrangement pathways lead to regioisomeric products which reveal the nature of the intermediate along the reaction pathway. The magnitude of the rate constants for the rearrangements is integral to the ability of **1.5** to behave as a mechanistic probe and the rate constants for rearrangement are large enough such that the rearrangement can effectively compete with other processes such as direct cyclization. Notably, the absence of a characteristic rearrangement can be construed as strong evidence against a given mechanism.¹⁴



Scheme 3.2

We have reported that alkyne **1.5** adds to tetramesityldigermene, containing a Ge-Ge double bond, via the formation of a biradical intermediate.¹⁵ Given the current interest in the addition of alkynes to digermynes, we have now investigated the addition of cyclopropyl alkyne **1.5** to digermene **1.3** in an attempt to evaluate the nature of the intermediates formed (if any).

3.2 Results

An excess of alkyne **1.5** was added to a red solution of digermene **1.3**^{2a} in hexanes at room temperature. The red colour of the solution changed to golden yellow after 30 min, and then faded to pale yellow within 24 hr. The solvent was removed under vacuum to give a colourless solid. The reaction was performed in the dark and under ambient light conditions with no difference in the outcome. Although the product is stable towards air and moisture, it decomposed during attempts to purify it by preparative thin layer chromatography. The product, **3.5c**, was characterized by ¹H, ¹³C, ¹H-¹H-COSY, ¹³C-¹H gHSQC and ¹³C-¹H gHMBC NMR spectroscopy and ESI-mass spectrometry; however, unambiguous identification of the structure was only possible by X-ray crystallography (Figure 3.1).

The skeletal framework of **3.5c** is analogous to those of **3.5a,b** previously reported by Power,^{7,8} however, the regiochemistry of the former alkynyl substituents about the digermene ring is opposite to that of **3.5b**, likely due to steric effects. The structural metrics of **3.5c** revealed similarities to those reported for **3.5b**.⁸ The distance between the two germanium atoms is 3.074 Å, indicating the absence of a germanium-germanium bond. Also, within the bridging aryl group, the C-C bond length (C34-C35) is

1.568(4) Å indicative of single bond. The C-C bond lengths in the digermine ring are consistent with C-C double bonds: C1-C2 and C3-C4 are 1.340(4) and 1.343(4) Å in length, respectively. The geometry about each germanium is quite distorted from tetrahedral: the intracyclic digermine C-Ge-C angles are both approximately 106 degrees; however, the exocyclic C-Ge-C angles range from approximately 90 (C27-Ge2-C34) to approximately 140 (C3-Ge2-C27) degrees.

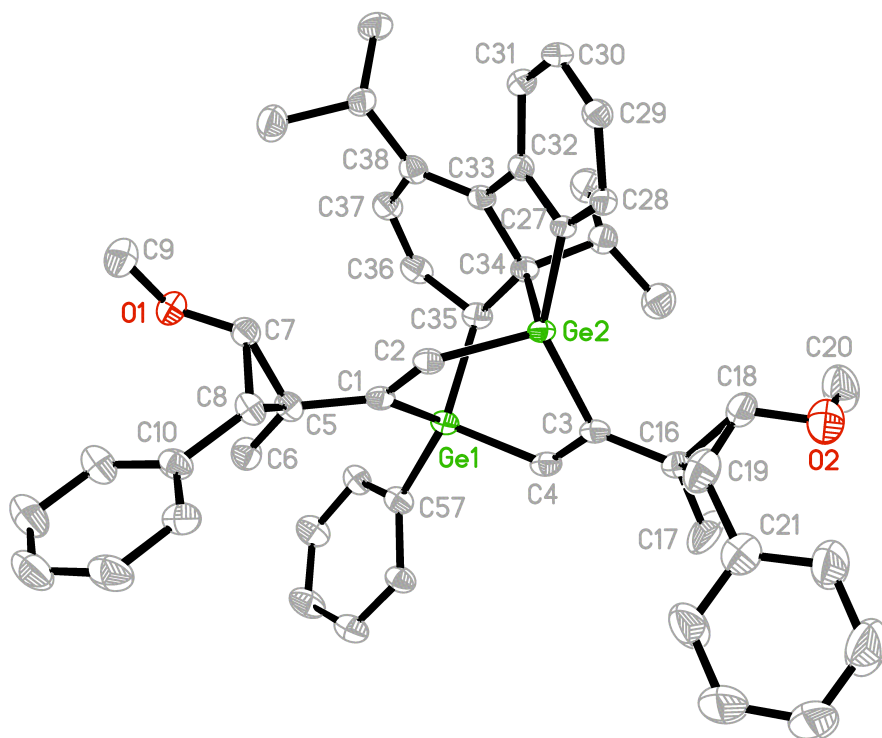
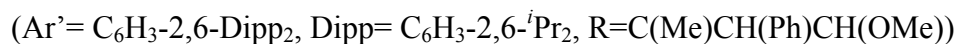
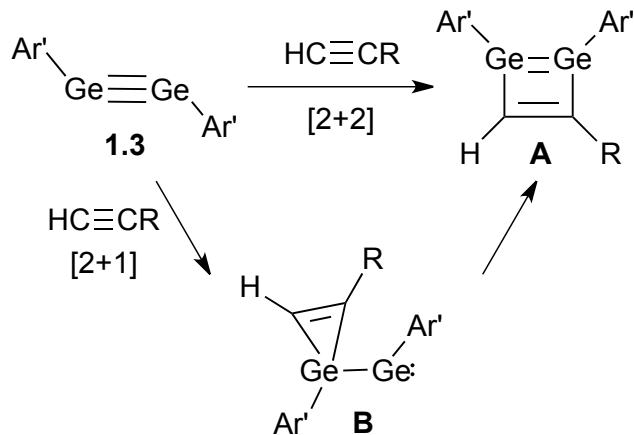


Figure 3.1 Displacement ellipsoid plot of the structure of **3.5c**; ellipsoids are at the 50% probability level. The hydrogen atoms and the Dipp groups were omitted for clarity. Selected bond lengths (Å) and angles (deg): Ge1-C4 = 1.960(3), Ge1-C1 = 1.995(3), Ge2-C2 = 1.945(3), Ge2-C3 = 1.959(3), C34-C35 = 1.568(4), C4-Ge1-C1 = 105.66(13), C2-Ge2-C3 = 106.05(13).

3.3 Discussion

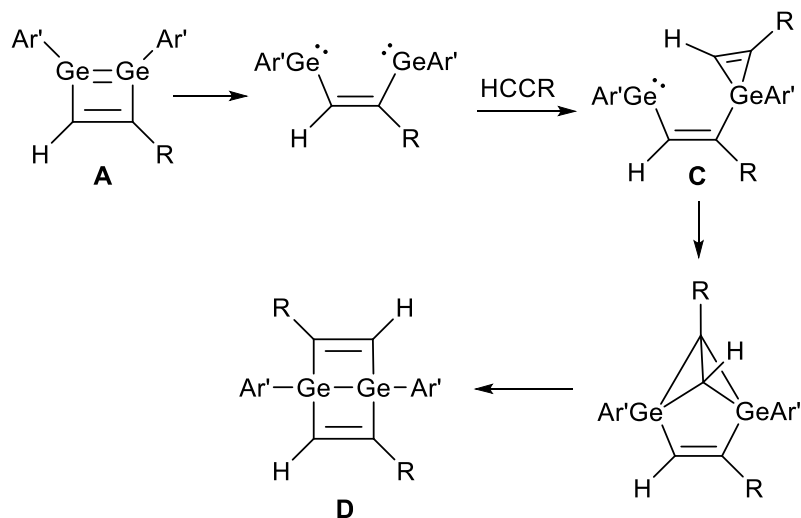
The addition of cyclopropylalkyne **1.5** to digermine **1.3** resulted in the formation of **3.5c** with the cyclopropyl ring still intact, which rules out the presence of a

cyclopropyl vinyl radical or cationic intermediate anywhere along the reaction pathway.¹⁴ In considering the implications of this result on the mechanism of the reaction, we make the assumption that the formation of **3.5c** proceeds via a digermete. This assumption is reasonable given that 1) Power observed the formation of a digermete in at least one addition of a substituted alkyne to a digermine,⁷ 2) the computed reaction pathway for the addition of acetylene to a silyl-substituted disilyne (silyl= Si^{*i*}Pr[CH(SiMe₃)₂]₂) located a disilene as an intermediate,⁵ 3) calculation of the energy profile for the addition of acetylene to a diamido-substituted digermine (Ph₂NGeGeNPh₂) revealed the formation of a related species which has a weak interaction between the two germaniums as evidenced by an elongated Ge-Ge bond¹⁰ and, 4) in the addition of ethene to a diaryldigermine (Ar = C₆H₂-2,6-[CH(SiMe₃)₂]₂-4-[C(SiMe₃)₃]), a 3,4-dihydrodigermete was isolated.¹⁶ Our results reveal, for the first time, that the formation of the digermete (i.e. **A** in Scheme 3.3) cannot involve a vinyl radical or a zwitterion along the reaction pathway. On the basis of the computed reaction pathways between acetylene and a disilyne,⁵ a digermine¹⁰ or a germene¹⁷ or between ethene and a digermine,¹⁶ the formation of a [2+1] complex/intermediate (**B** in Scheme 3.3) seems more probable and is consistent with the experimental results although a concerted asynchronous [2π_s + 2π_s],¹⁸ pseudoexcited¹⁹ or [2π_s + 2π_a]²⁰ reaction pathway cannot explicitly be eliminated. Notably, the transformation from **B** to **A** is the reverse of the well-known digermene to germylgermylene rearrangement.²¹



Scheme 3.3

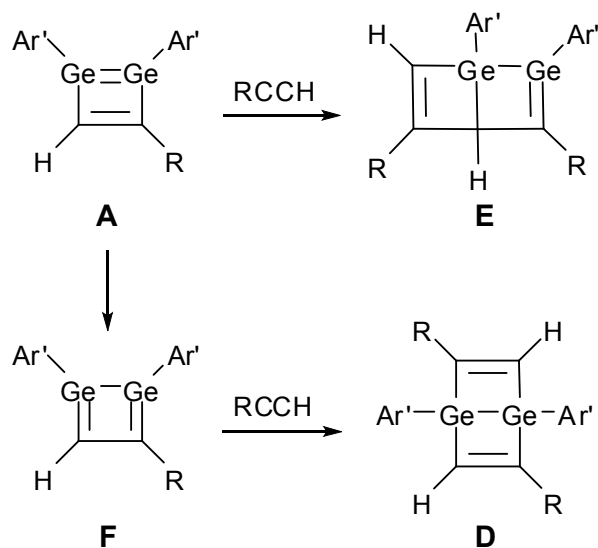
In the second stage of the reaction, the digermene **A** reacts with a second equivalent of alkyne to give **3.5c**. On the basis of the skeletal framework of **3.5c**, a Dewar benzene derivative (**D**) is reasonable as an intermediate. Given the complete absence of any cyclopropyl ring-opened products isolated from or detected in the crude reaction mixture, we eliminate the possibility of a cycloaddition between alkyne **1.5** and the digermenic moiety in a digermene through a diradical or zwitterionic intermediate as was observed in the addition of **1.5** to tetramesityldigermene.²² There are two pathways which seem reasonable to form **C**. As has been observed in the chemistry of several bulky digermenes, dissociation of the $\text{Ge}\text{-Ge}$ double bond²³ to give an ethene-bridged bis(germylene) followed by addition of **1.5** to one of the germylene centres would give the germirene intermediate (**C**) which could then react by insertion of the germylene moiety into the π -bond of the germirene followed by rearrangement, or by direct insertion of the germylene moiety into the $\text{Ge}\text{-C}$ σ -bond of the germirene, to give **D** (Scheme 3.4).



(Ar' = C₆H₃-2,6-Dipp₂, Dipp = C₆H₃-2,6-ⁱPr₂, R = C(Me)CH(Ph)CH(OMe))

Scheme 3.4

Alternatively, a [2+4] reaction between the alkyne and the digermene, similar to what Sekiguchi proposed in the formation of a disilabenzene, would give the wrong connectivity for the framework (See **E**, Scheme 3.5). However, rearrangement to a bis(germene), **F**, followed by a [2+4] cycloaddition would give **D** directly (Scheme 3.5). Although we have shown that the lowest energy pathway between an isolated germene and acetylene proceeds via a biradical intermediate,¹⁷ the addition of an alkyne to a conjugated germene likely follows a concerted [2+4] reaction pathway²⁴ and our current results are consistent with this finding. From **D**, insertion of the flanking aryl group can occur via a biradical intermediate, as was proposed earlier,⁷ or could occur via a [2+4]-type cycloaddition between the flanking aryl group and the 1,4-digermabenzene derived from rearrangement of **D**.



(Ar' = C₆H₃-2,6-Dipp₂, Dipp = C₆H₃-2,6-^{*i*}Pr₂, R = C(Me)CH(Ph)CH(OMe))

Scheme 3.5

3.4 Conclusions

In summary, the experimental results of the addition of alkyne probe **1.5** to digermene **1.3** have given us important insights into the reaction of alkynes with digermynes. Since no ring-opening of the cyclopropyl group was observed in the product, the reaction pathway to **3.5c** does not involve any vinylic radicals or cations derived from **1.5**. On this basis, we can conclude that the initial formation of a digermene does not proceed through a biradical, a possibility that had yet to be eliminated experimentally or computationally. Furthermore, the addition of a second equivalent of alkyne to the digermene also cannot proceed through a biradical. As a consequence, we have eliminated the addition of an alkyne to the digermenic moiety of the digermene as a possibility as it has been previously shown that a biradical intermediate occurs along such a reaction

pathway.¹⁵ Similarly, the addition of an alkyne to an isolated germenic moiety is also unlikely. With these insights, and the results of computational studies on analogous systems, a reasonable reaction pathway is proposed which helps to formulate a coherent picture of the reactivity of alkynes to both disilynes and digermynes. Notably, previous computational studies (with the exception of the computational study of the addition of acetylene to a germene¹⁷) did not examine the possibility of radical intermediates. Hopefully, this experimental study will inspire additional computational studies on this very important and fundamental reaction of digermynes.

3.5 Experimental

General Experimental Details

All air sensitive reactions were performed under an inert atmosphere of argon or nitrogen using standard Schlenk techniques or a glove box. Hexanes were obtained from a solvent purification system (SPS-400-5, Innovative Technology Inc) and was stored over 4Å molecular sieves. The NMR standards used were residual C₆D₅H (7.15 ppm) for ¹H NMR spectra, C₆D₆ central transition (128.00 ppm). Electrospray ionization mass spectra were recorded on a Bruker microTOF II mass spectrometer. X-ray data were obtained using a Bruker Apex II Diffractometer.

Addition of Alkyne Probe 1.5 to Digermine

A solution alkyne **1.5** (20 mg, 0.15 mmol) dissolved in hexanes (5 mL) was added to a red solution of digermine **1.3** (50 mg, 0.053 mmol) also dissolved in hexanes (5 mL). The red colour of the solution changed to golden yellow after 30 min, and then faded to pale yellow within 24 hr. The solvent was removed under vacuum to give a pale

yellow oil which was redissolved in a minimal amount of hexanes. The solution was placed in the freezer (-20 °C) for 24 hr to give **3.5c** as a colourless solid contaminated with residual alkyne **1.5** (0.22 mg, 31%). **3.5c**: δ ¹H (400 MHz, C₆D₆, Me₄Si) 7.5-6.9 (m, Ar-H), 6.57 (1 H, s, CH= on digermine), 6.52 (1 H, s, CH= on digermine), 5.9-5.8 (2 H, m, CH= on cyclohexadiene), 5.46 (m, 3 H), 3.60 (2 H, sept), 3.14, 3.05 (OMe), 2.57, 2.53 (each d, each 1 H, CH(OMe)), 2.33-2.10 (m, 5 H, CHMe₂), 2.02, 1.99 (each d, each 1 H, CHPh), 1.6-0.9 (52 H: (m, CHMe₂), 1.23 (s, Me on cyclopropyl), 1.20 (s, Me on cyclopropyl));²⁵ ESI-MS Exact mass calcd for C₈₆H₁₀₂NaO₂⁷⁰Ge⁷²Ge [M+Na⁺] 1331.7879; found 1331.6241.

Single Crystal X-ray Diffraction Experimental Details

Data Collection and Processing. The sample was mounted on a Mitegen polyimide micromount with a small amount of Paratone N oil. All X-ray measurements were made on a Bruker Kappa Axis Apex2 diffractometer at a temperature of 150 K. The unit cell dimensions were determined from a symmetry constrained fit of 9904 reflections with $5.3^\circ < 2\theta < 55.2^\circ$. The data collection strategy was a number of ω and φ scans which collected data up to 54.21° (2θ). The frame integration was performed using SAINT.²⁶ The resulting raw data were scaled and absorption corrected using a multi-scan averaging of symmetry equivalent data using SADABS.²⁷

Structure Solution and Refinement. The structure was solved by direct methods using the XS program.²⁸ All non-hydrogen atoms were obtained from the initial solution. The hydrogen atoms were introduced at idealized positions and were allowed to ride on the parent atom. The asymmetric unit contained three regions of included solvent molecules. The first region contained a hexane molecule which lay across a crystallographic center

of symmetry. The second region contained a hexane at a general position in the lattice. The C-C distances and anisotropic displacement parameters (ADP's) of the hexane molecules were restrained to keep the refinement stable and physically reasonable. The third region probably contained disordered or fractionally occupied CH₂Cl₂ molecule(s) as well as possibly some (disordered) hexane(s). No chemically sensible model could be found for this third region of solvation. To improve the fit of the known part of the structure, the SQUEEZE procedure²⁹ as implemented in PLATON³⁰ was used to subtract out the unaccounted for solvents' contribution to the diffraction pattern. The structural model was fit to the data using full matrix least-squares based on F^2 . The calculated structure factors included corrections for anomalous dispersion from the usual tabulation. The structure was refined using the SHELXL-2014 program from the SHELX suite of crystallographic software.³¹ Graphic plots were produced using the XP program suite.³² Additional information and other relevant literature references can be found in the reference section of this website (<http://xray.chem.uwo.ca>).

Table 3.1: Crystallographic data of compound **3.5c**

CCDC #	1434234
Formula	C ₉₅ H ₁₂₃ Ge ₂ O ₂
Formula Weight (<i>g/mol</i>)	1442.11
Crystal Color and Habit	colourless plate
Crystal System	triclinic
Space Group	P-1
Temperature, K	150
<i>a</i> , Å	12.871(7)
<i>b</i> , Å	16.645(10)
<i>c</i> , Å	23.354(13)
α , °	71.593(14)

$\beta, ^\circ$	87.449(7)
$\gamma, ^\circ$	67.404(8)
$V, \text{Å}^3$	4366(4)
Number of reflections to determine final unit cell	9904
Z	2
F(000)	1546
R_{merge}	0.0951
Number of parameters in least-squares	893
R_1	0.0532
wR_2	0.1288
R_1 (all data)	0.0915
wR_2 (all data)	0.1487
GOF	1.011
Maximum shift/error	0.001

3.6 References

1. (a) Sekiguchi, A.; Kinjo R.; Ichinohe, M. *Science* **2004**, *305*, 1755; (b) Wiberg, N.; Vasisht, S. K.; Fischer, G.; Mayer, P. *Z. Anorg. Allg. Chem.* **2004**, *630*, 1823; (c) Sasamori, T.; Hironaka, K.; Sugiyama, Y.; Takagi, N.; Nagase, S.; Hosoi, Y.; Furukawa, Y.; Tokitoh, N. *J. Am. Chem. Soc.* **2008**, *130*, 13856; (d) Ishida, S.; Sugawara, R.; Misawa Y.; Iwamoto, T. *Angew. Chem. Int. Ed.* **2013**, *52*, 12869.
2. (a) Stender, M.; Phillips, A. D.; Wright R. J.; Power, P. P. *Angew. Chem. Int. Ed.* **2002**, *41*, 1785; (b) Hadlington, T. J. Hermann, M.; Li, J.; Frenking G.; Jones, C. *Angew. Chem. Int. Ed.* **2013**, *52*, 10199; (c) Sugiyama, Y.; Sasamori, T.; Hosoi, Y.; Furukawa, Y.; Takagi, N.; Nagase S.; Tokitoh, N. *J. Am. Chem. Soc.* **2006**, *128*, 1023.
3. (a) Power, P. P. *Organometallics* **2007**, *26*, 4362; (b) Rivard, E.; Power, P. P. *Inorg.*

- Chem.* **2007**, *46*, 10047; (c) Sekiguchi, A. *Pure Appl. Chem.* **2008**, *80*, 447; (d) Fischer R. C.; Power, P. P. *Chem. Rev.* **2010**, *110*, 3877; (e) Asay M.; Sekiguchi, A. *Bull. Chem. Soc. Japan* **2012**, *85*, 1245; (f) Caputo C. A. Power, P. P. *Organometallics* **2013**, *32*, 2278.
4. (a) Power, P. P. *Nature* **2010**, *463*, 171; (b) Power, P. P. *Acc. Chem. Res.* **2011**, *44*, 627; (c) Power, P. P. *Chem. Rec.* **2012**, *12*, 238.
5. Kinjo, R.; Ichinohe, M.; Sekiguchi, A.; Takagi, N.; Sumimoto, M.; Nagase, S. *J. Am. Chem. Soc.* **2007**, *129*, 7766.
6. Han, J. S.; Sasamori, T.; Mizuhata Y.; Tokitoh, N. *Dalton Trans.* **2010**, *39*, 9238.
7. Cui, C.; Olmstead, M. M.; Power, P. P. *J. Am. Chem. Soc.* **2004**, *126*, 5062.
8. Cui, C.; Olmstead, M. M.; Fettinger, J. C.; Spikes G. H.; Power, P. P. *J. Am. Chem. Soc.* **2005**, *127*, 17530.
9. Hadlington, T. J.; Li, J.; Hermann, M.; Davey, A.; Frenking, G.; Jones, C. *Organometallics* **2015**, *34*, 3175.
10. Zhao, L.; Jones C.; Frenking, G. *Chem. Eur. J.* **2015**, *21*, 12405.
11. Sasamori, T.; Sugahara, T. Agou, T., Guo, J. D.; Nagase, S.; Streubel, R.; Tokitoh, N. *Organometallics* **2015**, *34*, 2106.
12. Milnes, K. K.; Pavelka L. C.; Baines, K. M. *Chem. Soc. Rev.* **2016**, *45*, 1019.
13. (a) Gottschling, S. E.; Grant, T. N.; Milnes, K. K.; Jennings M. C.; Baines, K. M. *J. Org. Chem.* **2005**, *70*, 2686; (b) Milnes, K. K.; Gottschling, S. E.; Baines, K. M. *Org. Biomol. Chem.* **2004**, *2*, 3530.
14. Bauld, N. L. *Radicals, Ion Radicals and Triplets*; Wiley-VCH, Chichester, 1997.
15. Hurni, K. L.; Baines, K. M. *Chem. Commun.* **2011**, *47*, 8382.

16. Sasamori, T.; Sugahara, T.; Agou, T.; Sugamata, K.; Guo, J. D.; Nagase S.; Tokitoh, N. *Chem. Sci.* **2015**, *6*, 5526.
17. Pavelka, L. C.; Hanson, M. A.; Staroverov V. N.; Baines, K. M. *Can. J. Chem.* **2015**, *93*, 134.
18. Woodward, R. B.; Hoffman, R. *Angew. Chem. Int. Ed.* **1969**, *8*, 781.
19. Nagasaki S.; Inagaki, S. *Tetrahedron Lett.* **2008**, *49*, 3578.
20. A $[2\pi_s + 2\pi_a]$ reaction pathway may be possible because of the long Ge-Ge bond and diffuse orbitals on germanium.
21. Baines, K. M.; Cooke J. A.; Vittal, J. J. *J. Chem. Soc. Chem. Commun.* **1992**, 1484.
22. A 1,2-dihydrodigermene was isolated in the addition of **3.5** to tetramesityldigermene, which was proposed to be formed from ring closure of an intermediate diradical prior to ring opening.¹⁵ Here, it is the *complete* absence of evidence for a ring-opened product that suggests the absence of a diradical intermediate.
23. For example see: (a) Summerscales, O. T.; Jiménez-Halla, J. O. C.; Merino G.; Power, P. P. *J. Am. Chem. Soc.* **2011**, *33*, 180; (b) Tokitoh, N.; Kishikawa, K.; Okazaki, R.; Sasamori, T.; Nakata, N.; Takeda, N. *Polyhedron* **2002**, *21*, 563; (c) Meiners, F.; Saak, W.; Weidenbruch, M. *Organometallics* **2000**, *19*, 2835; (d) Kishikawa, K.; Tokitoh N.; Okazaki, R. *Chem. Lett.* **1998**, *8*, 239.
24. Tashkandi, N. Y.; Pavelka, L. C.; Hanson, M. A.; Baines, K. M. *Can. J. Chem.* **2014**, *92*, 462.
25. Due to the complexity of the ¹H NMR spectrum of **3.5c** and the possible presence of isomers, all assignments are tentative.
26. Bruker-AXS, SAINT version 2013.8, **2013**, Bruker-AXS, Madison, WI 53711, USA.

27. Bruker-AXS, SADABS version 2012.1, **2012**, Bruker-AXS, Madison, WI 53711, USA.
28. Bruker-AXS, XS version 2013.12, **2013**, Bruker-AXS, Madison, WI 53711, USA.
29. Sluis, P. V. D.; Spek, A. L. *Acta Cryst.* **1990**, *A46*, 194 (in this manuscript, SQUEEZE is referred to as the BYPASS procedure).
30. Spek, A. L. *J. Appl. Cryst.* **2003**, *36*, 7.
31. Sheldrick, G. M. *Acta Cryst.* **2015**, *C71*, 3.
32. Bruker-AXS, XP version 2013.1, **2013**, Bruker-AXS, Madison, WI 53711, USA.

Chapter 4

Addition of Nitromethane to a Disilene and a Digermene: Comparison to Surface Reactivity and the Facile Formation of 1,3,2-dioxazolidines*

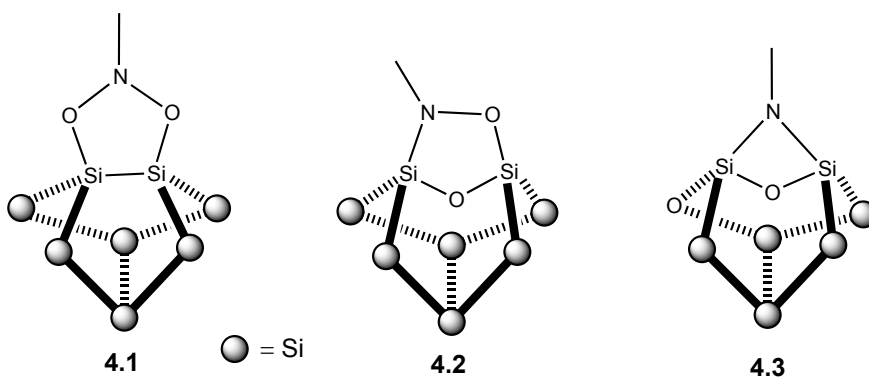
4.1 Introduction

By attaching complex organic molecules to Group 14 semiconductors, hybrid devices, having a semiconductor substrate and an organic surface, are possible with a range of potential applications designed to take advantage of the chemical function of the organic layer. With this objective in mind, the organic functionalization of silicon and germanium surfaces has been widely studied.¹ Of particular interest to us is the functionalization of Si- and Ge(100)- 2×1 reconstructed surfaces which are composed of rows of surface dimers isolated by trenches.^{1e} An effective molecular model for the dimers on the Si and Ge(100) reconstructed surfaces can provide valuable insight into the chemistry at the surface including the structure of surface adducts. Such insight will be critical if a complex functional molecule is to be attached to the surface through a primary layer. Based on our previous work,² we have proposed that tetramesityldisilene³ ($\text{Mes}_2\text{Si}=\text{SiMes}_2$, Mes = 2,4,6- $\text{Me}_3\text{C}_6\text{H}_2$) and tetramesityldigermene⁴ ($\text{Mes}_2\text{Ge}=\text{GeMes}_2$) can serve as effective molecular models for the corresponding Si or Ge(100)- 2×1 reconstructed surfaces, respectively.

* A version of sections 4.1, 4.2 and 4.3 of this chapter have been published. Nada Y. Tashkandi, Fredrick Parsons, Jiachang Guo, Kim M. Baines, Addition of Nitromethane to a Disilene and a Digermene: Comparison to Surface Reactivity and the Facile Formation of 1,3,2- Dioxazolidines. *Angew. Chem. Int. Ed.* **2014**, *54*, 1612.

The main differences between the molecular and surface species are the geometry about the double bond (planar in the case of the disilene⁵ and *trans*-bent in the case of the digermene^{2c} versus *cis* bent on the surface) and the nature of the substituents (aryl versus silyl/germyl). Despite these differences we have shown that the reactivity of surface disilenes and digermenes is comparable to their molecular counterparts.²

The addition of nitromethane to the Si(100)- 2×1 surface has been studied.⁶ Three different binding energy features were identified by N 1s X-ray photoelectron spectroscopy and assigned to three different *types* of adducts with the aid of DFT calculations: 1) cycloadduct **4.1**, with two NO bonds, present as a minor product, 2) adduct(s) **4.2** where one oxygen of the nitro group inserted into the silicon lattice; and 3) adduct(s) **4.3** where the two oxygen atoms of the nitro group have inserted into the silicon lattice (major product). The authors proposed that adduct **4.1** is metastable and rapidly undergoes rearrangement creating Si-O bonds at the expense of N-O bonds (Scheme 4.1).



Scheme 4.1

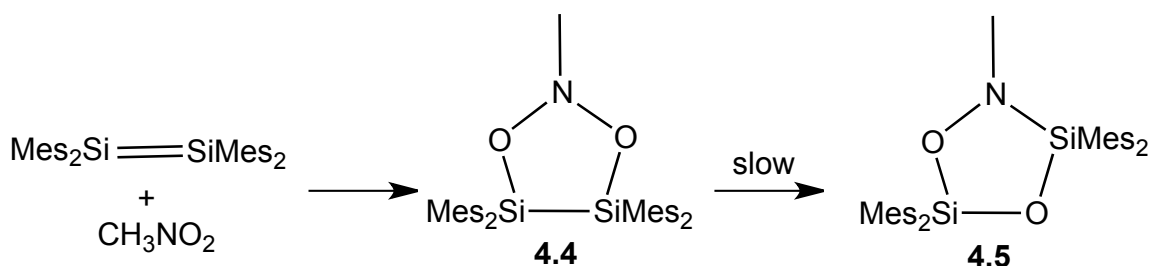
The formation of adduct **4.1** suggests a rather unusual and interesting reaction pathway for nitroalkanes: 1,3-dipolar cycloaddition through the nitro functional group. Thus, given our use of tetramesityldisilene as a model for the Si(100) reconstructed surface, we

have investigated the reaction of nitromethane with tetramesityldisilene and compared our results to those on the surface. For comparison purposes, we have also examined the addition of nitromethane to tetramesityldigermene.

4.2 Results

4.2.1 Addition of Nitromethane to Tetramesityldisilene

The addition of excess nitromethane to a bright yellow solution of tetramesityldisilene in hexanes or C_6D_6 at room temperature gave a pale yellow solution. Removal of the solvent yielded a pale yellow solid which revealed the presence of compound **4.4** along with minor amounts of at least two additional products (**4.5** and **4.6**) in a 10: 1: 1 ratio, respectively, by 1H NMR spectroscopy (Scheme 4.2 and 4.3). The high resolution mass spectral data of **4.4** and the isotopic pattern of the signal assigned to the molecular ion were consistent with the molecular formula, $Si_2C_{37}H_{47}NO_2$, a 1:1 adduct between tetramesityldisilene and nitromethane. The 1H NMR spectrum of **4.4** revealed the presence of two sets of signals assigned to two non-equivalent mesityl groups and a singlet at 3.10 ppm that integrated to 3H indicating that a methyl group, most likely attached to nitrogen, was present. Only one signal, at 1 ppm, in the ^{29}Si dimension of the ^{29}Si - 1H gHMBC spectrum of **4.4** correlated to the signal at 3.10 ppm in the 1H dimension. The structure of **4.4** was unambiguously identified in the solid state as 4,4,5,5-tetramesityl-1,3,2,4,5-dioxazadisilolidine by single crystal X-ray diffraction (Figure 4.1). All bond lengths and angles in **4.4** are within normal ranges; the structural metrics of the ONO linkage are similar to those of a carbon analog.⁷



Scheme 4.2

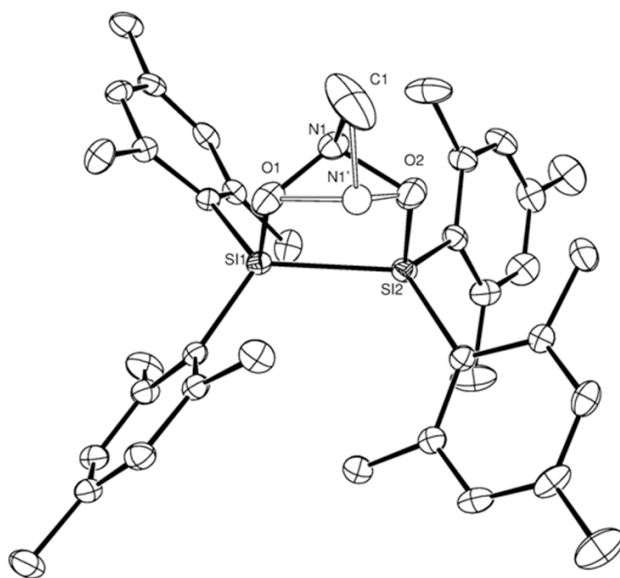
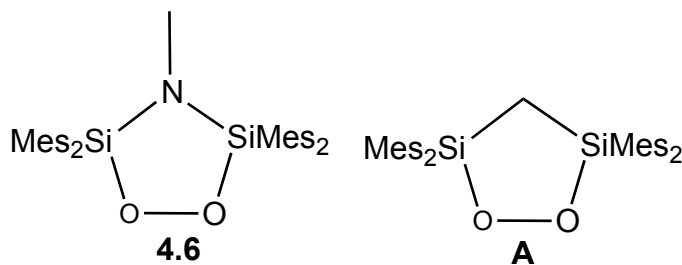


Figure 4.1 Displacement ellipsoid plot **4.4** (ellipsoids set at 50% probability level; hydrogen atoms are omitted for clarity) showing the disorder located at the nitrogen atom. Selected bond lengths (Å) and angles (deg): Si1-O1 = 1.701(17), Si1-Si2 = 2.41(9), Si2-O2 = 1.699(18), O1-N1 = 1.36(3), O2-N1 = 1.47(3); O1-Si1-Si2 = 88.47(6), O2-Si2-Si1 = 87.81(6), N1-O1-Si1 = 110.72(15), N1-O2-Si2 = 114.22(15), O1-N1-O2 = 109.7(2).

After a long period of time (months), adduct **4.4** was found to isomerize to **4.5** in solution. The ^1H NMR spectrum of **4.5** is similar to that of **4.4** with two sets of mesityl groups and a singlet at 3.20 ppm. The signal at 3.20 ppm, assigned to the NCH_3 group, and the signals at 2.36 and 6.64 ppm, assigned to one mesityl group, in the ^1H dimension of the ^{29}Si - ^1H gHMBC spectrum of **4.5** correlated to the signal at -21 ppm in the ^{29}Si

dimension and the signals at 2.55 and 6.64 ppm, assigned to a second mesityl group, correlated to the signal at -18 ppm in the ^{29}Si dimension. Based on the similarity of the ^{29}Si chemical shifts of **4.5** to those of the closely related N-phenyl analog,⁸ **4.5** was identified as 3,3,5,5-tetramesityl-1,4,2,3,5-dioxazadisilolidine.

The structures of a minor product (**4.6**) couldn't be assigned unambiguously as we were unable to separate the mixture either by TLC or recrystallization. Mass spectral data (EI and ESI) suggest the presence of only **4.4** and isomers; no signal could be assigned to a product of different mass. In the ^1H NMR spectrum of the crude reaction mixture, a signal was observed at 3.16 ppm and assigned to CH_3 on N. The signal at 3.16 ppm correlates to a signal at 18 ppm in ^{29}Si dimension of the ^{29}Si - ^1H gHMBC spectrum. The ^{29}Si chemical shift of 9.60 ppm was reported for the 1,2,3,5-dioxadisilolane **A**,⁹ and thus, we tentatively assign the structure of **4.6** as shown below in Scheme 4.3.

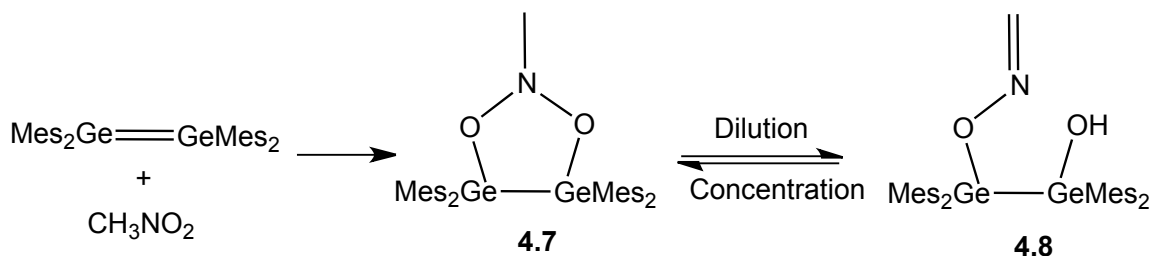


Scheme 4.3

4.2.2 Addition of Nitromethane to Tetramesityldigermene

The addition of excess nitromethane to a bright yellow solution of tetramesityldigermene in THF or hexanes at room temperature gave a clear, colorless solution. Evaporation of the solvent yielded a clear, pale yellow oil and analysis of the

product by ^1H NMR spectroscopy revealed the formation of compound **4.7**, which cleanly isomerizes to **4.8** when the concentration of the solution is lowered (Scheme 4.4).



Scheme 4.4

Adduct **4.7** was isolated by recrystallization from a saturated hexanes solution at low temperature. The ^1H NMR spectrum of a concentrated sample of **4.7** (~ 0.02 M) is similar to that of **4.4** with two sets of signals assigned to non-equivalent mesityl groups. The spectrum also revealed a singlet at 3.18 ppm assigned to a methyl group attached to nitrogen. Single crystal X-ray diffraction data unequivocally provided the structure of **4.7** (Figure 4.2), 4,4,5,5-tetramesityl-1,3,2,4,5-dioxadigermolidine. All bond lengths and angles are within normal ranges. The identity of the compound in solution was found to be dependent on the concentration of the solution. At higher concentration (~ 0.02 M), adduct **4.7** predominates, whereas at lower concentrations ($\sim 6 \times 10^{-3}$ M), **4.7** tautomerizes to **4.8**.

The ^1H and ^{13}C NMR spectra of **4.8** revealed the presence of two non-equivalent mesityl groups. Two doublets were also present in the ^1H NMR spectrum of **4.8**, at 5.87 and 6.68 ppm, with a coupling constant of 9 Hz. The chemical shifts of the two doublets suggest the presence of vinylic hydrogens. The magnitude of the geminal coupling

constant is consistent with that observed between the vinylic hydrogens in the structurally-related oxime, $(\text{HO}(\text{CH}_2)_2\text{ON}=\text{CH}_2, J = 8 \text{ Hz})$.¹⁰ After an extended period of time (months), compound **4.8** predominates in solution, concentration of the solution did not result in the isomerization of **4.8** back to **4.7**. Monitoring the conversion of **4.7** to **4.8** over two weeks by ^1H NMR spectroscopy revealed direct conversion with no evidence of any intermediate.

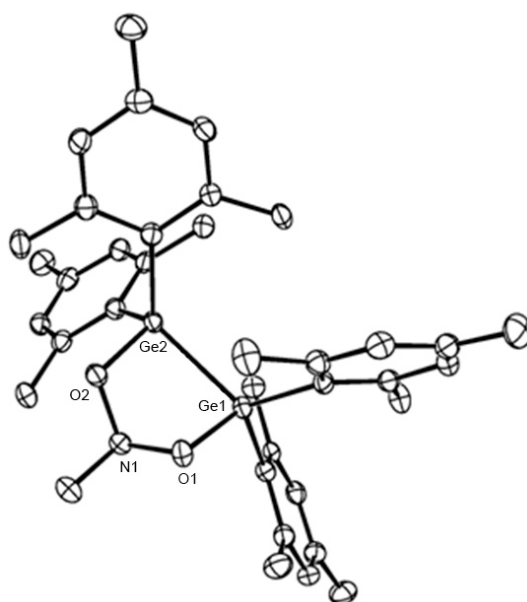


Figure 4.2 Displacement ellipsoid plot of **4.7** (ellipsoids set at 50% probability level; hydrogen atoms are omitted for clarity). Selected bond lengths (Å) and angles (deg): Ge1-O1 = 1.835(2), Ge2-O2 = 1.838(2), Ge1-Ge2 = 2.4963(7), O1-N1 = 1.447(3), O2-N1 = 1.454(3), N1-C1 = 1.461(4); O1-Ge1-Ge2 = 87.27(6); O2-Ge2-Ge1 = 86.74(6), N1-O2-Ge2 = 103.37(15), N1-O1-Ge1 = 100.68(15), O1-N1-O2 = 105.41(19).

4.3 Discussion

Adducts **4.4** and **4.7** appear to be derived from a formal [3+2] cycloaddition of nitromethane to the dimetallene to give the unusual 1,3,2-dioxazolidine ring system. The two different mesityl groups observed by ^1H NMR spectroscopy for **4.4** and **4.7** leads to

the conclusion that the nitrogen does not undergo the rapid inversion typically observed in amines. DFT calculations performed at the TPSS/TPSS¹¹/6-31G(d) level of theory show that the barrier for inversion at the nitrogen in the model compound MeN(OGeH₃)₂ is 112 kJ/mol, which is in reasonable agreement with the estimated inversion barrier for the nitrogen in the parent 2H-1,3,2-dioxazolidine (111 kJ/mol)¹² and sufficiently high for the nitrogen to be configurationally stable.¹³ As a consequence, the mesityl groups exhibit two sets of signals by NMR spectroscopy.

Compounds **4.4** and **4.7** are new heterocyclic ring systems containing the O-N-O moiety and are formed easily and in high yield. It is interesting to compare the chemistry of the disilene and digermene with nitromethane to that of an alkene. The reaction of alkenes with nitroalkanes generally proceeds through the nitronate isomer and not by cycloaddition through only the nitro group.¹⁴ The 1,3,2-dioxazolidine ring system can be generated by a limited number of methods;¹⁵ however, the synthesis of these ring systems via cycloaddition of a nitro group to an alkene only occurs under special circumstances. Thermally, the reaction proceeds only between highly strained alkenes and aromatic nitro compounds.¹⁶ The photochemical 1,3-addition of a nitro group to an alkene forming a 1,3,2-dioxazolidine is also known.^{6,17} Thus, the reactivity of nitromethane towards tetramesityldisilene and tetramesityldigermene in terms of both kinetics and reaction pathway was somewhat surprising. The addition reactions are undoubtedly facilitated by weakness of the M=M bond and the strength of M-O bond.

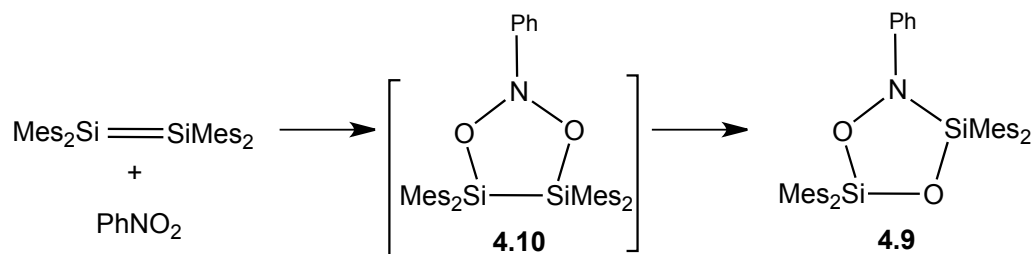
Although both the silicon and the germanium analogs of the 1,3,2-dioxazolidine ring systems are somewhat stable in solution at room temperature, both are prone to rearrangement albeit by two different pathways. In the case of silicon, the formation of

two isomeric products in minor yield was evident in the crude product mixture (i.e. **4.5** and **4.6**) and **4.5** grew in over time at the expense of **4.4**. Isomer **4.5** is derived from the cleavage of an N-O bond in favor of the formation of a Si-O bond to give the 1,4,2-dioxazolidine ring system, *i.e.* the oxygen inserted into the former Si-Si bond. The 1,4,2,3,5-dioxazadisilolidine ring system was found to be more stable than the 1,3,2-isomer by 342 kJ/mol as determined by DFT calculations (M06/6-31G(d)). In comparison, the addition of nitromethane to the Si(100) reconstructed surface produces an adduct(s) where both oxygen atoms have inserted into the underlying silicon matrix as the major product. With mesityl groups as the substituents in the molecular system, insertion of oxygen into the Si-C bond of the substituent is less thermodynamically stable in comparison to insertion into a Si-Si bond, and thus, does not occur; the substituents of the molecular disilene have a major influence on the products formed. In comparison, the analogous adduct where one oxygen has inserted between the silicon atoms of a surface dimer (**4.2**, Scheme 4.1) is only 82 kJ/mol more stable than adduct **4.1** because of the constrained geometry of the subsurface silicon substituents, and thus, is not formed in appreciable quantities.^{6b} Notably, neither the molecular nor the surface reactions were carried to equilibrium, and thus, the relative ratios of the products is kinetically-, and not thermodynamically-controlled.

In the case of germanium, the 1,3,2-dioxazolidine ring system opens to give oxime **4.8** which is stabilized by 236 kJ/mol compared to the 1,3,2-dioxazolidine ring system and by 40 kJ/mol compared to the 1,4,2- dioxazolidine isomer as determined by DFT calculations (M06/6-31G(d)). The weaker Ge-O bond apparently does not provide a sufficient driving force for rearrangement to the 1,4,2-dioxazolidine ring system and

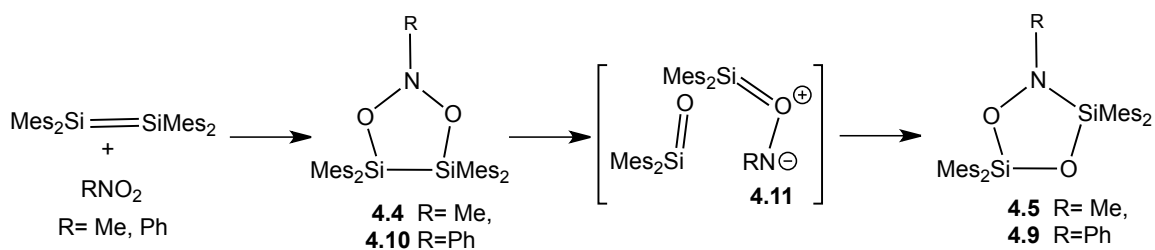
suggests that the addition of nitromethane to the Ge(100)- 2×1 reconstructed surface may be simpler in comparison to the multiple products formed on the silicon surface.

It is also interesting to compare the results of the addition of nitromethane to tetramesityldisilene to that of nitrobenzene performed by West and coworkers.⁸ The addition of nitrobenzene to $\text{Mes}_2\text{Si}=\text{SiMes}_2$ produces 1,4,2,3,5-dioxazadisilolidine **4.9** as the only product in comparison to the formation of **4.4**. The mechanism for the formation of **4.9** was postulated by West to proceed through one of two pathways: [3+2] cycloaddition to give **4.10** followed by rearrangement to form **4.9** (Scheme 4.5) or [2+2] cycloaddition to give a 1,2,3,4-oxazadisiletidine-*N*-oxide, followed by rearrangement to give **4.9**. Evidence for the former pathway was provided by monitoring the reaction at low temperature by ^{29}Si NMR spectroscopy. The formation of an intermediate with only one ^{29}Si NMR signal, at 0.64 ppm, was observed suggesting the formation of **4.10**. More recently, a DFT computational study of the relative stability of the adducts of nitromethane to a model of the Si(100) reconstructed surface suggests that the 1,2,3,4-oxazadisiletidine- *N*-oxide ring system is unstable relative to the 1,4,2,3,5-dioxazadisilolidine ring system.^{6b} Notably, the ^{29}Si chemical shift of **4.10** is similar to that of **4.4**, and thus, our results provide additional support for the [3+2] dipolar cycloaddition route as proposed by West. In contrast to **4.4**, **4.10** undergoes an apparently facile rearrangement to **4.9** compared to the slow conversion of **4.4** to the 1,4,2,3,5-dioxazadisilolidine ring system **4.5** which occurs over an extended period of time in solution at room temperature.



Scheme 4.5

We propose that the formation of **4.5** (and **4.9**) follows a mechanism similar to the well-known Criegee mechanism for the formation of ozonides (Scheme 4.6).¹⁸ Ring cleavage of **4.4** (or **4.10**) takes place initially to give dimesitylsilanone and the zwitterionic species, **4.11**. Recombination of these two species gives **4.5/4.9**. The rate of this rearrangement appears to depend on the stability of species **4.11**. With a substituent which can stabilize the negative charge at nitrogen, such as a phenyl substituent, rearrangement is rapid; however, with an alkyl substituent at nitrogen (such as methyl), rearrangement is slow (Scheme 4.6).



Scheme 4.6

4.4 Conclusions

In summary, we have presented a facile way to synthesize the unusual 1,3,2,4,5-dioxazadisilolidine and –digermolidine ring systems and provided some insight into their rearrangement chemistry. Our work allows for a coherent picture of the chemistry between nitro compounds and molecular and surface disilenes (and digermenes) to emerge. We continue to investigate the scope of the reaction between nitro compounds and Group 14 ditetrelenes.

4.5 Experimental

General Experimental Details

All air sensitive reactions were performed under an inert atmosphere of argon or nitrogen using standard Schlenk techniques or a glove box. Hexanes and THF were obtained from a solvent purification system (SPS-400-5, Innovative Technology Inc). Nitromethane was purified by distilling from CaH₂ and was stored over 4Å molecular sieves. Electron impact mass spectra were recorded on a MAT model 8400 mass spectrometer using an ionizing voltage of 70 eV. Mass spectral data are reported in mass-to-charge units, *m/z*. X-ray data were obtained using a Bruker Apex II Diffractometer. Ge₃MeS₆¹⁹ and (Me₃Si)₂SiMeS₂²⁰ were synthesized according to the literature procedures.

Addition of Nitromethane to Tetramesityldisilene

MeS₂Si(SiMe₃)₂ (50 mg, 0.12 mmol) was placed in a quartz tube and dissolved in hexanes (3 mL) and the solution was irradiated ($\lambda = 254$ nm) in a quartz Dewar for ~18 h. The yellow solution was cooled to -60 °C during the irradiation by circulating cold methanol through the quartz Dewar. Nitromethane (0.1 mL, 2 mmol) was added to the

yellow solution at room temperature and the reaction was allowed to stir. After 5 min, the solution became colorless. The hexanes were evaporated giving a pale yellow oil which was dissolved in a minimum amount of hexanes. The flask was placed in the freezer (-14 °C) for 24 h. A precipitate formed and the solid was isolated by decantation. The solid was triturated with pentane yielding a colorless, clear crystals (57 mg, 80%). After sitting in solution at room temperature for a long period of time (3 months), compound **4.4** converted to **4.5** and other unidentified compounds. All attempts to purify **4.4** or **4.5** resulted in decomposition.

4.4: colorless, clear solid; ^1H NMR (C_6D_6 , 600 MHz) δ [6.67 (s, Mes *m*-H), 6.63 (s, Mes *m*-H), together 8H], 3.10 (s, 3H, NCH₃), [2.43 (s, Mes *o*-CH₃), 2.42 (s, Mes *o*-CH₃), together 24H], [2.06 (s, Mes *p*-CH₃), 2.04 (s, Mes *p*-CH₃), together 12H]; ^{13}C NMR (C_6D_6 , 100 MHz) δ 145.49 (Mes *o*-C), 144.75 (Mes *o*-C), 139.46 (Mes *p*-C), 139.23 (Mes *p*-C), 133.90 (Mes *i*-C), 132.46 (Mes *i*-C), 129.46 (Mes *m*-CH), 53.10 (CH₃), 25.26 (Mes *o*-CH₃), 24.52 (Mes *o*-CH₃), 20.98 (Mes *p*-CH₃); ^{29}Si NMR (C_6D_6 , 50 MHz) δ 1 ppm; High-Resolution EI-MS for $\text{C}_{37}\text{H}_{47}\text{NO}_2\text{Si}_2$ (M^+) (m/z) calc. 593.3145, found 593.3149.

4.5: ^1H NMR (C_6D_6 , 600 MHz) δ 6.64 (s, 8H, Mes *m*-H), 3.21 (s, 3H, NCH₃), 2.55 (s, 12H, Mes *o*-CH₃), 2.36 (s, 12H, Mes *o*-CH₃), 2.05 (s, 6H, Mes *p*-CH₃), 2.03 (s, 6H, Mes *p*-CH₃); ^{13}C NMR (C_6D_6 , 100 MHz) δ 144.33 (Mes *o*-C), 143.55 (Mes *o*-C), 139.58 (Mes *p*-C), 139.56 (Mes *p*-C), 132.42 (Mes *i*-C), 131.04 (Mes *i*-C), 129.28 (Mes *m*-C), 129.23 (Mes *m*-C), 37.71 (CH₃), 23.22 (Mes *o*-CH₃), 22.80 (Mes *o*-CH₃), 21.08 (Mes *p*-CH₃), 21.06 (Mes *p*-CH₃); ^{29}Si NMR (C_6D_6 , 50 MHz) δ -22, -18 ppm; High-Resolution EI-MS for $\text{C}_{37}\text{H}_{47}\text{NO}_2\text{Si}_2$ (M^+) (m/z) calc. 593.3145, found 593.3146.

Addition of Nitromethane to Tetramesityldigermene

Ge₃Mes₆ (0.100 g, 0.107 mmol) was placed in a quartz tube^a and dissolved in THF (5 mL) and irradiated ($\lambda = 350$ nm) in a quartz Dewar^a at -60 °C for ~18 h to give yellow solution. The solution was cooled during the irradiation by circulating cold methanol through the quartz Dewar. Nitromethane (0.1 mL, 2 mmol) was added to the yellow solution at room temperature and the reaction was allowed to stir. After 5 min, the solution became colorless. The solvent was evaporated giving a clear, colorless oil. The oil was dissolved in a minimum amount of hexanes. The flask was placed in a freezer (-14 °C) for 24 h, yielding crystalline material, which was isolated by decantation. The crystals were triturated yielding colorless, clear crystals of **7** (65 mg, 89%). A suitable crystal was obtained by recrystallization of the material from pentane under an inert atmosphere. Compound **4.7** converted to **4.8** upon dilution ($\sim 6 \times 10^{-3}$ M). **4.7**: white solid; mp: 189-92 °C; ¹H NMR (C₆D₆, 400 MHz ~ 0.02 M) δ [6.67 (s, *m*-Mes), 6.66 (s, *m*-Mes), together 8H], 3.19 (s, 3H, NCH₃), 2.48 (s, 12H, Mes *o*-CH₃), 2.43 (s, 12H, Mes *o*-CH₃), 2.05 (s, 12H, Mes *p*-CH₃); ¹³C NMR (C₆D₆, 100 MHz) δ 143.78 (Mes *o*-C), 143.34 (Mes *o*-C), 139.18 (Mes *p*-C), 139.00 (Mes *p*-C), 138.67 (Mes *i*-C), 137.35 (Mes *i*-C), 129.48 (Mes *m*-CH), 129.38 (Mes *m*-CH), 52.96 (NCH₃), 24.64 (Mes *o*-CH₃), 23.93 (Mes *o*-CH₃), 20.94 (Mes *p*-CH₃); High resolution EI-MS *m/z* for C₃₇H₄₇NO₂⁷⁰Ge⁷²Ge Calc. 679.2070, found 679.2066; EI-MS *m/z* 683 (5), 655 (Mes₄⁷⁴Ge⁷²GeO₂H, 9), 535 (Mes₃⁷⁴Ge⁷²GeO₂, 9), 431 (Mes₃⁷⁴Ge, 35), 329 (Mes₂⁷⁴GeOH, 100), 312 (Mes₂⁷⁴Ge, 24), 192 (Mes⁷²GeH, 24), 119 (Mes, 32); Anal. Calc. for C₃₇H₄₇NO₂Ge₂: C 65.06, H 6.94, N 2.05, found C 65.00, H 6.90, N 1.99.

^a A quartz tube and Dewar were used but a Pyrex Dewar can be used instead.

4.8: Colorless liquid; ^1H NMR (C_6D_6 , 600 MHz $\sim 6 \times 10^{-3}\text{M}$) δ [6.71 (s, Mes *m*-H), 6.70 (s, Mes *m*-H), 6.69 (d, $J = 9.6$ Hz, $\text{CH}_2=\text{N}$), together 9H], 5.88 (d, 1H, $J = 9.0$ Hz, $\text{CH}_2=\text{N}$), [2.47 (s, Mes *o*- CH_3), 2.45 (s, Mes *o*- CH_3), together 24H], [2.08 (s, Mes *p*- CH_3), 2.07 (s, Mes *p*- CH_3), together 12H]; ^{13}C NMR (C_6D_6 , 150 MHz) δ 143.72 (Mes *o*-C), 143.62 (Mes *o*-C), 139.03 (Mes *p*-C or $\text{CH}_2=\text{N}$), 138.78 ($\text{CH}_2=\text{N}$ or Mes *p*-C), 138.57 (Mes *i*-C), 138.48 (Mes *i*-C), 137.83 (Mes *p*-C), 129.60 (Mes *m*-C), 24.34 (Mes *o*- CH_3), 23.96 (Mes *o*- CH_3), 20.95 (Mes *p*- CH_3); ESI-MS m/z for $\text{C}_{37}\text{H}_{47}\text{NO}_2$ $^{70}\text{Ge}^{70}\text{GeNa}$ Calc. 700.1990, found 700.1980.

DFT Calculations

First principles calculations were performed using Gaussian 09²¹ on the Shared Hierarchical Academic Research Computing Network (SHARCNET, www.sharcnet.ca). Calculations were performed on an 8 core Xeon 2.83 GHz CPU with 16 GB memory. All calculations were performed at the TPSSTPSS²²/6-31G(d) level of theory.

Crystallographic Details for 4.4

Data Collection and Processing. The sample was mounted on a Mitegen polyimide micromount with a small amount of Paratone N oil. All X-ray measurements were made on a Bruker Kappa Axis Apex2 diffractometer at a temperature of 110 K. The unit cell dimensions were determined from a symmetry constrained fit of 9432 reflections with $4.94^\circ < 2\theta < 64.86^\circ$. The data collection strategy was a number of ω and φ scans which collected data up to 65.33° (2θ). The frame integration was performed using SAINT.²³ The resulting raw data were scaled and absorption corrected using a multi-scan averaging of symmetry equivalent data using SADABS.²⁴

Structure Solution and Refinement. The structure was solved by direct methods using the SIR2011 program.²⁵ All non-hydrogen atoms were obtained from the initial solution. The hydrogen atoms were introduced at idealized positions and were allowed to ride on the parent atom. The N1 was disordered two sites giving rise to an alternative set of atomic position as N1 and N1' respectively. The major occupancy for the predominant conformation is 0.63. The structural model was fit to the data using full matrix least-squares based on F^2 . The calculated structure factors included corrections for anomalous dispersion from the usual tabulation. The structure was refined using the SHELXL-2014 program from the SHELXTL suite of crystallographic software.²⁶ Graphic plots were produced using the NRCVAX program suite.²⁷

Crystallographic details for 4.7

Data Collection and Processing. The sample was mounted on a Mitegen polyimide micromount with a small amount of Paratone N oil. All X-ray measurements were made on a Bruker Kappa Axis Apex 2 diffractometer at a temperature of 110(2) K. The unit cell dimensions were determined from a symmetry constrained fit of 7589 reflections with $5.2^\circ < 2\theta < 49.98^\circ$. The data collection strategy was a number of ω and φ scans which collected data up to 58.388° (2θ). The frame integration was performed using SAINT.²³ The resulting raw data were scaled and absorption corrected using a multi-scan averaging of symmetry equivalent data using SADABS.²⁴

Structure Solution and Refinement. The structure was solved using the SHELXL-XS program. All non-hydrogen atoms were obtained from the initial solution. The hydrogen atoms were introduced at idealized positions and were allowed to ride on the parent atom. The structural model was fit to the data using full matrix least-squares based on F^2 . The

calculated structure factors included corrections for anomalous dispersion from the usual tabulation. The structure was refined using the SHELXL-2013 (Sheldrick, 2013) program from the SHELXTL program package.²⁶ Graphic plots were produced using the NRCVAX program suite.²⁷

Table 4.1 Crystallographic data for compounds **4.4** and **4.7**

Parameter	4.7	4.4
Formula	C ₃₇ H ₄₇ Ge ₂ NO ₂	C ₃₇ H ₄₇ Si ₂ NO ₂
Formula Weight (g/mol)	682.93	593.93
Crystal Color and Habit	colourless prism	colourless prism
Crystal System	monoclinic	triclinic
Space Group	P 2 ₁ /c	P -1
Temperature, K	110	110
a, Å	11.597(3)	11.634(4)
b, Å	9.099(2)	12.088(3)
c, Å	31.324(8)	12.284(4)
α, °	90	88.658(14)
β, °	98.682(9)	89.621(15)
γ, °	90	72.271(15)
V, Å ³	3267.4(15)	1645.0(9)
Number of reflections to determine final unit cell	7589	9432
Min and Max 2θ for cell determination, °	5.2, 49.98	4.94, 64.86
Z	4	2
F(000)	1424	640
ρ (g/cm)	1.388	1.199
λ, Å, (MoKα)	0.71073	0.71073
μ, (cm ⁻¹)	1.873	0.141
Max 2θ for data collection, °	58.388	65.33
R _{merge}	0.0933	0.0317
R ₁	0.0450	0.0749
wR ₂	0.1134	0.2048
R ₁ (all data)	0.0767	0.1036
wR ₂ (all data)	0.1328	0.2285
GOF	0.961	1.042

4.6 References

1. (a) Kachian, J. S.; Wong, K. T.; Bent, S. F. *Acc. Chem. Res.* **2010**, *43*, 346; (b) Hamers, R. J. *Annu. Rev. Anal. Chem.* **2008**, *1*, 707; (c) Loscutoff, P. W.; Bent, S. F. *Annu. Rev. Phys. Chem.* **2006**, *57*, 467; (d) Bilić, A.; Reimers, J. R.; Hush, N. S. In *Properties of Single Organic Molecules on Crystal Surfaces*; Grütter, P.; Hofer W.; Rosei, F., Eds.; Imperial College Press, London, 2006; p. 333; (e) Buriak, J. M. *Chem. Rev.* **2002**, *102*, 1271.
2. (a) Hardwick, J. A.; Pavelka, L. C.; Baines, K. M. *Dalton Trans.* **2012**, *41*, 609; (b) Hurni, K. L.; Baines, K. M. *Chem. Comm.* **2011**, *47*, 8382; (c) Hurni, K. L.; Rupar, P. A.; Payne, N. C.; Baines, K. M. *Organometallics* **2007**, *26*, 5569; (d) Gottschling, S. E.; Milnes, K. K.; Jennings, M. C.; Baines, K. M. *Organometallics* **2005**, *24*, 3811; (e) Gottschling, S. E.; Jennings, M. C.; Baines, K. M. *Can. J. Chem.* **2005**, *83*, 1568; (f) Samuel, M. S.; Baines, K. M. *J. Am Chem. Soc.* **2003**, *125*, 12702; (g) Samuel, M. S.; Jenkins, H. A.; Hughes, D. W.; Baines, K. M. *Organometallics* **2003**, *22*, 1603.
3. For a review of disilene chemistry see: Kira, M.; Iwamoto, T. *Adv. Organomet. Chem.* **2006**, *54*, 73.
4. For a review of digermene chemistry see: Tokitoh, N.; Okazaki, R. In *Chemistry of Organic Germanium, Tin and Lead Compounds*; Rappoport, Z. Eds.; Wiley, New York, 2002; *2*, pp. 843.
5. Fink, M. J.; Michalczyk, M. J.; Haller, K. J.; West, R.; Michl, J. *J. Chem. Soc. Chem. Commun.* **1983**, 1010.
6. (a) Eng, J.; Hubner, Jr., I. A.; Barriocanal, J.; Opila, R. L.; Doren, D. J. *J. Appl. Phys.* **2004**, *95*, 1963; (b) Barriocanal, J.; Doren, D. J. *J. Phys. Chem. B* **2000**, *104*, 12269.

7. Okada, K.; Saito, Y.; Oda, M. *J. Chem. Soc., Chem. Commun.* **1992**, 1731.
8. Gillette, G. R.; Maxka, J.; West, R. *Angew. Chem. Int. Ed.* **1989**, 28, 54.
9. Ando, W.; Kako, M.; Akasaka, T.; Nagase, S. *Organometallics* **1993**, 12, 1514.
10. Dixon, D. W.; Weiss, R. H. *J. Org. Chem.* **1984**, 49, 1187.
11. Tao, J.; Perdew, J. P.; Staroverov, V. N.; Scuseria, G. E. *Phys. Rev. Lett.* **2003**, 91, 146401.
12. Chervin, I. I.; Nosova, V. S.; Rudchenko, V. F.; Shevenko, V. I.; Kostyanovskii, R. G. *Khim. Geterotskl. Soedin.* **1988**, 24, 396.
13. F. Davis, R. H. Jenkins Jr. *Asymm. Synth.* **1989**, 314.
14. Ono, N. In *The Nitro Group in Organic Synthesis*; John Wiley & Sons, Inc.: 2002; pp 231.
15. (a) Rudchenko, V. F.; Shevchenko, V. I.; Kostyanovskii, R. G., *Khim. Geterotskl. Soedin.* **1989**, 3, 393; (b) Rudchenko, V. F.; Shevchenko, V. I.; Kostyanovskii, R. G., *Izv. Akad. Nauk SSSR, Ser. Khim.* **1985**, 1685; (c) Rudchenko, V. F.; Shtamburg, V. G.; Nasibov, Sh. S.; Chervin, I. I.; Kostyanovskii, R. G., *Izv. Akad. Nauk SSSR, Ser. Khim.* **1980**, 2181.
16. Leitich, J. *Angew. Chem. Int. Ed.* **1976**, 15, 372.
17. (a) Charlton, J. L.; de Mayo, P. *Can. J. Chem.* **1968**, 46, 1041; (b) Charlton, J. L.; Liao, C.C.; de Mayo, P. *J. Am. Chem. Soc.* **1971**, 93, 2463; (c) Buchi, G.; Ayer, D. E. *J. Am. Chem. Soc.* **1956**, 78, 689.
18. Kuczkowski, R. L. *Chem. Soc. Rev.* **1992**, 21, 79.
19. Hurni, K. L.; Rupar, P. A.; Payne, N. C.; Baines, K. M. *Organometallics* **2007**, 26,

5569.

20. Fink, M. J.; Michalczyk, M. J.; Haller, K. J.; Michl, J.; West, R. *Organometallics* **1984**, *3*, 793.

21. Frisch, M. J.; Trucks, G. W.; Schlegel, H. B.; Scuseria, G. E.; Robb, M. A.; Cheeseman, J. R.; Scalmani, G.; Barone, V.; Mennucci, B.; Petersson, G. A.; Nakatsuji, H.; Caricato, M.; Li, X.; Hratchian, H. P.; Izmaylov, A. F.; Bloino, J.; Zheng, G.; Sonnenberg, J. L.; Hada, M.; Ehara, M.; Toyota, K.; Fukuda, R.; Hasegawa, J.; Ishida, M.; Nakajima, T.; Honda, Y.; Kitao, O.; Nakai, H.; Vreven, T.; Montgomery, J. A., Jr.; Peralta, J. E.; Ogliaro, F.; Bearpark, M.; Heyd, J. J.; Brothers, E.; Kudin, K. N.; Staroverov, V. N.; Kobayashi, R.; Normand, J.; Raghavachari, K.; Rendell, A.; Burant, J. C.; Iyengar, S. S.; Tomasi, J.; Cossi, M.; Rega, N.; Millam, N. J.; Klene, M.; Knox, J. E.; Cross, J. B.; Bakken, V.; Adamo, C.; Jaramillo, J.; Gomperts, R.; Stratmann, R. E.; Yazyev, O.; Austin, A. J.; Cammi, R.; Pomelli, C.; Ochterski, J. W.; Martin, R. L.; Morokuma, K.; Zakrzewski, V. G.; Voth, G. A.; Salvador, P.; Dannenberg, J. J.; Dapprich, S.; Daniels, A. D.; Farkas, Ö.; Foresman, J. B.; Ortiz, J. V.; Cioslowski, J.; Fox, D. J.; Revision A1 ed.; Gaussian Inc.: Wallingford, CT, **2009**.

22. Tao, J.; Perdew, J. P.; Staroverov, V. N.; Scuseria, G. E. *Phys. Rev. Lett.* **2003**, *91*, 146401.

23. Bruker-Nonius, SAINT version 2012.12, **2012**, Bruker-Nonius, Madison, WI 53711, USA.

24. Bruker-Nonius, SADABS version 2012.1, **2012**, Bruker-Nonius, Madison, WI 53711, USA.

25. Burla, M. C.; Caliendo, R.; Camalli, M.; Carrozzini, B.; Cascarano, G. L.;
Giacovazzo, C.; Mallamo, M.; Mazzone, A.; Polidori, G.; Spagna, R. *J. Appl. Cryst.*
2012, *45*, 357.
26. Sheldrick, G. M. *Acta Cryst.* **2008**, *A64*, 112.
27. Gabe, E. J.; Le Page, Y.; Charland, J. P.; Lee, F. L.; White, P. S. *J. Appl. Cryst.* **1989**,
22, 384.

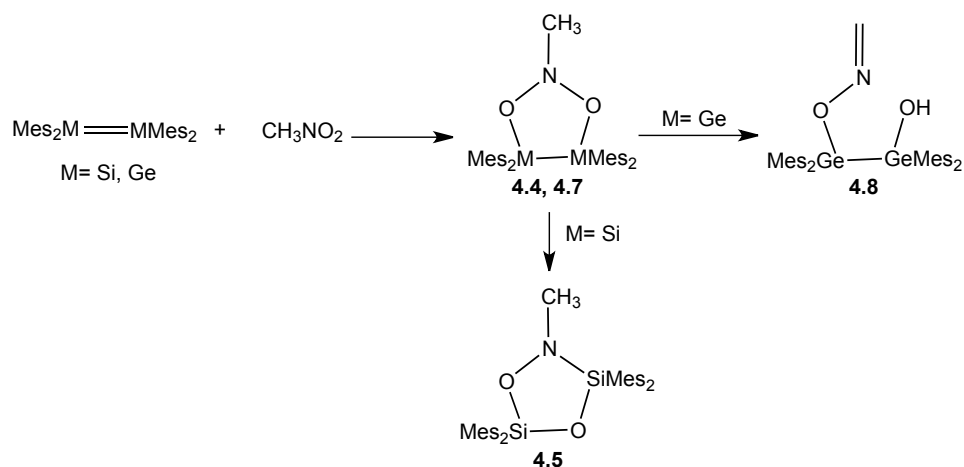
Chapter 5

The Addition of Nitro Compounds to Tetramesityldisilene and Tetramesityldigermene: Substituent Effects and Comparison to Surface Reactivity

5.1 Introduction

One of the fundamental developments in inorganic chemistry in the last decade was the discovery of stable ditetrelenes.¹ Reactivity studies of this novel class of compounds continue to feature in some of the more recent exciting developments chemistry. For example, doubly-bonded compounds of the heavy main group elements have proven to be powerful building blocks in organometallic/inorganic synthesis just as alkenes have proven to be in organic synthesis.¹ Also, ditetrelenes have been utilized as monomers in the development of novel organometallic oligomers.² Additionally, ditetrelenes are excellent models for the cycloaddition reactions of surface ditetrelenes.³

Recently, we reported the addition of nitromethane to tetramesityldisilene (**1.4**) which led to the facile formation of an unusual five membered ring 1,3,2,4,5-dioxazadisilolidine **4.4** that undergoes thermal rearrangement to **4.5**.⁴ Similarly, the addition of nitromethane to tetramesityldigermene (**1.2**) leads to the formation of the five-membered ring 1,3,2,4,5-dioxazadigermolidine **4.7**, which cleanly isomerizes to the oxime analogue **4.8** (Scheme 5.1).



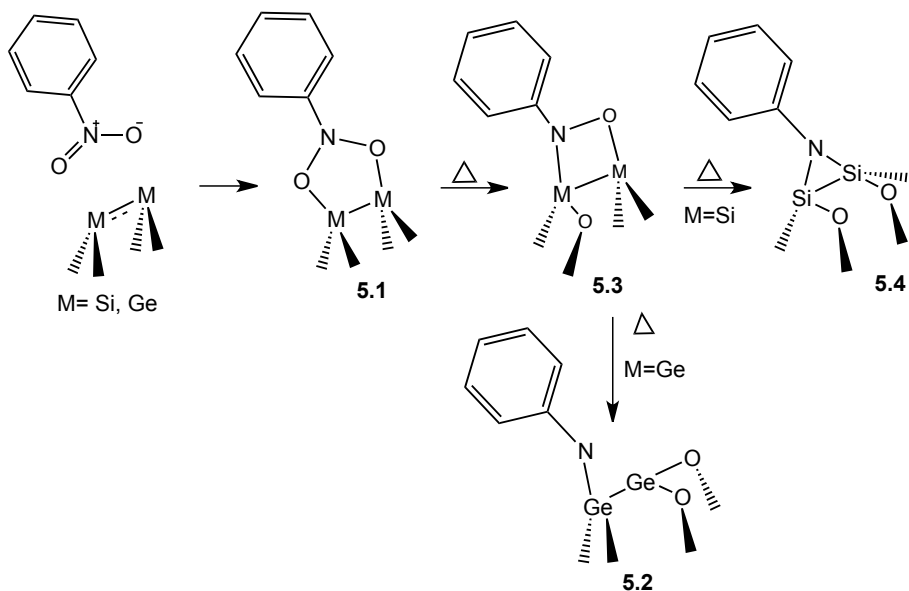
Scheme 5.1

1,3,2,4,5-dioxazadisil- and digermolidines are novel ring systems generated via a formal [3+2] cycloaddition, which is an efficient approach for the construction of the five-membered heterocyclic ring systems.

The addition of nitromethane to the reconstructed Si(100)- 2×1 surfaces has also been examined and three *types* of products were assigned with the aid of N 1s X-ray photoelectron spectroscopy (XPS) and DFT calculations: A) a [3+2] cycloadduct, similar to **4.4** and **4.7**, as the minor product, B) an adduct with one oxygen of the nitro group inserted into the silicon lattice, similar in structure to **4.5**, and C) an adduct with the two oxygen atoms of the nitro group inserted into the silicon lattice (major product).⁵ Our results from the molecular system were consistent with the formation of the formal [3+2] cycloadduct; however, no adducts similar to those derived from the insertion of the two oxygens of the nitro group between the underlying silicon lattice was observed.⁴

The addition of nitrobenzene to the Ge(100)- 2×1 reconstructed surface was examined at 300 K using IR, XPS and DFT calculations.⁶ The formation of a 1,3-dipolar cycloaddition product **5.1** from the addition of nitrobenzene to the Ge(100)- $2 \times$

1 surface dimer was observed in addition to some side products. Heating the surface resulted in desorption of some of the adsorbates; however, a significant fraction of the adducts undergo rearrangement resulting in oxygen atom insertion into the subsurface and the formation of a triplet nitrene **5.2** via the nitroso adduct **5.3** (Scheme 5.2).



Scheme 5.2

The addition of nitrobenzene to Si(100)- 2×1 surface has also been studied both experimentally and theoretically.^{7,8,9,10,11,12,13} In general, the [3+2] cycloadduct **5.1** forms initially. Adduct **5.1** revealed high stability toward thermal desorption,⁷ cycloadduct **5.1** rearranges by double oxygen migrations to form disilaazaridine **5.3** in addition to some minor side products.⁹ It's often hard to elucidate the exact structure of the surface adduct based on the limited availability of surface analytical methods, which include: IR spectroscopy, XPS and theoretical studies. An effective molecular model of surface dimers can be used to provide valuable insights into the surface chemistry by a comparative study of the adducts formed. We believe that tetramesityldisilene and

tetramesityldigermene can serve as appropriate molecular models for the corresponding Si and Ge(100)- 2×1 surfaces and have convincingly shown that the reactivity of surface disilenes and digermenes is comparable to their molecular counterparts.¹⁴

To expand the scope of our previous study,⁴ we were inspired to examine the addition of variety of nitro compounds to tetramesityldigermene and tetramesityldisilene in an effort to better understand the effects of the substituent on the nitro group on the reactivity and to compare the addition of nitrobenzene to the Ge and the Si(100)- 2×1 reconstructed surfaces to the chemistry of the molecular system.

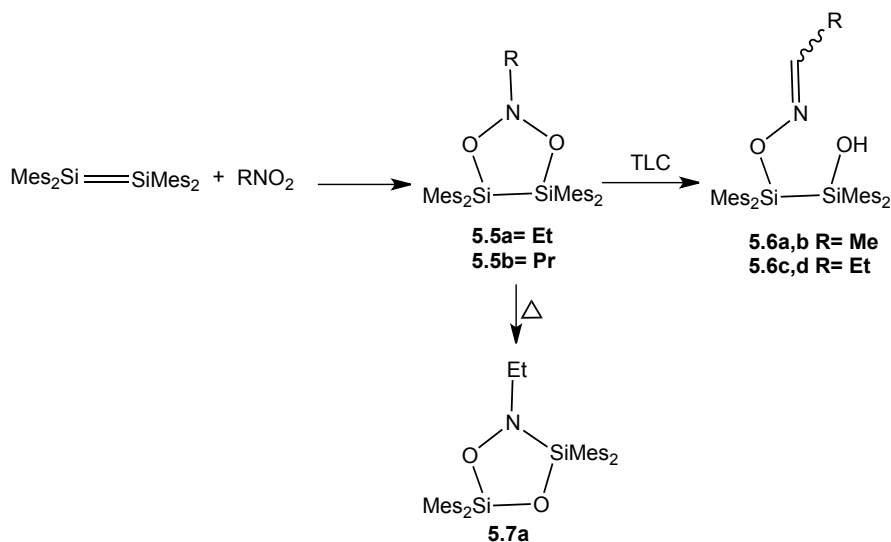
5.2 Results

Digermene **1.2** and disilene **1.4** were synthesized prior to each reaction in quantitative yield following the literature procedures^{14c,15} and used *in situ* without purification. The disilene or digermene was dissolved in C₆D₆, hexanes or THF, and the nitro compound was added in excess. The reaction was kept at room temperature and monitored by ¹H NMR spectroscopy. The products were isolated as either colourless or yellow oils/solids and were identified by ¹H, ¹³C, ¹H-¹H-COSY, ¹³C-¹H gHSQC and ¹³C-¹H gHMBC, ²⁹Si-¹H gHMBC (as appropriate) NMR spectroscopy, EI- (or ESI) mass spectrometry and, in some cases, X-ray crystallography.

5.2.1 Addition of Nitro Compounds to Disilene 1.4

The addition of nitroethane or nitropropane to a bright yellow solution of disilene **1.4** yielded a clear, pale yellow solution. Crystallization from pentane at -14 °C gave white solids. The ¹H NMR spectrum of the solids revealed the formation of 1,3,2,4,5-dioxazadisilolidine **5.5a,b**, respectively. The ¹H NMR spectral data of the adducts formed

from the addition of nitroethane, **5.5a**, and nitropropane, **5.5b**, were similar to those reported for the addition of nitromethane to disilene **1.4**, **4.4**.⁴ The ¹H NMR spectrum of **5.5a** revealed the presence of two sets of signals assigned to two non-equivalent mesityl groups revealing a lack of symmetry in the adduct. The structure of **5.5a** was unambiguously identified as 4,4,5,5-tetramesityl-1,3,2,4,5-dioxazadisilolidine by X-ray crystallography (Scheme 5.3, Figure 5.1). The geometry at the nitrogen atoms is trigonal pyramidal with the nitrogen being 0.525 Å out of the plane of the attached atoms. The sum of the angles at nitrogen is 322.1 degrees. The bond lengths and angles of **5.5a** are similar to those reported for its structurally related analogue, **4.1**.⁴



Scheme 5.3

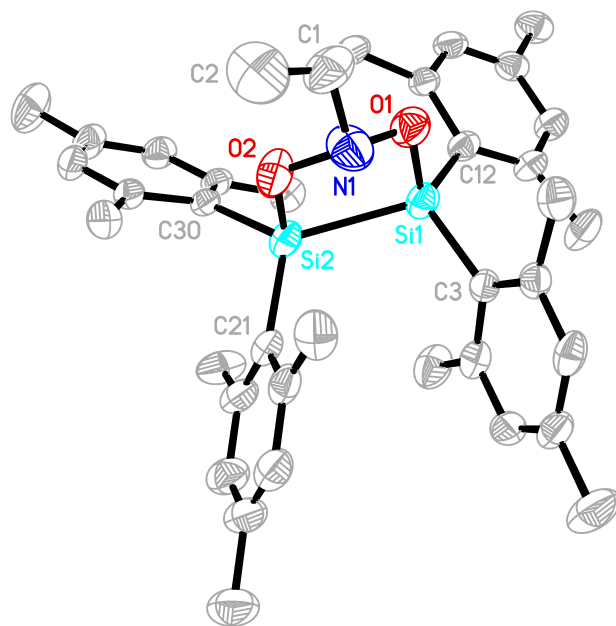
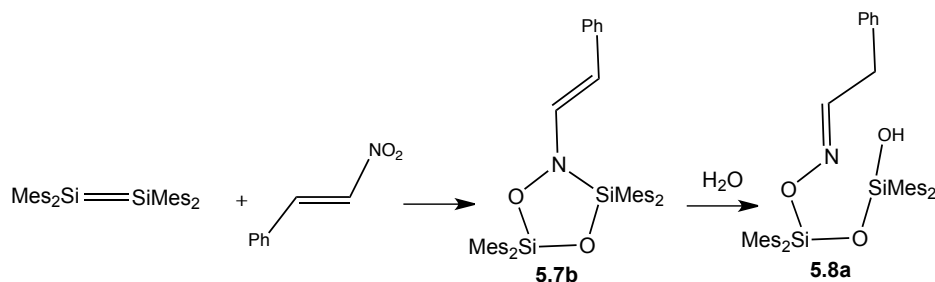


Figure 5.1 Thermal ellipsoid plot of **5.5a** (50% probability surface). Hydrogen atoms and the disorder located at carbon 2 were omitted for clarity. Selected bond lengths (Å) and angles (deg): Si1-O1 = 1.699(3), Si1-Si2 = 2.4046(16), Si2-O2 = 1.717(3), O1-N1 = 1.420(4), O2-N1 = 1.439(5), O1-Si1-Si2 = 90.61(11), O2-Si2-Si1 = 87.27(12), N1-O1-Si1 = 112.2(2), N1-O2-Si2 = 117.1(2), O1-N1-O2 = 110.6(3).

Adduct **5.5a** isomerizes to the oximes **5.6a,b** upon attempted purification by chromatography. Both the *E* and *Z* configurations of **5.6** were observed.¹⁶ The spectroscopic data for **5.6a,b** were similar to those reported for **4.8**.⁵ A solution of compound **5.5a** dissolved in C₆D₆ was heated in a sealed tube at 75 °C and the reaction was monitored by ¹H NMR spectroscopy. Clean conversion of **5.5a** to **5.7a** was observed over one week (Scheme 5.3). ¹H NMR spectrum of **5.7a** revealed the presence of two sets of mesityl groups and quartet at 3.55 ppm which was assigned to the CH₂ moiety and a triplet at 1.21 ppm assigned to the CH₃ group of the ethyl moiety. The ²⁹Si chemical shift of **5.6a** at 0 ppm changed significantly upon isomerization to **5.7a** (-22.6 and -16 ppm). In the ²⁹Si-¹H gHMBC spectrum of **5.7a** a correlation was observed between the signal at -22.6 ppm in the ²⁹Si dimension and the signals at 2.39 and 6.64 ppm in the ¹H dimension

which were assigned to one of the mesityl groups. The second mesityl group, at 2.59 ppm, correlated to the signal at -16 ppm in the ^{29}Si dimension. On the basis of the similarity of the ^{29}Si chemical shifts of **5.7a** to those of the closely related analog **4.5**,⁴ **5.7a** was identified as 2-ethyl-3,3,5,5-tetramesityl-1,4,2,3,5-dioxazadisilolidine.

Upon the addition of *trans*- β -nitrostyrene to a yellow solution of disilene **1.4**, the deep yellow solution became colourless in less than one hour. After drying the reaction mixture, a fine white powder, **5.7b**, was collected (Scheme 5.4). The ^1H NMR spectrum of **5.7b** is similar to that of **5.7a**. The ^{29}Si - ^1H HMBC spectrum of **5.7b** revealed a correlation between the signal at -14.2 ppm in the ^{29}Si dimension and the signal at 2.56 ppm in the ^1H dimension and assigned to one of the mesityl groups. The second signal at -22.2 ppm in the ^{29}Si dimension correlated to the signal at 2.38 ppm in the ^1H dimension, which was assigned to a second mesityl group. The chemical shifts of these signals were in reasonable agreement with the chemical shifts of the analogous signals assigned to the two nonequivalent silicons at -18 and -21 ppm for the structurally-related, 1,3,4,2,5-dioxazadisilolidine **4.5**⁴ and the N-Ph analogue.²⁰ The crystal structure unambiguously confirmed the structure of **5.7b** (Figure 5.2). All bond lengths and angles are within normal ranges. The geometry at the nitrogen atom is nearly trigonal planar with the nitrogen being 0.18 Å out of the plane of the attached atoms and the sum of the angles about nitrogen being 355.66°, close to 360°.



Scheme 5.4

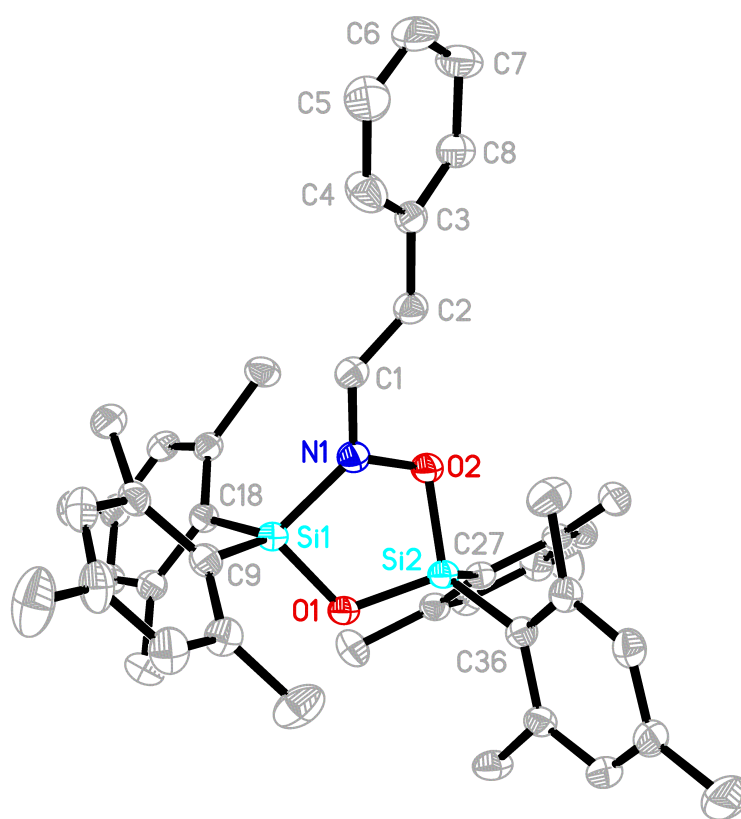


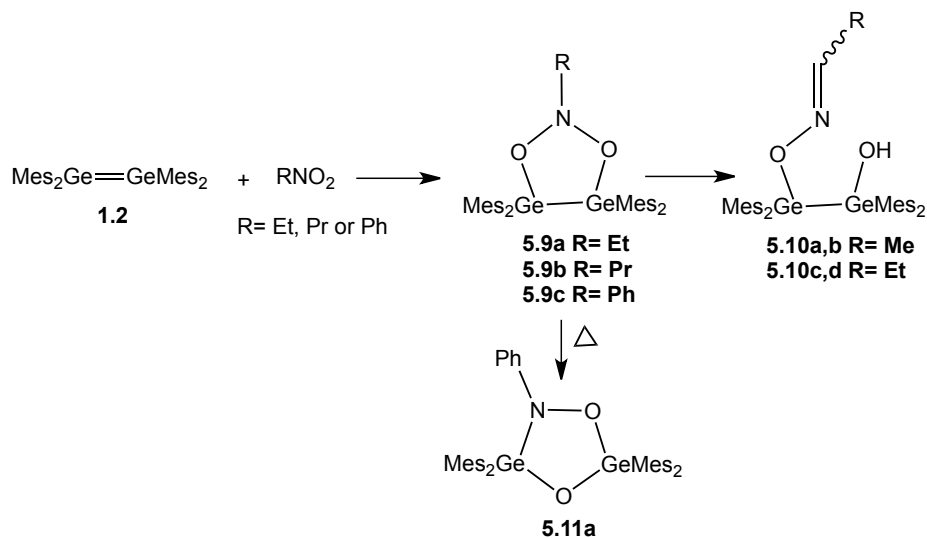
Figure 5.2 Thermal ellipsoid plot of **5.7b** (50% probability surface and hydrogen atoms were omitted for clarity). Selected bond lengths (Å) and angles (deg): Si1-O1 = 1.6492(11), Si1-N1 = 1.7690(13), Si2-O1 = 1.6485(12), Si2-O2 = 1.6837(11), O2-N1 = 1.4513(16), O1-Si1-N1 = 94.98(6), O1-Si2-O2 = 99.58(5), Si2-O1-Si1 = 114.79(6), N1-O2-Si2 = 107.79(8), O2-N1-Si1 = 109.13(9).

Compound **5.7b** hydrolyzed upon adsorption to silica to yield the oxime analogue **5.8a**. Only the *E* isomer of the oxime was isolated.¹⁶ The highest mass signal in the mass

spectrum of **5.8a** was observed at m/z 722.3483 corresponding to a 1:1 adduct between *trans*- β -nitrostyrene and disilene **1.4** and one molecule of H₂O. The ¹H NMR spectrum of **5.8a** revealed the presence of a doublet at 3.49 ppm, which was assigned to the CH₂ group, a triplet at 6.52 ppm which was assigned to the vinylic hydrogen, and a broad singlet at 4.4 ppm assigned to the OH group. The signal at 3.49 ppm in the ¹H dimension correlated to the signal assigned to the *ipso*-carbon of the phenyl substituent and the signal assigned to the vinylic carbon in the ¹³C-¹H HMBC spectrum of **5.8a** (Scheme 5.4).

5.2.2 Addition of Nitro Compounds to Tetramesityldigermene

1,3,2,4,5-dioxazadigermolindines **5.9a,b** were the only products initially formed from the reaction of digermene **1.2** with nitroethane or nitropropane paralleling the reaction of digermene **1.2** with nitromethane (Scheme 5.5).



Scheme 5.5

Adducts **5.9a,b** converted to the isomeric oxime **5.10a-d** after being left in solution under the ambient atmosphere for a few hours or rapidly upon exposure to air. All attempts to purify compounds **5.9a** or **b** resulted in rearrangement to **5.10a-d**

(Scheme 5.5). The *E* and *Z* isomers of the oximes were formed in different ratios. The ratio of *E* to *Z* in the case of **5.10a,b** is 1:1, whereas in the case of **5.10c,d** is 2:1. The ¹H NMR spectra of **5.10a,b** and **5.10c,d** are similar. A quartet at 6.38 ppm in the ¹H NMR spectrum of **5.10a** was assigned to the vinylic hydrogen of the *Z* isomer, whereas the vinylic hydrogen of the *E* isomer of **5.10a** was more deshielded at 7.17 ppm.¹⁶

The addition of nitrobenzene to digermene **1.2** in THF gave a brown oil after removal of the solvent. The oil was dissolved in hexanes and upon cooling to -14 C°, light brown crystals were formed. The ¹H NMR spectrum of **5.9c** revealed the presence of only one set of signals assigned to four equivalent mesityl groups (Scheme 5.5). Single crystal X-ray diffraction data unequivocally provided the structure of **5.9c** (Figure 5.3). All bond lengths and angles are within normal ranges. The structural metrics of the ONO linkage are similar to those of **4.7**.⁴ The geometry at the nitrogen atom is trigonal pyramidal with the nitrogen being 0.547 Å out of the plane of the attached atoms. The sum of the angles at nitrogen is 319.81°.

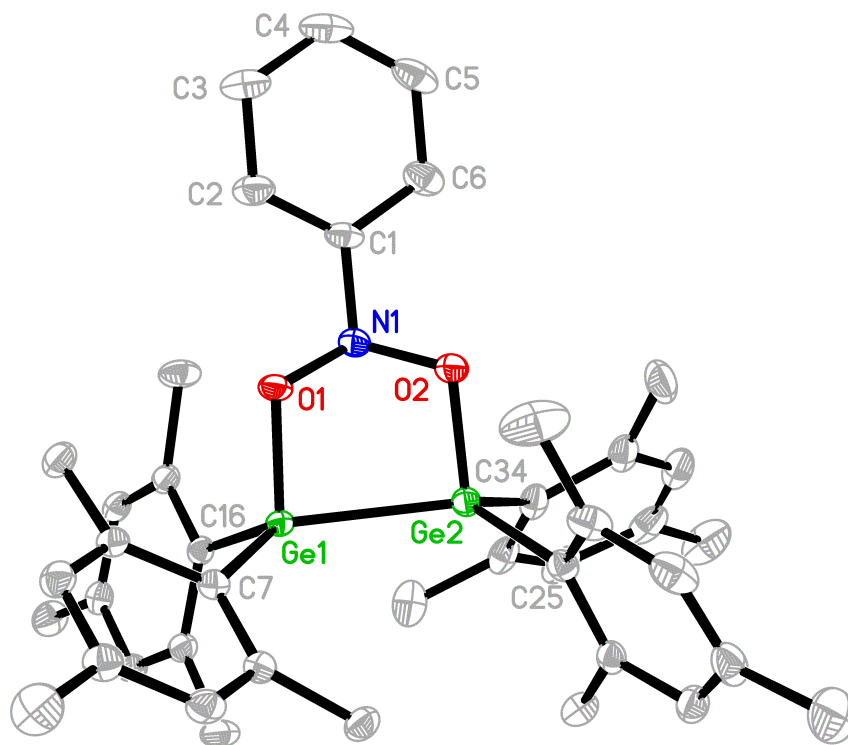
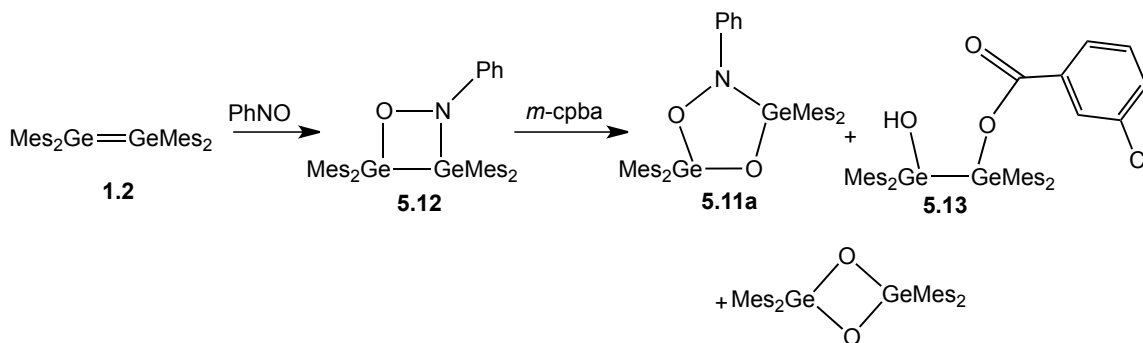


Figure 5.3 Thermal ellipsoid plot of **5.9c** (50% probability surface). Selected bond lengths (Å) and angles (deg): Ge1-O1 = 1.8409(12), Ge1-Ge2 = 2.4843(7), Ge2-O2 = 1.8417(13), O1-N1 = 1.4476(18), O2-N1 = 1.4492(18), N1-C1 = 1.441(2), O1-Ge1-Ge2 = 86.49(4), O2-Ge2-Ge1 = 88.34(4), N1-O1-Ge1 = 103.85(8), O1-N1-O2 = 106.32(11).

Heating a solution of compound **5.9c** in C_6D_6 sealed tube at $\sim 75^\circ C$ resulted in conversion to **5.11a**; the conversion was monitored by 1H NMR spectroscopy. The formation of 2,2,4,4-tetramesityl-1,3,2,4-dioxadigermetane, $Mes_4Ge_2O_2$,¹⁷ was also observed along with **5.11a** in the reaction mixture and was isolated and identified by 1H NMR spectroscopy and EI-mass spectrometry. Attempts to purify **5.11a** resulted in decomposition. Given that **5.11a** could not be purified, an attempt was made to confirm its identity by synthesizing it using an alternative route. Thus, the addition of nitrosobenzene to digermene **1.2** followed by oxidation was explored. The addition of nitrosobenzene to digermene **1.2** resulted in the formation of **5.12** as light green oil. The

structure of **5.12** was established by comparing the spectral of data **5.12** to those for the structurally-related silicon analogue.²⁰ Oxidation of **5.12** using *meta*-chloroperoxybenzoic acid (*m*-cpba) resulted in the formation of the anticipated adduct **5.11a**, as the ¹H NMR spectroscopy of the reaction mixture contained the same signals observed upon direct addition of nitrobenzene to digermene **1.2** followed by heating. Unfortunately, the formation of **5.11a** was accompanied by the formation of **5.13**, which was identified as 2-hydroxy-1,1,2,2-tetramesityldigermyl-3-chlorobenzoate by single crystal X-ray diffraction, as well as 2,2,4,4-tetramesityl-1,3,2,4-dioxadigermetane, Mes₄Ge₂O₂¹⁷ (Scheme 5.6 and Figure 5.4). Separation of mixture of **5.11a** and **5.13** by chromatography resulted in decomposition of **5.11a** and purification of **5.13**. The ¹H NMR spectrum of **5.13** revealed the presence of two sets of signals assigned to the two non-equivalent mesityl groups, and a broad signal assigned to the hydroxy group. Mass spectrometry confirmed the presence of 1:1 adduct between digermene **1.2** and *m*-cpba consistent with the proposed structure of **5.13** as well as a minor product with a formula of C₄₂H₅₀NO₃⁷⁰Ge₂ consistent with a 1:1 adduct between nitrobenzene and digermene **1.2** and one oxygen atom. The minor product may be 4,4,6,6-tetramesityl-2-phenyl-1,3,5,2,4,6-trioxazadigerminane, (Mes₄Ge₂O₃NPh), the oxidation product of **5.11a**.



Scheme 5.6

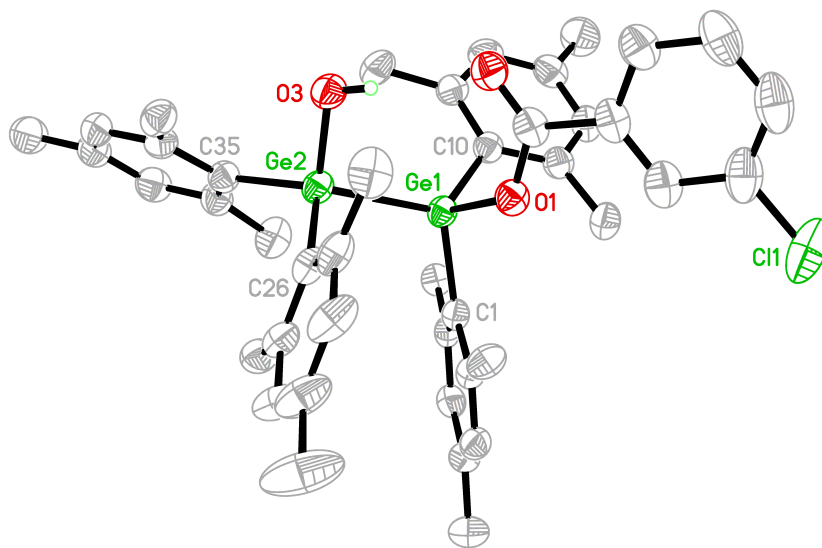
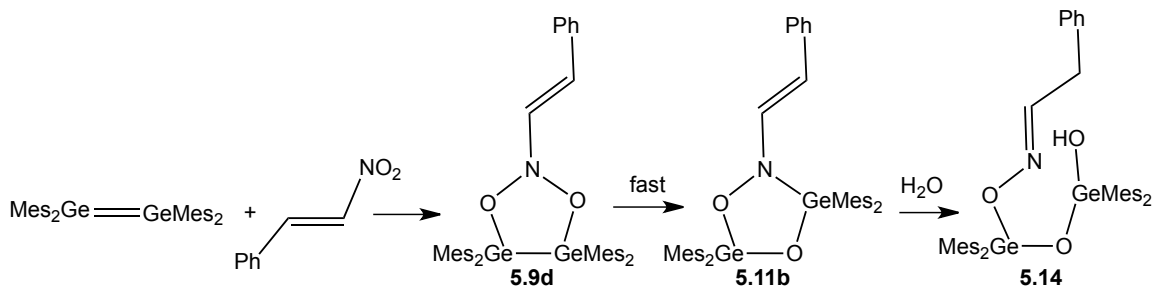


Figure 5.4 Thermal ellipsoid plot of **5.13** showing numbering scheme. Ellipsoids are at the 50% probability level and all hydrogen atoms except for H3A were omitted for clarity. A region of disorder was found near the *m*-chloro substituent on the phenyl ring of the *m*-cba fragment and is omitted for clarity. Selected bond lengths (Å) and angles (deg): Ge1-O1 = 1.8792(19), Ge1-Ge2 = 2.5004(7), Ge2-O3 = 1.784(2), O1-C19 = 1.323(4), O1-Ge1-C1 = 97.80(10), O1-Ge1-C1 = 103.30(10), C10-Ge1-C1 = 112.02(11), O1-Ge1-Ge2 = 101.04(6), C10-Ge1-Ge2 = 125.15(8), C1-Ge1-Ge2 = 112.80(8).

The results of the addition of *trans*- β -nitrostyrene to digermene **1.2** were similar to those of the addition of *trans*- β -nitrostyrene to disilene **1.4**. Upon the addition of the *trans*- β -nitrostyrene to the yellow solution of digermene **1.2**, the deep yellow solution of digermene **1.2** becomes colourless in less than one hour. The ^1H NMR spectrum of the intermediate **5.9d** is similar to that of **5.7a** with only one set of signals for the mesityl groups. Compound **5.9d** was not stable in solution; within ~ 1 hour, it begins to rearrange to **5.11b**. Attempts to purify **5.11b** by silica gel preparative thin layer chromatography led to hydrolysis to the open-chain oxime analogue, **5.14** (Scheme 5.7).



Scheme 5.7

The highest mass signal in the mass spectrum of **5.14** was observed at m/z 806.2405 corresponding to a 1:1 adduct between *trans*- β -nitrostyrene and digermene **1.2** and one molecule of H_2O . The ^1H NMR spectrum of **5.14** revealed two sets of mesityl groups and a doublet that integrates to two hydrogens at 3.57 ppm. The doublet was assigned to the CH_2 adjacent to the phenyl ring. A triplet at 6.61 ppm assigned to the vinylic hydrogen. In the ^1H - ^1H COSY spectrum of **5.14**, a correlation was observed between the signal assigned to the vinylic hydrogen and the signals assigned to the CH_2 attached to the phenyl group. In the ^1H - ^{13}C HMBC spectrum of **5.14**, a correlation was observed between the signal assigned to the CH_2 in the ^1H dimension and the signal assigned to the *ipso* and *ortho* carbons of the phenyl moiety in the ^{13}C dimension and the iminic carbon. All spectroscopic data support the structure of **5.14**. From elucidation of the structure of **5.14**, it became evident that the structure of **5.11b** has an oxygen inserted between the two germanium atoms, which is the most reasonable intermediate between **5.9d** and **5.14**.

5.3 Discussion

Adducts **5.5a,b** and **5.9a-d** appear to be generated by the formal [3+2] cycloaddition between the nitro functional group and the ditetrelene to form 1,3,2-dioxazolidines following the same reactivity that was observed in the addition of nitromethane to ditetrelenes.⁴ The ¹H NMR spectra of compounds **5.5a,b** and **5.9a,b** with an alkyl substituent at the nitrogen, are consistent with that of the structurally-related compounds **4.4**, **4.7**, **5.5** and **5.9a,b** revealing two sets of signals assigned to mesityl groups. DFT calculations show that the barrier for inversion at the nitrogen for cycloadduct **4.7**, modeled as MeN(OGeH₃)₂, is 112 kJ/mol, which is sufficiently high for the nitrogen to be configurationally stable.⁴ As a consequence, the mesityl groups on a given germanium or silicon are not equivalent and exhibit two sets of signals by NMR spectroscopy.

In contrast, the ¹H NMR spectra of the dioxazagermolides formed from the addition of nitrobenzene or *trans*-β-nitrostyrene to tetramesityldigermene (**5.9c,d**) reveals only one set of signals which can be assigned to the four mesityl groups. DFT calculations performed at the TPSS/TPSS¹⁸/6-31G(d) level of theory shows that the barrier for inversion at the nitrogen for cycloadduct **5.9c** as modeled by PhN(OGeH₃)₂ is -30.85 kJ/mol,¹⁹ and therefore, the barrier to inversion at the nitrogen is lowered by attachment of a phenyl group. Apparently, rapid inversion at the nitrogen in **5.9c** on the NMR time scale occurs, resulting in the observation of equivalent mesityl groups by NMR spectroscopy. The same is apparently true for **5.9d** where the conjugated styrenyl group can also be expected to lower the activation energy barrier.

The addition of nitrobenzene to tetramesityldisilene ($\text{Mes}_2\text{Si}=\text{SiMes}_2$) was reported by West.²⁰ The reaction gives the 1,3,2,4,5-dioxazadisilolidine **5.7c**. West did not report the crystal structure of **5.7c**, and thus, to unequivocally confirm the structure of **5.7c**, it was synthesized according to the literature procedure²⁰ and a suitable crystal of **5.7c** was obtained from a saturated pentane solution and the structure determined (Figure 5.5). The structural metrics **5.7c** are similar to those of the β -styrenyl analogue **5.7b**. The geometry at the nitrogen in **5.7c** is near trigonal planar with the nitrogen being displaced 0.195 Å from the plane of the attached atoms and the sum of the angles around nitrogen being 354.93°, close to 360°. It is noteworthy that the geometry at nitrogen of the adducts is either trigonal planar or trigonal pyramidal. 1,3,2,4,5-dioxazadisilolidines **5.5a** and 1,3,2,4,5-dioxazadigermolidine **5.9c** with an alkyl group attached to nitrogen have a trigonal pyramidal geometry at nitrogen, whereas 1,4,2,3,5-dioxazadisilolidines **5.7b,c**, with an aryl group attached to nitrogen, are trigonal planar at nitrogen.

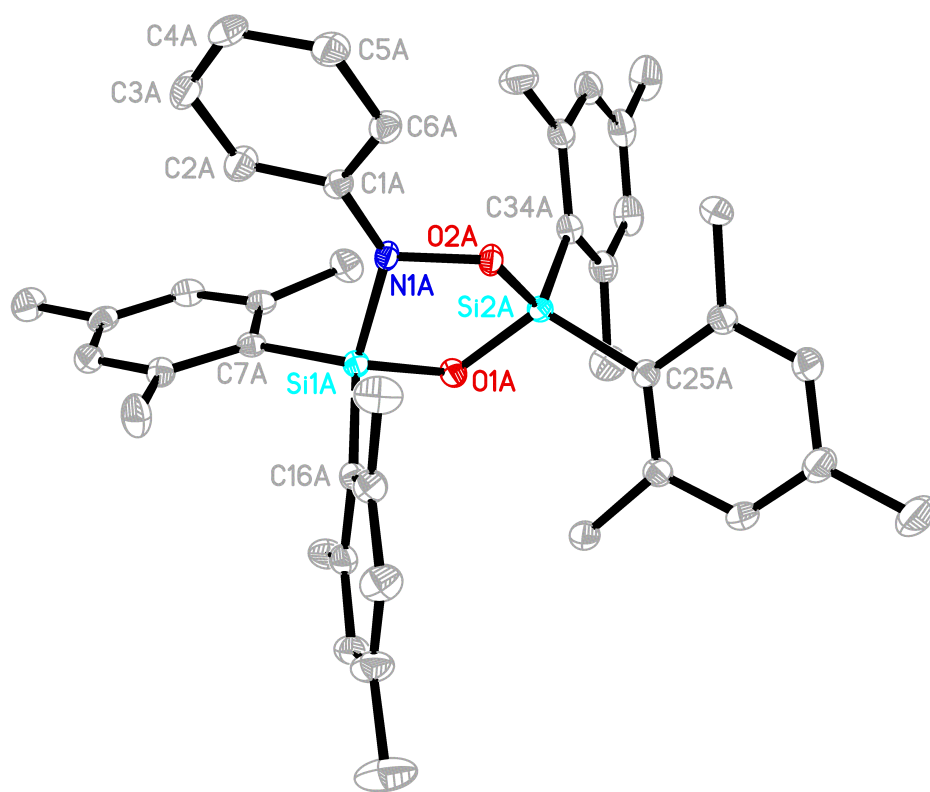
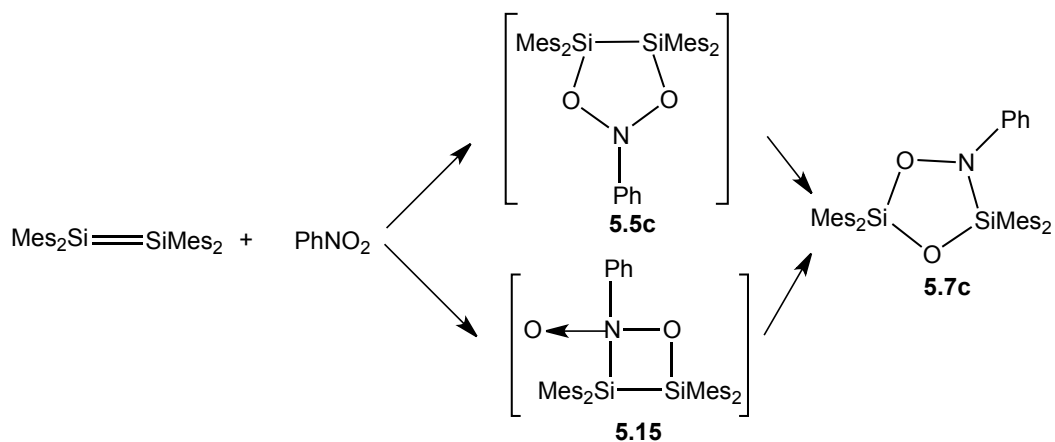


Figure 5.5 Thermal ellipsoid plot of **5.7c** (50% probability surface and hydrogen atoms were omitted for clarity). Selected bond lengths (Å) and angles (deg): Si1-O1 = 1.6584(11), Si1-N1 = 1.7569(14), Si2-O1 = 1.6592(12), Si2-O2 = 1.6847(11), O2-N1 = 1.4674(15), O1-Si1-N1 = 95.19(6), O1-Si2-O2 = 99.70(5), Si2-O1-Si1 = 113.42(6), N1-O2-Si2 = 107.28(8), O2-N1-Si1 = 107.28(8).

The mechanism for the formation of **5.7c** was postulated by West to proceed by one of two pathways: [3+2] cycloaddition forming either **5.5c** or [2+2] cycloaddition to give **5.15** followed by rearrangement to form **5.7c**, the isolated product. When the addition reaction was carried out at low temperature and monitored by ^{29}Si NMR spectroscopy, an intermediate was observed which possesses only one ^{29}Si NMR signal. This observation supports the structure of **5.5c** as the intermediate (Scheme 5.8).²⁰ Given that, in two cases, we have isolated and unambiguously determined the structure of the initially formed 1,3,2,4,5-dioxazolidine (**4.4** and **5.5c**) and observed the transformation to

the 1,4,2,3,5-isomer, we can conclude that the pathway for the formation of **5.7c** proceeds via **5.5c**. No evidence for any intermediate or product similar in structure to **5.15** was ever obtained.

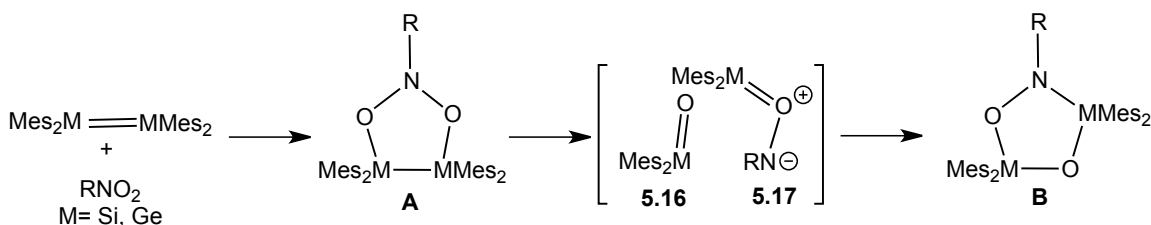


Scheme 5.8

The difference in the rate of conversion from 1,3,2,4,5-dioxazadisilolidine or -digermolidine to the disilyl- or digermyl-substituted oxime is interesting. 1,3,2,4,5-dioxazadisilolidine **5.5** converts to the oxime analogue **5.6** after exposure to the ambient atmosphere or upon preparative thin layer chromatography. In contrast, 1,3,2,4,5-dioxadigermolidine **5.9** converts to the oxime isomer **5.10** very rapidly under inert conditions in less than two hours suggesting that the silicon analogues are more stable than the germanium counterparts. Possibly, the silicon is better able to accommodate the high density of electrons O-N-O in the 5-membered rings through negative hyperconjugation.²¹ The σ^* orbital of the Si-Mes bond likely overlaps more effectively (in comparison to the Ge-Mes σ^*) with the lone pair of electrons on the adjacent oxygen resulting in delocalization of the electron density from the oxygen of the O-N-O linker in **5.5a,b**. As a consequence, the 1,3,2,4,5-dioxazadisilolidines rearrange at a slower rate in comparison to the germanium derivatives.

The addition of nitroalkanes (nitroethane and nitropropane) to tetramesityldisilene resulted in the formation of the 1,3,2,4,5-dioxazadisilolidine ring system; whereas, the addition of conjugated nitro compounds (nitrobenzene and *trans*- β -nitrostyrene) to tetramesityldisilene gave 1,4,2,3,5-dioxazadisilolidines. On the other hand, the addition of nitroalkanes and conjugated nitro compounds to tetramesityldigermene always gives a 1,3,2,4,5-dioxazadigermolidine. Heating the adduct formed from the addition of nitrobenzene to the digermene resulted in conversion to the 1,4,2,3,5-dioxazadigermolidine isomer; the 1,3,2,4,5-dioxazadigermolidine formed from the addition of *trans*- β -nitrostyrene to the digermene converts rapidly to the 1,4,2,3,5-dioxazadigermolidine. The differences observed in the rates of conversion from the 1,3,2,4,5-dioxazadisilolidine/ dioxazadigermolidine to the 1,4,2,3,5-isomer depends on the type of substituent attached to the nitro group. We propose that the formation of the 1,4,2,3,5 isomer (**5.7a-c** and **5.11a,b**) follows a mechanism similar to the well-known Criegee mechanism for the formation of ozonides (Scheme 5.9).²² Ring cleavage of the 1,3,2,4,5-isomer (**A**) takes place initially to give dimesitylsilanone/germanone (**5.16**) and the zwitterionic species, **5.17**. Recombination of these two species would give the 1,4,2,3,5-isomer (**B**). The rate of rearrangement appears to depend on the stability of the zwitterionic species **5.17**. With a substituent which can stabilize the negative charge at nitrogen, such as a phenyl or a styrenyl substituent, rearrangement is rapid; however, with an alkyl substituent at nitrogen (such as ethyl or propyl), rearrangement is slow (Scheme 5.9). Both disilene **1.4** and digermene **1.2** are similar in reactivity toward alkyl nitro compounds. However, for unsaturated substituents on the nitrogen, the reactivity of the disilene adducts differs from those of digermene. Rearrangement is rapid when the

substituent on nitrogen is styrenyl for both the germanium and the silicon system. When the substituent on the nitrogen is styrenyl, the extended conjugation stabilizes the zwitterionic specie **5.17** effectively and both the germanium and the silicon adducts rapidly rearrange to the 1,4,2,3,5-isomer. When substituent on nitrogen is phenyl, rearrangement is fast in the silicon system, while the rearrangement is slower in the germanium system. The stability of the conjugated species **5.17** (where R= styrenyl or Ph) should be similar, and thus, the rearrangement for both the germanium and the silicon analogue should be similar. It is not completely understood why rearrangement is fast when the substituent on nitrogen is phenyl in the silicon system compared to the germanium analogue. A detailed kinetic study is required to understand this difference.

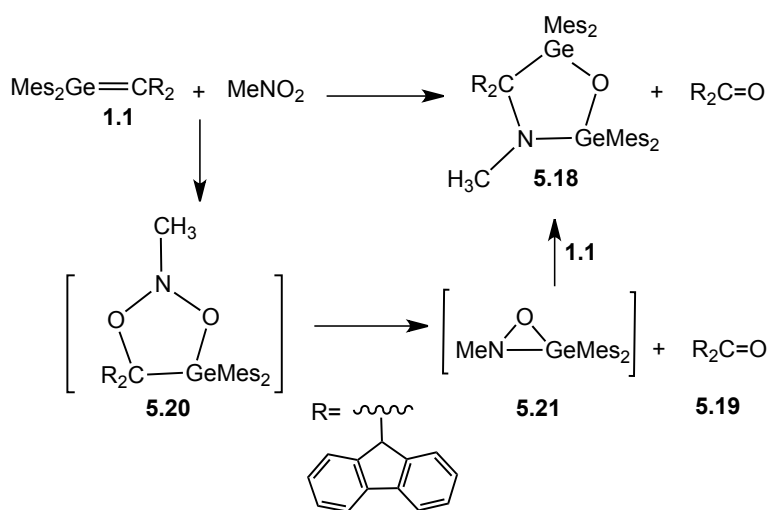


Scheme 5.9

The thermal conversion of **5.9c** to **5.11d** and **5.9d** to **5.11b** also afforded the 1,3,2,4-dioxadigermetane, $\text{Mes}_4\text{Ge}_2\text{O}_2$, which can be understood in the terms of the proposed mechanism. Dimerization of dimesitylgermanone (**5.16** where $\text{M} = \text{Ge}$) is expected to give the dioxadigermetane. The formation of the dimerization product of dimesitylgermanone **5.16** provides additional support for the proposed mechanism.

It's interesting to compare the reactivity of nitromethane towards disilenes and digermenes to the addition of nitromethane to germene **1.1**.²³ Compounds **5.18** and **5.19** were isolated from the addition of nitromethane to dimesitylfluorenyldienegermane **1.1** and postulated to form from the [3+2] cycloadduct **5.20** which underwent subsequent

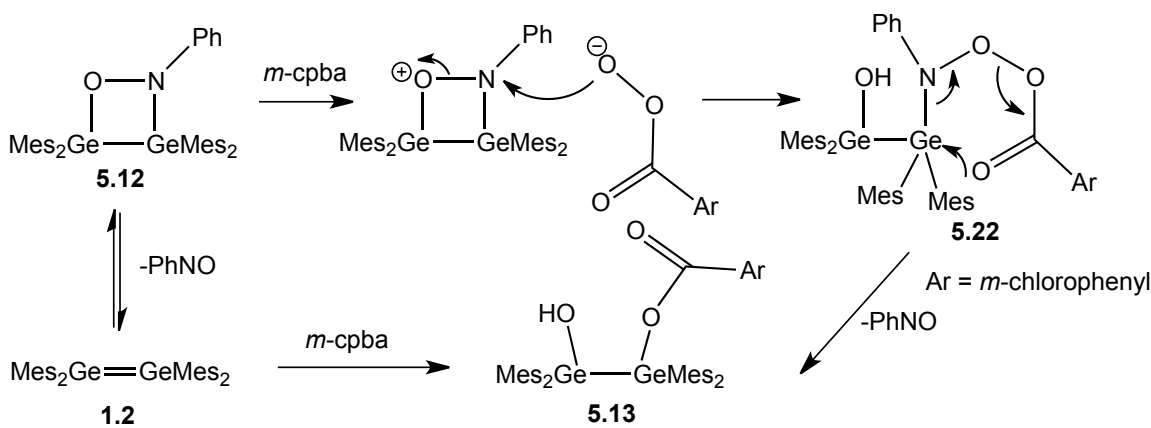
fragmentation to ketone **5.19** and oxazagermiridine **5.21** (Scheme 5.10). Another equivalent of germene **1.1** apparently then react with intermediate **5.21** to give the isolated product **5.18**. Interestingly, the fragmentation pathway proposed for **5.20** gives $R_2C=O$, the carbon analogue of **5.16**, and **5.21**, the cyclic analogue of **5.17**. One of the main factors that contribute to the difference in the observed reactivity of germene **1.1**, digermene **1.2** or disilene **1.4** towards nitromethane is the stability of the ketone formed. The ketone formed in the fragmentation of **5.18** is more stable than the analogous germanone/silanone (**5.16**), and thus, does not apparently undergo any further reaction.



Scheme 5.10

The formation of **5.13** was unexpected (see Scheme 5.6). In general, *m*-cpba acts as an oxygen donor and reacts with alkenes to give epoxides with *m*-chlorobenzoic acid as a by-product. Two reaction pathways to yield **5.13** were envisioned (Scheme 5.11). If the formation of **5.12** is reversible, in the presence of *m*-cpba, digermene **1.2** may react directly with *m*-cpba to give **5.13**. Alternatively, protonation of the oxygen in **5.12** by *m*-cpba, followed by nucleophilic attack of the oxyanion at the nitrogen would give **5.22**.

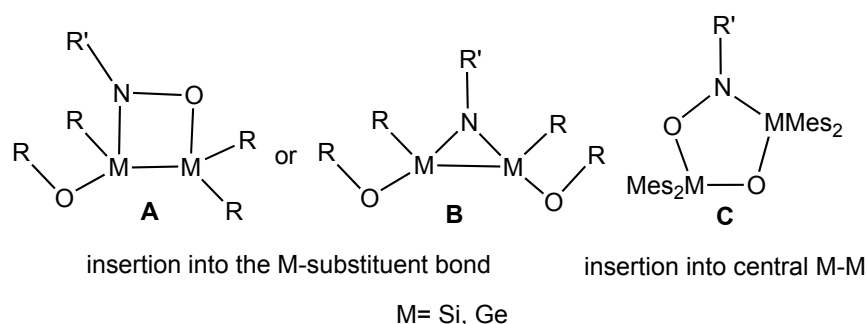
Rearrangement of **5.22** would regenerate nitrosobenzene and give **5.13**. To provide evidence for the operative pathway, we examined the addition of *m*-cpba to digermene **1.2**. Tetramesityloxadigermirane ($\text{Mes}_4\text{Ge}_2\text{O}$) and two isomers of tetramesityldigermoxetane¹⁷ were formed; no evidence of the formation of **5.13** was obtained. Therefore, the route via **5.22** is proposed to account for the formation of **5.13**.



Our findings are consistent with the formation of the [3+2] surface cycloadduct **5.1** generated from the addition of nitrobenzene to the $\text{Ge}(100)$ ⁹ and the $\text{Si}(100)$ ¹²- 2×1 reconstructed surfaces (Scheme 5.2). Upon heating, a triplet nitrene adduct was believed to form in the $\text{Ge}(100)$ - 2×1 by double insertion of the oxygen to the subsurface,⁹ while a disilaaziridine-type product is formed on the $\text{Si}(100)$ - 2×1 surface.¹² No evidence for a nitrene-type adduct was observed in any of the additions of nitro compounds to ditetrelenes in solution at room temperature. However, a nitrene is expected to be too reactive to be isolated in the molecular system at room temperature. Furthermore, no disilaaziridine-type product was observed in any of the additions of nitro compounds to ditetrelenes similar to those generated on the $\text{Si}(100)$ - 2×1 surface. A computational

study suggests that the strain enthalpy of formation of the parent disilirane (CSi_2H_6) is 155 kJmol^{-1} whereas the strain enthalpy of formation of the parent digermirane (CGe_2H_6) is 164 kJmol^{-1} .²⁴ Since the germanium derivatives are less stable than those of silicon derivatives, it is reasonable that no digermaazaridine was observed on the $\text{Ge}(100)\text{-}2 \times 1$ surface nor in the addition of nitro compounds to the molecular digermene **1.2**.

Oxygen migration from the surface into the lattice (Scheme 5.2) lead to the formation of adducts of type **A** or **B** (Scheme 5.12).



Scheme 5.12

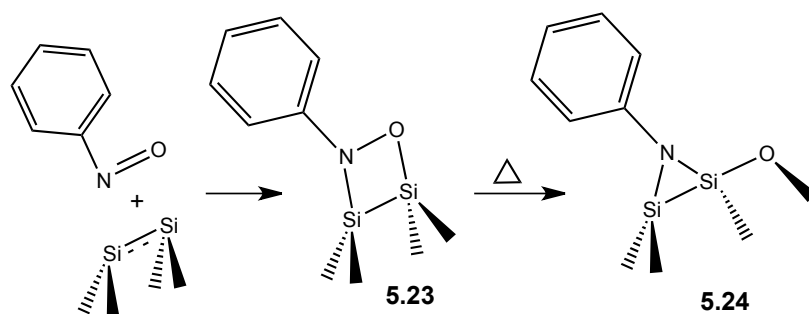
In the molecular system, no migration of oxygen into the Si- or Ge-substituent bond to give a product such as **A** or **B** (Scheme 5.12 where $\text{R} = \text{Mes}$) was observed in any addition reaction of a nitro compound to a ditetrelene. With mesityl groups as the substituents, insertion of oxygen into the M-C bond of the substituent is less thermodynamically favourable in comparison to insertion into a M-M bond, and thus, does not occur. Clearly, the nature of the substituents on the molecular disilene and digermene have a major influence on the products formed. The use of a silyl-substituted disilene or a germeryl- (or silyl) substituted digermene might facilitate the formation of oxygen migration products in the molecular system to form products similar in structure to **A** or **B** (Scheme 5.12 where $\text{R} = \text{SiR}_3$ or GeR_3). Notably, we do observe the migration of an oxygen to the Si-Si or the Ge-Ge bond of the initially formed [3+2] adduct (i.e. **5.7 a-c** and **5.11a,b**) to give

structures analogous to **C**. In the study of the reactivity of the Ge(100) surface toward nitrobenzene, the authors were not unable to distinguish between insertion into a surface Ge-Ge bond and insertion into a Ge-(lattice-Ge) bond using the available experimental methods (FTIR and XPS).⁶ DFT calculations suggested that oxygen insertion into the surface Ge-Ge and the Ge-(lattice- Ge) are energetically very similar, and thus, a mixture of isomers may have been formed.²⁵ Our results are certainly consistent with the migration of an oxygen to Ge-Ge surface bond.

The migration of oxygen into a surface Ge-Ge bond are also supported by the results obtained from a computational study of the addition of nitroethylene to the Si(100)- 2×1 surface. The authors determined that the [3+2] cycloaddition of nitroethylene to the Si(100)- 2×1 surface was the most reasonable reaction pathway and further isomerization to insert an oxygen into the surface silicon-silicon bond is also reasonable; however, the authors did not consider insertion of an oxygen into a Si(lattice) bond.²⁶ Furthermore, an IR spectroscopic and computational study of the addition of nitrobenzene and nitromethane to the Si(100)- 2×1 surface suggests that migration of an oxygen into the surface Si-Si bond is possible, albeit, only as a minor product in the reaction.^{5,11} Therefore, the formation of an adduct similar in structure to our 1,4,2,3,5-isomer on the Ge(100)- and Si(100)- 2×1 surfaces is very probable.

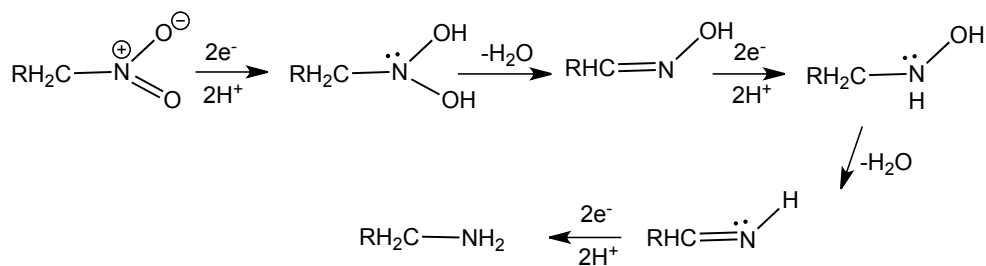
The addition of nitrosobenzene to the reconstructed Si(100) surface leads to the formation of the [2+2] cycloaddition product **5.23** (Scheme 5.13). Oxygen migration into the subsurface results in the formation of disilaziridine **5.24**.⁹ The addition of nitrosobenzene to digermene **1.2** gave the analogous [2+2] cycloadduct **5.12**. Also, the addition of nitrosobenzene to disilene **1.4** affords a similar [2+2] cycloadduct.²⁰ In this

case, the adducts formed in the molecular system are completely analogous to those formed in the surface.



Scheme 5.13

It's noteworthy that a $2e^-$ reduction of the nitro functional group to the corresponding 1,4,2,3,5-dioxazadisil- and digermolidine (essentially, the H_2O adduct of oxime) should be easily accomplished. The nitro functional group undergoes an overall $6e^-$ reduction to the corresponding amine, via a $2e^-$ reduction to the oxime followed by a $2e^-$ reduction to the imine and finally a $2e^-$ reduction the amine (Scheme 5.14). Oximes are known to serve as useful precursors to various compounds that have found numerous applications in material science, pharmaceuticals, and agrochemicals,²⁷ and great efforts have been made to develop efficient protocols enabling their facile preparations.²⁸



Scheme 5.14

The classical reduction of primary nitroalkanes, as well as α,β -unsaturated nitro compounds, to their oxime analogues is typically carried out using reducing agents such

as Se/NaBH₄, Bu₃SnH, SnCl₂/PhSH, or Au/TiO₂/H₂.²⁹ However, these established methods generally suffer from one or more limitations such as harsh reaction conditions, poor selectivity, or the use of toxic metal salts. A recent published mild method utilizes the irradiation of a substrate with visible light with Ru(bp)₃Cl₂ as a catalyst and Mg(ClO₄)₂ as an activator; however, it requires the use of a heavy metal catalyst.³⁰ Therefore, additional methods for the mild, convenient synthesis of oximes are needed. We have shown that the reduction of the nitro functional group using a disilene or a digermene is a convenient chemical method for the conversion of a nitro functional group to the water adduct of the oxime (1,4,2,3,5-dioxazadisil- and digermolidine) in a stepwise, controlled 2-electron reduction. Our results offer a potential chemical method for the controlled 2-electron reduction of nitro compounds.

5.4 Conclusions

In conclusion, the addition of a variety of nitro compounds to tetramesityldisilene and tetramesityldigermene was examined and leads to the facile formation of the novel 1,3,2,4,5-dioxazadisil and -digermolidine ring systems, respectively. In general, 1,3,2,4,5-dioxazadisilolidines and -digermolidines isomerize under thermal conditions to give the 1,4,2,3,5-dioxazadisilolidines and -digermolidines ring systems. The 1,3,2,4,5-dioxazadisilolidine and -digermolidine systems were found also to undergo ring opening to the isomeric oximes. Indeed, the addition of nitro compounds to ditetrelenes can be generalized and the variability of the products obtained from the reaction can be understood based on the nature of the substituents on the nitrogen.

By comparison of the reactivity of molecular disilenes and digermenes and their surface analogues towards nitro compounds, we conclude that our findings further

illustrate the use of tetramesityldisilene and -digermene as valuable molecular models for Si-(100) or Ge-(100) surfaces, respectively. For most part, the chemistries are quite comparable although the relative stabilities of the adducts varied. Notably, an alternative product (oxime isomers) was discovered in the molecular system, such compounds may also form on the surface. Thus, the study of the addition of nitro compounds to molecular disilenes and digermenes has provided valuable insights into the reactivity of Si-(100) and Ge-(100) surfaces.

5.5 Experimental

General Experimental Details

All manipulations were performed in flame-dried Schlenk tubes or NMR tubes sealed with a septum under an inert atmosphere of argon. Benzene- d_6 was distilled from LiAlH_4 , stored over 4 Å molecular sieves, and degassed prior to use. The NMR standards used were: residual $\text{C}_6\text{D}_5\text{H}$ (7.15 ppm) for ^1H NMR spectra, C_6D_6 central transition (128.00 ppm) for ^{13}C NMR spectra. Electron impact mass spectra were obtained using MAT model 8400 mass spectrometer using an ionizing voltage of 70 eV. Mass spectral data are reported in mass-to-charge units, m/z . $\text{Ge}_3\text{Mes}_6^{14\text{c}}$ and $(\text{Me}_3\text{Si})_2\text{SiMes}_2^{15}$ were synthesized according to the literature procedures.

General Procedure for the Reactions of Nitro Compound with Tetramesityldisilene

$\text{Mes}_2\text{Si}(\text{SiMe}_3)_2$ (100 mg, 0.24 mmol) was placed in a quartz tube, dissolved in hexanes (3 mL). The solution was irradiated ($\lambda = 254$ nm) in a quartz Dewar at -60 °C for ~ 18 h to give the yellow solution of **1.4**. The solution was cooled to -50 °C during the irradiation by circulating methanol in the quartz Dewar. The nitro compound (~ 0.40 mmol) was added and the reaction mixture was

stirred at room temperature. After 5 minutes, the solution became colourless. The hexanes were evaporated giving a pale yellow oil which was dissolved in a minimum amount of hexanes. The flask was placed in the freezer (-14 °C) for 24 h. A precipitate formed and the solid was isolated by decantation. The solid was triturated with pentane yielding either clear crystals or oils. **5.5a** White powder obtained from crystallization from pentane solution of the reaction mixture, contaminated with **5.5b** in (1: 0.1) ratio (61 mg, 81%): m.p.:144-146 °C ¹H NMR (C₆D₆, 600 MHz) δ 6.68, 6.64 (each s, 8H, Mes *m*-CH), 3.40 (q, 2H, CH₂N J = 8Hz), 2.43, 2.42 (each s, Mes *o*-CH₃), all together 24H], 2.06, 2.04 (each s, Mes *p*-CH₃) all together 12H], 1.16 (t, 3H, CH₃ J = 8Hz); ¹³C NMR (C₆D₆, 150 MHz) δ 145.43 (Mes *o*-C), 144.77 (Mes *o*-C), 139.41 (Mes *p*-C), 139.21 (Mes *p*-C), 134.03 (Mes *i*-C), 132.67 (Mes *i*-C), 129.46 (Mes *m*-C), 129.42 (Mes *m*-C), 60.32 (CH₂N), 25.29 (Mes *o*-CH₃), 24.64 (Mes *o*-CH₃), 20.99 (Mes *p*-CH₃), 11.54 (CH₃); ²⁹Si NMR (C₆D₆, 119 MHz) δ 0 ppm; high resolution EI-MS *m/z* for C₃₈H₄₉NO₂Si₂ calc. 607.3302, found 607.3314. **5.5b** White powder obtained by crystallization from the hexanes reaction mixture, contaminated with trace of [Mes₄Si₂O₂]³¹; (60 mg, 80%) ¹H NMR (C₆D₆, 600 MHz) δ [6.68 (s, Mes *m*-H), 6.65 (s, Mes *m*-H) all together 8H], 3.41 (t, 2H, J = 7 Hz CH₂N), [2.44 (s, Mes *o*-CH₃), 2.43 (s, Mes *o*-CH₃) all together 24H], [2.06 (s, Mes *p*-CH₃), 2.05 (s, Mes *p*-CH₃) all together 12H], 1.71 (tq, 2H, CH₂CH₃ J = 8, 7Hz), 0.76 (t, 3H, CH₃ J = 8 Hz); ¹³C NMR (C₆D₆, 150 MHz) δ 145.40 (Mes *o*-C), 144.78 (Mes *o*-C), 139.41 (Mes *p*-C), 139.22 (Mes *p*-C), 134.14 (Mes *i*-C), 132.77 (Mes *i*-C), 129.47 (Mes *m*-CH), 129.41 (Mes *m*-CH); 67.90 (CH₂N), 25.29 (Mes *o*-CH₃), 24.62 (Mes *o*-CH₃), 20.99 (Mes *p*-CH₃), 20.05 (CH₂CH₃), 11.89 (CH₃); ²⁹Si NMR (C₆D₆, 119 MHz) δ 0.5 ppm; high resolution EI-MS *m/z* for C₃₉H₅₁NO₂Si₂ calc. 621.3458, found 621.3459. **5.6a,b** The products were separated from nitroethane by preparative thin layer chromatography on silica gel (hexanes and dichloromethane, 50:50), (35.6 mg, 87%). Mixture of

two isomers *Z* and *E* in (3: 1) ratio, Yellow oil; ^1H NMR (C_6D_6 , 400 MHz) δ 7.19 (q, 1H, $=\text{CH}_E$ $J = 6$ Hz), 6.73 (s, 8H, *m*-Mes $_{E \text{ and } Z}$), 6.38 (q, 1H, $=\text{CH}_Z$, $J = 6$ Hz), 2.42, 2.34 (each s, 24H, Mes *o*-CH $_{3E \text{ and } Z}$), 2.11, 2.10 (each s, 12H Mes *p*-CH $_{3E \text{ and } Z}$), 1.44 (d, 3H, CH $_{3E}$ $J = 6$ Hz); ^{13}C NMR (C_6D_6 , 150 MHz) δ 150 ($=\text{CH}_E$)^a, 149 ($=\text{CH}_Z$)^a, 144.42 (Mes *o*-C $_{E \text{ and } Z}$), 138.94 (Mes *p*-C $_{E \text{ and } Z}$), 130.9 (Mes *i*-C $_{E \text{ and } Z}$), 129.71 (Mes *m*-CH $_{E \text{ and } Z}$), 24.42 (Mes *o*-CH $_{3E \text{ and } Z}$), 21.03 (Mes *p*-CH $_{3E \text{ and } Z}$); 14.91 (CH $_{3E}$), 12.70 (CH $_{3E}$), high resolution EI-MS m/z for $\text{C}_{38}\text{H}_{49}\text{NO}_2\text{Si}_2$ Calc. 607.3302 found 607.3287. **5.6c,d** The products were purified by preparative thin layer chromatography on silica gel (hexanes and dichloromethane, 50:50), (36 mg, 86%). Mixture of two isomers *Z* and *E* in (2: 1) ratio, yellow oil; ^1H NMR (C_6D_6 , 400 MHz) δ 7.28 (t, 1H, $=\text{CH}_E$ $J = 6$ Hz), 6.74 (s, 16H, Mes *m*-H $_{E+Z}$), 6.37 (t, 1H, $=\text{CH}_Z$, $J = 5$ Hz), 2.04-2.49 (br s, 38H, Mes *o*-CH $_{3E+Z}$), 2.14 (dq, 2H, CH $_{2Z}$, $J = 2, 8$ Hz), 2.12-2.09 (br s, 24H, Mes *p*-CH $_{3E+Z}$), 1.68 (m, 2H, CH $_{2E}$), 0.63 (t, 3H, CH $_{3E}$, $J = 8$ Hz), 0.61 (t, 3H, CH $_{3Z}$, $J = 8$ Hz); ^{13}C NMR (C_6D_6 , 150 MHz) δ 156.37 ($=\text{CH}_{E+Z}$), 144.76 (Mes *o*-C $_{E+Z}$), 138.97 (Mes *p*-C $_{E \text{ or } Z}$), 138.80 (Mes *p*-C $_{E \text{ or } Z}$), 133.51 (Mes *i*-C $_{E,Z}$), 129.73 (Mes *m*-CH $_{E+Z}$), 24.54 (Mes *o*-CH $_{3E+Z}$), 23.25 (CH $_{2E}$), 21.02 (Mes *p*-CH $_{3E,Z}$), 20.21 (CH $_{2Z}$), 10.46 (CH $_{3E,Z}$); high resolution EI-MS m/z for $\text{C}_{39}\text{H}_{51}\text{NO}_2\text{Si}_2$ calc. 621.3458, found 621.3462. **5.7a** White powder contaminated with unknown compound (59 mg, 79%); ^1H NMR (C_6D_6 , 600 MHz) δ 6.65 (s, 8H, Mes *m*-H), 3.56 (q, 2H, CH $_2$, $J = 7$ Hz), 2.59 (s, 12H, Mes *o*-CH $_3$), 2.39 (s, 12H, Mes *o*-CH $_3$), 2.05, 2.03 (each s, 12H, Mes *p*-CH $_3$), 1.21 (t, 3H, CH $_3$ $J = 7$ Hz); ^{13}C NMR (C_6D_6 , 150 MHz) δ 144.29 (Mes *o*-C), 143.72 (Mes *o*-C), 139.53 (Mes *p*-C), 139.50 (Mes *p*-C), 132.65 (Mes *i*-C), 131.19 (Mes *i*-C), 129.41 (Mes *m*-CH), 129.26 (Mes *m*-CH), 46.33 (CH $_2$), 23.59 (Mes *o*-CH $_3$), 23.10 (Mes *o*-CH $_3$), 21.07 (Mes *p*-CH $_3$), 21.03 (Mes *p*-CH $_3$), 15.24 (CH $_3$); ^{29}Si NMR (C_6D_6 , 119 MHz) δ -22.6 (SiNO), -16.0 (SiO $_2$); high resolution EI-

^a Chemical shift extracted from gHMBC spectrum

MS m/z for $C_{38}H_{49}NO_2Si_2$ calc. 607.3302, found 607.3284. **5.7b** Colourless crystals (69 mg, 85 %); m.p.165-168 °C; 1H NMR (C_6D_6 , 400 MHz) δ 7.27 (d, 2H, Ph *o*-CH J = 8 Hz), 7.26 (d, 1H, =CHN J =13 Hz), 7.10 (t, 2H, Ph *m*-CH J = 8, 8 Hz), 6.94 (t, 1H, Ph *p*-CH J = 8, 7 Hz), [6.62 (s, Mes *m*-CH), 6.61 (s, Mes *m*-CH), all together 8H], 6.56 (d, 1H, =CHPh, J =13 Hz), 2.56 (s, 12H, Mes *o*-CH₃), 2.38 (s, 12H, Mes *o*-CH₃), [2.01 (s, Mes *p*-CH₃), 2.00 (s, Mes *p*-CH₃), all together 12H]; ^{13}C NMR (C_6D_6 , 100 MHz) δ 144.41 (Mes *o*-C), 143.90 (Mes *o*-C), 140.52 (Mes *p*-C), 140.15 (Mes *p*-C), 139.51 (Ph *i*-C+ Mes *i*-C), 130.66 (Ph *o*-C), 130.10 (Mes *i*-C)^b; 129.66 (Mes *m*-CH), 129.38 (Mes *m*-CH), 128.91 (Ph *m*-CH), 124.67 (=CHN), 124.44 (Ph *p*-C), 103.13 (=CHPh), 23.31 (Mes *o*-CH₃), 22.94 (Mes *o*-CH₃), 21.10 (Mes *p*-CH₃); ^{29}Si NMR (C_6D_6 , 119 MHz) δ -14.2, -22.2 ppm; high resolution EI-MS m/z for $C_{44}H_{51}NO_2Si_2$ calc. 681.3458, found 681.3441. **5.8a** separated from **5.7b** by preparative thin layer chromatography on silica gel (hexanes and dichloromethane, 50:50) (77 mg, 77%); Yellow oil contaminated with nitrostyrene; 1H NMR (C_6D_6 , 400 MHz) δ 7.05-6.98 (m, 3H, Ph *o*-CH+ Ph *p*-CH), 6.81-6.77 (m, 2H, Ph *m*-CH), [6.70 (s, Mes *m*-CH), 6.69 (s, Mes *m*-CH), all together 8H], 6.52 (t, 1H, =CH, J = 6 Hz), 4.43 (br s, 1H, OH), 3.49 (d, 2H, CH₂, J = 5.6 Hz), 2.56 (s, 12H, Mes *o*-CH₃), 2.47 (s, 12H, Mes *o*-CH₃), [2.10 (s, Mes *p*-CH₃), 2.08 (s, Mes *p*-CH₃), all together 12H]; ^{13}C NMR (C_6D_6 , 150 MHz) δ 156.05 (=CH), 144.48 (Mes *o*-C), 144.30 (Mes *o*-C), 139.51 (Mes *p*-C), 139.03 (Mes *p*-C), 136.26 (Ph *i*-C), 132.82 (Mes *i*-C), 131.41 (Mes *i*-C), 129.61 (Mes *m*-CH), 129.50 (Mes *m*-CH), 129.01 (Ph *o*-CH), 128.83 (Ph *m*-CH), 126.84 (Ph *p*-CH), 33.33 (CH₂), 23.91 (Mes *o*-CH₃), 23.68 (Mes *o*-CH₃), 21.05 (Mes *p*-CH₃); high resolution ESI-MS m/z for $C_{44}H_{53}NaNO_3Si_2$ calc. 722.3462, found 722.3483.

^b Both Mes *ipso*-C are assigned tentatively, no correlations were observed in 1H - ^{13}C - HMBC spectrum.

General Procedure for the Reaction of Nitro Compounds with

Tetramesityldigermene

Ge₃Mes₆ (100 mg, 0.107 mmol) was placed in a quartz tube and dissolved in THF (5 mL) and then irradiated ($\lambda = 350$ nm) in a quartz Dewar at -60 °C for ~ 18 h to give a bright yellow solution of digermene **1.2**. The solution was cooled during the irradiation by circulating cold methanol in the quartz Dewar. The nitro compound (~ 0.2 mmol) was added and the reaction was allowed to stir at room temperature. After 5 minutes, the colour of the reaction mixture changed. The solvent was evaporated giving a clear oil. The oil was dissolved in a minimum amount of hexanes. The flask was placed in a freezer (-14 °C) for 24 h, yielding crystalline material, which was isolated by decantation. **5.9a** Yellow oil (50 mg, 67 %); ¹H NMR (C₆D₆, 400 MHz) δ 6.67 (s, 4H, Mes *m*-H), 6.65 (s, 4H, Mes *m*-H), 3.46 (q, 2H, NCH₂, J = 7 Hz), 2.47 (s, 12H, Mes *o*-CH₃), 2.42 (s, 12H, Mes *o*-CH₃), 2.04 (s, 12H, Mes *p*-CH₃), 1.19 (t, 3H, CH₃, J = 7 Hz); ¹³C NMR (C₆D₆, 100 MHz) δ 143.71 (Mes *o*-C), 143.33 (Mes *o*-C), 139.12 (Mes *p*-C), 139.97 (Mes *p*-C), 138.78 (Mes *i*-C), 137.54 (Mes *i*-C), 129.43 (Mes *m*-CH), 129.38 (Mes *m*-CH), 59.71 (NCH₂), 24.64 (Mes *o*-CH₃), 24.00 (Mes *o*-CH₃), 20.94 (Mes *p*-CH₃), 11.54 (CH₃); high resolution EI-MS *m/z* for C₃₈H₄₉NO₂⁷⁰Ge⁷²Ge calc. 693.3763, found 693.2216. **5.9b** Yellow oil (68 mg, 89 %); ¹H NMR (C₆D₆, 600 MHz) δ 6.68 (s, 4H, Mes *m*-H), 6.65 (s, 4H, Mes *m*-H), 3.45 (t, 2H, NCH₂ J= 7Hz), 2.48 (s, 12H, Mes *o*-CH₃), 2.43 (s, total 12H, Mes *o*-CH₃), 2.05, 2.04 (each s, 12H, Mes *p*-CH₃), 1.73 (sext, 2H, CH₂CH₃ J= 7 Hz, 8 Hz), 0.75 (t, 3H, CH₃, J= 7 Hz); ¹³C NMR (C₆D₆, 150 MHz) δ 143.67 (Mes *o*-C), 143.33 (Mes *o*-C), 139.13 (Mes *p*-C), 138.71 (Mes *p*-C), 137.64 (Mes *i*-C), 129.79 (Mes *i*-CH), 129.56 (Mes *m*-CH), 129.38 (Mes *m*-CH), 67.23 (NCH₂), 24.63 (Mes *o*-CH₃), 23.97 (Mes *o*-CH₃), 20.95 (Mes *p*-CH₃), 20.56 (CH₂CH₃),

11.99 (CH₃); high resolution EI-MS m/z for C₃₉H₅₁NO₂⁷⁰Ge₂ calc. 705.2405, found 705.2400.

5.9c Brown solid contaminated with nitrobenzene and (Mes₂GeO)₂³² in a ratio 1:3:0.06, respectively (41 mg, 76.7 %); ¹H NMR (C₆D₆, 400 MHz) δ 7.86 (d, 2H, Ph *o*-H, J = 8 Hz), 7.21 (t, 2H, Ph *m*-H, J = 9 Hz), 6.96 (t, 1H, Ph *p*-H, J = 7 Hz), 6.64 (s, 8H, Mes *m*-H), 2.45 (s, 24H, Mes *o*-CH₃), 2.04 (s, 12H, Mes *p*-CH₃); ¹³C NMR (C₆D₆, 100 MHz) δ 155.19 (Ph *i*-C), 143.57 (br s, Mes *o*-C), 139.38 (Mes *p*-C), 137.64 (Mes *i*-C),^c 129.52 (Mes *m*-H), 128.49 (Ph *m*-CH), 124.92 (Ph *p*-CH), 120.40 (Ph *o*-CH), 24.38 (br s, Mes *o*-CH₃), 20.94 (Mes *p*-CH₃); high resolution EI-MS m/z for C₄₂H₄₉NO₂⁷²Ge⁷⁴Ge calc. 745.2196 found 745.2190. **5.9d** Yellow oil contaminated with decomposition products (78 mg, 94%); ¹H NMR (C₆D₆, 400 MHz) δ 7.34 (d, 1H, =CHN J= 14 Hz), 7.17 (d, 2H, Ph, J= 7.2 Hz), 7.04 (t, 2H, Ph, J= 8 Hz), 6.96 (d, 2H, =CHPh J= 13.6 Hz), 6.70-6.68 (m, Ph), 6.66 (s, 8H, Mes *m*-CH), 2.47 (s, 24H, Mes *o*-CH₃), 2.04 (s, 12H, Mes *p*-CH₃); ¹³C NMR (C₆D₆, 150 MHz) δ 143.67 (Mes *o*-C), 141.52 (=CH), 139.38 (Mes *p*-C), 137.35 (Mes *i*-C), 136.92 (Ph *i*-C), 130.06 (Ph *p*-CH), 129.54 (Mes *m*-CH), 128.71 (Ph *m*-CH), 126.77 (Ph *o*-CH), 117.16 (=CH), 24.00 (Mes *o*-CH₃), 20.94 (Mes *p*-CH₃).

5.10a,b The products were separated from residual nitroethane by preparative thin layer chromatography on silica gel (hexanes and dichloromethane, 90:10). Mixture of two isomers *E* and *Z* in (1: 1) ratio, yellow oil (36 mg, 46%); ¹H NMR (C₆D₆, 600 MHz) δ 7.16 (q, 1H, =CH_{*E*}, J = 5.4 Hz), 6.71 (s, 12H, Mes_{*E* or *Z*} *m*-CH), 6.63 (s, 4H, Mes_{*Z* or *E*} *m*-CH), 6.38 (q, 1H, =CH_{*Z*}, J = 5.4 Hz), 2.52 (s, 12H, Mes *o*-CH_{3 *Z* or *E*}), 2.51 (s, 12H, Mes *o*-CH_{3 *E*}), 2.48 (s, 12H, Mes *o*-CH_{3 *E* or *Z*}), 2.45 (s, 12H, Mes *o*-CH_{3 *E* or *Z*}), [2.09 (s, Mes *p*-CH_{3 *Z* or *E*}), 2.08 (s, Mes *p*-CH_{3 *Z* or *E*}), 2.06 (s, Mes *p*-CH_{3 *Z+E*}), all together 24H] 1.5 (d, 3H, J = 4.8 Hz, CH_{3 *Z*}), 1.23 (d, 3H, J = 6 Hz, CH_{3 *E*}); ¹³C NMR (C₆D₆, 150 MHz) δ 148.66 (=CH_{*E*}), 148.02 (=CH_{*Z*}), 143.72 (Mes _{*Z* or *E*} *o*-C), 143.23

^c Chemical shift extracted from gHMBC spectrum

(Mes *Z* or *E* *o*-C), 139.34 (Mes *Z* or *E* *p*-C), 138.95 (Mes *Z* or *E* *p*-C), 138.90 (Mes *Z* or *E* *p*-C), 138.70 (Mes *Z* or *E* *p*-C), 138.18 (Mes *Z* or *E* *i*-C), 137.80 (Mes *Z* or *E* *i*-C), 135.27 (Mes *Z* or *E* *i*-C), 129.62 (Mes *Z* or *E* *m*-CH), 129.60 (Mes *Z* or *E* *m*-CH), 129.57 (Mes *Z* or *E* *m*-CH), 129.55 (Mes *Z* or *E* *m*-CH), 129.42 (Mes *Z* or *E* *m*-CH), 24.40 (Mes *o*-CH₃*Z* or *E*), 24.22 (Mes *o*-CH₃ *Z* or *E*), 23.09 (Mes *o*-CH₃ *Z* or *E*), 21.00 (Mes *p*-CH₃ *Z* or *E*), 20.97 (Mes *p*-CH₃ *Z* or *E*), 14.91 (CH₃*E*), 11.69 (CH₃*Z*); high resolution ESI-MS *m/z* for C₃₈H₄₉NNaO₂⁷⁰Ge₂ calc. 714.2146, found 714.2140. **5.10c,d**: The product was separated from **5.9b** by preparative thin layer chromatography on silica gel (hexanes and dichloromethane, 30:70). Mixture of two isomers *E* and *Z* in (1: 0.3) ratio, contaminated with water adduct; yellow oil (34 mg, 46%); ¹H NMR (C₆D₆, 400 MHz) δ 7.24 (t, 1H, =CH_E, J = 6 Hz), 6.71 (s, 16H, Mes *m*-H_{*E+Z*}), 6.35 (t, 1H, =CH_Z J = 6 Hz), 2.54 (s, 12H, Mes *o*-CH₃*E* or *Z*), 2.50 (s, 12H, Mes *o*-CH₃*Z* or *E*), 2.48 (s, 12H, Mes *o*-CH₃*E*), 2.46 (s, 12H, Mes *o*-CH₃*Z*), 2.18 (dq, 2H, CH₂CH₃*Z*, J = 2, 7 Hz), 2.08 (s, 12H, Mes *p*-CH₃*E*), 2.07 (s, 6H, Mes *p*-CH₃*Z*), 2.06 (s, 6H, Mes *p*-CH₃*E*), 1.67 (dq, 2H, CH₂CH₃*E*, J = 1, 8 Hz), 0.66 (t, 3H, CH₃*Z*, J = 8 Hz), 0.61 (t, 3H, CH₃*E*, J = 8 Hz); ¹³C NMR (C₆D₆, 100 MHz) δ 154.45 (=CH_Z), 154.02 (=CH_E), 143.71 (Mes *o*-C_{*Z/E*}), 143.66 (Mes *o*-C_{*E/Z*}), 138.92 (Mes *p*-C_{*E/Z*}), 138.70 (Mes *p*-C_{*E/Z*} and Mes *i*-C_{*E*}), 138.16 (Mes *i*-C_{*Z*}), 137.83 (Mes *i*-C_{*E*}), 129.57 (Mes *m*-CH_{*E/Z*}), 129.53 (Mes *m*-CH_{*Z/E*}), 24.36 (Mes *o*-CH₃*E/Z*), 24.24 (Mes *o*-CH₃ *Z* or *E*), 24.12 (Mes *o*-CH₃ *E*), 23.99 (Mes *o*-CH₃*Z*), 23.26 (CH₂*E*), 20.97 (Mes *p*-CH₃*E*), 20.95 (Mes *p*-CH₃*Z/E*), 19.30 (CH₂*Z*), 10.92 (CH₃*E*), 10.53 (CH₃*Z*); high resolution ESI-MS *m/z* for C₃₉H₅₁NO₂⁷⁰Ge₂Na calc. 728.2298, found 728.2303. **5.11a** Brown oil; ¹H NMR (C₆D₆, 600 MHz) δ 7.35 (d, 2H, Ph *o*-H, J = 7 Hz), 7.16 (t, 2H, Ph *m*-H, J = 8 Hz), 6.6-6.7 (m, 1H, Ph *p*-H), 6.63 (s, 4H, Mes *m*-H), 6.58 (s, 4H, Mes *m*-H), 2.58 (s, 12H, Mes *o*-CH₃), 2.41 (s, 12H, Mes *o*-CH₃), 1.99, 1.97 (each s, 6H, Mes *p*-CH₃); ¹³C NMR (C₆D₆, 150 MHz) δ 152.61 (Ph *i*-C), 143.42 (Mes *o*-C), 143.26 (Mes *o*-C), 140.16 (Mes *p*-C), 139.81 (Mes *p*-C),

139.85 (Mes *i*-C), 129.61 (Mes *m*-CH), 129.42 (Ph *m*-CH), 129.27 (Mes *m*-CH), 118.21 (Ph *p*-CH), 113.01 (Ph *o*-C), 23.54 (Mes *p*-CH₃), 22.63 (Mes *p*-CH₃), 21.02 (Mes *o*-CH₃), 20.96 (Mes *o*-CH₃). **5.11b** Yellow oil contaminated with **5.9d** plus two isomers of Mes₄Ge₂O₂³²; (78 mg, 94%); ¹H NMR (C₆D₆, 400 MHz) δ 7.30 (d, 1H, =CH, J = 13 Hz), 7.29 (d, 2H, Ph *o*-CH, J = 8 Hz), 7.11 (t, 2H, Ph *m*-CH, J = 8 Hz), 6.70-6.67 (m, Ph *p*-CH), 6.61 (s, 8H, Mes *m*-CH), 6.57 (d, 1H, =CH J = 13 Hz), 2.59 (s, 12H, Mes *o*-CH₃), 2.44 (s, 12H, Mes *o*-CH₃), 2.00, 1.99 (each s, total 12H Mes *o*-CH₃); ¹³C NMR (C₆D₆, 100 MHz) δ 143.32 (Mes *o*-C), 143.03 (Mes *o*-C), 140.25 (Ph *i*-C), 134.47 (Ph *o*-C), 133.78 (Mes *i*-C), 133.66 (Mes *i*-C), 129.34 (Mes *m*-CH), 129.09 (Ph *p*-C), 128.98 (Ph *m*-CH), 124.27 (=CH), 101.43 (=CH), 23.06 (Mes *o*-CH₃), 22.65 (Mes *o*-CH₃), 21.02 (Mes *p*-CH₃) 20.99 (Mes *p*-CH₃); high resolution EI-MS *m/z* for C₄₄H₅₁NO₂⁷⁴Ge⁷²Ge calc. 771.2352, found 771.2315. **5.14** The products were separated from **5.11b** by preparative thin layer chromatography on silica gel (hexanes and dichloromethane, 50:50) Yellow oil (; ¹H NMR (C₆D₆, 600 MHz) δ 7.04- 7.7.00 (m, Ph *o*-CH), 6.87 (d, 1H, Ph *p*-CH, J = 8 Hz), 6.70- 6.69 (m, Ph *m*-CH), [6.67 (s, Mes *m*-H), 6.66 (s, Mes *m*-H) all together 8H], 6.62 (t, 1H, =CH, J = 5 Hz), 3.57 (d, 2H, J = 5 Hz), 2.59 (s, 12H, Mes *o*-CH₃), 2.53 (s, 12H, Mes *o*-CH₃), [2.02 (s, Mes *p*-CH₃), 2.06 (s, Mes *p*-CH₃), all together 12H)]; ¹³C NMR (C₆D₆, 150 MHz) δ 153.71 (=CH), 143.54 (Mes *o*-C), 143.33 (Mes *o*-CH), 139.60 (Mes *p*-C), 139.14 (Mes *p*-C), 137.19 (Ph *i*-C), 135.50 (Mes *i*-C), 134.63 (Mes *i*-C), 129.35 (Mes *m*-CH), 128.99 (Ph *m*-CH), 128.74 (Ph *p*-CH), 126.57 (Ph *o*-CH), 47.16 (CH₂), 23.19 (Mes *o*-CH₃), 23.03 (Mes *o*-CH₃), 20.99 (Mes *p*-CH₃); high resolution ESI-MS *m/z* for C₄₄H₅₃NO₃⁷⁰Ge₂Na calc. 806.2408, found 806.2405.

Addition of Nitrosobenzene to Tetramesityldigermene

Ge₃Mes₆ (0.100 g, 0.107 mmol) was placed in a quartz tube and dissolved in THF (5 mL) and then irradiated ($\lambda = 350$ nm) in a quartz Dewar at -60 °C for ~ 18 h to give a bright yellow solution of digermene **1.2**. The solution was cooled during the irradiation by circulating cold methanol in the quartz Dewar. Nitrosobenzene (21 mg, 0.2 mmol) was added and the reaction was allowed to stir at room temperature. After 5 minutes, the colour of the reaction mixture changed to light green. **5.12** Green oil (69 mg, 88 %); ¹H NMR (C₆D₆, 600 MHz) δ 7.59 (d, 2H, Ph *o*-H, J = 8 Hz), 7.10-6.90 (m, Ph *m*-H), 6.70-6.60 (m, Ph *p*-H), 6.59 and 6.55 (each s, 8H, Mes *m*-H), 2.47 (s, total 12H, Mes *o*-CH₃), 2.35 (s, 12H, Mes *o*-CH₃), 2.01 and 1.96 (each s, 12H, Mes *p*-CH₃); ¹³C NMR (C₆D₆, 150 MHz) δ 153.66 (Ph *i*-C), 143.55 (Mes *o*-C), 143.05 (Mes *o*-C), 139.83 (Mes *p*-C), 139.30 (Mes *p*-C), 137.75 (Mes *i*-C), 135.47 (Mes *i*-C), 129.69 (Mes *m*-CH), 129.29 (Mes *m*-CH), 128.49 (Ph *m*-CH), 120.67 (Ph *o*-CH), 116.48 (Ph *p*-CH), 24.01 (Mes *o*-CH₃), 23.18 (Mes *o*-CH₃), 20.93 (Mes *p*-CH₃); high resolution ESI-MS *m/z* for C₄₂H₅₀NO⁷⁰Ge₂ calc. 724.2377, found 724.2368.

Addition of *m*-cpba to **5.12**

To the light green hexanes solution of **5.12**, (20 mg, 0.2 mmol) *m*-cpba was added. The colour of the solution changed to colourless. The reaction mixture was separated on silica gel chromatography (70:30, DCM: hexanes) **5.13** Colourless oil (35 mg, 41%) ; ¹H NMR (C₆D₆, 400 MHz) δ 8.14 (s, 1H, Ph *o*-CH), 7.84 (d, 1H, Ph *p*-CH, J = 8Hz), 7.02 (d, 1H, Ph *o*-CH, J = 8Hz), 6.68 (t, 1H, Ph *m*-CH, J = 8Hz), 6.63 (s, 4H, Mes *m*-H), 5.05 (br s, 1H, OH), 2.55 (s, 12H, Mes *o*-CH₃), 2.50 (s, 12H, Mes *o*-CH₃), 2.05 (s, 6H, Mes *p*-CH₃), 2.02 (s, 6H, Mes *p*-CH₃); ¹³C NMR (C₆D₆, 150 MHz) δ 169.04 (CO), 143.45 (Mes *o*-C), 143.34 (br s, Mes *o*-C), 139.53 (Mes *p*-C),

139.05 (Mes *p*-C), 138.54 (Mes *i*-C), 137 (Mes *i*-C)^d, 134.83 (Ph *i*-C), 132.70 (Ph *o*-C), 130.5 (Ph *m*-CH), 130.12 (Mes *m*-CH), 130 (Ph *m*-CH)^e, 129.63 (Mes *m*-CH), 129 (Ph *p*-C)^e, 24.59 (Mes *o*-CH₃), 20.92 (Mes *p*-CH₃), high resolution ESI-MS *m/z* for C₄₃H₄₉Na³⁵ClO₃⁷⁰Ge₂ calc. 811.17529, found 811.17679, for (Mes₂GeO₃NPhGeMes₂) high resolution ESI-MS *m/z* for C₄₂H₅₀NO₃⁷⁰Ge₂ calc. 756.2264, found 724.2276.

DFT Calculations

First principles calculations were performed using Gaussian 09³³ on the Shared Hierarchical Academic Research Computing Network (SHARCNET, www.sharcnet.ca). Calculations were performed on an 8 core Xeon 2.83 GHz CPU with 16 GB memory. All calculations were performed at the TPSS/6-31G(d) level of theory.

Single Crystal X-ray Diffraction Experimental Details

Data Collection and Processing. The sample was mounted on a Mitegen polyimide micromount with a small amount of Paratone N oil. All X-ray measurements were made on a Bruker Kappa Axis Apex2 diffractometer or Nonius Bruker KappaCCD Apex2 diffractometer for **5.13** at a temperature of 110 K. For **5.7a**, before intensity data collection, the sample crystal was recognized as a non-merohedral twin. A second domain was rotated relative to the first by an approximately 2.8° rotation about the [-0.799, 0.030, 1.000] reciprocal space axis. The frame integration was performed using SAINT.³⁵ The resulting raw data was scaled and absorption corrected using a multi-scan averaging of symmetry equivalent data using SADABS or TWINABS for **5.7a**.³⁵

^d Chemical shift extracted from gHMBC spectrum

^e Chemical shift extracted from gHSQC spectrum

Structure Solution and Refinement. The structure was solved by using a dual space methodology using the SHELXT program.³⁶ All non-hydrogen atoms were obtained from the initial solution. The hydrogen atoms were introduced at idealized positions and were allowed to ride on the parent atom. For **5.7a**, the ethyl group exhibited a disorder which distributed the methyl group over two sites. The occupancies were refined and normalized and converged to a value of 0.738(10) for the major conformer. For **5.13**, a region of disorder was found in the meta-chlorine atoms on the phenyl ring of the MCPBA fragment. A rotation of 180° about the C19-C20 bond was found, and the normalized occupancy refined to a value of 0.574(3) for Cl(1). The structural model was fit to the data using full matrix least-squares based on F^2 . The calculated structure factors included corrections for anomalous dispersion from the usual tabulation. The structure was refined using the SHELXL-2014 program from the SHELX suite of crystallographic software.³⁷ Graphic plots were produced using the XP program suite.³⁸

Table 5.1: Crystallographic data of compounds **5.5a**, **5.7b**, **5.7c**, **5.9c** and **5.13**

Data	5.7a	5.7b	5.7c	5.9c	5.13
Formula	C ₃₈ H ₄₉ NO ₂ Si ₂	C ₄₄ H ₅₁ NO ₂ Si ₂	C ₈₄ H ₉₈ N ₂ O ₄ Si ₄	C ₄₂ H ₄₉ Ge ₂ NO ₂	C ₄₃ H ₄₉ ClGe ₂ O ₃
Formula Weight (g/mol)	607.96	682.03	1312.00	745.00	794.45
Crystal System	triclinic	monoclinic	monoclinic	triclinic	orthorhombic
Space Group	P-1	P2 ₁ /n	P2 ₁ /c	P-1	Pbca
<i>a</i> , Å	10.0666(14)	11.097(4)	18.477(7)	8.878(3)	14.446(3)
<i>b</i> , Å	11.886(2)	14.196(4)	18.323(6)	11.984(4)	22.041(5)
<i>c</i> , Å	15.146(2)	24.907(8)	21.958(8)	18.814(6)	23.719(5)
α , °	73.729(13)	90	90	87.195(10)	90
β , °	79.030(9)	96.187(7)	97.525(16)	78.020(11)	90
γ , °	81.360(8)	90	90	69.010(12)	90
<i>V</i> , Å ³	1698.9(5)	3901(2)	7370(4)	1827.3(10)	7552(3)
<i>Z</i>	2	4	4	2	8

R ₁	0.0684	0.0504	0.0516	0.0383	0.0367
wR ₂	0.1680	0.1222	0.1156	0.0801	0.0935
R ₁ (all data)	0.1303	0.0896	0.1071	0.0689	0.0471
wR ₂ (all data)	0.2038	0.1410	0.1359	0.0892	0.1006
GOF	1.041	1.037	1.028	1.018	1.029

5.6 References

- For recent accounts on various aspects of ditetrelenes chemistry: (a) Iwamoto, T.; Ishida, S. *Struct. Bonding* **2014**, *156*, 125; (b) Sasamori, T.; Tokitoh, N. *Bull. Chem. Soc. Jpn.* **2013**, *86*, 1005; (c) Kira, M. *Proc. Jpn. Acad., Ser. B* **2012**, *88*, 167; (d) Matsuo, T. Kobayashi M.; Tamao, K. *Dalton Trans.* **2010**, *39*, 9203; (e) Abersfelder, K.; Scheschkewitz, D. *Pure Appl. Chem.* **2010**, *82*, 595; (f) Scheschkewitz, D. *Chem. Eur. J.* **2009**, *15*, 2476; (g) Kira, M. *J. Organomet. Chem.* **2004**, *689*, 4475; (h) Weidenbruch, M. *Organometallics* **2003**, *22*, 4348; (i) Plyusnin, V. F.; Kaletina M. V.; Leshina, T. V. *Russ. Chem. Rev.* **2007**, *76*, 931; (j) Takeda, N.; Tokitoh N.; Okazaki, R. *Science of Synthesis*; Moloney, M. G., Eds.; Thieme, Stuttgart, 2003; Chapters 5.1.2.
- Majumdar, M.; Bejan, L.; Huch, V.; White, A. J. P.; Whittell, G. R.; Schäfer, A.; Manners, I.; Scheschkewitz, D. *Chem. Eur. J.* **2014**, *20*, 9225.
- For recent reviews, see: (a) Kachian, J. S. Wong, K. T. Bent, S. F. *Acc. Chem. Res.* **2010**, *43*, 346; (b) Hamers, R. J. *Annu. Rev. Anal. Chem.* **2008**, *1*, 707; (c) Loscutoff, P. W. Bent, S. F. *Annu. Rev. Phys. Chem.* **2006**, *57*, 467; (d) Bilic, A. J. Reimers, R. Hush N. S. in *Properties of Single Organic Molecules on Crystal Surfaces*; Grütter, P.; Hofer, W. Rosei F., Eds.; Imperial College Press, London, 2006; p. 333; (e) Hamers, R. J.;

- Coulter, S. K.; Ellison, M. D.; Hovis, J. S.; Padwitz, D. F.; Schwartz, M. P.; Greenlief, C. M.; Russell Jr., N. *Acc. Chem. Res.* **2000**, *33*, 617.
4. Tashkandi, N. Y.; Parsons, F.; Guo, J.; Baines, K. M. *Angew. Chem. Int. Ed.* **2015**, *54*, 1612.
5. (a) Eng, J.; Hubner, Jr., I. A.; Barriocanal, J.; Opila, R. L.; Doren, D. J. *J. Appl. Phys.* **2004**, *95*, 1963; (b) Barriocanal, J.; Doren, D. J. *J. Phys. Chem. B* **2000**, *104*, 12269.
6. Shong, B.; Bent, S. *J. Phys. Chem. C* **2014**, *118*, 29224.
7. Bocharov, S.; Teplyakov, A. V. *Surf. Sci.* **2004**, *573*, 403.
8. Méndez De Leo, L.P.; Teplyakov, A.V. *J. Phys. Chem. B* **2006**, *110*, 6899.
9. Perrine, K. A.; Leftwich, T. R.; Weiland, C. R.; Madachik, M. R.; Opila, R. L.; Teplyakov, A. V. *J. Phys. Chem. C* **2009**, *113*, 6643.
10. Madachik, M. R.; Teplyakov, A. V. *J. Phys. Chem. C* **2009**, *113*, 18270.
11. Leftwich, T. R.; Teplyakov, A. V. *J. Electron Spectrosc. Relat. Phenom.* **2009**, *175*, 31.
12. Peng, G.; Seo, S.; Ruther, R. E.; Hamers, R. J.; Mavrikakis, M.; Evans, P. G. *J. Phys. Chem. C* **2011**, *115*, 3011.
13. Madachik, M. R.; Teplyakov, A. V. *J. Phys. Chem. C* **2009**, *113*, 18270.
14. (a) Hardwick, J. A.; Pavelka, L. C.; Baines, K. M. *Dalton Trans.* **2012**, *41*, 609; (b) Hurni, K. L.; Baines, K. M. *Chem. Comm.* **2011**, *47*, 8382; (c) Hurni, K. L.; Rupar, P. A.; Payne, N. C.; Baines, K. M. *Organometallics* **2007**, *26*, 5569; (d) Gottschling, S. E.; Milnes, K. K.; Jennings, M. C.; Baines, K. M. *Organometallics* **2005**, *24*, 3811; (e) Gottschling, S. E.; Jennings, M. C.; Baines, K. M. *Can. J. Chem.* **2005**, *83*, 1568; (f)

- Samuel, M. S.; Baines, K. M. *J. Am Chem. Soc.* **2003**, *125*, 12702; (g) Samuel, M. S.; Jenkins, H. A.; Hughes, D. W.; Baines, K. M. *Organometallics* **2003**, *22*, 1603.
15. Fink, M. J.; Michalczyk, M. J.; Haller, K. J.; Michl, J.; West, R. *Organometallics* **1984**, *3*, 793.
16. Assignment of the configuration about the C=N double bond was made based on a comparison of the chemical shifts of vinylic hydrogen in structurally-related compounds: Pretsch, E.; Buhlmann, P.; Badertscher, M. *Structure Determination of Organic Compounds*; Springer, 2009; 4th edition.
17. Samuel, M. S.; Jennings, M.C.; Baines, K. M. *J. Organomet. Chem.* **2001**, *636*, 130.
18. Tao, J.; Perdew, J. P.; Staroverov, V. N.; Scuseria, G. E. *Phys. Rev. Lett.* **2003**, *91*, 146401.
19. It is unlikely that the transition state is of a lower energy than the product but clearly it is lower than the saturated analogue; however, under the chosen level of theory the transition state is negative.
20. Gillette, G. R.; Maxka J.; West, R. *Angew. Chem. Int. Ed.* **1989**, *28*, 54.
- 21 Lambert, J. B.; Zhao, Y.; Emblidge, R. W.; Salvador, L. A.; Liu, X.; So, J- H.; Chelius, E. C. *Acc. Chem. Res.* **1999**, *32*, 183.
22. Kuczkowski, R. L. *Chem. Soc. Rev.* **1992**, *21*, 79.
23. El Kettani, S.; Lazraq, M.; Ranaivonjatovo, H.; Escudie, J.; Couret, C.; Gornitzka, H.; Atmani, A. *Organometallics* **2005**, *24*, 5364.
24. Horner, D.; Grev, R.; Schaefer, H. F. *J. Am. Chem. Soc.* **1992**, *114*, 2093.
25. Dr. Bonggeun Shong, private communication.

26. Wang, Y.; Ma, J. *J. Phys. Chem. B* **2006**, *110*, 5542.
27. (a) Fawcett, C. H. *Nature* **1964**, *204*, 1200. (b) Park, J.; Pei, D. *Biochemistry* **2000**, *43*, 15014; (c) Gergely, A.; Gyimesi-Forrás, K.; Horvath, P.; Hosztafi, S.; Koekoesi, J.; Nagy, P. I.; Szasz, G.; Szentesi, A. *Curr. Med. Chem.* **2004**, *11*, 2555; (d) Mokaya, R.; Poliakov, M. *Nature* **2005**, *437*, 1243.
28. For other metal reductions of nitroalkanes to oximes, see: (a) Akita, Y.; Inaba, M.; Uchida, H.; Ohta, A. *Synthesis* **1977**, 792; (b) Johnson, K.; Degering, E. F. *J. Am. Chem. Soc.* **1939**, *61*, 3194.
29. (a) Braun, V. J.; Sobel, W. *Ber. Dtsch. Chem. Ges.* **1911**, *44*, 2526; (b) Hughes, C. C.; Trauner, D. *Angew. Chem., Int. Ed.* **2002**, *41*, 4556; (c) Grundmann, C. *Angew. Chem.* **1950**, *62*, 558; For other methods, see: (d) Barton, D. H. R.; Fernandez, I.; Richard, C. S.; Zard, S. Z. *Tetrahedron* **1987**, *43*, 551; (e) Albanese, D.; Landini, D.; Penseo, M. *Synthesis* **1990**, 333; (f) Wang, K. W.; Qian, X. H.; Cui, J. N. *Tetrahedron* **2009**, *65*, 10377; (g) Czekelius, C.; Carreira, E. M. *Angew. Chem. Int. Ed.* **2005**, *44*, 612; (h) Miralles-Roch, F.; Tallec, A.; Tardivel, R. *Electrochim. Acta.* **1993**, *38*, 2379; (i) Corma, A.; Serna, P.; Garcia, H. *J. Am. Chem. Soc.* **2007**, *129*, 6358; For a recent account of oxime chemistry, see: Chiba, S.; Narasaka, K., *Science of Synthesis, Knowledge Updates*; Thieme, 2011; p. 445.
30. Cai, S.; Zhang, S.; Zhao, Y.; Wang, D. *Org. Lett.* **2013**, *15*, 2660.
31. McKillop, K., L.; Gillette, G., R.; Powell, D., R.; West, R. *J. Am. Chem. Soc.* **1992**, *114*, 5203.
32. Samuel, M. S.; Jennings, M. C.; Baines, K. M. *J. Organomet. Chem.* **2001**, *636*, 130.

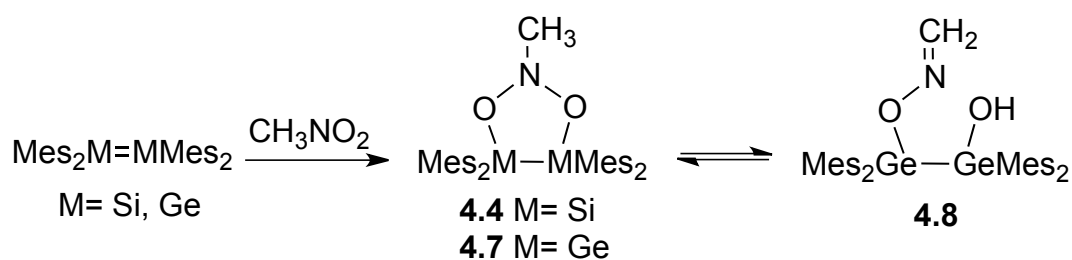
33. Frisch, M. J.; Trucks, G. W.; Schlegel, H. B.; Scuseria, G. E.; Robb, M. A.; Cheeseman, J. R.; Scalmani, G.; Barone, V.; Mennucci, B.; Petersson, G. A.; Nakatsuji, H.; Caricato, M.; Li, X.; Hratchian, H. P.; Izmaylov, A. F.; Bloino, J.; Zheng, G.; Sonnenberg, J. L.; Hada, M.; Ehara, M.; Toyota, K.; Fukuda, R.; Hasegawa, J.; Ishida, M.; Nakajima, T.; Honda, Y.; Kitao, O.; Nakai, H.; Vreven, T.; Montgomery, J. A., Jr.; Peralta, J. E.; Ogliaro, F.; Bearpark, M.; Heyd, J. J.; Brothers, E.; Kudin, K. N.; Staroverov, V. N.; Kobayashi, R.; Normand, J.; Raghavachari, K.; Rendell, A.; Burant, J. C.; Iyengar, S. S.; Tomasi, J.; Cossi, M.; Rega, N.; Millam, N. J.; Klene, M.; Knox, J. E.; Cross, J. B.; Bakken, V.; Adamo, C.; Jaramillo, J.; Gomperts, R.; Stratmann, R. E.; Yazyev, O.; Austin, A. J.; Cammi, R.; Pomelli, C.; Ochterski, J. W.; Martin, R. L.; Morokuma, K.; Zakrzewski, V. G.; Voth, G. A.; Salvador, P.; Dannenberg, J. J.; Dapprich, S.; Daniels, A. D.; Farkas, Ö.; Foresman, J. B.; Ortiz, J. V.; Cioslowski, J.; Fox, D. J.; Revision A1 ed.; Gaussian Inc.: Wallingford, CT, **2009**.
34. Tao, J.; Perdew, J. P.; Staroverov, V. N.; Scuseria, G. E. *Phys. Rev. Lett.* **2003**, *91*, 146401.
35. Bruker-AXS, SAINT version 2013.8, **2013**, Bruker-AXS, Madison, WI 53711, USA.
36. Beta version, Sheldrick, G. M. **2014**, University of Göttingen.
37. Sheldrick, G. M. *Acta Cryst.* **2008**, *A64*, 112.
38. Bruker-AXS, SAINT version 2013.8, **2013**, Bruker-AXS, Madison, WI 53711, USA.

Chapter 6

Reactivity of Sulfonyl-Containing Compounds with Ditetrelenes

6.1 Introduction

The use of main group compounds as reducing agents is well-established and includes common reagents such as PR_3 , Bu_3SnH , and SnX_2 .¹ The notion of using (di)tetrelenes specifically as reducing agents is known although it has not been well-explored. For example, the addition of nitro compounds to the ditetrelenes results in the nitrogen of the nitro moiety being reduced (**4.4** and **4.7**).²

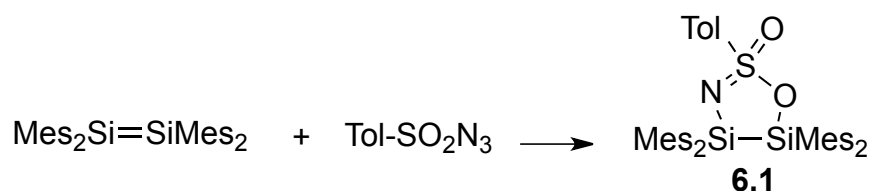


Scheme 6.1

In a similar fashion, 2,6-dimethylphenyl isocyanide reacts with tetraxlyldisilene to yield disilacyclopropanimine where the oxidation number of nitrogen has been reduced from +5 in the isocyanide to +3 in the product.² Other examples include the addition of azides to tetramesityldisilene, forming disilaaziridines.³ These reactions illustrate the potential use of ditetrelenes as effective reducing agents as the reductions occur rapidly, at room temperature and under mild conditions.

The potential of using unsaturated silicon and germanium compounds as reducing agents prompted us to explore the reactivity of sulfonyl-compounds with ditetrelenes.

Sulfonyl compounds are the sulfur analogues of nitro compounds and the sulfur oxidation number varies from +6 to -2, and thus, they are good candidates to explore in this context. Only one example of the addition of a sulfonyl derivative to a ditetrelene has been reported in the literature; the addition of *p*-toluenesulfonyl azide to tetramesityldisilene was reported by West and co-workers and resulted in the formation of **6.1** (Scheme 6.2).⁴ In this case, no reduction of the sulfur atom occurred.



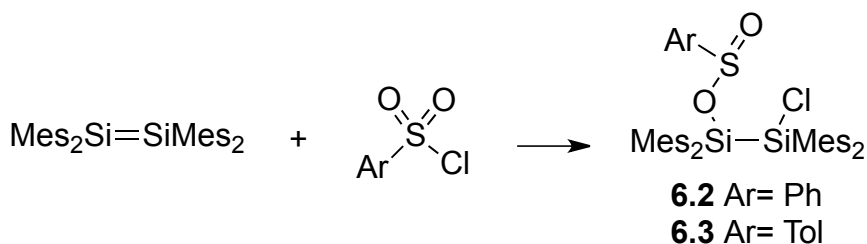
Scheme 6.2

The reactivity of RSO_2X derivatives where $\text{R} = \text{Ph}, \text{Tol}$; $\text{X} = \text{Cl}, \text{F}, \text{OH}, \text{Ph}$ and diphenylphosphine oxide towards ditetrelenes is the subject of this study.

6.2 Results

The addition of benzenesulfonyl chloride to a bright yellow solution of disilene **1.4** dissolved in hexanes or C_6D_6 at room temperature gave a colourless solution and removal of the solvent resulted in a white solid, identified as **6.2**. In a similar fashion, the addition of *p*-toluenesulfonyl chloride to the disilene yielded **6.3** (Scheme 6.3). The products were purified by recrystallization from a saturated hexanes solution at low temperature to yield colourless solids. The compounds were identified as adducts between the sulfonyl chlorides and disilene **1.4** by ^1H , ^{13}C , ^1H - ^1H gCOSY, ^1H - ^{13}C gHSQC, ^1H - ^{13}C gHMBC and ^{29}Si - ^1H gHMBC NMR spectroscopy, and ESI-TOF mass

spectrometry. The structures of **6.2** and **6.3** were unequivocally determined by single crystal X-ray diffraction as β -chlorotetramesityldisilyl benzenesulfinate, **6.2**, and β -chlorotetramesityldisilyl *p*-methylbenzenesulfinate, **6.3** (Figures 6.1 and 6.2).



Scheme 6.3

The structural metrics of **6.2** and **6.3** are similar; the bond angles and bond lengths for both adducts are within expected ranges. The sulfur atoms exhibit pyramidal geometry, indicating the presence of a stereochemically active lone pair. The sulfur is displaced from the plane of the attached atoms by 0.6882(19) Å for **6.2**. The Si-Cl bond lengths in **6.2** and **6.3** (2.0981(13) and 2.0949(8) Å, respectively), are not significantly different from the average Si-Cl bond lengths found in similar four-coordinate silicon compounds (2.116 ± 0.071 Å), based on a search of the Cambridge Structural Database.⁵ Likewise the Si-O bond lengths (1.700(2) Å for **6.2** and 1.6953(14) Å for **6.3**) are not significantly different from the average Si-O bond length found in similar four-coordinate silicon compounds (1.643 ± 0.032 Å).⁵ The Si-Si bond distances (2.3993(14) Å for **6.2** and 2.3997(10) Å for **6.3**), are near the mean of four-coordinate Si-Si compounds with single bonds (2.364 ± 0.032 Å).⁵ The non-bridging oxygen-sulfur bond distances are 1.462(3) and 1.4601(17) Å, for **6.2** and **6.3**, respectively, indicative of terminal oxygen-sulfur bonds, while the bridging oxygen-sulfur bonds have lengths of 1.637(2) and 1.6318(14) Å for **6.2** and **6.3**, respectively, that are longer. Compounds **6.2** and **6.3** are

air- and moisture-sensitive and decompose upon exposure to air or upon chromatography to unidentified compounds.

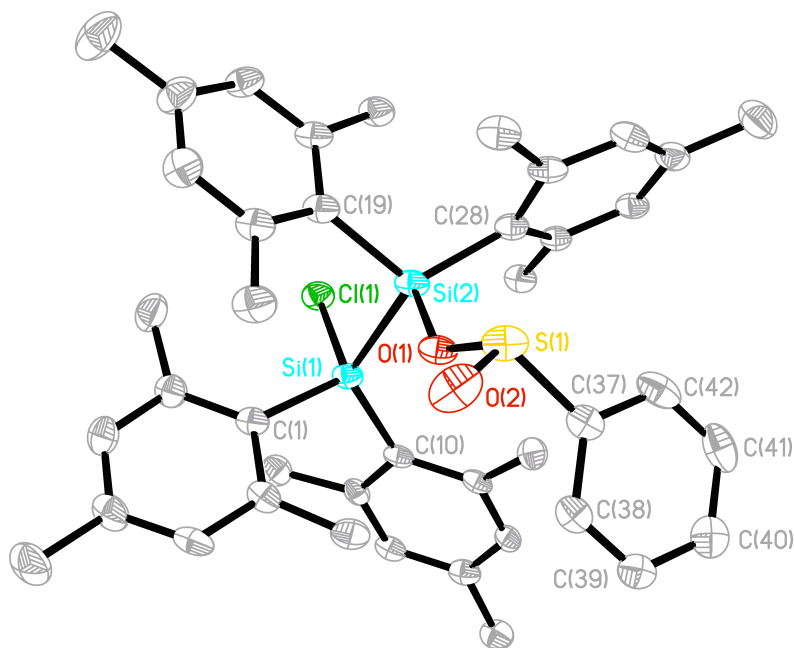


Figure 6.1 Displacement ellipsoid plot of **6.2**. Ellipsoids are at the 50% probability level and hydrogen atoms were omitted for clarity. Selected bond lengths (Å) and angles (deg): Si1-C11 = 2.0981(13), Si1-Si2 = 2.3993(14), S1-O2 = 1.462(3), S1-O1 = 1.637(2), Si2-O1 = 1.700(2); Cl1-Si1-Si2 = 99.86(5), O2-S1-O1 = 105.23(14), O2-S1-C37 = 105.88(16), O1-Si2-Si1 = 101.47(9), S1-O1-Si2 = 134.54(15).

Due to the presence of the chiral sulfur centre, the two mesityl groups on each silicon are diastereotopic. Accordingly, the ^1H NMR spectra of **6.2** and **6.3** reveal the presence of four nonequivalent mesityl groups in addition to an aryl group. Two of the signals assigned to the *o*-methyl groups on the mesityl groups in each spectrum are broad due to the slow rotation of the mesityl groups on the NMR time scale; these signals can be assigned to the mesityl groups on the silicon bearing the sulfinate moiety. Heating the sample to 70 °C resulted in sharpening of the signals in the ^1H NMR and ^{13}C NMR spectra of **6.2** and **6.3**.

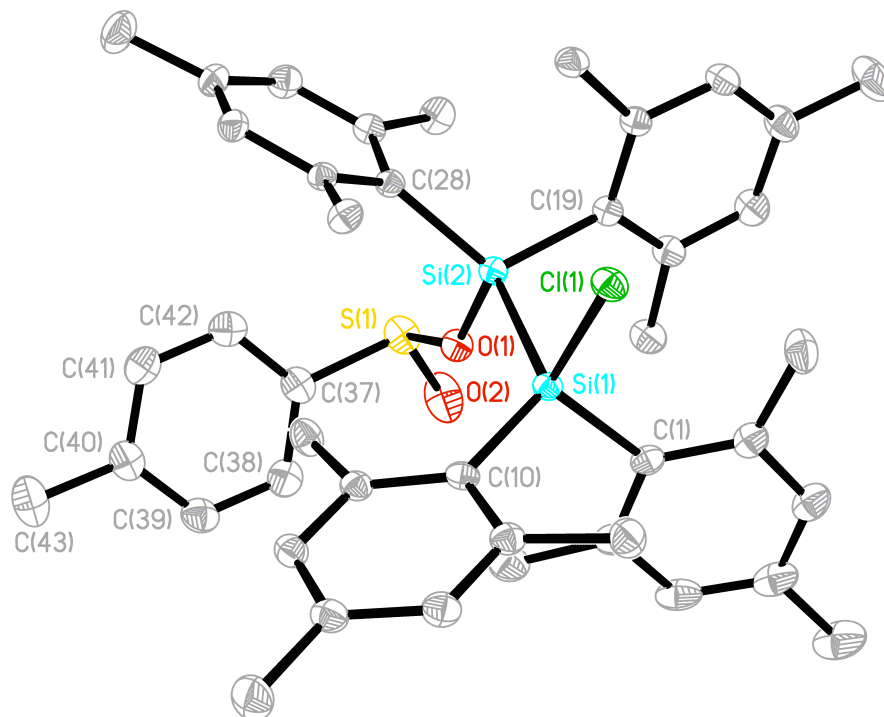
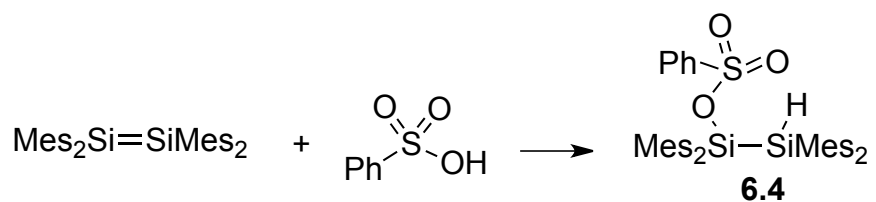


Figure 6.2 Displacement ellipsoid plot of **6.3** ellipsoids are at the 50% probability level and hydrogen atoms were omitted for clarity. Selected bond lengths (Å) and angles (deg): Si1-Cl1 = 2.0949(8), Si1-Si2 = 2.3997(10), Si2-O1 = 1.6953(14), O1-S1 = 1.6318(14), S1-O2 = 1.4601(17); Cl1-Si1-Si2 = 99.69(3), O1-Si2-Si1 = 100.92(5), S1-O1-Si2 = 136.06(9), O2-S1-O1 = 105.12(9), O2-S1-C37 = 105.95(10).

To explore the effect of the halide on the outcome of the reaction, the addition of benzenesulfonyl fluoride and diphenyl sulfone to disilene **1.4** was examined. Surprisingly, no reaction was observed in either case. To explore whether or not the lack of reaction between the disilene and diphenyl sulfone may be caused by high steric congestion, the reaction of dimethyl sulfone and the disilene was investigated as well. Again, no reaction was observed.

The addition of benzenesulfonic acid to a yellow solution of disilene **1.4** in hexanes yielded a clear, colourless solution within a few minutes. The ^1H NMR spectrum of **6.4** showed two sets of mesityl signals and a singlet at 5.71 ppm, which was assigned

to a Si-H bond. Accordingly, the IR spectrum of **6.4** revealed an absorption at 2200 cm^{-1} , which is in the range typical for the stretching vibration of an Si-H bond. The strong absorption at 1349 cm^{-1} in the IR spectrum of **6.4** was assigned to the terminal S=O bond stretch, and the absorption at 909 cm^{-1} was assigned to the bridging S-O bond stretch. The structure of **6.4** was confirmed by X-ray crystallography as 1,1,2,2-tetramesityldisilyl benzenesulfonate (Scheme 6.4 and Figure 6.3). All bond lengths and angles are within normal ranges.



Scheme 6.4

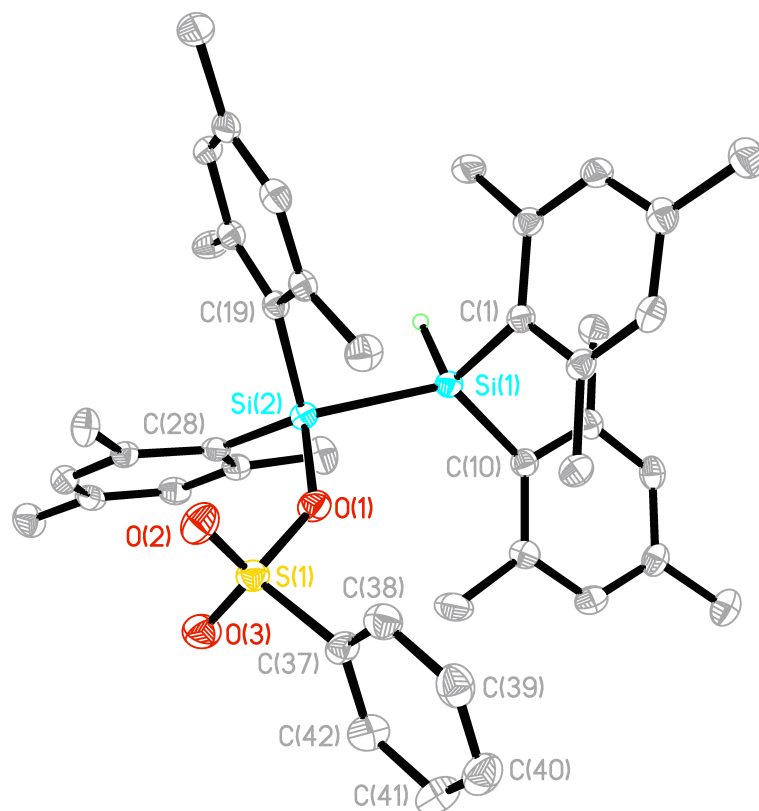
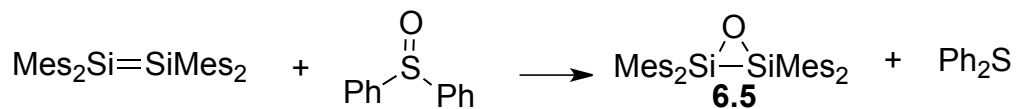


Figure 6.3 Displacement ellipsoid plot of **6.4** Ellipsoids are at the 50% probability level and hydrogen atoms were omitted for clarity except the hydrogen on Si(1). Selected bond lengths (Å) and angles (deg): Si1-Si2 = 2.3757(10), Si1-H1 = 1.46(2), Si2-O1 = 1.7127(16), S1-O3 = 1.4253(17), S1-O2 = 1.4274(16), S1-O1 = 1.5486(16); C1-Si1-Si2 = 110.96(7), C1-Si1-H1 = 106.3(8), C10-Si1-H1 = 107.2(8), Si2-Si1-H1 = 96.6(8), O1-Si2-Si1 = 106.10(6).

The addition of excess diphenyl sulfoxide to a bright yellow solution of disilene **1.4** in hexanes at room temperature gave a colourless solution. Removal of the solvent yielded a white solid, which revealed the presence of tetramesityloxadisilirane, Mes₄Si₂O **6.5**,⁶ and diphenylsulfide as confirmed by ¹H NMR spectroscopy (Scheme 6.5).



Scheme 6.5

To compare the addition of sulfonyl compounds to tetramesityldisilene with a heavier congener of silicon, the reaction of sulfonyl compounds with tetramesityldigermene was also examined. In a similar fashion, the addition of benzenesulfonyl chloride to digermene **1.2** in THF at room temperature produced β -chlorotetramesityldigermeryl benzenesulfinate **6.6**, as confirmed by X-ray crystallography. All bond lengths and angles of **6.6** are within normal ranges. The sulfur exhibits pyramidal geometry similar to **6.2** and **6.3**; in this case, the sulfur is displaced from the plane by 0.6615(20) Å (Scheme 6.6 and Figure 6.4).

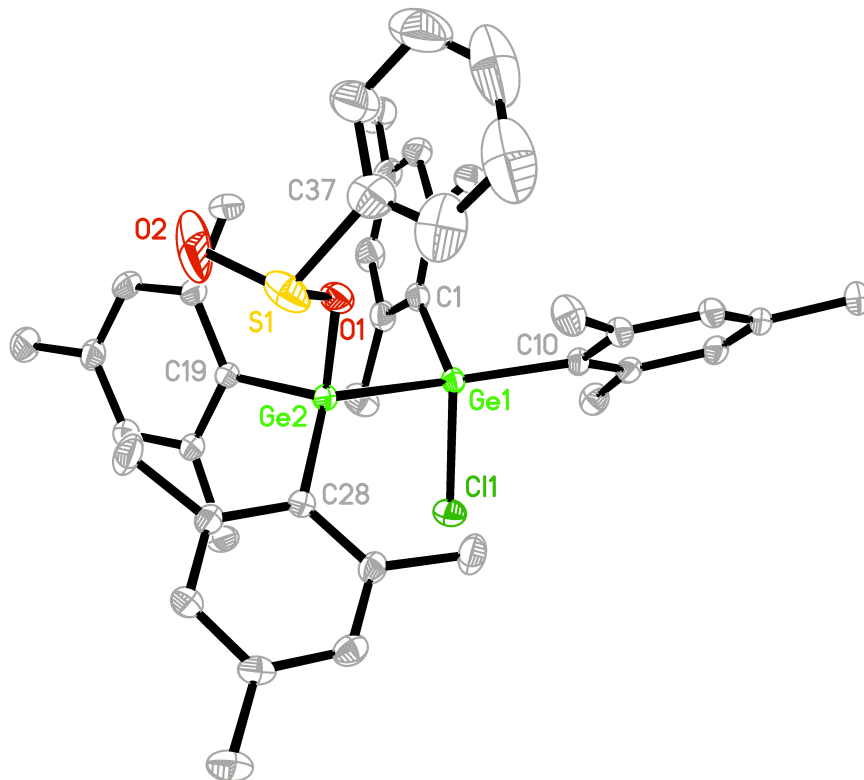
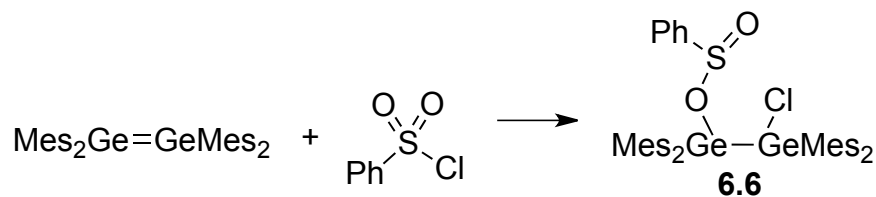


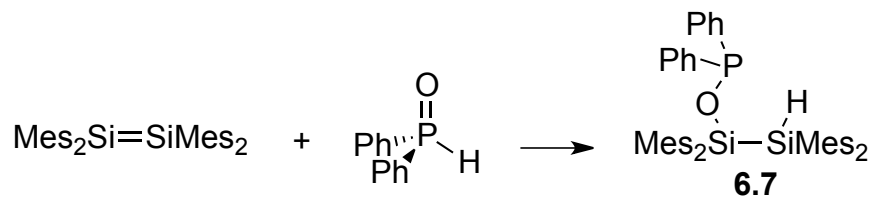
Figure 6.4 Displacement ellipsoid plot of **6.6**. Ellipsoids are at the 50% probability level; hydrogen atoms and the disorder at the benzenesulfinate moiety were omitted for clarity. Selected bond lengths (Å) and angles (deg): Ge1-C11 = 2.2200(7), Ge1-Ge2 = 2.4748(9), Ge2-O1' = 1.8574(12), Ge2-O1 = 1.8574(12), O1-S1 = 1.5599(15), O2-S1 = 1.436(3), O1'-S1' = 1.726 (2), O2'-S1' = 1.504 (6); C11-Ge1-Ge2 = 95.89(3), O1-Ge2-Ge1 = 102.44(4), S1-O1-Ge2 = 122.37(7), O2-S1-O1 = 109.94(15).



Scheme 6.6

Similar to the reactivity of the disilene **1.4**, no reaction was observed upon the addition of benzenesulfonyl fluoride and diphenyl sulfone to digermene **1.2**.

Diphenylphosphine oxide is the phosphorus analogue of diphenyl sulfoxide, and therefore, we examined the addition of diphenylphosphine oxide to disilene **1.4** for comparison purposes. The addition of excess diphenylphosphine oxide to a bright yellow solution of disilene **1.4** in hexanes at room temperature gave a colourless solution. Removal of the solvent yielded colourless crystals (Scheme 6.7). The high resolution mass spectral data of the product, **6.7**, and the isotopic pattern of the signal assigned to the molecular ion were consistent with the molecular formula, $\text{C}_{48}\text{H}_{56}\text{Si}_2\text{OP}$ corresponding to, a 1:1 adduct between tetramesityldisilene and diphenylphosphine oxide. The ^1H NMR spectrum of **6.7** revealed the presence of two sets of signals assigned to two non-equivalent mesityl groups and a singlet at 5.66 ppm that integrated to 1H and was assigned to an Si-H moiety. The ^{31}P NMR signal for **6.7** was observed at 107.2 ppm, in close agreement with similar germanium oxyphosphine complexes.⁷ The structure of **6.7** was unambiguously identified by single crystal X-ray diffraction (Figure 6.5). The phosphorus atom in compound **6.7** exhibits pyramidal geometry; the displacement of the phosphorus from the plane of the attached atoms is 0.814(11) Å. All bond lengths and angles in **6.7** are within normal ranges.



Scheme 6.7

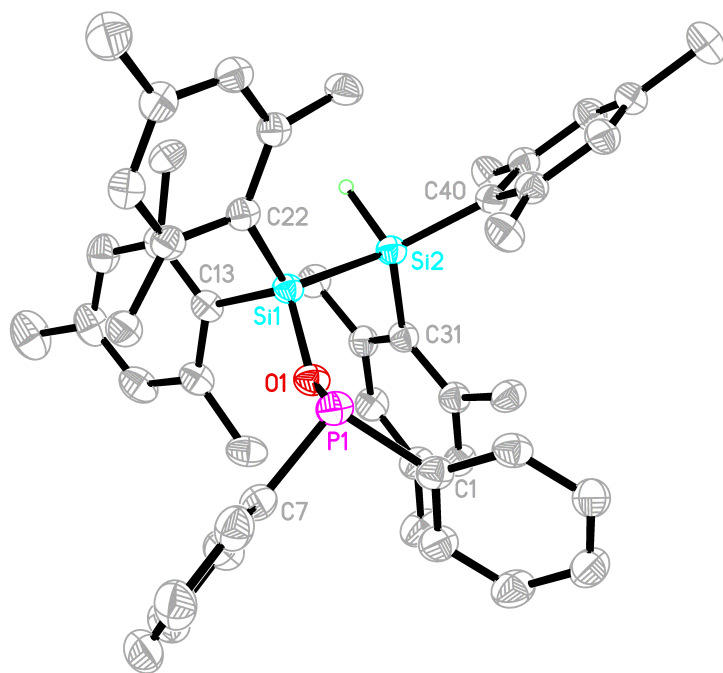


Figure 6.5 Displacement ellipsoid plot of **6.7**. Ellipsoids are at the 50% probability level and hydrogen atoms were omitted for clarity except the hydrogen on Si2. Selected bond lengths (Å) and angles (deg): Si1-O1 = 1.6834(14), Si1-Si2 = 2.3791(8), Si2-H1 = 1.52(2), P1-O1 = 1.6433(13), O1-Si1-Si2 = 110.85(5), Si1-Si2-H1 = 97.9(8), P1-O1-Si1 = 132.60(8).

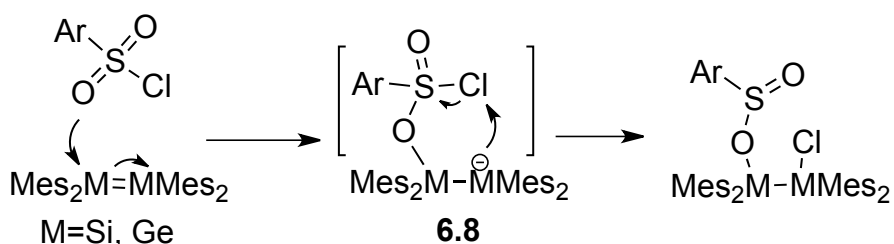
6.3 Discussion

The addition of benzenesulfonyl chloride and *p*-toluenesulfonyl chloride to disilene **1.4** and digermene **1.2** generated the chiral sulfinate adducts **6.2**, **6.3** and **6.6**. Sulfonates are an important class of molecules; for example, they have been recently utilized for the C-H functionalization of heteroarenes.⁸ Various procedures have been

reported for the preparation of chiral sulfinates and most are multistep reactions using strong oxidants, activated by heat or light and give a relatively low yield of product.⁹ The use of main group compounds to generate chiral sulfinates provides an exciting potential for development in sulfinate chemistry. A known method for the synthesis of sulfinates which utilizes a main group reagent involves the use of stoichiometric amount of trialkoxyphosphine combined with triethylamine, which provides the sulfinates through the reduction of sulfonyl chlorides in the presence of alcohols to give the sulfinate esters over several hours (1 h – 27 h) in CH₂Cl₂.¹⁰ Using triphenylphosphine and triethylamine, sulfonyl chlorides can be reduced in CH₂Cl₂ at 0 °C to give sulfinates in good yields in approximately one hour.¹¹ The generation of silylated/germylated sulfinates **6.2**, **6.3** and **6.6** via the addition of sulfonyl chlorides to ditetrelenes offers a facile, rapid new route for the formation of chiral sulfinates, which proceeds without the use of heat or a catalyst under very mild conditions. However, there are some difficulties associated with the generation of sulfinates using ditetrelenes. Disilene **1.4** and digermene **1.2** are quite reactive and require strict handling under inert conditions. Furthermore, the ditetrelenes are not commercially available and must be synthesized. Also, the final step of hydrolysis of silylated/germylated sulfinates **6.2**, **6.3** and **6.6** to generate the free sulfinates has not yet been tested to assess the yields and the optimum conditions.

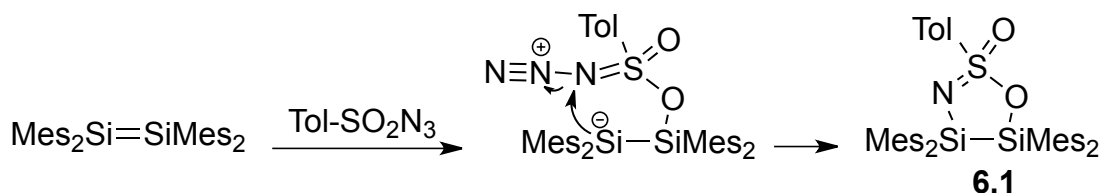
We propose the following mechanism to account for the formation of the sulfinate adducts **6.2**, **6.3** and **6.6**. Nucleophilic attack by one of the sulfonyl oxygens on the ditetrelene gives intermediate **6.8** (Scheme 6.8). This step is also consistent with the mechanism postulated for the addition of alcohols or water to disilenes, which begins with nucleophilic attack of the water or alcohol on one of the silicon atoms. The

nucleophilic addition of water and alcohol is strongly exothermic with a small activation energy.¹² In a second step, the negatively charged silicon (or germanium) abstracts the chlorine, reducing the sulfur atom and forming the final product (Scheme 6.8).



Scheme 6.8

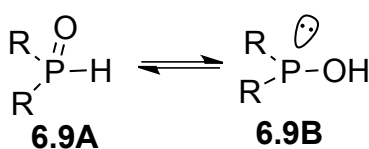
The reaction may occur stepwise as described in Scheme 6.7 or in a concerted fashion. The addition of *p*-toluenesulfonyl azide to tetramesityldisilene was also proposed to be stepwise, where nucleophilic attack of oxygen on the disilene was followed by ring closure and simultaneous loss of N₂ resulted in the formation of the five-membered ring system **6.1** (Scheme 6.9).⁴



Scheme 6.9

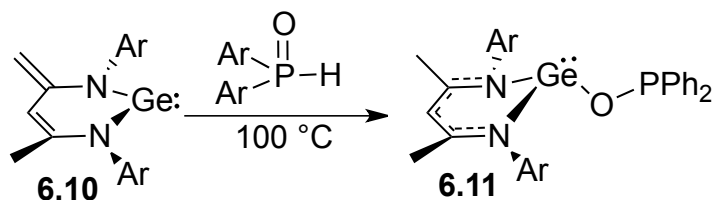
The addition of diphenyl sulfoxide to disilene **1.4** resulted in the formation of **6.5** and diphenylsulfide. In this case, diphenyl sulfoxide acts as an oxygen donor to the disilene. Oxygen donation to disilenes has also been reported for N₂O where disilaoxetanes were formed by the donation of two oxygens.¹³ The reactivity of diphenyl sulfoxide was compared to the reactivity of diphenylphosphine oxide. In the addition of

diphenylphosphine oxide, a 1:1 adduct was observed (**6.7**) rather than complete reduction to a phosphine, R_2PH . An equilibrium exists between the pentavalent and the trivalent phosphorus species; diphenylphosphine oxide (**6.9A**) is a weak acid¹⁴ and can tautomerize in solution to give hydroxydiphenylphosphine (**6.9B**) (Scheme 6.10).¹⁵ When $R = Ph$, the equilibrium lies strongly in favour of diphenylphosphine oxide **6.9A** in neutral conditions.¹⁶



Scheme 6.10

The addition of diphenylphosphine oxide to the N-heterocyclic germylene **6.10** afforded **6.11**⁷ (Scheme 6.11) exhibiting similar reactivity to the disilene **1.4**.



Scheme 6.11

Two mechanisms are postulated for the formation of **6.7**, although both are quite similar. Addition of diphenylphosphine oxide **6.9A** may begin with nucleophilic attack by the oxygen in **6.9A** to one of the silicon atoms of disilene **1.4** followed by hydrogen abstraction by the silyl anion to generate **6.7**. Alternatively, addition of hydroxydiphenylphosphine, **6.9B**, may begin with nucleophilic attack by the oxygen in

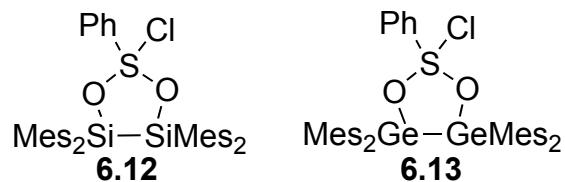
6.9B to one of the silicon atoms of disilene **1.4** followed by the silyl anion abstracting the hydrogen, forming **6.7**. It is unclear whether the disilene reacts with isomer **6.9A** or **6.9B**; however, in either case, the phosphorus is reduced in **6.7**.

The proposed mechanism for the formation of the sulfinates adducts **6.2**, **6.3** and **6.6** is consistent with the observed lack of reactivity of benzenesulfonyl fluoride towards tetramesityldisilene and tetramesityldigermene. The nucleophilicity of a terminal oxygen in benzenesulfonyl fluoride is expected to be lower than that in benzenesulfonyl chloride, slowing the rate of the first step. Furthermore, the low polarizability of fluorine compared to chlorine would further inhibit the addition reaction, as the halide abstraction would not be facile for the fluoride derivative.

The lack of the addition of dimethyl- and diphenyl sulfones to disilene **1.4** and digermene **1.2** is interesting. Three different modes of addition can be envisioned for the addition. First, considering that diphenyl sulfoxide reacted with the disilene by donation of an oxygen to give **6.5**, oxygen donation may also be possible for diphenyl- and dimethyl sulfone forming either the disilaoxirane or digermaoxirane and diphenyl sulfoxide by donation of one oxygen (Scheme 6.12, **A**) or formation of a 1,2- or 1,3-dimetalloxetane and diphenylsulfide by donation of two oxygens (Scheme 6.12, **B**). A second possible reaction pathway involves a cycloaddition reaction between one of the terminal oxygen-sulfur bonds and the disilene or the digermene to give the diphenyl-1,2,3,4-oxathiadisiletane 2-oxide or diphenyl-1,2,3,4-oxathiadigermene-2-oxide, respectively (Scheme 6.12, **C**).¹⁷ A third possible reaction pathway is a formal [3+2] cycloaddition reaction forming 1,3,2,4,5-dioxathiadisilolane or 1,3,2,4,5-dioxathiadigermolane (Scheme 6.12, **D**). Although these cycloaddition reaction pathways

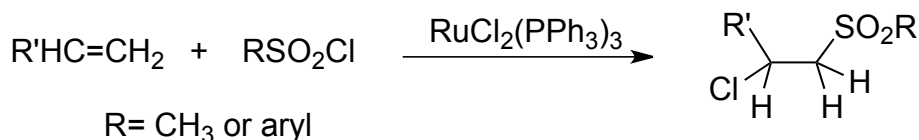
potential for N_2O_2 (oxidation number +4) to HNO_2 (oxidation number +3) is 1.07 V in acidic medium/ 0.867 in basic medium which is greater (more positive) than the reduction potential for HSO_4^- (oxidation state +6) to H_2SO_3 (oxidation number +4) at 0.15 in acidic medium/ -0.9 in basic medium.²¹ The less positive potential of the sulfate compared to nitrogen oxide is consistent with the lack of reactivity of sulfones compared to nitro compounds toward ditetrelenes. Substitution of the halide in benzenesulfonyl chloride with a methyl or a phenyl group, as in dimethyl- and diphenyl sulfone is expected to increase the nucleophilicity of the oxygen; however, the nucleophilicity of the oxygen in sulfones is apparently insufficient to overcome the activation barrier to form either a cycloadduct or an oxygen donor adduct. Another explanation for the lack of reaction between dimethyl- and diphenyl sulfone and the disilene or the digermene relies on the electronic structure of sulfonyl compounds. The two oxygen-sulfur bonds are highly polarized. The best Lewis representation of the sulfonyl moiety has a negative charge on the oxygen and a double positive charge on sulfur ($\text{O}^--\text{S}^{2+}-\text{O}^-$).²² As the bonding between sulfur and oxygen is quite polarized, the sulfonyl group is not a 1,3-dipole, and therefore, a formal [3+2] cycloadduct is expected to be inhibited.

The optimized geometries of **6.2**, **6.6** and their isomeric cycloadducts were calculated at the B3LYP/6-311+G* level of theory (Scheme 6.13).²³ For the silicon derivatives, the 1,3,2,4,5-dioxathiadisilolane cycloadduct, **6.12**, was 92.1 kJ/mol higher in energy than the 1,2-adduct **6.2**. A similar trend is observed in the germanium derivatives, as the 1,3,2,4,5-dioxathiadigermolane **6.13** was 119.2 kJ/mol higher in energy than the 1,2-adduct **6.6**. The relative lower energies of the acyclic isomer compared to the cyclic derivative is also consistent with the formation of the observed products, **6.2** and **6.6**.



Scheme 6.13

It is interesting to compare the observed reactivity of ditetrelenes towards sulfonyl chlorides with the chemistry of the analogous alkenes. Alkyl- and arylsulfonyl chlorides add to alkenes to form β -halosulfones (Scheme 6.14), in the presence of catalysts such as peroxide, light or metal salts; however, the yields of the reactions are low due to the presence of by-products.²⁴ In the presence of a catalytic amount of dichlorotris(triphenylphosphine)ruthenium(II), the addition of alkyl- and arylsulfonyl chlorides to alkenes at high temperature ($\approx 100^\circ \text{C}$) proceeds cleanly in high yield.²⁵ The use of the Ru(III) complex, $[\text{Cp}^*\text{RuCl}_2(\text{PPh}_3)]$ in combination with AIBN as a co-catalyst improved the yield of the halosulfones at lower temperatures.²⁶ The influence of substituents on the sulfonyl chlorides (i.e. alkyl vs. aryl) were investigated as well; however, no distinctive change in the rate of the reaction or the yield of the products was observed.²⁵ The reactions of sulfonyl chlorides and alkenes is believed to proceed via a radical redox mechanism.²⁷



Scheme 6.14

In contrast to the carbon chemistry, the addition of sulfonyl compounds to ditetrelenes proceeds almost instantly without a catalyst or heat. Also, β -halosulfonates are formed in the silicon/germanium systems in contrast to carbon chemistry where β -halosulfones are formed. The formation of the strong Si-O bond is thermodynamically favourable, and thus, the Si-O bond is preferentially formed over the weaker Si-S bond. Furthermore, the sulfur in the β -halosulfones, resulting from the addition of sulfonyl chlorides to alkenes, has the same oxidation number (+6) whereas, in the β -halosulfonate esters, resulting from the addition of sulfonyl chlorides to the disilene (or digermene), the sulfur is reduced from the +6 to the +4 oxidation number.

Similarly, the sulfur in diphenyl sulfoxide has an oxidation number of +4 and it was reduced to +2 in diphenylsulfide through the reaction with the disilene. The reduction of sulfoxides to their corresponding sulfides has been reported using main group compounds and metal complexes.²⁸ Similarly, the oxidation number of the phosphorus in **6.7** was reduced from +5 to +3 when diphenylphosphine oxide reacted with the disilene. In contrast, the product formed from the addition of the benzenesulfonic acid to the disilene, benzenesulfonate **6.4**, has the same oxidation number (+6) as the sulfonic acid. The sulfur also maintains the same oxidation number of (+6) in **6.1** during the addition of *p*-toluenesulfonyl azide to tetramesityldisilene. The addition of an OH across a double bond is, in general, not considered a redox reaction; however, formally, one silicon of the disilene has been oxidized and one has been reduced. In the addition of *p*-toluenesulfonyl azide, both silicons have been oxidized and the nitrogen has been reduced. These reactions demonstrate the potential use of ditetrelenes as effective reducing agents as the reductions occur rapidly, at room

temperature and under mild conditions. Further expanding the theme of ditetrelenes as reducing agents might open new possibilities in synthesis.

6.4 Summary and Conclusions

In conclusion, the addition of sulfonyl compounds to tetramesityldisilene and tetramesityldigermene leads to the facile formation of the 1,2-addition products, β -chlorotetramesityldisilyl benzenesulfinate and β -chlorotetramesityldigermyl benzenesulfinate, respectively. On the other hand, the addition of benzenesulfonyl fluoride and diphenyl sulfone to both disilene and digermene gave no reaction. The addition of dimethyl sulfone to the disilene also did not give a product. The addition of diphenylphosphine oxide to tetramesityldisilene leads to the formation diphenyl((1,1,2,2-tetramesityldisilyl)oxy)phosphine. The formation of sulfinate compounds (**6.2**, **6.3** and **6.6**) as well as the oxyphosphine compound (**6.7**) revealed an interesting, mild 2-electron reduction of the sulfur and phosphorus centers using ditetrelenes. The addition reactions of sulfonyl compounds illustrate the potential use of ditetrelenes as effective reducing agents as the reductions occur rapidly, at room temperature and under mild conditions.

6.5 Experimental

General Experimental Details

All air sensitive reactions were performed under an inert atmosphere of argon or nitrogen using standard Schlenk techniques or a glove box. Hexanes and THF were obtained from a solvent purification system (SPS-400-5, Innovative Technology Inc). The NMR standards used were residual C_6D_5H (7.15 ppm) for 1H NMR spectra and C_6D_6 central transition of C_6D_6 (128.00 ppm) for ^{13}C NMR spectra. IR spectra were recorded (cm^{-1}) from thin films on a Bruker Tensor 27 FT-IR spectrometer. Electron impact mass

spectra were recorded on a MAT model 8400 mass spectrometer using an ionizing voltage of 70 eV. ESI-TOF mass spectra were obtained using a Micromass LCT instrument. Mass spectral data are reported in mass-to-charge units, m/z . X-ray data were obtained using a Bruker Apex II Diffractometer. Ge_3Mes_6 ²⁹ and $(\text{Me}_3\text{Si})_2\text{SiMes}_2$ ³⁰ were synthesized according to the literature procedures.

Addition of Benzenesulfonyl Chloride (or *p*-Toluenesulfonyl Chloride) to Tetramesityldisilene

$\text{Mes}_2\text{Si}(\text{SiMe}_3)_2$ (50 mg, 0.12 mmol) was placed in a quartz tube, dissolved in hexanes (3 mL), and then placed in a quartz Dewar. The solution was irradiated ($\lambda = 254 \text{ nm}$) for ~18 h to give a bright yellow solution. The solution was cooled to $-60 \text{ }^\circ\text{C}$ during the irradiation by circulating cold methanol. Excess benzenesulfonyl chloride (14 mg, 0.08 mmol) (or *p*-toluenesulfonyl chloride (13 mg, 0.08 mmol)) was added to the yellow solution at room temperature and the mixture was allowed to stir. After 5 min, the solution became pale yellow. The hexanes were evaporated giving a pale yellow oil which was redissolved in a minimal amount of hexanes. ^1H NMR spectroscopy revealed the presence of only one product. The solution was placed in the freezer ($-20 \text{ }^\circ\text{C}$) for 24 h to give a colourless solid, which was isolated by decantation. The solid was triturated with pentane yielding colourless, clear crystals of **6.2** (30 mg, 53%). m.p. $174\text{-}176 \text{ }^\circ\text{C}$; ^1H NMR (C_6D_6 , 600 MHz, $70 \text{ }^\circ\text{C}$) δ 7.59 (br s, 2H, Ph *o*-H), 7.00 (3H, Ph *m*-H+*p*-H), 6.75 (br s, 2H, Mes *m*-H), 6.69 (s, 4H, Mes *m*-H), 6.59 (s, 2H, Mes *m*-H), [2.40 (br s, Mes *o*-CH₃), 2.21 (br s, Mes *o*-CH₃), 2.11 (s, Mes *o*-CH₃), 2.08 (s, Mes *p*-CH₃), 2.07 (s, Mes *p*-CH₃), 2.01 (s, Mes *p*-CH₃) all together 36H]; ^{13}C NMR (C_6D_6 , 150 MHz, $70 \text{ }^\circ\text{C}$) δ 150.16

(Ph *i*-C), 144 (Mes *o*-C)^a, 140.25 (Mes *p*-C), 140.01 (Mes *p*-C), 139.72 (Mes *p*-C), 139.60 (Mes *p*-C), 131.69 (Mes *i*-C+ Ph *p*-CH), 130.20 (Mes *m*-CH), 130.17 (Mes *m*-CH), 129.5 (br s, Mes *m*-CH), 128.77 (Ph *m*-CH), 124.67 (Ph *o*-CH), 25 (Mes *o*-CH₃)^b, 20.99 (Mes *p*-CH₃), 20.89 (Mes *p*-CH₃), 20.87 (Mes *p*-CH₃), 20.81 (Mes *p*-CH₃); ²⁹Si (C₆D₆, 119 Hz, 70 °C)^c -4.19 ppm; FTIR (thin film, cm⁻¹) 2920 (br s), 1603 (s), 1445 (s), 1143 (m), 819 (m), 755 (m); high resolution ESI-MS *m/z* for C₄₂H₄₉O₂Na Si₂S³⁵Cl calc. 731.2578 found 731.2568.

Colourless, clear crystals **6.3** (35 mg, 50%) m.p. 172-174 °C; ¹H NMR (C₆D₆, 600 MHz, 70 °C) δ 7.54 (br s, 2H, Ph *o*-CH), 6.84 (m, 2H, Ph *m*-CH), 6.76 (s, 2H, Mes *m*-CH), 7.00 (br s, 4H, Mes *m*-CH), 6.60 (s, 2H, Mes *m*-CH), [2.42 (br s, Mes *o*-CH₃), 2.24 (br s, Mes *o*-CH₃), 2.12 (s, Mes *o*-CH₃), 2.08 (s, Mes *p*-CH₃), 2.07 (s, Mes *p*-CH₃), 2.01 (s, Mes *p*-CH₃), 1.94 (s, Tol *p*-CH₃) all together 39H]; ¹³C NMR (C₆D₆, 150 MHz, 70 °C) δ 147.50 (Ph *i*-C), 145.20 (br s, Mes *o*-C), 142.18 (Ph *p*-C), 140.20 (Mes *p*-C), 139.95 (Mes *p*-C), 139.68 (Mes *p*-C), 139.57 (Mes *p*-C), 131.96 (br s, Mes *i*-C), 130.17 (Mes *m*-CH), 129.97 (br s, Mes *m*-CH), 129.44 (Ph *m*-CH), 124.79 (Ph *o*-CH), 25.39 (br s, Mes *o*-CH₃), 21.13 (Tol. *p*-CH₃), 21.00 (Mes *p*-CH₃), 20.90 (Mes *p*-CH₃), 20.87 (Mes *p*-CH₃), 20.81 (Mes *p*-CH₃); ²⁹Si (C₆D₆, 70 °C) 67, -4 ppm; FTIR (thin film, cm⁻¹) 3017 (s), 2958 (s), 2921 (s), 1603 (s), 1449 (s), 1139 (m), 824 (s), 757 (s); high resolution ESI-MS *m/z* for C₄₃H₅₁O₂NaSi₂SCl calcd. 745.2735 found 745.2749.

Addition of Benzenesulfonic Acid to Tetramesityldisilene

^a Chemical shift extracted from the ¹H-¹³C gHMBC spectrum

^b Chemical shift extracted from the ¹H-¹³C gHSQC spectrum

^c Attempts to detect a second signal by direct detection ²⁹Si and ²⁹Si-HMBC spectroscopy using various J couplings weren't successful.

Mes₂Si(SiMe₃)₂ (100 mg, 0.24 mmol) was placed in a quartz tube, dissolved in hexanes (3 mL), and then placed in a quartz Dewar. The solution was irradiated ($\lambda = 254$ nm) for ~18 h to give a bright yellow solution. The solution was cooled to -60 °C during the irradiation by circulating cold methanol. Excess benzenesulfonic acid (23.7 mg, 0.15 mmol) was added to the yellow solution at room temperature and the reaction was allowed to stir. After 5 min, the solution became colourless. The hexanes were evaporated giving a pale yellow powder, which was redissolved in a minimal amount of hexanes. The flask was placed in the freezer (-20 °C) for 24 h. A fine precipitate formed which was isolated by centrifugation. The solid was triturated with pentane yielding colourless, clear crystals of **6.4** (80 mg, 77%) White powder; m.p. 188- 190 °C; ¹H NMR (C₆D₆, 400 MHz) δ 7.82 (d, 2H, Ph *o*-H J = 8 Hz), 6.89 (t, 1H, Ph *p*-H J = 7 Hz), 6.84 (t, 2H, Ph *m*-H J = 8 Hz), [6.66 (s, Mes *m*-H) 6.63 (s, Mes *m*-H) all together 8H], 5.68 (s, 1H, Si-H), 2.30 (br s, 24H, Mes *o*-CH₃), 2.06 (s, Mes *p*-CH₃), 2.04 (s, Mes *p*-CH₃) all together 12H]; ¹³C NMR (C₆D₆, 150 MHz) δ 145.51 (Mes *o*-C), 144.58 (Mes *o*-C), 140.63 (Ph *i*-C), 140.10 (Mes *p*-C), 139.12 (Mes *p*-C), 132.48 (Ph *p*-CH), 131.69 (Mes *i*-C), 129.99 (Mes *m*-CH), 129.96 (Mes *m*-CH), 129.94 (Mes *m*-CH), 129.93 (Mes *m*-CH), 129.02 (br s, Mes *m*-CH), 128.99 (Mes *m*-CH), 128.54 (Ph *m*-CH), 127.92 (Ph *o*-CH), 24.72 (br s, Mes *o*-CH₃), 24.67 (Mes *o*-CH₃), 24.65 (Mes *o*-CH₃), 21.04 (Mes *p*-CH₃), 21.12 (Mes *p*-CH₃), 21.00 (Mes *p*-CH₃), 20.98 (Mes *p*-CH₃); FTIR (thin film, cm⁻¹) 3022 (s), 2961 (s), 2920 (s), 2200(m), 1604 (s), 1448 (s), 1350 (s), 1185 (s), 909 (s), 757 (s), 597 (s); ²⁹Si 5 (Si-O), -55 (Si-H) ppm; high resolution ESI-MS *m/z* for C₄₂H₅₀O₃NaSi₂S calc. 713.2917 found 713.2918.

Addition of Benzenesulfonyl Chloride to Tetramesityldigermene

Ge₃Mes₆ (100 mg, 0.107 mmol) was placed in a quartz tube^d and dissolved in THF (5 mL) and then irradiated ($\lambda = 350$ nm) in a quartz Dewar^d at -60 °C for ~18 h to give a yellow solution. Excess benzenesulfonyl chloride (30 mg, 0.17 mmol) was added to the yellow solution at room temperature and the reaction was allowed to stir. After 5 min, the solution became colourless. The solvent was evaporated giving a clear, colourless oil. The oil was redissolved in a minimal amount of hexanes. The solution was placed in a freezer (-20 °C) for 24 h, yielding crystalline material, which was isolated by decantation. The crystals were triturated with hexanes yielding colourless clear, crystals of **6.6** (110 mg, 80%). The crystalline material was contaminated with an unidentified compound. Attempts to purify **6.6** by chromatography (50:50 hexanes: DCM) resulted in the decomposition of **6.6**: m.p. 160-162 °C; ¹H NMR (C₆D₆, 600 MHz, 70 °C) δ 7.65 (dd, 2H, Ph *o*-CH, J = 8, 2 Hz), 7.06-7.02 (m, 3H, Ph *m*-H+*p*-H), 6.71 (s, 4H, Mes *m*-H), 6.64 (s, 4H, Mes *m*-H), 2.47 (s, 12H, Mes *o*-CH₃), 2.31 (s, 12H, Mes *o*-CH₃), [2.07 (s, Mes *p*-CH₃), 2.03 (s, Mes *p*-CH₃), all together 12H)];^e ¹³C NMR (C₆D₆, 150 MHz, 70 °C) δ 152.31 (Ph *i*-C), 143.89 (Mes *p*-C), 143.65 (Mes *p*-C), 139.97 (br s, Mes *o*-C), 139.82 (br s, Mes *o*-C), 136.78 (br s, Mes *i*-C), 136.71 (br s, Mes *i*-C), 130.97 (Ph *p*-CH), 130.09 (Mes *m*-CH), 130.06 (Mes *m*-CH), 128.69 (Ph *m*-CH), 124.45 (Ph *o*-CH), 25.11 (br s, Mes *o*-CH₃), 24.77 (br s, Mes *o*-CH₃), 20.86 (Mes *p*-CH₃), 20.81 (Mes *p*-CH₃);^f FTIR (thin film, cm⁻¹) 3017 (s), 2964 (s), 2923 (s), 1601 (s), 1446 (s), 1405 (m), 1382 (m), 1147 (s), 849 (s), 754 (s); high resolution ESI-MS for C₄₂H₄₉O₂S⁷⁰Ge₂ [M-Cl]⁺ (*m/z*) calc.

^d A quartz tube and Dewar were used but a Pyrex Dewar also can be used.

^e Additional signals were observed in the ¹H NMR spectrum of **6.6** at 6.69, 2.42, 2.40, 2.06, 1.20, 1.99 ppm in ratio of 1:0.06.

^f We did not observe a signal which could be assigned to the *ipso*-carbon of the phenyl ring.

757.1938, found 757.1928; low resolution ESI-MS: 757-769 [M-Cl]⁺, 815-828

[M+Na⁺]⁺.^g

Addition of Diphenylphosphine Oxide to Tetramesityldisilene

Mes₂Si(SiMe₃)₂ (100 mg, 0.24 mmol) was placed in a quartz tube, dissolved in hexanes (3 mL), and then placed in a quartz Dewar. The solution was irradiated ($\lambda = 254$ nm) for ~18 h to give a bright yellow solution. The solution was cooled to -60 °C during the irradiation by circulating cold methanol. Excess diphenylphosphine oxide (30 mg, 0.15 mmol) was added to the yellow solution at room temperature; the colour of the solution immediately changed to pale yellow. The hexanes were evaporated giving a colourless oil which was redissolved in a minimal amount of hexanes. The flask was placed in the freezer (-20 °C) for 24 h. A precipitate formed and the solid was isolated by decantation. The solid was triturated with hexanes yielding colourless, clear crystals of **6.7** (70 mg, 63 %). ¹H NMR (C₆D₆, 400 MHz) δ 7.55 (t, 2H, Ph *m*-H), 7.05- 7.01 (m, 3H, Ph *o*- and *p*-H), [6.67 (s, Mes *m*-H), 6.63 (s, Mes *m*-H), all together 8H], 5.66 (s, 1H, Si-H), [2.32 (s, Mes *o*-CH₃), 2.31 (s, Mes *o*-CH₃), Mes *o*-CH₃), all together 24H], 2.07 (br s, 12H, Mes *p*-CH₃); ¹³C NMR (C₆D₆, 150 MHz) δ 145.41 (s, Mes *o*-C), 144.19 (Mes *o*-C), 144.03 (*i*-Ph), 139.15 (Mes *p*-C), 138.56 (Mes *p*-C), 135.06 (Mes *i*-C), 131.81 (Ph *o*-CH), 131.65 (Mes *i*-C), 129.70 (Mes *m*-CH), 129.22 (Ph *p*-CH), 128.86 (Mes *m*-CH), 128.54 (Ph *o*-CH), 25.17 (br s, Mes *o*-CH₃), 21.07 (br s, Mes *o*-CH₃); ²⁹Si (C₆D₆) 2 (Si-O), -56 (Si-H); ³¹P (C₆D₆, 162 MHz) δ 107.19 ppm; ESI-TOF for [C₄₈H₅₅Si₂OP+ H⁺] calcd.: 735.3607, found: 735.3604.

^g The high-resolution ESI-MS data are for [M-Cl]⁺. We were unable to obtain satisfactory high-resolution Ms data of M+Na⁺ due to overlap with an unknown contaminant or an additional ion (i.e. M+H⁺).

Addition of Benzenesulfonyl Fluoride, Diphenyl Sulfone or Dimethyl Sulfone to Tetramesityldisilene

Mes₂Si(SiMe₃)₂ (100 mg, 0.24 mmol) was placed in a quartz tube, dissolved in hexanes (3 mL), placed in a quartz Dewar and then the solution was irradiated ($\lambda = 254$ nm) for ~18 h to give a bright yellow solution. The solution was cooled to -60 °C during the irradiation by circulating cold methanol. Excess diphenyl sulfone (32 mg, 0.15 mmol) or dimethylsulfone (14 mg, 0.15 mmol) or benzenesulfonyl fluoride (24 mg, 0.15 mmol) were added to the yellow solution at room temperature and the reaction was allowed to stir. For the addition of diphenyl sulfone the reaction mixture was heated to 80 °C in C₆D₆ in a sealed tube for two days. The reaction mixtures were allowed to stir up to 3 days and were monitored by ¹H NMR spectroscopy. No reaction was observed.

Addition of Benzenesulfonyl Fluoride or Diphenyl Sulfone to Tetramesityldigermene

Ge₃Mes₆ (100 mg, 0.107 mmol) was placed in a quartz tube^h and dissolved in THF (5 mL) and irradiated ($\lambda = 350$ nm) in a quartz Dewar^d at -60 °C for ~18 h to give yellow solution. The solution was cooled during the irradiation by circulating cold methanol through the quartz Dewar. Excess benzenesulfonyl fluoride (26 mg, 0.16 mmol) or diphenyl sulfone (34 mg, 0.16 mmol) were added to the yellow solution at room temperature and the reaction was allowed to stir. For the addition of diphenyl sulfone, the reaction mixture was heated to 80 °C in C₆D₆ in a sealed tube for two days with no change in colour. The reactions were monitored by ¹H NMR spectroscopy; no reaction was observed for either addition.

Addition of Diphenyl Sulfoxide to Tetramesityldisilene

^h A quartz tube and Dewar were used but a Pyrex Dewar also can be used.

Mes₂Si(SiMe₃)₂ (50 mg, 0.12 mmol) was placed in a quartz tube, dissolved in hexanes (3 mL), placed in a quartz Dewar. The solution was irradiated ($\lambda = 254$ nm) for ~18 h to give a bright yellow solution. The solution was cooled to -60 °C during the irradiation by circulating cold methanol. Excess diphenylsulfoxide (16 mg, 0.08 mmol) dissolved in (1mL) of hexanes was added to the yellow solution at room temperature, the reaction mixture turned out colourless immediately. Tetramesityloxadisilirane,³¹ Mes₄Si₂O, and diphenylsulfide were observed as determined by ¹H NMR spectroscopy.

Computational Details

All calculations were performed using Gaussian 09²³ on the Shared Hierarchical Academic Research Computing Network (SHARCNET, www.sharcnet.ca). Computations were run using two AMD Opteron 2.2 GHz 24 core CPUs with 32 GB of memory. Initial optimization was performed from either crystal structures or modified from previously obtained crystal structures. Optimization was initially performed at the Opt=Loose level until convergence was achieved, upon which the default optimization restraints were used. All optimization and frequency calculations were performed at the B3LYP level of theory,³² using the 6-31G* basis set, and an ultra fine integration grid. Molecular orbital and single-point energy calculations were performed using the normal population method, using the M06 functional,³³ and the 6-311+G* basis set and using an ultra fine integration grid.

Crystallographic Details

Data Collection and Processing The samples were mounted on a Mitegen polyimide micromount with a small amount of Paratone N oil. All X-ray measurements were made on a Bruker Kappa Axis Apex2 diffractometer or Nonius Bruker KappaCCD Apex2

diffractometer for **6.5** at a temperature of 110 K. The frame integration was performed using SAINT.³⁴ The resulting raw data was scaled and absorption corrected using a multi-scan averaging of symmetry equivalent data using SADABS.³⁵ For **6.2**, following data collection, the sample crystal was recognized as a non-merohedral twin. A second domain was rotated relative to the first by an approximately 3.1° rotation about the [1.000 -0.167 -0.387] reciprocal space axis.

Structure Solution and Refinement. The structure was solved by using a dual space methodology using the SHELXT program.³⁶ All non-hydrogen atoms were obtained from the initial solution. The hydrogen atoms were introduced at idealized positions and were allowed to ride on the parent atom. The structural model was fit to the data using full matrix least-squares based on F^2 . The calculated structure factors included corrections for anomalous dispersion from the usual tabulation. The structure was refined using the SHELXL-2014 program from the Shelx suite of crystallographic software.³⁷ Graphic plots were produced using the XP program suite.³⁴

For **6.2**, the crystal was found to be a non-merohedral twin, with a refined fraction for the major component of 0.6713. As a result, the model was refined using only the reflections for the major component. For **6.3**, the asymmetric unit demonstrated a region of disorder in the benzenesulfonate group. The benzenesulfonate group was rotated approximately 165° about C37, giving rise to two sulfur and oxygen positions, and two separate phenyl rings, related by a 33° rotation about the midpoint between the two sulfur positions. The normalized occupancy for the major component of this disorder refined to a value of 0.680(2). For **6.6**, the asymmetric unit demonstrated two regions of disordered solvent, initially modeled as molecules of THF using several restraints, but were unsuccessful. The

data were then subject to the SQUEEZE procedure³⁸ as implemented in the PLATON program.³⁹ For **6.4**, the hydrogen bound to Si1 was refined isotropically, whereas the rest of the hydrogen atoms were allowed to ride on their parent atom. For **6.6**, the hydrogen atoms were introduced at idealized positions allowed to ride on the parent atom, other than H2, which was found in the difference map.

Table 6.1: Crystallographic data of compounds **6.2**, **6.3**, **6.4**, **6.6** and **6.7**

	6.2	6.3	6.4	6.6	6.7
Formula	C ₄₂ H ₄₉ ClO ₂ SSi ₂ . C ₆ H ₁₄	C ₄₃ H ₅₁ ClO ₂ SSi ₂	C ₄₂ H ₅₀ O ₃ SSi ₂	C ₄₂ H ₄₉ ClGe ₂ O ₂ S	C ₄₈ H ₅₅ OPSi ₂
Formula Weight (g/mol)	795.67	723.52	691.06	798.50	735.07
Crystal System	triclinic	triclinic	monoclinic	triclinic	triclinic
Space Group	P-1	P-1	P 2 ₁ /c	P-1	P-1
Temperature, K	110	110	110	110	110
<i>a</i> , Å	10.124(3)	10.079(3)	14.176(4)	10.346(3)	12.1010(15)
<i>b</i> , Å	13.745(3)	13.524(4)	10.516(3)	12.097(5)	12.3337(11)
<i>c</i> , Å	17.836(5)	18.630(6)	24.432(8)	16.393(7)	14.9570(12)
α , °	107.93(2)	109.589(17)	90	96.469(18)	93.583(5)
β , °	97.174(7)	96.277(17)	92.040(13)	92.688(11)	112.275(7)
γ , °	98.522(6)	97.257(14)	90	111.538(8)	93.783(5)
<i>V</i> , Å ³	2296.7(11)	2342.0(12)	3640(2)	1887.6(13)	2052.0(4)
<i>Z</i>	2	2	4	2	2
μ , (cm ⁻¹)	0.217	0.207	0.194	1.753	1.411
R _{merge}	0.0652	0.0498	0.0795	0.0332	0.0512
R ₁	0.0656	0.0585	0.0491	0.0411	0.0403
wR ₂	0.1687	0.1643	0.1126	0.0964	0.1035
R ₁ (all data)	0.1223	0.0980	0.0833	0.0717	0.519
wR ₂ (all data)	0.1867	0.1851	0.1294	0.1058	0.1112
GOF	1.053	1.063	1.033	1.027	1.016

6.6 References

1. Revunova K.; Nikonov, G. I. *Dalton Trans.* **2015**, *44*, 840.
2. Yokelson, H. B.; Millevolte, A. J.; Haller, K. J.; West, R. *J. Chem. Soc., Chem. Commun.* **1987**, *21*, 1605.

3. Gillette, G. R.; West, R. *J. Organomet. Chem.* **1990**, *45*, 394.
4. Gillette, G.; West, R. *J. Organomet. Chem.* **1990**, *394*, 45.
5. CSD search performed using Conquest software, CSD version 5.36.0, <http://www.ccdc.cam.ac.uk/Solutions/CSDSsystem/pages/CSDSsystem.aspx>, Retrieved on 28/3/2015.
6. McKillop, K. L.; Gillette, G. R.; Powell, D. R.; West, R. *J. Am. Chem. Soc.* **1992**, *114*, 5203.
7. Wu, Y.; Liu, L.; Su, J.; Yan, K.; Wang, T.; Zhu, J.; Gao, X.; Gao, Y.; Zhao, Y. *Inorg. Chem.* **2015**, *54*, 4423.
8. (a) Fujiwara, Y.; Dixon, J. A.; Rodriguez, R. A.; Baxter, R. D.; Dixon, D. D.; Collins, M. R.; Blackmond, D. G.; Baran, P. S. *J. Am. Chem. Soc.* **2012**, *134*, 1494; (b) Fujiwara, Y.; Dixon, J. A.; O'Hara, F.; Daa Funder, E.; Dixon, D. D.; Rodriguez, R. A.; Baxter, R. D.; Herle, B.; Sach, N.; Collins, M. R.; Ishihara, Y.; Baran, P. S. *Nature* **2012**, *492*, 95; (c) Zhou, Q.; Ruffoni, A.; Gianatassio, R.; Fujiwara, Y.; Sella, E.; Shabat, D.; Baran, P. S. *Angew. Chem.* **2013**, *125*, 4041.
9. (a) Miyaji, Y.; Minato, H.; Kobayashi, M. *Bull. Chem. Soc. Jp.* **1971**, *44*, 862; (b) Furukawa, M.; Okawara, T.; Noguchi, Y.; Nishikawa, M. *Synthesis* **1978**, 441; (c) Boar, R. B.; Patel, A. C. *Synthesis* **1982**, 584; (d) Fernandez, I.; Khiar, N.; Llera, J. M.; Alcludia, F. *J. Org. Chem.* **1992**, *57*, 6789; (e) Field, L.; Hoelzel, C. B.; Locke, J. M. *J. Am. Chem. Soc.* **1962**, *84*, 847; (f) Solladié, G.; Hutt, J.; Girardin, A. *Synthesis* **1987**, 173; (g) Kobayashi, M.; Terao, M. *Bull. Chem. Soc. Jp.* **1966**, *39*, 1292; (h) Meek, J. S.; Fowler, J. S. *J. Org. Chem.* **1968**, *33*, 3422; (i) Gianatassio, R.; Kawamura, S.; Eprile, C.

- L.; Foo, K.; Ge, J.; Burns, A. C.; Collins, M. R.; Baran, P. S. *Angew. Chem. Int. Ed.* **2014**, *53*, 9851; (j) Whitesell, J. K.; Wong, M. S. *J. Org. Chem.* **1994**, *59*, 597.
10. Klunder, J. M.; Sharpless, K. B. *J. Org. Chem.* **1987**, *52*, 2598.
- 11 Watanabe, Y.; Mase, N.; Tateyama, M. A.; Toru, T. *Tetrahedron: Asymm.* **1999**, *10*, 737.
12. Veszpremi, T.; Takahashi, M.; Hajgato, B.; Kira, M. *J. Am. Chem. Soc.* **2001**, *123*, 6629.
13. Khan, S.; Michel, R.; Koley, D.; Roesky, H. W.; Stalke, D. *Inorg. Chem.* **2011**, *50*, 10878.
14. (a) Grayson, M.; Farley, C. E.; Streuli, C. A. *Tetrahedron* **1967**, *23*, 1065; (b) Quin, L. D., *A Guide to Organophosphorus Chemistry*; Wiley-Interscience, New York, 2000.
15. Chatt, J.; Heaton, B. T. *J. Chem. Soc. A* **1968**, 2745.
16. Dixon, K. R.; Rattray, A. D. *Can. J. Chem.* **1971**, *49*, 3997.
17. (a) Raabe, G.; Michl, J., *In The Chemistry of Organic Silicon Compounds*; Patai, S.; Rappoport, Z., Eds.; Wiley: New York, 1989; p 1015; (b) Barrau, J.; Escudié, J.; Satgé, J. *Chem. Rev.* **1990**, *90*, 283; (c) Morkin, T. L.; Owens, T. R.; Leigh, W. J., *In The Chemistry of Organic Silicon Compounds*; Rappoport, Z.; Apeloig, Y., Eds.; John Wiley and Sons, Ltd.: New York, 2001; Vol. 3, p 949; (d) Wiberg, N.; Fischer, G.; Schurz, K. *Chem. Ber.* **1987**, *120*, 1605; (e) Leigh, W. J.; Li, X. *Organometallics* **2002**, *21*, 1197; (f) Trommer, M.; Miracle, G. E.; Eichler, B. E.; Powell, D. R.; West, R. *Organometallics* **1997**, *16*, 5737.
18. Simpkins, N. S. *Sulfones in Organic Synthesis*; Pergamon Press, 1993; Chapter 9.

19. Ono, N. *In The Nitro Group in Organic Synthesis*; John Wiley & Sons, Inc. 2002; pp 231.
20. Bordwell, F. G.; McKellin, W. H. *J. Am. Chem. Soc.* **1951**, *73*, 2251.
21. Atkins, P.; Overton, T.; Rourke, L.; Weller, M.; Armstrong, F. *Inorganic Chemistry*; Freeman, 2006; pp 775.
22. Denehy, E.; White, J. M.; Williams, S. J. *Inorg. Chem.* **2007**, *46*, 8871.
23. Frisch, M. J.; Trucks, G. W.; Schlegel, H. B.; Scuseria, G.; Robb, M. A.; Cheeseman, J. R.; Scalmani, G.; Barone, V.; Mennucci, B.; Petersson, G. A.; Nakatsuji, H.; Caricato, M.; Li, X.; Hratchian, H. P.; Izmaylov, A. F.; Bloino, J.; Zheng, G.; Sonnenberg, J. L.; Hada, M.; Ehara, M.; Toyota, K.; Fukuda, R.; Hasegawa, J.; Ishida, M.; Nakajima, T.; Honda, Y.; Kitao, O.; Nakai, H.; Vreven, T.; Montgomery, J. A.; Peralta, Jr., J. E.; Ogliaro, F.; Bearpark, M.; Heyd, J. J.; Brothers, E.; Kudin, K. N.; Staroverov, V. N.; Kobayashi, R.; Normand, J.; Raghavachari, K.; Rendell, A.; Burant, J. C.; Iyengar, S. S.; Tomasi, J.; Cossi, M.; Rega, N.; Millam, M. J.; Klene, M.; Knox, J. E.; Cross, J. B.; Bakken, V.; Adamo, C.; Jaramillo, J.; Comperts, R.; Stratmann, R. E.; Yazyev, O.; Austin, A. J.; Cammi, R.; Pomelli, C.; Ochterski, J. W.; Martin, R. L.; Morokuma, K.; Zakrzewski, V. G.; Voth, G. A.; Salvador, P.; Dannenberg, J. J.; Dapprich, S.; Daniels, A. D.; Farkas, Ö.; Foresman, J. B.; Ortiz, J. V.; Cioslowski, J.; Fox, D. J. *Gaussian 09*, Revision D.01, Gaussian, Inc., Wallingford, CT, **2009**.
24. Goldwhite, H.; Gibson, M. S.; Harris, T. *Tetradydron* **1964**, *20*, 1657.
25. (a) Kamigata, N.; Sawada, H.; Suzuki, N.; Kobayashi, M. *Phosphorus, Sulfur Silicon Relat. Elem.* **1984**, *19*, 199; (b) Kamigata, N.; Shimizu, T. *Rev. Heteroat. Chem.* **1997**,

- 17, 1.
26. Quebatte, L.; Thommes, K.; Severin, K. *J. Am. Chem. Soc.* **2006**, *128*, 7440.
27. Kameyama, M.; Kamigata, N.; *Bull. Chem. Soc. Jpn.* **1989**, *62*, 648.
28. Firouzabadi, H.; Jamalian, A. *J. Sulfur Chem.* **2008**, *29*, 53.
29. Hurni, K. L.; Rupar, P. A.; Payne, N. C.; Baines, K. M. *Organometallics* **2007**, *26*, 5569.
30. Fink, M. J.; Michalczyk, M. J.; Haller, K. J.; Michl, J.; West, R. *Organometallics* **1984**, *3*, 793.
31. McKillop, K. L.; Gillette, G. R.; Powell, D. R.; West, R. *J. Am. Chem. Soc.* **1992**, *114*, 5203.
32. Becke, A. D. *J. Chem. Phys.* **1993**, *98*, 5648.
33. Zhao, Y.; Truhlar, D. G. *Theor. Chem. Acc.* **2008**, *120*, 215.
34. Bruker-AXS, SAINT version 2013.8, **2013**, Bruker-AXS, Madison, WI 53711, USA.
35. Bruker-AXS, SADABS version 2012.1, **2012**, Bruker-AXS, Madison, WI 53711, USA.
36. Sheldrick, G. M. **2014**, University of Göttingen.
37. Sheldrick, G. M. *Acta Cryst.* **2008**, *A64*, 112.
38. Van der Sluis, P.; Spek, A. L. *Acta Cryst.* **1990**, *A46*, 194.
39. Spek, A. L. *J. Appl. Cryst.* **2003**, *36*, 7.

Chapter 7

The Reactivity of Ditetrelenes Toward Isocyanides

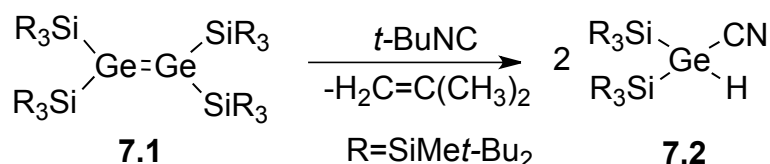
7.1 Introduction

Since the first isolation of a stable disilene by West *et al.* and silene by Brook *et al.* in 1981,¹ the chemistry of these doubly-bonded species has been the subject of many extensive studies.^{2,3} They are not only the subject of fundamental investigations;⁴ due to their unique electronic properties and high reactivity, they are also increasingly moving into focus as functional materials.⁵ The reactions of these low coordinate Group 14 compounds reactions feature in some exciting developments. The addition of nitriles to tetramesityldigermene has been reported and found to be reversible as evident from trapping reactions using dimethylbutadiene (DMB).⁶ This is the first example of a reversible formal cycloaddition of a doubly-bonded heavier Group 14 species and suggests that main group ditetrelenes may have potential in catalytic applications. The idea of multiply-bonded main group compounds acting as catalysts was unprecedented until the report of the reversible addition of ethylene to a distannyne, which implies the use of low-valent main Group 14 species as catalyst.¹²

Isocyanides are structural isomers of nitriles, and thus, it seems plausible that these compounds may also react with digermenes in a reversible manner. Although the addition of isocyanides to tetramesityldigermene or tetramesityldisilene has never been investigated, isocyanides are known to react with other unsaturated Group 14 species. Reactions between isocyanides and unsaturated Group 14 species often involve the isocyanide carbon acting as a Lewis base. Several modes of reactivity have been observed: cleavages of the metalloid-metalloid bond, 1:1 adduct formation of the isocyanide to the metalloid atom without cleavage. Some of the

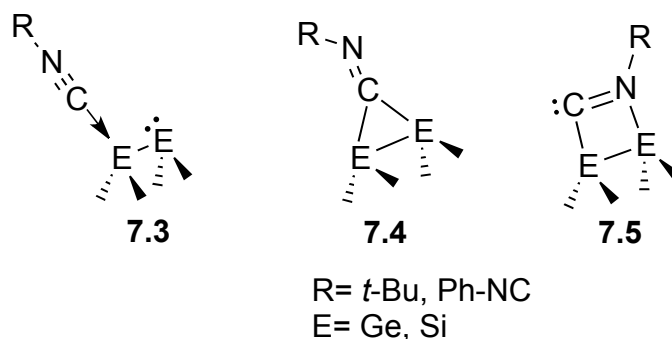
reactions have been shown to be reversible. Therefore, the addition reaction of isocyanides to a digermene and disilene, respectively, will be briefly introduced.

Only one reaction between an isocyanide and a digermene has been reported to date. *t*-Butyl isocyanide reacts with digermene **7.1**, to give **7.2** through loss of $\text{H}_2\text{C}=\text{C}(\text{CH}_3)_2$ and cleavage of the Ge=Ge double bond (Scheme 7.1).⁷



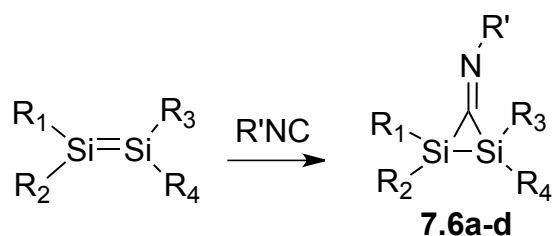
Scheme 7.1

The addition of isocyanides towards the Ge(100)- 2×1 reconstructed surface has also been investigated. Three possible adsorption modes were considered for the addition of *t*-butyl isocyanide to the Ge(100)- 2×1 surface; a Lewis base adduct **7.3**, a [2+1] cycloadduct **7.4**, and a [2+2] cycloadduct **7.5** (Scheme 7.2). Through the use of FTIR spectroscopy, temperature-programmed desorption and DFT calculations the surface adduct is believed to have the structure of **7.3**.⁸ In a similar fashion, investigation of the reaction of 1,4-phenylene diisocyanide with the Ge(100)- 2×1 surface revealed the formation of a coordination compound with one isocyanide moiety, although several modes of reactivity were considered.⁹



Scheme 7.2

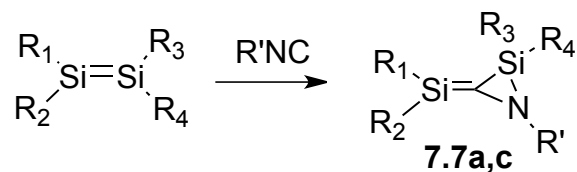
The formation of the [2+1] cycloadduct, iminodisilirane **7.6**, was observed in the addition of 2,6-dimethylphenyl isocyanide to tetrakis(2,6-dimethylphenyl)disilene (Scheme 7.3),¹⁰ and disilene, $R^H_2Si=Si(t-Bu)R^{Ar}$.¹⁵ The formation of the iminodisilirane was also reported for the addition of *t*-butyl isocyanide to $Ph(t-Bu_3Si)Si=SiPh(Si^i-Bu_3)$ as the primary product of the reaction, **7.6c**.¹¹ The addition several isocyanides to cyclotrisilenes was also investigated, and leads to the formation of analogues of **7.6**, which often undergo subsequent rearrangement with the cyclic silicon moiety.¹²



7.6a $R_1, R_2, R_3, R_4, R' = 2,6$ dimethylphenyl¹⁰ **7.6b** $R_1, R_2 = 1,1,4,4$ - tetrakis(trimethylsilyl)butane-1,4-diyl, $R_3 = t-Bu$, $R_4 = Ant$, 1-naphthyl, $R' = 2,6$ - dimethylphenyl;¹⁵ **7.6c** $R_1, R_3 = Si^i-Bu_3$, $R_2, R_4 = Ph$, $R' = t-Bu$;¹¹ **7.6d** $R_1, R_2, R_3 = Tip$ (2,4,6-*i*-Pr₃C₆H₂), $R_4 = Ph$, $R' = t-Bu$, CMe_2CH_2t-Bu , 2,6-Me₂C₆H₃¹³

Scheme 7.3

Rearrangement of iminodisilirane **7.6** to silaaziridines was reported in few cases for the addition of isocyanides to disilenes. One equivalent of *t*-butyl isocyanide added to the asymmetric disilene, $Tip_2Si=SiPh(Tip)$, to yield a silaaziridine with an exocyclic Si=C double bond **7.7a** through rearrangement of **7.6d**.¹³ The formation of a silaaziridine was also observed in the addition of *t*-butyl isocyanide to $Tip_2Si=Si(Tip)TMOP$ (TMOP= 2,4,6-(MeO)₃C₆H₂)¹⁴ as well as to $R^H_2Si=Si(t-Bu)R^{Ar}$ ($R^H_2 = 1,1,4,4$ -tetrakis(trimethylsilyl)butane-1,4-diyl, $R^{Ar} = Ant$, 1-naphthyl)¹⁵ (Scheme 7.4).



7.7a $R_1, R_2, R_3 = \text{Tip}$ (2,4,6-*i*-Pr₃C₆H₂), $R_4 = \text{Ph}$, $R' = t\text{-BuCMe}_2\text{CH}_2t\text{-Bu}$, 2,6-Me₂C₆H₃¹³; **7.7b** $R_1, R_2 = 1,1,4,4\text{-tetrakis(trimethylsilyl)butane-1,4-diyl}$, $R_3 = t\text{-Bu}$, $R_4 = \text{Ant}$, $R' = 2,6\text{-dimethylphenyl}$,¹⁵ **7.7c** $R_1, R_2, R_3 = \text{Tip}$ (2,4,6 *i*-Pr₃C₆H₂), $R_4 = 2,4,6\text{-(MeO)}_3\text{C}_6\text{H}_2$, $R' = t\text{-Bu}$ ¹⁵

Scheme 7.4

The addition of isocyanides to the Si (100)- 2×1 reconstructed surface was examined using X-ray photoelectron spectroscopy (XPS) and *ab-initio* calculations. *t*-Butyl and 2,6-dimethylphenyl isocyanide add to the Si (100)- 2×1 surface, disilaazaridines **7.4** were postulated as the products of the addition reaction.¹⁶

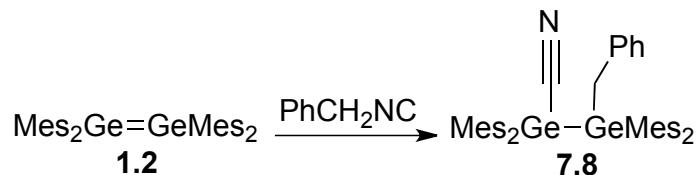
Given our previous work, we believe that tetramesityldisilene (Mes₂Si=SiMes₂, Mes = 2,4,6-Me₃C₆H₂), and tetramesityldigermene (Mes₂Ge=GeMes₂) can serve as useful molecular models for the corresponding Si and Ge(100)- 2×1 surfaces.¹⁷ Indeed, we have shown that the reactivity of the silicon and germanium surfaces are comparable to their molecular counterparts.¹⁷ Herein, the addition of isocyanides to tetramesityldigermene and tetramesityldisilene is explored in an effort to give a broader understanding of the chemistry and, in particular, an understanding of the influence of the substituents on the ditetrelene and on the isocyanide on the outcomes of the reaction. Furthermore, the chemistry of the molecular systems will be compared to that found on the Si/Ge(100)- 2×1 surfaces.

7.2 Results

7.2.1 The Addition of Isocyanides to Tetramesityldigermene

7.2.1.1 Addition of Small Isocyanide to Tetramesityldigermene

The addition of excess of benzyl isocyanide to a THF solution of tetramesityldigermene **1.2** at room temperature gave a dark orange oil upon removal of the solvent. ^1H NMR spectroscopic analysis of the crude product revealed that **7.8** is the only product formed. The mass spectrum of **7.8** revealed a molecular ion at m/z 756.2388, which is consistent with a 1:1 adduct between digermene **1.2** and benzyl isocyanide. Two sets of signals assigned to mesityl groups were evident in both the ^1H and the ^{13}C NMR spectra of **7.8**. One of the signals on the mesityl substituent (2.24 ppm) appeared as a very broad singlet. The broadness is attributed to slow rotation about the Mes-Ge bond on the NMR timescale, and thus, this signal was assigned to the *ortho*-methyl groups on the mesityl rings located on the germanium bearing the benzyl substituent. In the ^{13}C - ^1H HMBC spectrum of **7.8**, a correlation between the signal assigned to the *ipso*-C of the Mes group in the ^{13}C dimension and the signal assigned to the two hydrogens of the benzyl moiety was observed consistent with the assigned structure. Notably, the iminodigermirane structure analogous to **7.6** would not be expected to give rise to such a correlation. The IR spectrum of **7.8** revealed an absorption at 2168 cm^{-1} which falls outside the range of a typical nitrile stretching vibration ($2260\text{--}2240\text{ cm}^{-1}$);¹⁸ however, this value is consistent with the CN stretching vibration of $\text{Mes}_2\text{Ge}(\text{CN})_2$ (2186 cm^{-1}).¹⁹ Unambiguous identification of **7.8** in the solid state was obtained from X-ray crystallography; the product was identified as 2-benzyl-1,1,2-tetramesityldigermeryl nitrile (Scheme 7.5 and Figure 7.1).



Scheme 7.5

X-ray crystallography revealed that the C1-N1 fragment in **7.8** was disordered, with a reverse of the atom order (nitrile vs. isonitrile) in a 91% to 9% ratio, respectively. Attempts to separate the isomer with the N bonded to the germanium using Et₃B were not successful possibly due to the low concentration of the isomer with the N bonded to the germanium in comparison to **7.8**. The presence of the isomeric mixture was not evident by NMR spectroscopy at 25 °C. The N1-C1-Ge1 angle is slightly bent at 174.07° (17). The C20-Ge2-Ge1 angle at 96.85(5)° deviates from the standard tetrahedral angle of 109°. All remaining bond lengths and angles in **7.8** are within normal ranges.

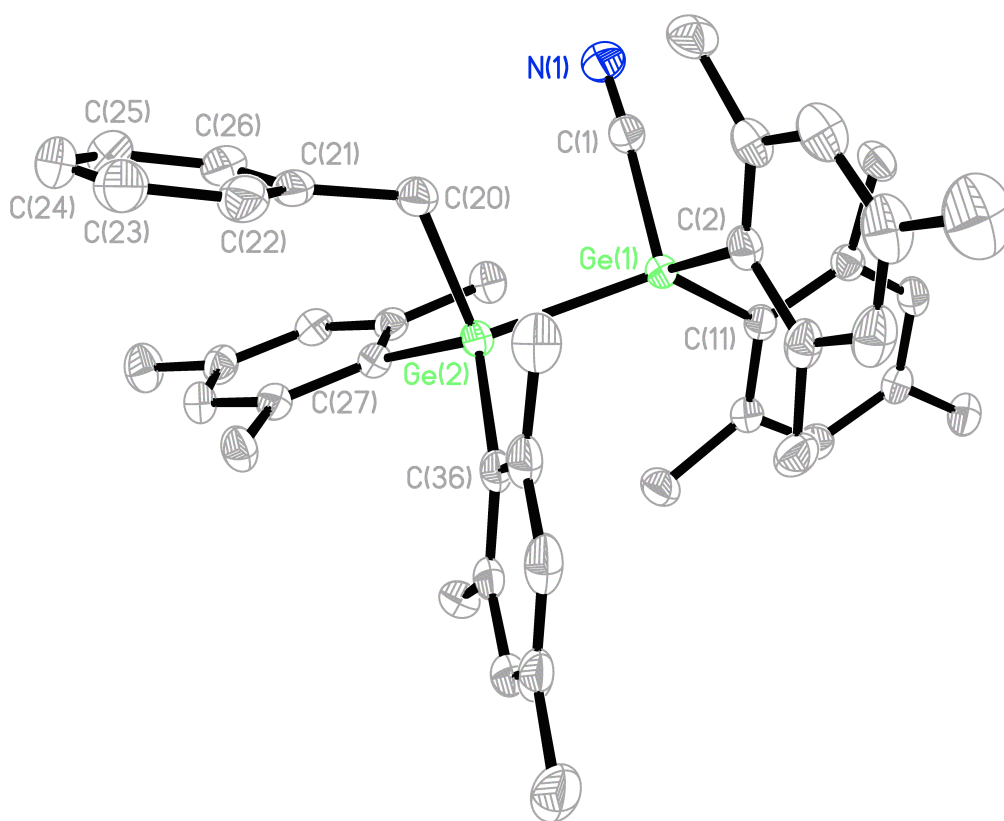


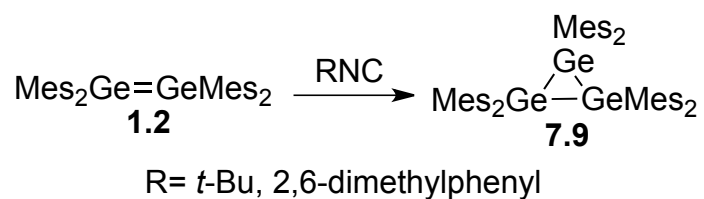
Figure 7.1 Displacement ellipsoid plot of **7.8**. Ellipsoids are at the 50% probability level and hydrogen atoms were omitted for clarity. The disorder at C1-N1 is omitted for clarity. Selected bond lengths (Å) and angles (deg): Ge1-N1' = 1.9759(18), Ge1-C1 = 1.9759(18), Ge1-Ge2 = 2.5031(3), Ge2-C20 = 2.0120(18), C1-N1 = 1.142(2), N'1-Ge1-Ge2 = 100.98(5), C1-Ge1-Ge2 = 100.98(5), C2-Ge1-C11 = 107.80(7), C27-Ge2-C36 = 114.21(7), C20-Ge2-Ge1 = 96.85(5), N1-C1-Ge1 = 174.07(17), C1'-N1'-Ge1 = 174.07(17).

The thermal stability of **7.8** was investigated by heating a THF-*d*₈ solution of **7.8** to 145 °C in the presence of DMB; **7.8** was recovered unchanged.

7.2.1.2 Addition of Bulky Isocyanides to Tetramesityldigermene

The addition of 2,6-dimethylphenyl or *t*-butyl isocyanide to a THF solution of tetramesityldigermene did not result in the formation of an adduct, even upon prolonged heating at 100 °C. Interestingly, both isocyanides accelerated the conversion of digermene **1.2** to cyclotrigermene **7.9** (Scheme 7.6). When a solution of **1.2** and **7.9** (1:1 ratio) was left to stir at room temperature for three weeks, the ratio of digermene **1.2** to the cyclotrigermene **7.9** increased slightly to 1.0:1.3.^{17b} After two weeks of refluxing in THF, the ratio of digermene **1.2** to cyclotrigermene **7.9** changed to 1.0:7.1. In contrast, in the presence of 2,6-dimethylphenyl or *t*-butyl isocyanide, the conversion of digermene **1.2** to **7.9** was accelerated; the conversion is nearly complete after one week at room temperature. The addition of *t*-butyl isocyanide to cyclotrigermene **7.9** did not show any reaction after stirring at room temperature for one week.

The reaction between digermene **1.2**, and 2,6-dimethylphenyl isocyanide was monitored in THF-*d*₈ in a J. Young tube. A solution of digermene **1.2** dissolved in THF-*d*₈ was monitored simultaneously as a control experiment. The amount of **7.9** present in each solution, relative to an internal standard, was plotted against time (Figure 7.2). Clearly, the presence of 2,6-dimethylphenyl isocyanide has a significant effect on the rate of conversion of digermene **1.2** to cyclotrigermene **7.9** with a significant amount of cyclotrigermene observed even after 20 hours. The accelerated conversion of digermene **1.2** to **7.9** in the presence of an anionic gallium NHC analogue has previously been reported.²⁰



Scheme 7.6

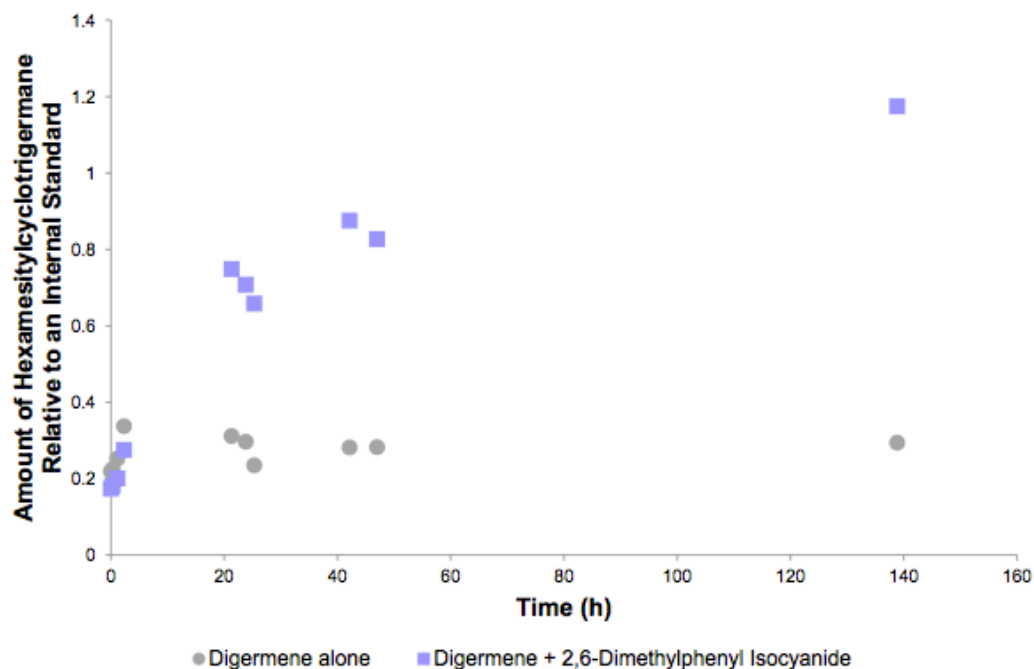
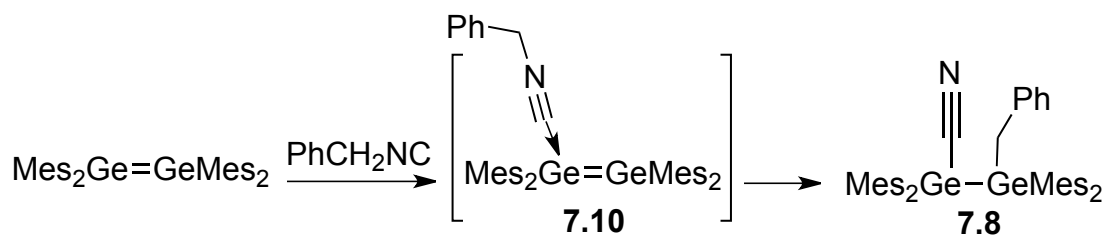


Figure 7.2: Effect of adding 2,6-dimethylphenyl isocyanide on the conversion of **1.2** to **7.9**

7.3 Discussion

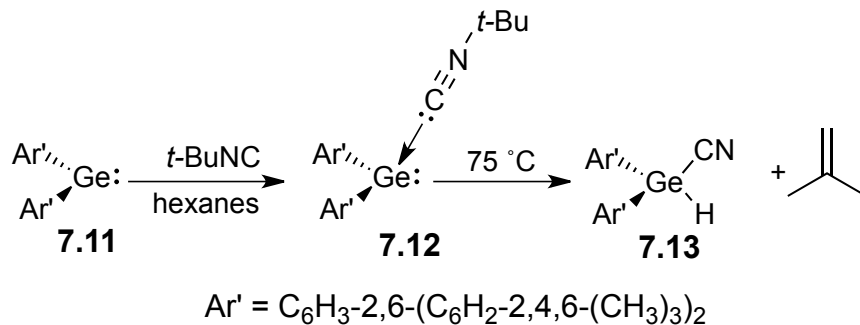
7.3.1 The Addition of Isocyanides to Tetramesityldigermene

A possible pathway for the formation of adduct **7.8** begins with the coordination of the isocyanide carbon to one of the germanium atoms of digermene **1.2** to afford **7.10**, followed by cleavage of the alkyl nitrogen bond to give a benzyl carbocation, which can then recombine with the germyl anion to yield **7.8** (Scheme 7.7).



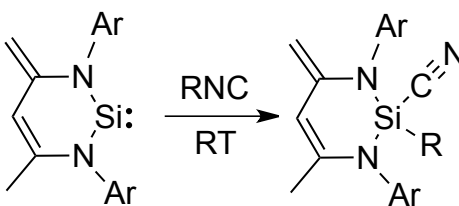
Scheme 7.7

The relative energies of the proposed intermediate **7.10** and the isolated product **7.8** were calculated using DFT at the M06/6-311+G**/ B3LYP/6-31G* level. The energies of **7.10** and **7.8** were lower than the reactants at -13.0 kJ/mol and -236.5 kJ/mol, respectively. The formation of **7.10** is reasonable as many reports on the reaction between isocyanides and unsaturated Group 14 species involving the isocyanide carbon acting as a Lewis base. For example: a similar coordination motif was reported in the addition of one equivalent of *t*-butyl isocyanide to a bis(terphenyl)digermene ($\text{Ar}'=\text{C}_6\text{H}_2-2,6-(\text{C}_6\text{H}_3-2,6-^i\text{Pr}_2)_2$).^{21,22} The addition of two equivalents of *t*-butyl or mesityl isocyanide to a bis(terphenyl)distannyne also resulted in the coordination of both equivalents to the distannyne.^{17,23} Activation of the C-N bond of an isocyanide by a low coordinate germanium species, has also been observed in the addition of *t*-butyl isocyanide to germylene **7.11** (Scheme 7.8).²⁴ In this case, the initially formed Lewis acid-base adduct **7.12** undergoes elimination of isobutylene at higher temperatures to give the germyl nitrile, **7.13**.



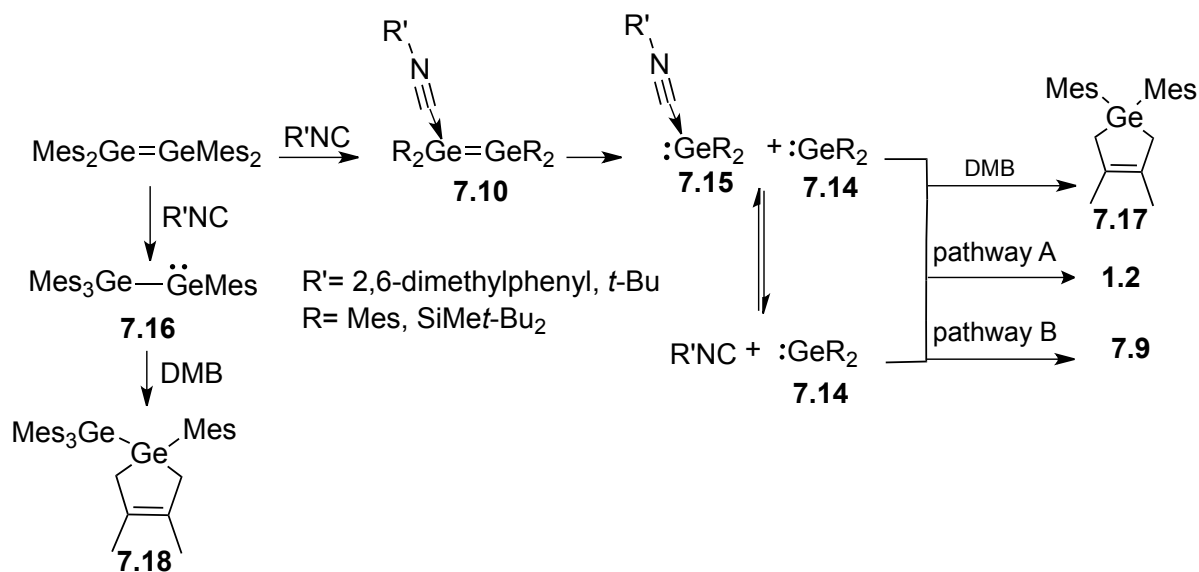
Scheme 7.8

In a similar fashion, the dealkylation of metal–isocyanide complexes has been reported. The activation of *t*-butyl isocyanide by the iron(0) phosphine complex, $\text{Fe}(\text{PMe}_3)_2(\text{CN}t\text{-Bu})_3$, gave $\text{Fe}(\text{PMe}_3)_2(\text{CN}t\text{-Bu})_2(\text{H})(\text{CN})$ and was speculated to proceed via homolytic cleavage of the N- *t*-butyl bond, with the subsequent *t*-butyl radical acting as a hydrogen donor to yield isobutene.²⁵ Insertion into the N–R bond of cyclohexyl isocyanide by silylenes has been also reported (Scheme 7.9).²⁶



Scheme 7.9

The formation of cyclotrigermane **7.9** in the presence of 2,6-dimethylphenyl and *t*-butyl isocyanide can be explained as follows: initial coordination of the bulky isocyanide to the digermene would give **7.10** (Scheme 7.10). Loss of germylene **7.14** from **7.10** would result in the formation of the germylene-isocyanide complex **7.15**. Complex **7.15** is likely in equilibrium with the free isocyanide and germylene **7.14**; the reversible complexation of dimesitylgermylene with donors has been reported.²⁷ Germylene **7.14** could dimerize to form digermene **1.2** (Pathway A) or react with digermene **1.2** to produce cyclotrigermane **7.9** (Pathway B). A similar mechanism was proposed for the addition of anionic gallium hetrocyclic carbene analogue to digermene **1.2**. The gallium NHC analogue was proposed to facilitate the conversion of digermene **1.2** to cyclotrigermane **7.9** through the initial coordination of the gallium atom to the digermene.²⁰



Scheme 7.10

The isolation of the adduct **7.12** was facilitated by the addition of a five-fold excess of *t*-butyl isocyanide to germylene **7.11** (Scheme 7.8).²⁴ Thus, the addition of a five-fold excess of *t*-butyl isocyanide to digermene **1.2** was performed. Although an adduct was not isolated, a 1:1 adduct between the isocyanide and the digermene was observed by mass spectrometry which supports the formation of **7.10**. In an effort to provide evidence for the formation of germylene **7.14** as an intermediate along the reaction pathway, the reaction was repeated in the presence of DMB. When a THF solution of digermene **1.2**, 2,6-dimethylphenyl isocyanide and large excess of DMB was stirred at room temperature overnight the formation of germacyclopentenes **7.17** and **7.18** were observed. The formation of **7.17** provides convincing evidence for the formation of germylene **7.14** during the reaction as germacyclopentene **7.17** is the well-known product of the reaction between dimesitylgermylene and DMB.²⁸ Notably, a THF solution of digermene **1.2** was stirred in the presence of excess DMB at room temperature for three weeks and **7.18** was observed as the only product indicating that digermene **1.2** does not dissociate to give **7.14** under these reaction conditions. Obviously, hexamesitylcyclotrigermane **7.9** acts as a thermodynamic

sink in the reaction. Evidently, the larger terphenyl substituents in germylene **7.11** prevent dimerization and thus, germylene-isocyanide complex **7.12** can be isolated.

The addition of *t*-butyl isocyanide to digermene **7.1** (Scheme 7.1) appears to be analogous to the addition of *t*-butyl isocyanide to tetramesityldigermene, even though the outcomes of the reaction are quite different (yields **7.2** and **7.9**, respectively). The initial step for formation of **7.2** was proposed to occur via coordination of the isocyanide carbon to one of the germanium atoms of digermene **7.1** to give a structure analogous to **7.10**. Cleavage of the germanium-germanium bond forms the germylene-isocyanide complex **7.15**. (Scheme 7.10 where R= SiMe*t*-Bu₂). The difference in reactivity can be attributed to where the equilibrium lies: when R= Mes, the equilibrium lies on the side of free germylene, which then undergoes reaction pathway A or B (Scheme 7.10). While when R= SiMe*t*-Bu₂, the equilibrium appears to lie toward the germylene-isocyanide complex **7.15**, loss of H₂C=C(CH₃)₂ forms **7.2**. The germylene complex **7.15** must exist long enough to form **7.2** in comparison to the short-lived species **7.10**. We speculate that the silyl substituents stabilize the germylene-isocyanide complex through negative hyperconjugation,²⁹ and thus, the complex is long-lived allowing subsequent insertion and elimination steps to occur. A Ge(IV) cyanide product does not apparently form between *t*-butyl isocyanide and digermene **1.2** because the germylene and isocyanide are not coordinated long enough for the insertion reaction to proceed.

The interaction between electron donors and ditetrelenes is an interesting topic that has received little attention. Electron donors are proposed to coordinate to one of the metalloid atoms in ditetrelenes to give a structure similar to **7.10**. Strong Lewis bases, such as NHCs, are able to form a stable donor-germylene complex analogous to **7.15**, through extrusion of a germylene.^{20,30} Weak Lewis bases, such as nitriles, are proposed to form an initial donor-digermene species (e.g. **7.10**) and, although the reactivity of the digermene is influenced, extrusion of germylene **7.14**

does not occur.⁹ Molecules with moderate Lewis basicity, such as isocyanides, cleave the Ge=Ge bond and form donor-germylene complexes when intramolecular cyclization cannot occur. The formation of the germylene-donor complex is proposed to be reversible and under these conditions, subsequent reactivity of the germylene is observed.

The reactivity of *t*-butyl isocyanide toward the Ge(100)- 2×1 surface revealed the formation of **7.3**, which is similar in structure to **7.10**.⁸ Although the authors considered the formation of cycloadducts as possible products, the formation of the C-N bond activation product similar to **7.8** was not considered. Although the majority of the characterization data obtained for **7.3** cannot be compared to the data of **7.8**, the FTIR spectroscopic data for **7.8** can be directly compared to the data obtained for **7.3**. The value of 2168 cm^{-1} assigned, to the nitrile bond stretching vibration of **7.8**, is similar in the value to the isonitrile stretching vibration of **7.3** (2190 cm^{-1}). The stretching vibration for the surface bound isonitrile was blue-shifted from that of the *t*-butyl isocyanide stretching vibration at 2134 cm^{-1} .⁸ We observed the same trend; the stretching vibration for **7.8** was blue-shifted from the free benzyl isocyanide (2151 cm^{-1}). The IR stretching vibration for the CN moiety in **7.8** (2168 cm^{-1}) falls outside the normal range for nitriles ($2260\text{-}2220 \text{ cm}^{-1}$) and lies closer to the normal range for isocyanides ($2110\text{-}2165 \text{ cm}^{-1}$).¹⁸ However, the wavenumber for the nitrile stretching vibration in germyl nitriles is known to be much less than organic nitriles (e.g. $\text{Mes}_2\text{Ge}(\text{CN})_2$ at 2186 cm^{-1}). A similar trend was also observed for silyl nitriles, the nitrile stretching vibration of $\text{H}_3\text{SiH}_2\text{SiCN}$ is at 2188 cm^{-1} .³¹ Thus, it is entirely reasonable that the structure on the Ge(100)- 2×1 surface is analogous to **7.8** and not the Lewis acid-base donor adduct. Consideration of this possibility needs further investigation from surface scientists.

Notably, the addition of *t*-butyl isocyanide to digermene **1.2** did not result in the formation of a stable adduct, unlike the Ge(100)- 2×1 surface chemistry. The underlying germyl

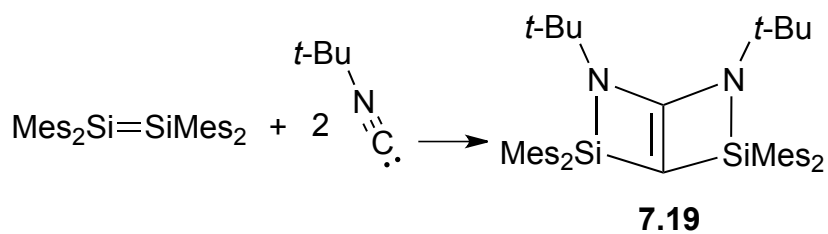
substituents on the surface dimers of the Ge(100)- 2×1 surface are in a *cis*-bent geometry about the dimer. In contrast, digermene **1.2** possesses bulky mesityl substituents oriented in a *trans*-bent geometry.^{17b} The increased bulk of the digermene **1.2** as a result of its stabilizing ligands may prevent the formation of a stable adduct with bulky isocyanides. The Ge(100)- 2×1 surface dimer is tilted even at room temperature. The “up” atom exhibits a nucleophilic character since it possesses most of the electron density and the “down” atom is expected to exhibit significant electrophilic character since it possesses the least electron density.³² This tilting might make the Ge(100)- 2×1 surfaces prefer to react in donor/acceptor fashion (i.e. to form the donor adduct **7.3**) or enable the formation of a C-N activation product analogous to **7.8**.

In summary, we have shown that tetramesityldigermene can serve as a valuable model for the Ge(100)- 2×1 surface providing insights into the reactivity of the surfaces not previously considered.

7.2.2 The Addition of Isocyanides to Tetramesityldisilene

7.2.2.1 Addition of *t*-Butyl Isocyanide to Tetramesityldisilene

The addition of excess *t*-butyl isocyanide to the bright yellow solution of disilene **1.4** in hexanes at room temperature gave a white solid, **7.19**, upon removal of the solvent. The product was purified by recrystallization from a saturated hexanes solution at low temperature to yield colourless crystals. The compound was identified as a 2:1 adduct between *t*-butyl isocyanide and the disilene by ¹H, ¹³C, ¹H-¹H gCOSY, ¹H-¹³C gHSQC, ¹H-¹³C gHMBC and ²⁹Si-¹³C gHMBC NMR spectroscopy, and ESI mass spectrometry (Scheme 7.11).



Scheme 7.11

The structure of **7.19** was unequivocally determined by single crystal X-ray diffraction as 2,6-di-*t*-butyl-3,3,5,5-tetramesityl-2,6-diaza-3,5-disilabicyclo[2.2.0]hex-1(4)-ene referred to herein as the butterfly adduct **7.19**. All bond lengths and angles are within normal ranges; the distance between C2 and C1 is 1.377(2)Å, consistent with a C-C double bond (Figure 7.3). Compound **7.19** has a double enamine structure, with two distinctive chemical shifts for the signals assigned to the unsaturated carbons at 178 and 86.7 ppm, similar to other double enamines.³³ The structure of **7.19** is unique; no similar structures have been reported either for carbon or other main group elements.

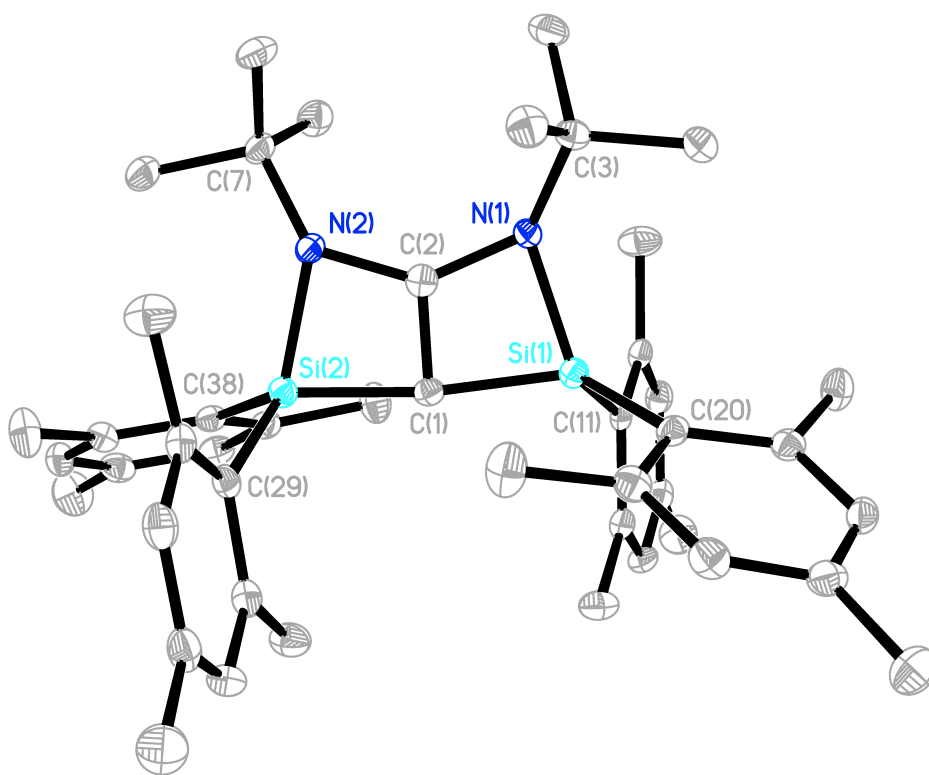


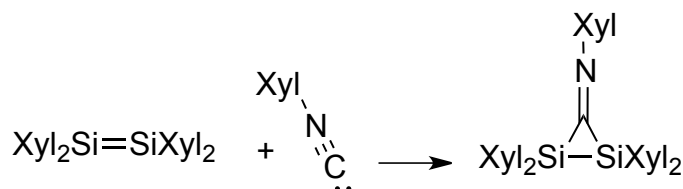
Figure 7.3 Displacement ellipsoid plot of **7.19**. Ellipsoids are at the 50% probability level and hydrogen atoms were omitted for clarity. Selected bond lengths (Å) and angles (deg): Si1-C1 = 1.8049(17), Si1-N1 = 1.8164(16), Si2-C1 = 1.8073(17), Si2-N2 = 1.8239(17), N1-C2 = 1.425(2), N2-C2 = 1.424(2), C1-C2 = 1.377(2); C1-Si1-N1 = 78.82(7), C1-Si1-N2 = 78.82(7), C1-Si2-N2 = 78.50(7), C1-C2-N2 = 110.22(14), C1-C2-N1 = 110.25(14).

To gain insight into the reaction pathway, the addition of one equivalent of *t*-butyl isocyanide to the bright yellow solution of disilene **1.4** in hexanes (or THF or C₆D₆) at room temperature was examined. ¹H NMR spectroscopy of the deep orange solution revealed the formation of an intermediate, **7.20**, which was determined to be a 1:1 adduct between *t*-butyl isocyanide and the disilene by integration of the appropriate signals in the ¹H NMR spectroscopy of the reaction mixture. The intermediate transformed, within 30 min, to a mixture of a disilene **1.4** and **7.19** in a 2:1 ratio. Two ²⁹Si signals were observed and assigned to **7.20**, at -64.1 ppm and -53.3 ppm. In an effort to elucidate the structure of the **7.20**, trapping experiments with a variety of scavengers was attempted. No reaction was observed upon the addition of *t*-butylacetylene to a hexane solution of **7.20**. Other trapping experiments included the addition of the soft Lewis acid

W(CO)₅; again no reaction was observed. The addition of GaCl₃ to **7.20** resulted in cleaving the isocyanide from **7.20**, forming an adduct between GaCl₃ and the *t*-butyl isocyanide along with some unidentified material.³⁴ The addition of AuCl, acetonitrile, I₂ and CH₃I gave complex mixtures as determined by ¹H NMR spectroscopy.

7.2.2.2 Addition of 2,6-Dimethylphenyl Isocyanide to Tetramesityldisilene

The addition of excess 2,6-dimethylphenyl isocyanide to a bright yellow solution of tetramesityldisilene in hexanes at room temperature gave a red solid, **7.21**, upon removal of the solvent. The product was purified by recrystallization from a saturated hexanes solution at low temperature to yield red crystals. The compound was identified as the 1:1 adduct between 2,6-dimethylphenyl isocyanide and disilene **1.4** by ¹H, ¹³C, ¹H-¹H gCOSY, ¹H-¹³C gHSQC and ¹H-¹³C gHMBC and ²⁹Si-¹³C gHMBC NMR spectroscopy. The structure of **7.21** was unequivocally determined by single crystal X-ray diffraction as the iminodisilirane (Scheme 7.12 and Figure 7.4). All bond lengths and angles are within normal ranges and are similar to those reported for structurally-related compounds.^{10,15}



Scheme 7.12

Only one signal in the ²⁹Si dimension in the ²⁹Si-¹H HMBC spectrum of **7.21** was observed at 37 ppm. This is in an excellent agreement with the ²⁹Si chemical shift reported for **7.6a** (37 ppm).⁷ Also, in the ¹³C NMR spectrum of **7.21** a signal at 216 ppm was assigned to the iminic carbon and is in excellent agreement with the analogous chemical shift in **7.6a** (214.0 ppm).¹⁵ Compound **7.21** is unstable and decolourises in less than 24 h under an inert atmosphere

forming a yellow solid. The yellow solid revealed the formation of a 1:2 adduct between disilene **1.4** and 2,6-dimethylphenyl isocyanide as determined by mass spectrometry; however, the structure of the compound was not unambiguously elucidated.

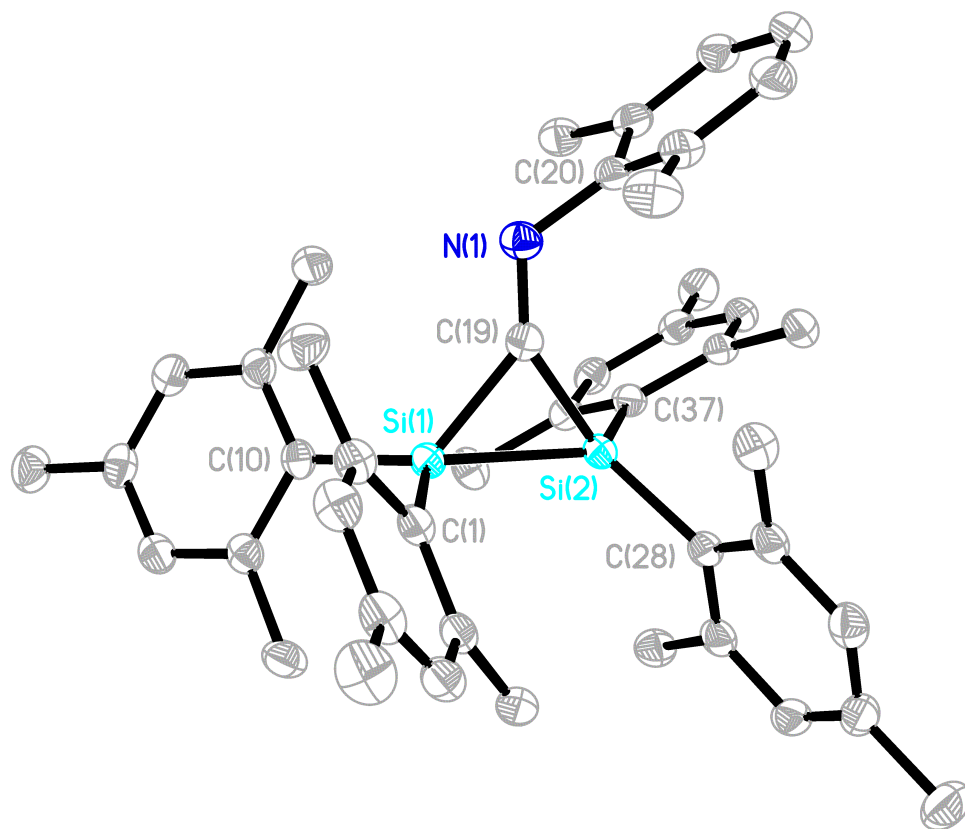


Figure 7.4 Displacement ellipsoid of **7.21** showing naming and numbering scheme. Ellipsoids are at the 50% probability level and hydrogen atoms were omitted for clarity. Selected bond lengths (Å) and angles (deg): Si1-C10 = 1.898(3), Si1-C19 = 1.914(3), Si1-Si2 = 2.3316(11), C19-N1 = 1.276(4), N1-C20 = 1.424(4); C19-Si1-Si2 = 53.58(9), C19-Si2-Si1 = 52.17(9), Si1-C19-Si2 = 74.25(11), C19-N1-C20 = 122.5(3).

Interestingly, only one signal was observed in the ^{29}Si - ^1H HMBC spectrum of **7.21**; West also reported only one signal for iminodisilirane **7.6a** as well.¹⁰ The appearance of only one signal in the ^{29}Si NMR spectrum of **7.21** suggests that the barrier to inversion at the iminic nitrogen is low as proposed by West.¹⁰

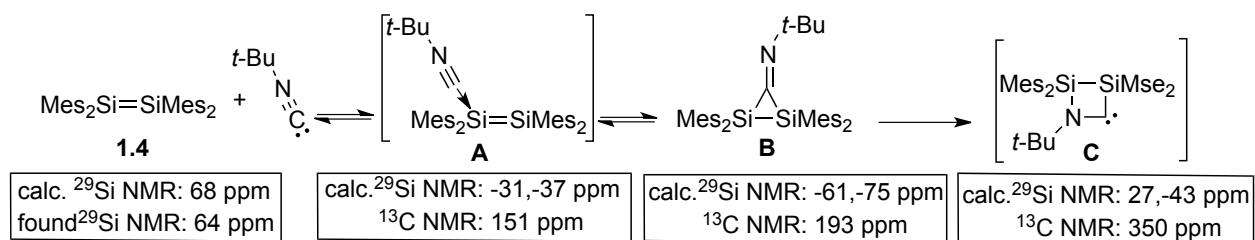
7.3.2 The Addition of Isocyanides to Tetramesityldisilene

The assignment of the structure of **7.20**, the intermediate observed along the reaction pathway in the addition of *t*-butyl isocyanide to disilene **1.4**, was not evident from a comparison of the ^{29}Si chemical shifts of **7.20** (-53 and -64 ppm) with either that of the iminodisilirane reported by West for **7.6a** (37 ppm), that of **7.21** (37 ppm) or the silaaziridine derivative **7.7a** reported by Scheschkewitz (-4 and -80 ppm). Notably, Scheschkewitz also observed three sets of ^{29}Si signals in the early stages of the addition reaction of *t*-butyl isocyanide to the asymmetric disilene, $\text{Tip}_2\text{Si}=\text{Si}(\text{Tip})\text{Ph}$ which were also assigned to an intermediate along the reaction pathway. The major signals at (-53 and -80 ppm) were identified as iminodisilirane **7.6d** on the basis of ^{29}Si chemical shifts calculations. The ^{29}Si chemical shifts of the intermediate reported by Scheschkewitz are close to the observed ^{29}Si chemical shifts for **7.20** suggesting the formation of the iminodisilirane along the reaction pathway. However, the chemical shifts of **7.6a** and **7.21** cast some uncertainty on the assignment.

To determine the structure of **7.20**, the ^{29}Si and ^{13}C NMR chemical shifts of relevant intermediates at the M06-L/6-311G(2d,p)/M06-2X/6-311+G(d,p) level of theory were calculated. The reaction pathway was proposed on the basis of the work of Scheschkewitz¹³, Nguyen³⁵ and Iwamoto¹⁵ (see Schemes 7.13 and 7.14). Significant differences in the ^{29}Si chemical shifts of the iminodisilirane reported by West and Scheschkewitz were noted, which suggested there might be a large influence of the substituent at the nitrogen on the chemical shifts, and thus, we performed the calculations on the actual structures (i.e. with mesityl groups on the disilene and *t*-butyl on the isocyanide moiety). As a test of the method, the structures of disilene **1.4** and the adduct **7.19** were optimized and the ^{29}Si chemical shifts were calculated and compared to the experimental values. There is excellent agreement between the experimentally determined and the calculated ^{29}Si chemical shifts of disilene **1.4** (64 ppm and 68 ppm,

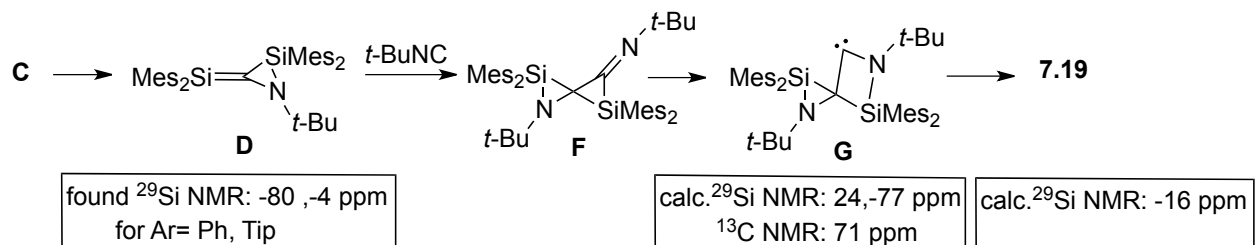
respectively) and there is excellent agreement between the experimental and calculated ^{29}Si chemical shifts of **7.19** (-12 and -16 ppm, respectively). The excellent agreement between the experimental and calculated values gave us confidence in the reliability of the selected computational method.

The reaction pathway is believed to begin by coordination of *t*-butyl isocyanide to the disilene **1.4** to give the donor adduct **A**. The calculated ^{29}Si NMR chemical shifts for **A** are -31 and -37 ppm while the ^{13}C chemical shift of the iminic carbon is at 151 ppm.



Scheme 7.13

Rearrangement of **A** to form the three-membered ring **B** may then occur. The calculated ^{29}Si NMR shifts of **B** are at -61 and -75 ppm, while the ^{13}C chemical shift of the iminic carbon is at 193 ppm. The formation of the [2+1] cycloadduct is reasonable given that the addition of 2,6-dimethylphenyl isocyanide to disilene **1.4** produced iminodisilirane **7.21** as a stable product.



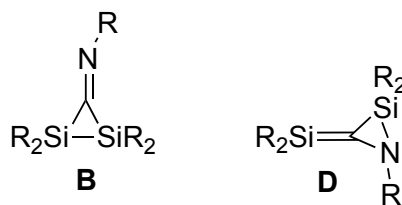
Scheme 7.14

Migration of a silyl group from the iminic carbon to the iminic nitrogen gives the 4-membered ring, **C**. The calculated ^{29}Si NMR shifts of **C** are 27 and -43 ppm, while the ^{13}C NMR shift of the carbenic-like carbon is at 350 ppm. For **C**, one of the ^{29}Si NMR shifts and the ^{13}C chemical shift are quite deshielded and are not consistent with the observed chemical shifts of **7.20**.

Isomerization of **C** to form silaaziridine **D** with an exocyclic Si=C double bond gives a structure analogous to that observed by Scheschkewitz (**7.1a**).¹³ The addition of a second *t*-butyl isocyanide to the Si=C of **D** gives **F**. Another 1,2-silyl shift transforms **F** to **G** which, after a 1,2-N shift, gives the final product **7.19**. The calculated ^{29}Si chemical shifts of **G** are 24 and -77 ppm, while the ^{13}C chemical shift of the carbenic carbon is at 71 ppm.

Upon comparison of the ^{13}C and ^{29}Si NMR chemical shifts of compound **7.20** with the shifts of those calculated for **A**, **B**, **C**, **D** and **G**; we see there is excellent agreement between the observed signal for the iminic carbon at 197 ppm as well as for the ^{29}Si shifts at -53 and -64 ppm with the values calculated for compound **B**; ^{29}Si shifts at -61 and -75 ppm, ^{13}C shift of the iminic carbon at 193 ppm. On the basis of the similarity of the calculated and experimentally observed chemical shifts, the structure of the **7.20** was assigned as the three-membered ring iminodisilirane **B**. Thus, the addition of *t*-butyl isocyanide to disilene **1.4** appears to be completely analogous to that observed by Scheschkewitz's and West's up to the formation of disilaziridine **B**. However, in our system, a second equivalent of *t*-butyl isocyanide appears to add to the Si=C bond, presumably the weakest bond in the molecule. Subsequent migration of the C-N bond is apparently preferred over migration of C-Si bond in compound **G** to form **7.19**. Selective migration of the C-N bond is likely because the lone pair on the nitrogen effectively overlaps with the empty p orbital at the carbenic carbon.

It is interesting to compare the reactivity of different disilenes towards isocyanides (Table 7.1).

Table 7.1: Summary of the reactivity of disilenes towards isocyanides

Disilene	Mes ₂ Si=SiMes ₂	Xyl ₂ Si=SiXyl ₂ ¹⁰	Tip ₂ Si=SiTip ₂ ¹³	Tip ₂ Si=Ph(Tip) ¹³	R ^H ₂ Si=Si(<i>t</i> -Bu)R ^{Ar15}
RNC	(This work)			Tip ₂ Si=Tip(TMOP) ¹⁴	
XylNC	Structure B isolated. Unstable, evidence of 2:1 adduct between disilene and XylNC.	Structure B isolated. Unstable, forms another unidentified compound after some time.	-	-	Structure B isolated and rearranges to D .
<i>t</i> -BuNC 1eq.	Structure B as an intermediate.	-	No reaction.	Addition of one equivalent forming B then rearranges to D . Heating D forms an unidentified compound in the absence of a scavenger.	-
<i>t</i> -BuNC 2eq.	Butterfly adduct 7.19 .	-	-	-	-

The steric bulk of the substituents on both the isocyanide and the disilene has a substantial effect on the observed reaction pathway. Increasing the steric bulk of the substituent on the isocyanide (2,6-dimethylphenyl isocyanide in contrast to *t*-butyl isocyanide) to the same disilene enables the isolation of the [2+1] cycloadduct **B**. For example, **7.20**, with a *t*-butyl substituent on the isocyanide moiety, could not be isolated while **7.21**, with a 2,6-dimethylphenyl substituent on

the isocyanide moiety, was isolated when the corresponding isocyanides were added to the same disilene, **1.4**.

On the other hand, increasing the bulk on the disilene may hinder the reaction completely or enable isolation of initially formed adduct **B**. For example, keeping the bulk of the isocyanide constant (i.e. *t*-BuNC), Tip₂Si=SiTip₂ does not react and (*t*-Bu₃Si)PhSi=SiPh(Si*t*-Bu₃) allows the formation of an isolable adduct.¹¹ When the steric bulk is reduced for example in Mes₂Si=SiMes₂, Tip₂Si=Si(Tip)Ph, Tip₂Si=Si(Tip)TMOP or R^H₂Si=Si(*t*-Bu)R^{Ar} the iminodisilirane **B**, is only observed as an intermediate. Finally, if the substituents on both the disilene and the isocyanide are small (i.e. Mes and *t*-butyl, respectively), two equivalents of the isocyanide adds to the disilene and enables the isolation of the 2:1 adduct, **7.19**.

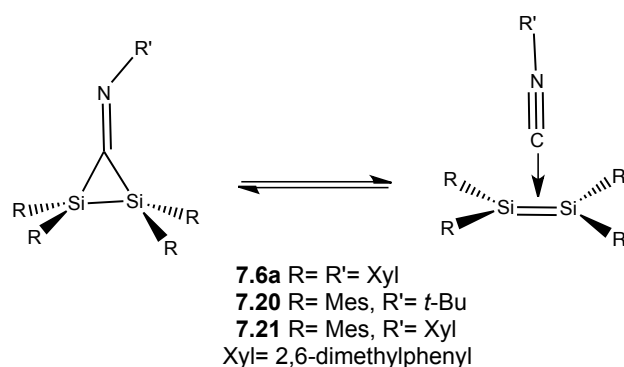
Scheschkewitz reported that heating an analogue of **D** (**7.7a**) released the free *t*-butyl isocyanide, which then reacted with another equivalent of **D** forming unidentified product.¹³ West reported that **7.6a** decolourized over a period of time to an unidentified compound,¹⁰ and we also observed decolourization of **7.21**. However, in our case, we were able to identify the compound by mass spectrometry as the 2:1 adduct between 2,6-dimethylphenyl isocyanide and disilene **1.4** or by X-ray crystallography as **7.19**, the butterfly adduct. Taking into consideration our results, we postulate that the instability of iminodisilirane **7.6a** and **7.21** and of silaazaridene **7.7a** are due to subsequent reactions to give structures analogous to **7.19**, the butterfly adduct.

Thus, depending on the of steric bulk of the substituents on the disilene and the isocyanide, compound **B** may be isolated or rearrange to **D** and **D** may react with a second equivalent of isocyanide to give a stable adduct. Presumably, the energy of **D** is lower than that of **B**. Iwamoto calculated the energies of **B** and **D** with methyl groups as substituents. The rearrangement to **D** was calculated to be endothermic with the energy of **D** being higher than that

of **B** by 21.5 kJ/mol;¹⁵ however, with methyl groups on the disilene and the isocyanide, the steric interactions would be diminished and reflected in the calculated values of the energies.

Notably, a structure similar to **A** has never been isolated or observed in the chemistry of disilene and isocyanide. The energy of **A** at the M06/6-311+G* level of theory was calculated and was found to be lower than the energy of the individual reactants, disilene **1.4** and *t*-butyl isocyanide by -15.6 kJ/mol. Nguyen³⁵, Scheschkewitz¹³ and Iwamoto¹⁵ have also considered intermediates such as **A**; however, given the lack of any experimental evidence for the presence of such a complex, they may not exist as discrete intermediates.

The unusual difference in the ²⁹Si chemical shifts of **7.20** and **7.21/7.6** is not completely understood. The ²⁹Si chemical shifts of compound **7.20** are very shielded at -53 and -64 ppm while the ²⁹Si chemical shift for compounds **7.6** and **7.21** are deshielded at 37 ppm. The effect of the substituent on the isocyanide clearly has a significant influence. West postulated a π -complex structure for **7.6a** rather than the covalent three-membered ring (Scheme 7.15). Interestingly, the geometry around each silicon in **7.21** is quite planar; the sum of the angles around Si1 is nearly 360° (356.93°) and around Si2 is 354.98° (Figure 7.4). The geometries around the silicons in **7.21** are very similar to the geometry around silicons in the free disilene **1.4** (356.3).⁴⁰ The geometry about silicon in a metallacycle (the formal 3-membered iminodisilirane) are expected to be significantly different.^{3c} It is possible that compound **7.21** exists in dynamic equilibrium between the π complex and the iminodisilirane and the π -complex structure dominates in solution while the cyclic structure dominates in solid state (Scheme 7.15).



Scheme 7.15

The π -character in the Si-Si double bond is expected to greatly deshield the ^{29}Si chemical shifts, and therefore, ^{29}Si chemical shifts of 37 ppm would be reasonable. Furthermore, the observation of one chemical shift for **7.21** is also consistent with a π -complex. In contrast, compound **7.20** may exist as the cyclic (iminodisilirane) exclusively, rather than the π -complex, and therefore, exhibit shielded ^{29}Si chemical shifts.

The π -complex character of disilenes in transition metals complexes is known.^{3c} There is a continuum between the π -complex and metallacycle structure which depends on the nature of the ligand on the metal.³⁶ We calculated the ^{29}Si chemical shifts for **7.21** and **7.6a**, (-48.5, -69.6 ppm) and (-55, -69 ppm) and found that they are significantly different from the observed ^{29}Si chemical shifts (both at 37 ppm). Taking into consideration that the calculated structures were optimized from the crystal structure data for **7.21**, the calculated structure may have minimized to the iminodisilirane structure as a local minimum with shielded ^{29}Si chemical shift values. However, in solution, the π -complex may be a better description of the bonding of **7.21**. Although many π -complexes of disilenes with transition metals such as Pd, Hf, Zr, Mo and W, have been reported,^{3c} or with oxygen³⁷ and sulphur³⁸, to the best of our knowledge, **7.21**, along with West's **7.6a**, are the only examples of π -complex of disilene with organic molecule.

The reactivity of isocyanides toward the Si(100)- 2×1 surface revealed the formation of **7.4**, which is similar in structure to **7.20** and **7.21**. Our results further support the formation of the iminodisilirane on the surface. A computational study determined that the strain enthalpy of formation of the three-membered ring disilirane (CSi_2H_6) is 155 kJ mol^{-1} whereas the strain enthalpy of formation of digermirane 164 J mol^{-1} for (CGe_2H_6),³⁹ and therefore, it is not surprising that the formation of iminodisiliranenes has been observed frequently in disilene chemistry, whereas, the analogous structures have not observed in the digemene chemistry.

7.4 Conclusions

In conclusion, digermene **1.2** reacts with benzyl isocyanide to form the C-N bond activation product, 2-benzyl-1,1,2,2-tetraimesityldigermyl nitrile. In the presence of the bulkier 2,6-dimethylphenyl or *t*-butyl isocyanide, the conversion of digermene **1.2** to cyclotrigermane **7.9** is accelerated. The observed results can be understood in terms of an initial coordination of the isocyanide to the digermene **1.2** to give a donor complex **7.10** (Scheme 7.10). If the isocyanide substituent is small, activation of the C-N bond occurs. Alternatively, if the isocyanide substituent is large, dissociation occurs to give the germylene-isocyanide coordination complex and free germylene, which undergoes subsequent reaction accelerating the conversion of digermene **1.2** to cyclotrigermane **7.9** where bulky isocyanide act as catalyst.

While one equivalent of *t*-butyl isocyanide or 2,6-dimethylphenyl isocyanide adds to disilene **1.4** to give the [2+1] cycloadduct, the addition of two equivalents of *t*-butyl isocyanide yields the novel double enamine cycloadduct **7.19**. Our results, in addition to the results of Scheschkewitz¹³, Nguyen³⁵ and Iwamoto,¹⁵ now gives a coherent understanding of the reactivity of disilenes towards isocyanides. The investigation of the reactivity of ditetrelenes towards isocyanides has contributed to understanding the influence of Lewis bases on ditetrelene

chemistry. The results of these experiments suggest that electron donors may have a much larger effect on the reactivity of digermenes in comparison to disilenes chemistry.

7.5 Experimental

General Experimental

All experiments were carried out under an atmosphere of argon or nitrogen using standard Schlenk techniques or a glove box. THF was purified by passage through a column of alumina and was degassed and stored over 4 Å molecular sieves prior to use. C₆D₆ was distilled from lithium aluminum hydride, degassed and stored over 4 Å molecular sieves prior to use. THF-*d*₈ was stored over 4 Å molecular sieves. Liquid isocyanides were degassed and stored over 4 Å molecular sieves prior to use. Ge₃Mes₆^{17b} and (Me₃Si)₂SiMes₂⁴⁰ were synthesized according to the literature procedures. All other chemicals were purchased from commercial sources and used without further purification, except as noted above. NMR spectra were recorded on a Varian Inova 400 or Inova 600 MHz NMR spectrometer using C₆D₆ or THF-*d*₈ as the solvent. The NMR standards used are as follows: ¹H NMR spectra were referenced to residual C₆D₅H (7.15 ppm) or THF-*d*₇H (3.58 ppm); ¹³C NMR spectra were referenced to the central transition of C₆D₆ (128.00 ppm). Representative example of NMR characterization of new compounds (compound **7.8**) is presented in Appendix 1. FTIR spectra were recorded as thin films using a Bruker Tensor 27 Spectrometer (resolution of 4 cm⁻¹). ESI-TOF mass spectra were obtained using a Micromass LCT instrument.

The Addition of Benzyl Isocyanide to Digermene 1.2

Ge₃Mes₆ (100 mg, 0.107 mmol) was placed in a quartz tube^a and dissolved in THF (5 mL) and then irradiated ($\lambda = 350$ nm) in a quartz Dewar^a at -60 °C for ~18 h to give a yellow solution. The

^a A quartz tube and Dewar were used but a Pyrex Dewar also can be used.

bright yellow solution of digermene **1.2** (0.084 mol) was transferred to a round-bottomed flask. Additional THF was added (5.0 mL) followed by a THF solution of benzyl isocyanide (1.05 mL, 0.082 M, 0.086 mmol). After stirring for 30 minutes at room temperature the solution became dark orange. The solution was stirred overnight. The THF was then removed under vacuum and a pale pink, sticky solid was obtained. Product **7.8** was purified by crystallization from saturated solution of hexanes at -22 °C to give **7.8** as a white solid (14 mg, 23%). **7.8** ¹H NMR (C₆D₆, 600 MHz) δ 7.25- 6.98 (m, 2H, Ph *o*-H), 6.95- 6.87 (m, 3H, Ph *m*- and *p*-H), 6.61 (s, 8H, Mes *m*-H), 3.63 (br s, 2H, CH₂), 2.33 (s, 12H, Mes *o*-CH₃), 2.24 (br s, 12H, Mes *o*-CH₃)^b, 2.05, 2.04 (each s, 12 H total Mes *p*-CH₃); ¹³C NMR (C₆D₆, 100 MHz) δ 143.93 (br s, Mes *o*-C), 143.44 (Mes *o*-C), 139.72 (Ph *i*-C), 139.17 (Mes *p*-C), 138.66 (Mes *p*-C), 136.15 (Mes *i*-C), 134.36 (Mes *i*-C), 130.16 (CN), 130.02 (Ph *m*-CH), 129.93 (Mes *m*-CH), 129.90 (Mes *m*-CH), 127.8^c (Ph *p*-CH), 125.31 (Ph *o*-CH), 31.84 (br s, CH₂), 25.73 (br s, Mes *o*-CH₃), 25.15 (br s, Mes *o*-CH₃), 20.86 (Mes *p*-CH₃), 20.83 (Mes *p*-CH₃); FTIR (thin film, cm⁻¹) 3016 (s), 2922 (s), 2855 (s), 2168 (w), 1601 (s), 1556 (m), 1451 (s), 1405 (m), 1378 (m), 1289 (m), 1216 (m), 1029 (m), 848 (s), 758 (s), 698 (m); high resolution ESI-MS for C₄₄H₅₁⁷⁰Ge₂NNa calcd.: 756.2388, found: 756.2404.

Thermal Stability of **7.8**

7.8 (13 mg, 0.017 mmol) was dissolved in THF-*d*₈ in a J. Young tube and excess DMB (4 drops) was added to the solution. The J. Young tube was placed in an oil bath at 100 °C for 20 hours. The solution was allowed to cool to room temperature and then analyzed by ¹H NMR spectroscopy. **7.8** appeared unchanged. The J. Young tube was subsequently placed in an oil bath at 145 °C for 18.5 hours. After cooling to room temperature, the solution was analyzed by ¹H

^b ¹H NMR δ 2.24 (Mes *o*-CH₃); ¹³C NMR δ 143.93 (Mes *o*-C), 136.15 (Mes *i*-C) have been tentatively assigned to the mesityl groups closest to the phenyl ring based on ¹H-¹³C gHMBC correlations to the broad ¹H signal at 2.24 ppm.

^c Chemical shift extracted from the ¹H-¹³C gHSQC spectrum

NMR spectroscopy; once again, **7.8** appeared unchanged. The THF-*d*₈ and excess DMB were then removed from the solution under vacuum and the white solid was redissolved in C₆D₆. In addition to the signals assigned to **7.8**, a number of signals were observed from 1.72 – 1.85 ppm inferring some decomposition. The mixture was separated by preparative TLC (silica gel, 1:1 CH₂Cl₂-hexanes). **7.8** was recovered as a colourless solid.

The Addition of 2,6-Dimethylphenyl Isocyanide to Digermene 1.2

Mes₆Ge₃ (49 mg, 0.053 mmol) was dissolved in THF (4.0 mL) and irradiated at -40 °C overnight in a Pyrex Schlenk tube. The bright yellow solution of tetramesityldigermene (0.079 mmol) was transferred to a round-bottomed flask. Additional THF was added (4.0 mL) followed by a THF solution of 2,6-dimethylphenyl isocyanide (1.03 mL, 0.076 M, 0.079 mmol). The solution was stirred at room temperature and monitored by ¹H NMR spectroscopy. After five days, the ratio of **1.2:7.9** was determined to be ~1.0:14 by integration of the signals at 6.71 ppm (**1.2**, 8H) and 6.67 ppm (**7.9**, 12H) in C₆D₆.

Monitoring the Conversion of Digermene 1.2 to 7.9 in the Presence of 2,6-Dimethylphenyl Isocyanide

Mes₆Ge₃ (35 mg, 0.037 mmol) was dissolved in THF-*d*₈ (1.4 mL) and irradiated at -40 °C overnight in a Pyrex Schlenk tube. The bright yellow solution of **1.2** (0.056 mmol) was divided equally and transferred to two NMR tubes (0.028 mmol of **1.2** in each tube). A THF-*d*₈ solution of 2,6-dimethylphenyl isocyanide was added (0.30 mL, 0.076 M, 0.023 mmol) to one of the NMR tubes. The reactions were monitored using ¹H NMR spectroscopy. The ratio of **1.2: 7.9** was determined at intervals by integration of the signals at 6.75 ppm (**1.2**, 8H) and 6.64 ppm (**7.9**, 12H) in THF-*d*₈. The THF-*d*₇H signal at 3.58 ppm was used as an internal standard. After six days, the THF-*d*₈ was removed and the mixture was redissolved in C₆D₆. The ratio of **1.2: 7.9** was determined to be ~1.0:3.1 by integration of the signals at 6.71 ppm (**1.2**, 8H) and 6.67 ppm (**7.9**, 12H).

The Addition of 2,6-Dimethylphenyl Isocyanide to Digermene 1.2 in the Presence of DMB

Mes₆Ge₃ (25 mg, 0.026 mmol) was dissolved in THF (2.2 mL) and irradiated at -40 °C overnight in a Pyrex Schlenk tube. The bright yellow solution of **1.2** (0.035 mmol) was transferred to a round-bottomed flask. Additional THF was added (2.0 mL) followed by a THF solution of 2,6-dimethylphenyl isocyanide (0.46 mL, 0.076 M, 0.035 mmol) and excess DMB (0.40 mL, 100 eq.). After stirring at room temperature for 21.5 hours, an aliquot was removed and examined by ¹H NMR spectroscopy. The ratio of **7.17**:**7.18** was determined to be ~1.0: 2.2 by integration of the signals at 1.65 ppm (**7.17**, 6H) and 1.73 ppm (**7.18**, 6H) in C₆D₆.

The Addition of *t*-Butyl Isocyanide to Digermene 1.2

Mes₆Ge₃ (55 mg, 0.059 mmol) was dissolved in THF (5.0 mL) and irradiated at -40 °C overnight in a Pyrex Schlenk tube. The bright yellow solution of **1.2** (0.088 mmol) was transferred to a round-bottomed flask. Additional THF was added (5.0 mL) followed by a THF solution of *t*-butyl isocyanide (1.00 mL, 0.088 M, 0.088 mmol). The solution was stirred at room temperature and monitored by ¹H NMR spectroscopy. After four days, the ratio of **1.2**: **7.9** was determined to be ~1.0:4.2 by integration of the signals at 6.71 ppm (**1.2**, 8H) and 6.67 ppm (**7.9**, 12H) in C₆D₆.

The Addition of Excess *t*-Butyl Isocyanide to Digermene 1.2

Mes₆Ge₃ (55 mg, 0.059 mmol) was dissolved in THF (5.0 mL) and irradiated at -40 °C overnight in a Pyrex Schlenk tube. The bright yellow solution of **1.2** (0.088 mmol) was transferred to a round-bottomed flask. Additional THF was added (5.0 mL) followed by a 5 equivalents of *t*-butyl isocyanide (5.00 mL, 0.44 M, 0.44 mmol). The solution was stirred at room temperature and monitored by ¹H NMR spectroscopy. The ¹H NMR spectrum of the crude solution revealed broad signals of Ge₃Mes₆ plus some low intensity signals. Mass spectrometry revealed a signal which was assigned to the 1:1 adduct between digermene **1.2** and *t*-butyl isocyanide (ESI-TOF) for C₄₁H₅₃⁷⁰Ge₂N+H calcd.: 700.2747, found: 700.2741. The low intensity signals disappeared after few days; only Ge₃Mes₆ was recovered after a week as determined by ¹H NMR spectroscopy.

Addition of 1 Equivalent of *t*-Butyl Isocyanide to Disilene 1.4

Mes₂Si(SiMe₃)₂ (100 mg, 0.24 mmol) was placed in a quartz tube and dissolved in hexanes (3 mL) and the solution was irradiated ($\lambda = 254$ nm) in a quartz Dewar for ~18 h. The yellow solution was cooled to -60 °C during the irradiation by circulating cold methanol through the quartz Dewar. One equivalent of *t*-butyl isocyanide (52 mg, 3 mmol) was added to the yellow solution at room temperature; the colour of the solution immediately changed to deep orange. The hexanes were evaporated giving a deep orange oil. Compound **7.20** transformed within 30 min to a mixture of a disilene **1.4** and **7.19** in a 2:1 ratio at room temperature. **7.20** (50 mg, 68%). ¹H NMR (C₆D₆, 600 MHz, 25 °C) δ 6.67 (s, 4H, Mes *m*-H), 6.61 (s, 4H, Mes *m*-H), 2.72 (br s, 12H, Mes *o*-CH₃), 2.26 (br s, 12H, Mes *o*-CH₃), 2.04 (s, 6H, Mes *p*-CH₃), 2.01 (s, 6H, Mes *p*-CH₃), 1.37 (s, 9H, *t*-but); ¹³C NMR (C₆D₆, 150 MHz) δ 197.64 (C=N), 146.00 (Mes *o*-C), 145.97 (Mes *o*-C), 144.58 (Mes *o*-C), 144.55 (Mes *o*-C), 139.01 (Mes *p*-C), 138.98 (Mes *p*-C), 138.94 (Mes *p*-C), 132.76 (Mes *i*-C), 132.75 (Mes *i*-C), 131.34 (Mes *i*-C), 131.30 (Mes *i*-C), 129.15 (Mes *m*-CH), 128.85 (Mes *m*-CH), 64.30 (C(CH₃)₃), 28.91 ((CH₃)₃), 25.49 (Mes *o*-CH₃), 25.39 (Mes *o*-CH₃), 21.08 (Mes *p*-CH₃), 21.06 (Mes *p*-CH₃), ²⁹Si NMR (C₆D₆, 119 MHz) -53.3, -64.1 ppm.

Addition of 2 Equivalents *t*-Butyl Isocyanide to Disilene 1.4

Mes₂Si(SiMe₃)₂ (100 mg, 0.24 mmol) was placed in a quartz tube and dissolved in hexanes (3 mL) and the solution was irradiated ($\lambda = 254$ nm) in a quartz Dewar for ~18 h. The yellow solution was cooled to -60 °C during the irradiation by circulating cold methanol through the quartz Dewar. Two equivalent of *t*-butyl isocyanide (100 mg, 6 mmol) was added to the yellow solution at room temperature; the colour of the solution immediately changed to pale yellow. The hexanes were evaporated giving a pale yellow orange oil which was redissolved in a minimal amount of hexanes. The flask was placed in a freezer (-20 °C) for 24 h. A precipitate formed and

the solid was isolated by decantation. The solid was triturated with hexanes yielding colourless, clear crystals of **7.19** (50 mg, 60%) ^1H NMR (C_6D_6 , 600 MHz, 25 °C) δ 6.95 (s, 2H, Mes *m*-H), 6.69 (s, 2H, Mes *m*-H), 6.57, 6.56 (each s, 2H, Mes *m*-H), 3.06 (br s, 6H, Mes *o*-CH₃), 2.25, 2.23, 2.23 (each s, 6H, Mes *o*-CH₃), 2.16 (s, 6H, Mes *p*-CH₃), 1.96 (s, 6H, Mes *p*-CH₃), 1.50 (s, 18H, *t*-but); ^{13}C NMR (C_6D_6 , 150 MHz) δ 178.21 (=CN₂), 145.86 (Mes *o*-C), 142.56 (Mes *o*-C), 141.38 (Mes *o*-C), 139.48 (Mes *p*-C), 137.81 (Mes *p*-C), 137.22 (Mes *i*-C), 133.04 (Mes *i*-C), 130.04 (Mes *m*-CH), 129.30 (Mes *m*-CH), 128.99 (Mes *m*-CH), 86.77 (=CSi₂), 53.58 (CCH₃), 31.84 ((CH₃)₃), 30.04 (Mes *o*-CH₃), 25.38 (Mes *p*-CH₃), 22.25 (Mes *o*-CH₃), 20.97 (Mes *p*-CH₃) ^{29}Si NMR (C_6D_6 , 119 MHz) δ -12 ppm; high resolution ESI-MS *m/z* for C₄₆H₆₂Si₂+H calc. 699.4530 found 699.4543.

Addition of 2,6-Dimethylphenyl Isocyanide to Disilene 1.4

Mes₂Si(SiMe₃)₂ (100 mg, 0.24 mmol) was placed in a quartz tube and dissolved in hexanes (3 mL) and the solution was irradiated ($\lambda = 254$ nm) in a quartz Dewar for ~18 h. The yellow solution was cooled to -60 °C during the irradiation by circulating cold methanol through the quartz Dewar. 2,6-Dimethylphenyl isocyanide (20 mg, 0.2 mmol) was added to the yellow solution at room temperature the colour of the solution immediately changed to deep red. The hexanes were evaporated giving a deep red oil. **7.21** (70 mg, 76%). ^1H NMR (C_6D_6 , 600 MHz, 70 °C) δ 6.8-6.84 (m, *m*-CH₃-Ph), 6.73-6.7 (m, *p*-CH₃-Ph), 6.66 (s, 8H, Mes *m*-H), 2.35 (br s, 24H, Mes *o*-CH₃), 2.06 (s, 12H, Mes *p*-CH₃), 1.7 (s, 6H, CH₃, CH₃-Ph I); ^{13}C NMR (C_6D_6 , 150 MHz) δ 215.18 (C=N), 155.43 (*i*-C, CH₃-Ph), 145.85 (Mes *o*-C), 139.52 (Mes *p*-C), 132.5 (Mes *i*-C)^d, 128.86 (Mes *m*-CH), 128.28 (*m*-CH), 125.28 (*o*-C, CH₃-Ph), 123.43 (*o*-C, CH₃-Ph), 24.73 (Mes *o*-CH₃), 21.00 (Mes *p*-CH₃), 18.12 (*o*-CH₃); ^{29}Si NMR (C_6D_6) 37 ppm. After 4 days, a yellow

^d Chemical shift extracted from the ^1H - ^{13}C gHMBC spectrum

powder was obtained after evaporating the solvent; high resolution ESI-MS m/z for $C_{54}H_{62}N_2Si_2+H$ calc. 795.4529 found 795.4507.

Computational Details for Calculating the Relative Energies

All calculations were performed using Gaussian 09⁴¹ on the Shared Hierarchical Academic Research Computing Network (SHARCNET, www.sharcnet.ca). Computations were run using two AMD Opteron 2.2 GHz 24 core CPUs with 32 GB of memory. Initial optimization was performed from crystal structures. Optimization was initially performed at the Opt=Loose level until convergence was achieved, upon which the default optimization restraints were used. All optimization and frequency calculations were performed at the B3LYP level of theory,⁴² using the 6-31G* basis set, and an ultra fine integration grid. Molecular orbital and single-point energy calculations were performed using the normal population method, using the M06 functional,⁴³ and the 6-311+G* basis set and using an ultra fine integration grid.

Computational Details for Calculating the Chemical Shifts

All quantum chemical calculations were carried out using the Gaussian09 package.⁴¹ The molecular structure optimizations were performed using the M06-2X functional⁴⁴ along with the 6-311+G(d,p) basis set. Every stationary point was identified by a subsequent frequency calculation either as minimum (Number of imaginary frequencies (NIMAG): 0) or transition state (NIMAG: 1). NMR chemical shift computations were performed using the GIAO method as implemented in Gaussian 09 and the M06-L functional along with the 6-311G(2d,p) basis set for molecular structures obtained at the M06-2X/6-311+G(d,p) level of theory.⁴³ The obtained

absolute shieldings $\sigma(29\text{Si})$ were transferred to the chemical shift δ -scale by using the absolute shielding of tetramethylsilane calculated at the same level of theory ($\sigma(29\text{Si}) = 362.2$).

Crystallographic Details

Data Collection and Processing. The sample was mounted on a Mitegen polyimide micromount with a small amount of Paratone N oil. All X-ray measurements were made on a Bruker Kappa Axis Apex2 diffractometer or Nonius Bruker KappaCCD Apex2 diffractometer for **7.21** at a temperature of 110 K. The frame integration was performed using SAINT.⁴⁵ The resulting raw data was scaled and absorption corrected using a multi-scan averaging of symmetry equivalent data using SADABS.⁴⁶

Structure Solution and Refinement. The structure was solved by using a dual space methodology using the SHELXT program.⁴⁷ All non-hydrogen atoms were obtained from the initial solution. The hydrogen atoms were introduced at idealized positions and were allowed to ride on the parent atom. The structural model was fit to the data using full matrix least-squares based on F^2 . The hydrogen atoms were introduced at idealized positions and were treated in a mixed fashion. The calculated structure factors included corrections for anomalous dispersion from the usual tabulation. The structure was refined using the SHELXL-2014 program from the SHELXTL suite of crystallographic software.⁴⁸ Graphic plots were produced using the XP program suite.⁴⁵ For **7.8**, the C1-N1 fragment was found to be disordered, with a reverse of the atom order. The occupancy value for the main component, with C1 bound to Ge1 refined to 0.91(2). For **7.20**, all hydrogen atoms were refined isotropically, except those on C27, C44 and C45, which were allowed to ride on the parent atoms. The hydrogen atoms on C45 were treated as an idealized disordered methyl group.

Table 7.2: Crystallographic data of compounds **7.8**, **7.20** and **7.21**

Data	7.8	7.20	7.21
Formula	C ₄₄ H ₅₁ Ge ₂ N	C ₄₆ H ₆₂ N ₂ Si ₂	C ₅₄ H ₆₂ N ₂ Si ₂
Formula Weight (g/mol)	739.03	699.15	795.23
Crystal Color and Habit	colourless prism	colourless plate	red plate
Crystal System	monoclinic	triclinic	triclinic
Space Group	P 2 ₁ /n	P-1	P-1
Temperature, K	110	110	110
a, Å	15.5920(16)	12.163(5)	11.929(2)
b, Å	14.5156(14)	12.543(6)	14.425(2)
c, Å	18.1735(18)	16.006(8)	15.631(3)
α, °	90	103.178(14)	108.318(9)
β, °	114.855(4)	107.442(9)	111.719(8)
γ, °	90	108.215(11)	98.458(7)
V, Å ³	3732.2(7)	2068.9(17)	2264.0(7)
Z	4	2	2
F(000)	1544	760	856
ρ, (g/cm)	1.315	1.122	1.167
λ, Å,	1.54178	0.71073	1.54178
μ, (cm ⁻¹)	2.202	0.119	0.988
R _{merge}	0.0363	0.0828	0.0309
R ₁	0.0253	0.0430	0.0668
wR ₂	0.0659	0.0854	0.1924
R ₁ (all data)	0.0275	0.0780	0.0724
wR ₂ (all data)	0.0672	0.0939	0.1978
GOF	1.043	0.918	1.040

7.6 References

1. (a) West, R.; Fink, M. J.; Michl, J. *Science* **1981**, *214*, 1343; (b) Brook, A. G.; Abdesaken, F.; Gutekunst, B.; Gutekunst, G.; Kallury, R. K. *J. Chem. Soc. Chem. Commun.* **1981**, 191.
2. For recent accounts on various aspects of silene chemistry: (a) Ottosson, H.; Rouf, A. M., In *Science of Synthesis: Knowledge Updates*; 2011/3; M. Oestreich, Thieme, Stuttgart, 2011; ch. 4.4.25; (b) Ottosson H.; Ohshita, J. In *Science of Synthesis: Knowledge Updates*; 2011/3; M. Oestreich, Thieme, Stuttgart, 2011; ch. 4.4.26; (c) Baines, K. M. *Chem. Comm.* **2013**, *49*, 6366; (d) Ottosson H.; Eklof, A. M. *Coord. Chem. Rev.* **2008**, *252*, 1287; (e) Ottosson H.; Steel, P. G.,

- Chem. Eur. J.* **2006**, *12*, 1576; (f) Gusel'nikov, L. E. *Coord. Chem. Rev.* **2003**, *244*, 149; (g) Escudie, J.; Couret C.; Ranaivonjatovo, H. *Coord. Chem. Rev.* **1998**, *565*, 178.
3. For recent accounts on various aspects of disilene chemistry: (a) Iwamoto, T.; Ishida, S. *Struct. Bonding*, **2014**, *156*, 125; (b) Sasamori, T.; Tokitoh, N. *Bull. Chem. Soc. Jpn*, **2013**, *86*, 1005; (c) Kira, M. *Proc. Jpn. Acad. Ser. B* **2012**, *88*, 167; (d) Matsuo, T.; Kobayashi M.; Tamao, K. *Dalton Trans.* **2010**, *39*, 9203; (e) Abersfelder K.; Scheschkewitz, D. *Pure Appl. Chem.* **2010**, *82*, 595; (f) Scheschkewitz, D. *Chem. Eur. J.* **2009**, *15*, 2476; (g) Kira, M. *J. Organomet. Chem.* **2004**, *689*, 4475; (h) Weidenbruch, M. *Organometallics* **2003**, *22*, 4348.
4. For comprehensive reviews, see: (a) Okazaki, R.; West, R. *Adv. Organomet. Chem.* **1996**, *39*, 231; (b) Kira, M.; Iwamoto, T. *Adv. Organomet. Chem.* **2006**, *54*, 73; (c) Lee, V. Ya; Sekiguchi, A., In *Organometallic Compounds of Low-Coordinate Si, Ge, Sn and Pb: From Phantom Species to Stable Compounds*; Wiley, Chichester, 2010; Chapter 5.
5. For examples see: (a) Fukazawa, A.; Li, Y.; Yamaguchi, S.; Tsuji, H.; Tamao, K. *J. Am. Chem. Soc.* **2007**, *129*, 14164; (b) Tamao, K.; Kobayashi, M.; Matsuo, T.; Furukawa, S.; Tsuji, H. *Chem. Commun.* **2012**, *48*, 1030.
6. Hardwick J. A.; Baines, K. M. *Angew. Chem. Int. Ed.* **2015**, *54*, 6600.
7. Lee, V. Y.; McNeice, K.; Ito, Y.; Sekiguchi, A. *Chem. Commun.* **2011**, *47*, 3272.
8. Shong, B.; Wong, K.; Bent, S. F. *J. Am. Chem. Soc.* **2014**, *136*, 5848.
9. Shong, B.; Sandoval, T. E.; Crow, A. M. Bent, S. F. *J. Phys. Chem. Lett.* **2015**, *6*, 1037.
10. Yokelson, H. B.; Millevolte, A. J.; Haller, K. J.; West, R. *J. Chem. Soc. Chem. Commun.* **1987**, *21*, 1606.
11. Wiberg, N.; Niedermayer, W.; Polborn, K.; Mayer, P. *Chem. Eur. J.* **2002**, *8*, 2730.
12. Ohmori, Y.; Ichinohe, M.; Sekiguchi, A.; Cowley, M. J.; Huch, V.; Scheschkewitz, D. *Organometallics* **2013**, *32*, 191.

13. Majumdar, M.; Huch, V.; Bejan, I.; Meltzer, A.; Scheschkewitz, D. *Angew. Chem. Int. Ed.* **2013**, *52*, 3516.
14. Meltzer, A.; Majumdar, White, A. J. P. M.; Huch, V.; Meltzer, A.; Scheschkewitz, D. *Organometallics* **2013**, *32*, 6844.
15. Iwamoto, T.; Ohnishi, N.; Akasaka, N.; Ohno, K.; Ishida, S. *J. Am. Chem. Soc.* **2013**, *135*, 10606.
16. (a) Kugler, T.; Ziegler, C.; Göpel, W. *J. Mol. Struct.* **1993**, *293*, 257; (b) Kugler, T.; Ziegler, C.; Göpel, W. *Mater. Sci. Eng. B* **1996**, *37*, 112.
17. (a) Hardwick, J. A.; Baines, K. M. *Angew. Chem. Int. Ed.* **2015**, *54*, 6600; (b) Tashkandi, N. Y.; Parsons, F.; Guo, J.; Baines, K. M. *Angew. Chem. Int. Ed.* **2015**, *54*, 1612; (c) Hardwick, J. A.; Pavelka, L. C.; Baines, K. M. *Dalton Trans.* **2012**, *41*, 609; (d) Hurni, K. L.; Baines, K. M. *Chem. Comm.* **2011**, *47*, 8382; (e) Hurni, K. L.; Rupar, P. A.; Payne, N. C.; Baines, K. M. *Organometallics* **2007**, *26*, 5569; (f) Gottschling, S. E.; Milnes, K. K.; Jennings, M. C.; Baines, K. M. *Organometallics* **2005**, *24*, 3811; (g) Gottschling, S. E.; Jennings, M. C.; Baines, K. M. *Can. J. Chem.* **2005**, *83*, 1568; (h) Samuel, M. S.; Baines, K. M. *J. Am. Chem. Soc.* **2003**, *125*, 12702; (i) Samuel, M. S.; Jenkins, H. A.; Hughes, D. W.; Baines, K. M. *Organometallics* **2003**, *22*, 1603.
18. Pavia, D.L.; Lampman, G. M.; Kriz, G. S., *Introduction to Spectroscopy*; 3rd ed.; Thomson Learning, Inc.: Toronto, 2001.
19. Hihara, G.; Hynes C. R.; Lebuis, A. M.; Riviere-Baudet, M.; Wharf, I.; Onyszchuk, M. J. *Organomet. Chem.* **2000**, *598*, 276.
20. Rupar, P. A.; Jennings, M. C.; Baines, K. M. *Can. J. Chem.* **2007**, *85*, 141.
21. Cui, C.; Olmstead, M. M.; Fettingner, J. C.; Spikes, G. H.; Power, P. P. *J. Am. Chem. Soc.* **2005**, *127*, 17530.

22. Spikes, G. H.; Power, P. P. *Chem. Commun.* **2010**, 46, 943.
23. Peng, Y.; Wang, X.; Fettinger, J. C.; Power, P. P. *Chem. Commun.* **2007**, 46, 943.
24. Brown, Z. D.; Vasko, P.; Fettinger, J. C.; Tuononen, H. M.; Power, P. P. *J. Am. Chem. Soc.* **2012**, 134, 4045.
25. Tennent, C. L.; Jones, W. D. *Can. J. Chem.* **2005**, 83, 626.
26. Xiong, Y.; Yao, S.; Driess, M. *Chem. Eur. J.* **2009**, 15, 8542.
27. Leszczynska, K.; Abersfelder, K.; Mix, A.; Neumann, B.; Stammeler, H. G.; Cowley, M. J.; Jutzi, P.; Scheschkewitz, D. *Angew. Chem. Int. Ed.* **2012**, 51, 6785.
28. Baines, K. M.; Cooke, J. A.; Dixon, C. E.; Liu, H. W.; Netherton, M. R. *Organometallics* **1994**, 13, 631.
29. Lambert, J. B.; Zhao, Y.; Emblidge, R. W.; Salvador, L. A.; Liu, X.; So, J-H.; Chelius, E. C. *Acc. Chem. Res.* **1999**, 32, 183.
30. Rugar, P. A.; Jennings, M. C.; Ragogna, P. J.; Baines, K. M. *Organometallics* **2007**, 26, 4109.
31. Durig, J. R.; Brletic, P. A.; Church, J. S.; Li, Y. S. *J. Chem. Phys.* **1982**, 76, 2210.
32. Tao, F.; Bernasek, S. *Functionalization of Semiconductor Surfaces*; Wiley: 2012; Chapter 3.
33. Kihara, N.; Sugimoto, Y.; Endo, T. *J. Polymer Sci. A* **1999**, 37, 3079.
34. Bourque, J. L.; Tashkandi, N. Y.; Baines, K. M. *IUCrData* **2016**, 1, x160389.
35. Nguyen, M. T.; Vansweevelt, H.; Neef, A. D.; Vanquickenborne, L. G. *J. Org. Chem.* **1994**, 59, 8015.
36. Iwamoto, K.; Sekiguchi, Y.; Yoshida, N.; Kabuto, C.; Kira, M. *Dalton Trans.* **2006**, 177.
37. Yokelson, H. B.; Millevolte, A. J.; Gillette, G. R.; West, R. *J. Am. Chem. Soc.* **1987**, 109, 6865.
38. West, R.; De Young, D. J.; Haller, K. J. *J. Am. Chem. Soc.* **1985**, 107, 4942.
39. Horner, D.; Grev, R.; Schaefer, H. F. *J. Am. Chem. Soc.* **1992**, 114, 2093.

40. Fink, M. J.; Michalczyk, M. J.; Haller, K. J.; Michl, J.; West, R. *Organometallics* **1984**, *3*, 793.
41. Frisch, M. J.; Trucks, G. W.; Schlegel, H. B.; Scuseria, G.; Robb, M. A.; Cheeseman, J. R.; Scalmani, G.; Barone, V.; Mennucci, B.; Petersson, G. A.; Nakatsuji, H.; Caricato, M.; Li, X.; Hratchian, H. P.; Izmaylov, A. F.; Bloino, J.; Zheng, G.; Sonnenberg, J. L.; Hada, M.; Ehara, M.; Toyota, K.; Fukuda, R.; Hasegawa, J.; Ishida, M.; Nakajima, T.; Honda, Y.; Kitao, O.; Nakai, H.; Vreven, T.; Montgomery, J. A.; Peralta, Jr., J. E.; Ogliaro, F.; Bearpark, M.; Heyd, J. J.; Brothers, E.; Kudin, K. N.; Staroverov, V. N.; Kobayashi, R.; Normand, J.; Raghavachari, K.; Rendell, A.; Burant, J. C.; Iyengar, S. S.; Tomasi, J.; Cossi, M.; Rega, N.; Millam, M. J.; Klene, M.; Knox, J. E.; Cross, J. B.; Bakken, V.; Adamo, C.; Jaramillo, J.; Comperts, R.; Stratmann, R. E.; Yazyev, O.; Austin, A. J.; Cammi, R.; Pomelli, C.; Ochterski, J. W.; Martin, R. L.; Morokuma, K.; Zakrzewski, V. G.; Voth, G. A.; Salvador, P.; Dannenberg, J. J.; Dapprich, S.; Daniels, A. D.; Farkas, Ö.; Foresman, J. B.; Ortiz, J. V.; Cioslowski, J.; Fox, D. J. *Gaussian 09, Revision D.01*, Gaussian, Inc., Wallingford, CT, **2009**.
42. Becke, A. D. *J. Chem. Phys.* **1993**, *98*, 5648.
43. Zhao, Y.; Truhlar, D. G. *Theor. Chem. Acc.* **2008**, *120*, 215.
44. Zhao, Y.; Schultz, N. E.; Truhlar, D. G. *J. Chem. Theory Comput.* **2006**, *2*, 364.
45. Bruker-AXS, SAINT version 2013.8, **2013**, Bruker-AXS, Madison, WI 53711, USA.
46. Bruker-AXS, SADABS version 2012.1, **2012**, Bruker-AXS, Madison, WI 53711, USA.
47. Sheldrick, G. M. *Acta Cryst.* **2015**, *A71*, 3.
48. Sheldrick, G. M. *Acta Cryst.* **2008**, *A64*, 112.

Chapter 8

Summary, Conclusions and Future Directions

8.1 Summary and Conclusions

This thesis has examined the reactivity of many multiply-bonded Group 14 species with a focus on cycloaddition reactions. Two perspectives were investigated: the mechanism of the cycloaddition reactions of multiply-bonded main group compounds by use of a mechanistic probe and the reactivity studies of ditetrelenes as models of their surface dimers.

In Chapter 2, the addition of terminal alkynes to dimesitylfluorenylidienegermane, $\text{Mes}_2\text{Ge}=\text{CR}_2$ (where CR_2 =fluorenylidene), was described. The addition of terminal alkynes to dimesitylfluorenylidienegermane yielded germacyclohexenes quantitatively. The adducts arise from a [4+2] cycloaddition where the germene acts as the 4π component by the participation of the C-fluorenyl substituent in addition to the Ge=C bond. Following cycloaddition, a H-shift allowed for the re-aromatization of the fused six-membered ring. A concerted reaction pathway was proposed for the formation of the germacyclohexenes as the diagnostic ring opening of the cyclopropyl moiety did not occur ruling out the presence of a radical or cationic intermediate along the reaction pathway. The addition of ethoxyacetylene to the germene produced both a germacyclobutene and a germacyclohexene. The germacyclobutene is likely formed via a stepwise [2+2] cycloaddition through a zwitterionic intermediate. The difference in reaction rate between aromatic and aliphatic alkynes and

dimesitylfluorenyldienegermane reveals that germenes mimic carbon-based dienes in terms of their reactivity.

An investigation of the mechanism of the addition of alkynes to digermyne **1.3** was described in Chapter 3. The addition of the alkyne mechanistic probe to the digermyne yielded the 1,4-dihydro-1,4-digermine **3.5c**. Given that no ring-opening of the cyclopropyl group was observed, the reaction pathway to form the 1,4-dihydro-1,4-digermine **3.5c** does not involve a vinylic radical or cation. On this basis, it was concluded that the initial formation of a digermete does not proceed through a biradical, a possibility that had yet to be eliminated experimentally or computationally. Notably, previous computational studies (with the exception of the computational study of the addition of acetylene to a germene¹) did not examine the possibility of radical intermediates. Furthermore, the addition of a second equivalent of alkyne to the digermete also cannot proceed through a biradical. As a consequence, we have eliminated the addition of an alkyne to the digermenic moiety of the digermete as a possibility as it has been previously shown that a biradical intermediate occurs along such a reaction pathway. Our experimental work, combined with the results of computational studies on analogous systems, has provided an insightful prediction of the reaction pathway and contributes to the formulation of a coherent picture of the reactivity of alkynes towards both disilynes and digermynes.

Germenes and digermynes exhibit similar reactivity towards alkynes, both form cycloaddition products via a concerted reaction mechanism. Our results and previous studies in the area² have demonstrated that germenes and digermynes in addition to silenes, disilenes and digermenes all mimic their carbon analogues in terms of their

pericyclic reactions and suggests that the heavy Group 14 alkene and alkyne derivatives do indeed obey the Woodward-Hoffmann rules for pericyclic reactions established for carbon compounds.³

Another focus of this thesis is the utilization of ditetrelenes as effective molecular models of surface dimers as a means of providing valuable insights into the surface chemistry. In Chapters 4 and 5, the addition of a variety of nitro compounds to tetramesityldisilene and tetramesityldigermene was examined. The facile formation of the novel 1,3,2,4,5-dioxazadisilidine and -digermolidine ring systems, respectively, was observed. In general, 1,3,2,4,5-dioxazadisilolidines and -digermolidines isomerize under thermal conditions to the 1,4,2,3,5-dioxazadisilolidines and -digermolidines ring system. The 1,3,2,4,5-dioxazadisilolidine and -digermolidine systems were also found to undergo ring opening to the isomeric oxime. The addition of nitro compounds to ditetrelenes is a general reaction; the variability of products obtained from the reactions can be understood based on the nature of the substituent on the nitrogen in the starting nitro compound.

By a comparison of the reactivity of molecular disilenes and digermenes and their surface analogues towards nitro compounds, we can conclude that, indeed, tetramesityldisilene and -digermene are valuable models for the reactivity of the Si(100) or the Ge(100) surface dimers, respectively. For most the part, the chemistries are quite comparable although the apparent relative stabilities of the adducts varies. Notably, a product (the oxime isomers) was uncovered in the molecular system which had not been considered in the surface systems and implies that such compounds may also be present

on the surface. Thus, our study has provided valuable insights into the reactivity of Si(100) and Ge(100) surface dimers towards nitro compounds.

The addition of sulfonyl chlorides to tetramesityldisilene (or tetramesityldigermene) was examined and leads to the formation of a 1,2 addition product, a β -disilyl (or digermyl) halosulfinate (Chapter 6). On the other hand, benzenesulfonyl fluoride, diphenyl- and dimethylsulfone did not react with either the disilene or the digermene. The addition of diphenylphosphine oxide to tetramesityldisilene leads to the formation of a diphenyl ((disilyl)oxy)phosphine. The formation of the sulfinate compounds as well as the oxyphosphine revealed an interesting 2-electron reduction of the sulfur and phosphorus centres using ditetrelenes. The addition reactions of sulfonyl compounds illustrates the potential of ditetrelenes to serve as effective reducing agents which react rapidly, at room temperature and under mild conditions. Further studies are required to realize this potential.

In Chapter 7, a C-N bond activation product was obtained from the reaction of tetramesityldigermene with benzyl isocyanide. In the presence of the bulkier 2,6-dimethylphenyl or *t*-butyl isocyanides, the conversion of the digermene to the cyclotrigermane is accelerated. The observed results can be understood in terms of initial coordination of the isocyanide to the tetramesityldigermene to give a donor complex. If the isocyanide substituent is small, activation of the C-N bond occurs. Alternatively, if the isocyanide substituent is large, dissociation occurs to form a germylene-isocyanide coordination complex and a germylene, which undergoes subsequent reaction. While one equivalent of *t*-butyl isocyanide or 2,6-dimethylphenyl isocyanide can add to the disilene to give a [2+1] cycloadduct the addition of two equivalents of *t*-butyl isocyanide yields a

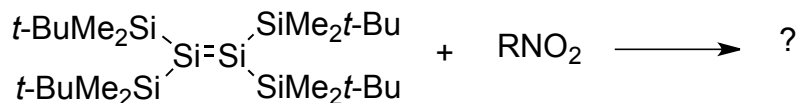
novel double enamine butterfly cycloadduct. Our work, with that of Scheschkewitz,⁴ Nguyen⁵ and Iwamoto⁶, provides a complete and comprehensive understanding of the reactivity of disilenes towards isocyanides.

Our results of the addition of unsaturated functional groups, such as nitro compounds and isocyanides, to ditetrelenes revealed the formation of unexpected compounds not previously considered by surface scientists in the addition of similar compounds to Si and Ge(100)- 2×1 surfaces. Our work emphasizes the benefits, and the necessity, of examining a research question from multiple viewpoints to reveal aspects of the science that may not be obvious. In general, the addition of nitro and sulfonyl compounds revealed interesting new chemistry including the ability of ditetrelenes to act as reducing agents. Hopefully, our work will inspire additional reactivity studies to examine the ability of ditetrelenes to serve as reducing agents for other functional groups. Furthermore, the addition of sulfonyl chlorides to ditetrelenes highlighted the important differences between alkene chemistry and ditetrelene chemistry where completely different products are possible and emphasizes the uniqueness of the chemistry of the heavier Group 14 unsaturated analogues. Indeed, by examination of the reactivity of multiple derivatives of certain class of molecules (i.e. nitro compounds, isocyanides, oxygen-containing sulfur functional groups) with ditetrelenes, the substantial effect of the substituent on the observed chemistry was revealed and a much broader and comprehensive understanding of the chemistry was obtained. We continue to investigate the cycloaddition reactions of the heavy Group 14 alkene analogues with the goal of understanding their reactivity and to develop useful applications of the chemistry of this fundamental class of molecules.

8.2 Future Work

The addition of nitro compounds to ditetrelenes proceeds via a [3+2] cycloaddition reaction followed by rearrangement and parallels the well-known Criegee mechanism for the formation of molozonides and rearrangement to ozonides.⁷ The reactivity of ozone towards ditetrelenes has not been investigated. We have carried out a preliminary study of the addition of ozone to tetramesityldisilene and tetramesityldigermene and obtained very promising results. The investigation of the addition of ozone to (di)tetrelenes will bring further insight to the potential operation of the Criegee mechanism in this chemistry.

The addition of many nitro compounds to the reconstructed Si and Ge(100)- 2×1 surfaces demonstrated the formation of the [3+2] cycloadduct as well as surface structures where the oxygen atoms of the nitro group inserted into the silicon or germanium lattice.^{8,9} In the molecular system, no migration of oxygen into the Si- or Ge-substituent bond was observed. Not surprisingly, with mesityl groups as the substituents, the insertion of oxygen into the M-C bond of the substituent is less thermodynamically favourable in comparison to the insertion of oxygen into a M-M bond. Clearly, the nature of the substituents on the molecular disilene and digermene has a major influence on the products formed. The use of a silyl-substituted disilene such as $R_2Si=SiR_2$ where $R=SiMe_2t-Bu$ ¹⁰ might facilitate the migration of oxygen into the Si-substituent bond. Indeed, in general, silyl-substituted disilenes and digermenes would be a second excellent model for the Si(100) and Ge(100) reconstructed surfaces, respectively.



Scheme 8.1

Through our investigations of the reactivity of disilenes towards diphenylphosphine oxide, it became evident that little is known about the addition of oxyphosphorus derivatives to ditetrelenes and it would be interesting to compare the reactivity of sulfonyl and phosphonyl compounds towards ditetrelenes. For example, the reactivity of arylphosphine dioxide, arylphosphinic acid and aryl phosphinic chloride toward ditetrelenes can be explored and compared to our results on the sulfur-containing derivatives.

8.3 References

1. Pavelka, L. C.; Hanson, M. A.; Staroverov, V. N.; Baines, K. M. *Can. J. Chem.* **2015**, *93*, 134.
2. Milnes, K. K.; Pavelka, L. C.; Baines, K. M. *Chem. Soc. Rev.* **2015**, *45*, 1019.
3. Lee, V. Y.; Sekiguchi, A., *Organometallic Compounds of Low-Coordinate Si, Ge, S, and Pb, From Phantom Species to Stable Compounds*; John Wiley & Sons, Ltd., Chichester, 2010; Chapter 5.
4. Majumdar, M.; Huch, V.; Bejan, I.; Meltzer, A.; Scheschkewitz, D. *Angew. Chem. Int. Ed.* **2013**, *52*, 3516.
5. Nguyen, M. T.; Vansweevelt, H.; Neef, A. D.; Vanquickenborne, L. G. *J. Org. Chem.*

1994, 59, 8015.

6. Iwamoto, T.; Ohnishi, N.; Akasaka, N.; Ohno, K.; Ishida, S. *J. Am. Chem. Soc.* **2013**, 135, 10606.

7. (a) Criegee, R. *Angew. Chem. Int. Ed.* **1975**, 14, 745; (b) Kuczkowski, R. L. *Chem. Soc. Rev.* **1992**, 21, 79.

8. (a) Eng, J.; Hubner, Jr., I. A.; Barriocanal, J.; Opila, R. L.; Doren, D. J. *J. Appl. Phys.* **2004**, 95, 1963; (b) Barriocanal, J.; Doren, D. J., *J. Phys. Chem. B* **2000**, 104, 12269.

9. (a) Shong, B.; Bent, S. *J. Phys. Chem. C* **2014**, 118, 29224; (b) Bocharov, S.; Teplyakov, A. V. *Surf. Sci.* **2004**, 573, 403; (c) Méndez De Leo, L.P.; Teplyakov, A.V. *J. Phys. Chem. B* **2006**, 110, 6899; (d) Perrine, K. A.; Leftwich, T. R.; Weiland, C. R.; Madachik, M. R.; Opila, R. L.; Teplyakov, A. V. *J. Phys. Chem. C* **2009**, 113, 6643; (e) Madachik, M. R.; Teplyakov, A. V. *J. Phys. Chem. C* **2009**, 113, 18270; (f) Leftwich, T. R.; Teplyakov, A. V. *J. Electron Spectrosc. Relat. Phenom.* **2009**, 175, 31; (g) Peng, G.; Seo, S.; Ruther, R. E.; Hamers, R. J.; Mavrikakis, M.; Evans, P. G. *J. Phys. Chem. C* **2011**, 115, 3011; (h) Madachik, M. R.; Teplyakov, A. V. *J. Phys. Chem. C* **2009**, 113, 18270.

10. Kira, M.; Iwamoto, T.; Maruyama, M.; Kuzuguchi, T.; Yin, D.; Kabuto, C.; Sakurai, H. *J. Chem. Soc. Dalton Trans.* **2002**, 1539.

Appendix 1

Illustrative Example of NMR Spectra for Characterization of New Compounds

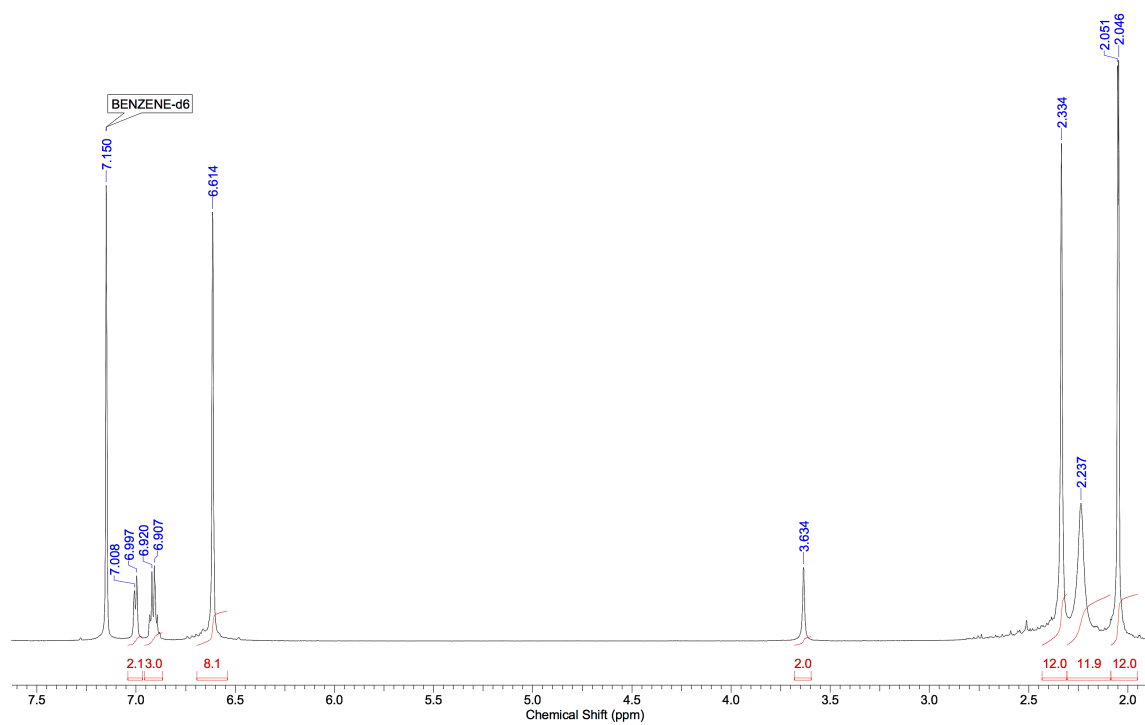


Figure A1.1 ^1H NMR spectrum of **7.8** 600 MHz in C_6D_6 .

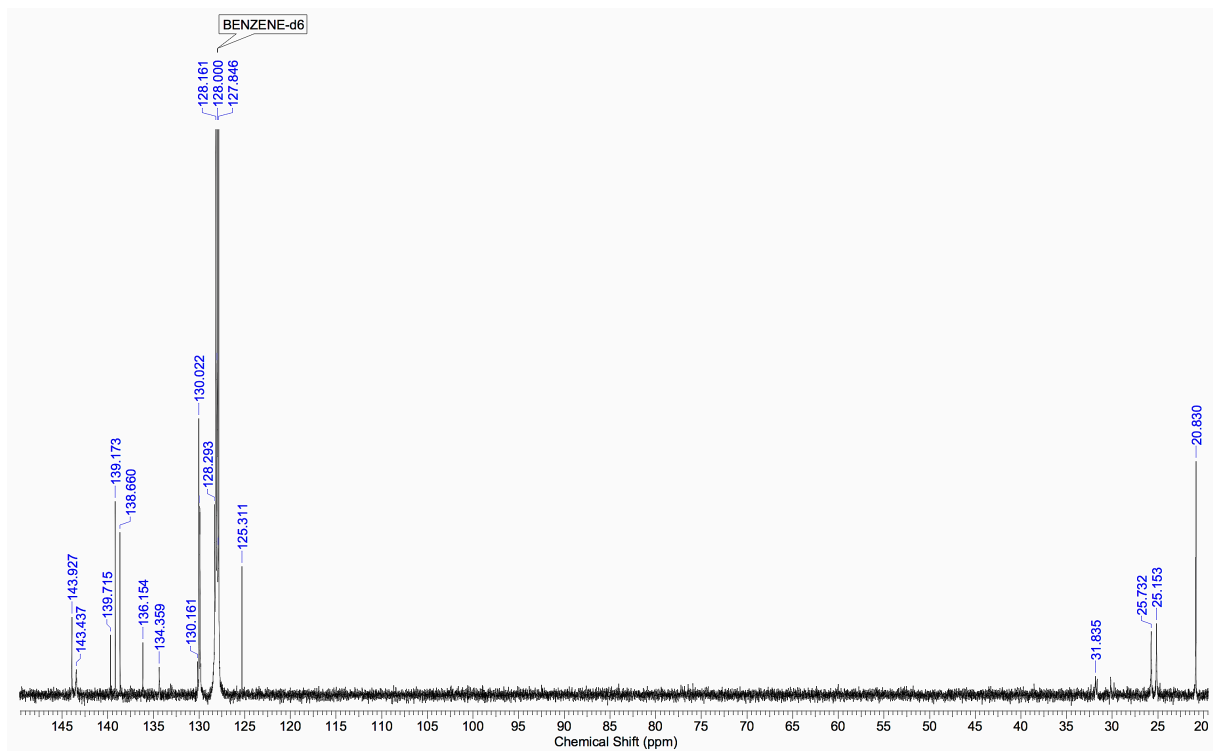


Figure A1.2 ^{13}C NMR spectrum of 7.8 100 MHz in C_6D_6 .

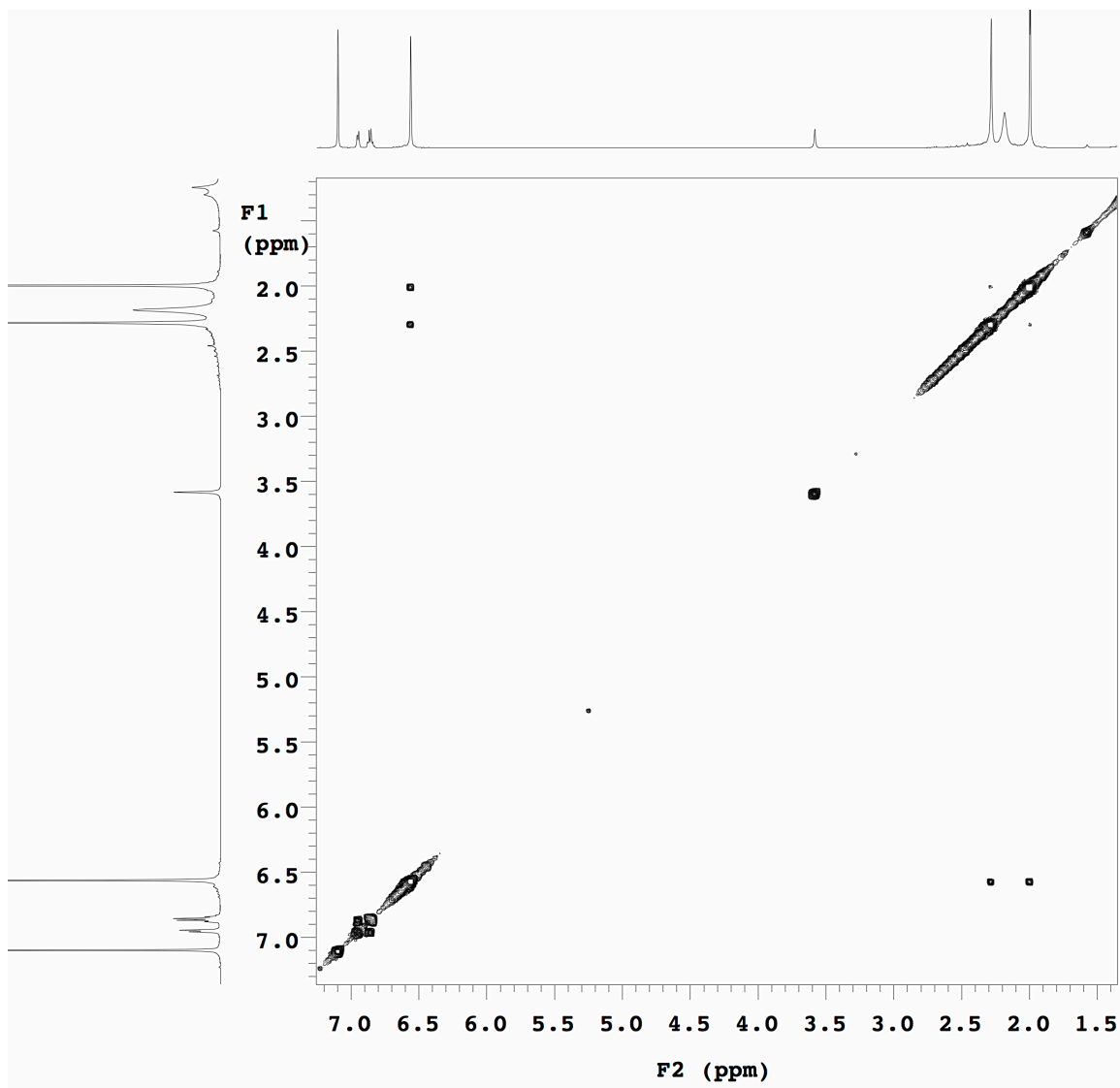


Figure A1.3 ^1H - ^1H COSY spectrum of 7.8 in C_6D_6 .

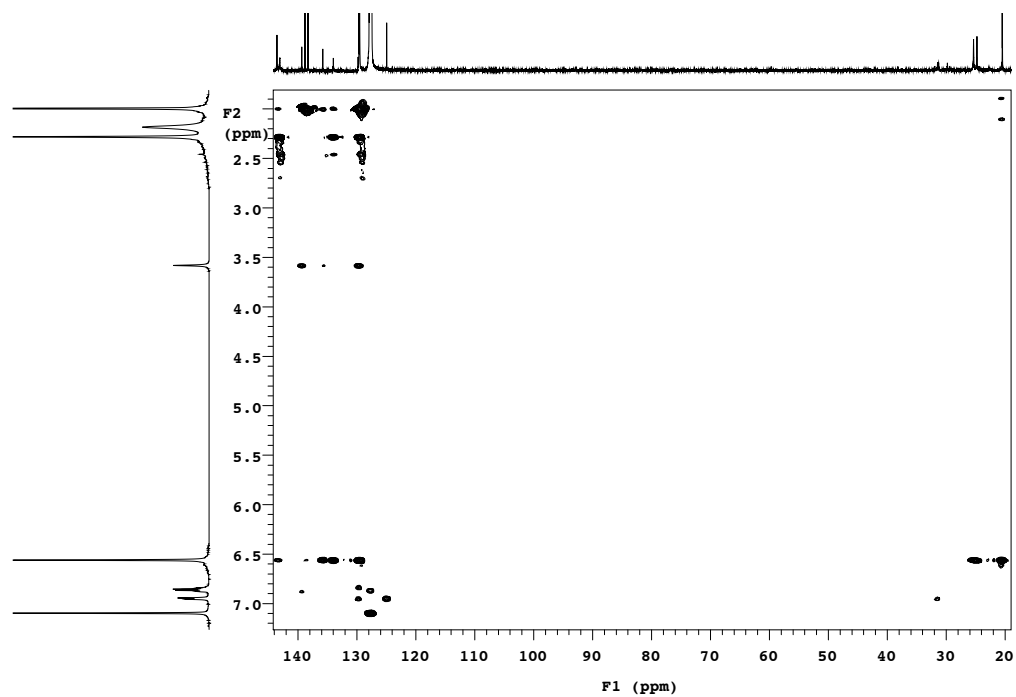


Figure A1.4 ^1H - ^{13}C gHMBC spectrum of **7.8** in C_6D_6 .

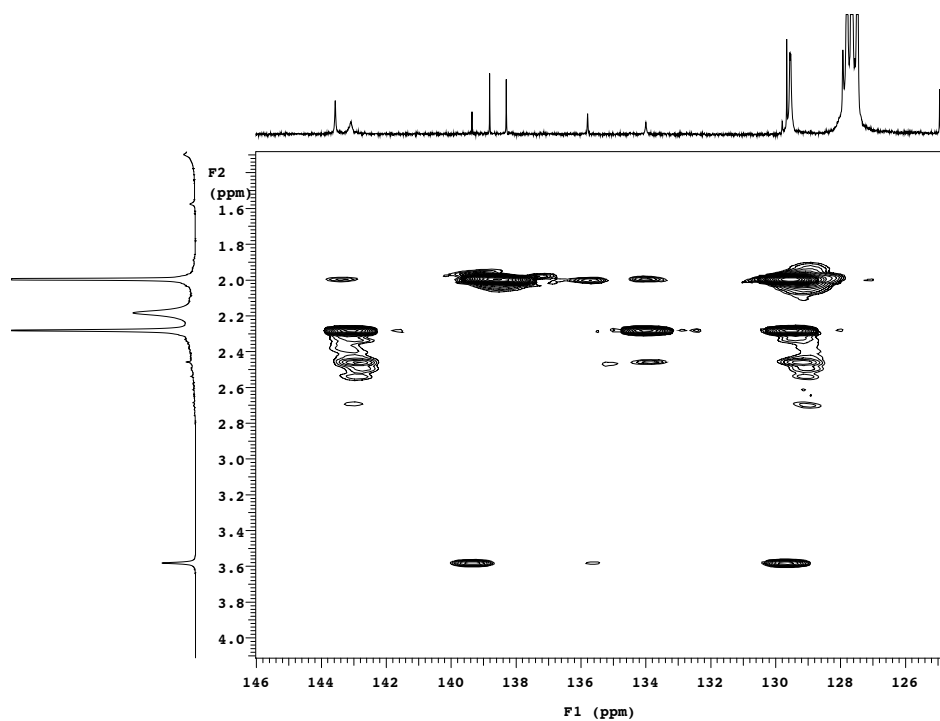


Figure A1.5 Expansion of ^1H - ^{13}C gHMBC spectrum of **7.8** in C_6D_6 .

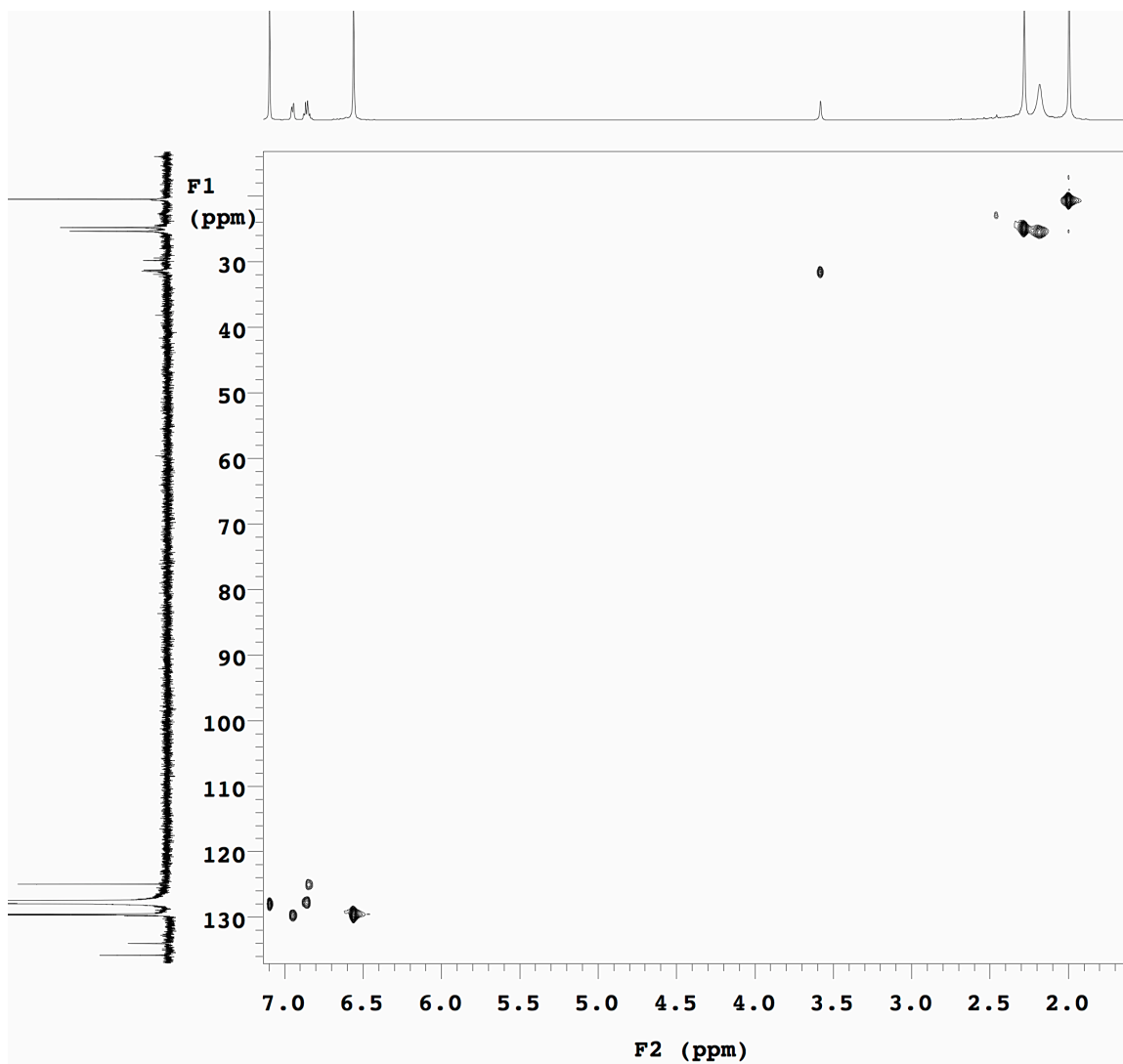


Figure A1.6 ^1H - ^{13}C gHSQC spectrum of 7.8 in C_6D_6 .

Appendix 2

Copyrighted Material and Permissions

A1 National Research Council Research Free Policy on Authors' Rights

All articles in NRC Research Press journals are copyright NRC Research Press or its licensors (see Copyright).

However, NRC Research Press recognizes the importance of sharing significant research among the scholarly community. With this in mind, we grant authors who have transferred copyright or granted a license to the NRC Research Press the following privileges to support this effort.

Authors will retain the right to

- Place a draft of a submitted article(s) (pre-acceptance) on their web site or their organization's server, provided that it is not amended once accepted for publication by NRC Research Press. We encourage authors to insert hypertext links from their preprints to the NRC Research Press web site, <http://pubs.nrc-cnrc.gc.ca>
- Post a published article on their web site or their organization's server six months after the NRC Research Press' original electronic publication date. The author must include NRC Research Press' copyright notice and acknowledge the article's source.
- Make copies of their article(s) in electronic or paper format, for personal or educational use within the home institution provided no financial gain is realized.

- Reproduce their article(s) in paper format for placement in the home institution's reserve collection.
- Re-use all or part of their article(s) in subsequent publications provided the source is acknowledged and no financial gain is realized.

NRC Research Press must retain certain rights in order to conduct day-to-day business for the benefit of the authors, the scholarly community and NRC.

NRC Research Press will retain the right to

- Negotiate agreements with secondary publishers and other third parties to further the dissemination of the published information.
- Administer copyright for all published materials to permit the above negotiations and to facilitate the process of granting permission to reproduce.
- Republish articles in alternative formats and editions.

A2 Wiley-VCH Verlag GmbH & Co. KGaA's Copyright release

We hereby grant permission for the requested use expected that due credit is given to the original source.

For material published before 2007 additionally: Please note that the author's permission is also required.

➤ Please note that we only grant rights for a printed version, but not the rights for an electronic/ online/ web/ microfiche publication, but you are free to create a link to the article in question which is posted on our website (<http://www3.interscience.wiley.com>)

If material appears within our work with credit to another source, authorisation from that source must be obtained.

Journal: Angewandte Chemie, International Edition

Authors: Nada Tashkandi; Frederick Parsons, Jiacheng Guo and Kim M. Baines

Pages: 1612-1615

Year: 2015

Volume: 54

Copyright Wiley-VCH Verlag GmbH & Co. KGaA. Reproduced with permission.

A3 Royal Society of Chemistry Copyright release

Author reusing their own work published by the Royal Society of Chemistry

You do not need to request permission to reuse your own figures, diagrams, etc, that were originally published in a Royal Society of Chemistry publication. However, permission should be requested for use of the whole article or chapter except if reusing it in a thesis. If you are including an article or book chapter published by us in your thesis please ensure that your co-authors are aware of this.

Reuse of material that was published originally by the Royal Society of Chemistry must be accompanied by the appropriate acknowledgement of the publication. The form of the acknowledgement is dependent on the journal in which it was published originally, as detailed in 'Acknowledgements'.

Curriculum Vitae

Name: Nada Y. Tashkandi

Post-secondary Education:

The University of Western Ontario

London Ontario, Canada

Ph. D (Chemistry)

2011-2016

King Abdul Aziz University, Jeddah, Kingdom of Saudi Arabia

M. Sc. (Chemistry)

2004-2007

King Abdul Aziz University, Jeddah, Kingdom of Saudi Arabia

B. Sc. (Honors Chemistry)

2000-2004

Honors and Awards:

King Abdul Aziz University Scholarship

2010

2nd prize; oral presentation award

14th International Conference on the Coordination and Organometallic Chemistry of Germanium, Tin and Lead (GTL 2013), Cape Breton, Baddeck, Nova Scotia, July 2013.

Related Work Experience:

Teaching assistant

King Abdul Aziz University

2004-2009

Lecturer

King Abdul Aziz University

2009-2010

Courses taken:

2011	Chem 9553a	Mechanistic Organic Chemistry	Wisner	87
2012	Chem 9555r	Organic Photochemistry	Workentin	91
2012	Chem 9503s	Advances NMR spectroscopy	Baines	91
2012	Chem 9603t	Advances NMR spectroscopy II	Wisner	83
2013	Chem 9658	Departmental Seminar		83
2013	Chem 9671t	Synthesis with Organometallics	Puddephatt	82
2013	Chem 9723t	Advanced Synthetic methods	Kerr	89
2014	Chem 9653t	Polymers: Synthesis and Function	Gilroy	82
2014	Chem 9823t	Heterocycles	Kerr	89

Publications:

Tashkandi, N. Y.; Pavelka, L. C.; Hanson, M. A.; Baines, K. M. "The addition of terminal alkynes to dimesitylfluorenylidene-germane", *Can. J. Chem.* **2014**, *92*, 462. (Special issue on ICCOC-GTL 2013).

Tashkandi, N. Y.; Parsons, F.; Guo, J.; Baines, K. M. "Addition of Nitromethane to a Disilene and a Digermene: Comparison to Surface Reactivity and the Facile Formation of 1,3,2-Dioxazolidines" *Angew. Chem. Int. Ed. Eng.* **2014**, *54*, 1612.

Bourque, J. L.; Tashkandi, N. Y.; Baines, K. M. "(*tert*-Butyl isocyanide- κ C)tri-chlorido-gallium(III)", *IUCrData*, **2016**, 1, x160389

Tashkandi, N. Y.; Pavelka, L. C.; Caputo, C. A.; Boyle, P. D.; Power, P. P.; Baines, K. M. " Addition of alkynes to digermynes: experimental insight into the reaction pathway", *Dalton Trans.* **2016**, *45*, 7226.

Tashkandi, N. Y.; Cook, E. E.; Bourque, J. L.; Baines, K. M. "The Addition of Isocyanides to Tetramesityldigermene: A Comparison of the Reactivity between Surface and Molecular Digermenes", *Chem. Euro. J.* **2016**, accepted.

Tashkandi, N. Y.; Bourque, J. L.; Baines, K. M. "Reduction of Aryl Sulfonyl Chlorides to Aryl Sulfinates using Ditetrelenes", manuscript in preparation.

Tashkandi, N. Y.; Bourque, J. L.; Baines, K. M. "The Reactivity of a Disilene Towards Isocyanides: The End of the Story", manuscript in preparation.

Tashkandi, N. Y.; Guo, J.; Bourque, J. L.; Baines, K. M. "Addition of Nitro Compounds to a Disilene and a Digermene: Comparison to Surface Reactivity and the Facile Formation of 1,3,2- Dioxazolidines", manuscript in preparation.

Presentations (Oral and poster):

Tashkandi, N. Y.; Pavelka, L. C.; Hanson, M. A.; Baines, K. M. "The Addition of Terminal Alkynes to Dimesitylfluorenylidene-germane", Poster, 44th Silicon Symposium, St. Cathrines, Ontario, June 15-17, 2012.

Tashkandi, N. Y.; Pavelka, L. C.; Hanson, M. A.; Baines, K. M. "The Addition of Terminal Alkynes to Dimesitylfluorenylidene-germane", Oral presentation, 14th International Conference on the Coordination and Organometallic Chemistry of Germanium, Tin and Lead (GTL 2013), Cape Breton, Baddeck, Nova Scotia, July 2013.

Tashkandi, N. Y.; Guo, J.; Baines, K. M. "Addition of Nitro compounds to a Disilene and a Digermene: Comparison to Surface Reactivity and the Facile Formation of 1,3,2- Dioxazolidines", Poster, 98th Canadian Chemistry Conference and Exhibition, Ottawa, Ontario, June, 13-17, 2015.